การกำจัดก๊าซอะเซทัลดีไฮด์ แอมโมเนีย และไทรเมทีลอะมีนโดยปฏิกิริยาเติมอิเล็กตรอนที่อุณหภูมิสูง

นายจินตวัฒน์ ไชยชนะวงศ์

วิทยานิพนธ์นี้เป็นส่วนหนึ่งของการศึกษาตามหลักสูตรปริญญาวิศวกรรมศาสตรมหาบัณฑิต
สาขาวิชาวิศวกรรมเคมี ภาควิชาวิศวกรรมเคมี
คณะวิศวกรรมศาสตร์ จุฬาลงกรณ์มหาวิทยาลัย
ปีการศึกษา 2545

ISBN 974-17-1960-4

REMOVAL OF ACETALDEHYDE, AMMONIA AND TRIMETHYLAMINE GASES USING ELECTRON ATTACHMENT REACTION AT HIGH TEMPERATURE

Mr. Jintawat Chaichanawong

A Thesis Submitted in Partial Fulfillment of the Requirements
for the Degree of Master of Engineering in Chemical Engineering
Department of Chemical Engineering
Faculty of Engineering
Chulalongkorn University
Academic Year 2002

ISBN 974-17-1960-4

Thesis Title	Removal of Acetaldehyde, Ammonia and Trimethylamine Gases Using Electron Attachment Reaction at High Temperature
By	Mr. Jintawat Chichanawong
Field of Study	Chemical Engineering
Thesis Advisor	Professor Wiwut Tanthapanichakoon, Ph.D.
Thesis Co-advisor	Associate Professor Tawatchai Charinpanitkul, D.Eng

---

Accepted by the Faculty of Engineering, Chulalongkorn University in Partial Fulfillment of the Requirements for the Master 's Degree

……………………………………………Dean of Faculty of Engineering
(Professor Somsak Panyakaow, D.Eng.)

THESIS COMMITTEE

…………………………………………….. Chairman
(Assistant Professor Vichitra Chongvisal, Ph.D.)

…………………………………………….. Thesis Advisor
(Professor Wiwut Tanthapanichakoon, Ph.D.)

…………………………………………….. Thesis Co-advisor
(Associate Professor Tawatchai Charinpanitkul, D.Eng.)

…………………………………………….. Member
(Assistant Professor Prasert Pavasant, Ph.D.)

…………………………………………….. Member
(Miss Nattaporn Tonanon, M.Sc.)

จินตวัฒน์ ไชยชนะวงศ์ : การกำจัดก๊าซอะเซทัลดีไฮด์ แอมโมเนีย และไทรเมทีลอะมีนโดยปฏิกิริยาเติมอิเล็กตรอนที่อุณหภูมิสูง. (REMOVAL OF ACETALDEHYDE, AMMONIA AND TRIMETHYLAMINE GASES USING ELECTRON ATTACHMENT REACTION AT HIGH TEMPERATURE). อ. ที่ปรึกษา : ศ.ดร .วิวัฒน์ ตัณฑะพานิชกุล, อ.ที่ปรึกษาร่วม : รศ.ดร . ธวัชชัย ชรินพาณิชกุล จำนวนหน้า 240 หน้า. ISBN 974-17-1960-4.

จุดประสงค์หลักของงานวิจัยนี้คือ ศึกษาผลของอุณหภูมิที่มีต่อการกำจัดก๊าซอะเซทัลดีไฮด์ แอมโมเนียและไทรเมทีลอะมีนออกจากกระแสก๊าซไนโตรเจนโดยใช้เครื่องปฏิกรณ์แบบเติมอิเล็กตรอน ก๊าซเป้าหมายเหล่านี้มีกลิ่นเหม็นและเป็นก๊าซองค์ประกอบของก๊าซที่ปล่อยจากเตาเผาศพที่อุณหภูมิสูง เนื่องจากก๊าซที่ปล่อยจากเตาเผาศพจะมีทั้งออกซิเจนและไอน้ำผสมอยู่ ดังนั้นปัจจัยที่ทำการศึกษาทดลองได้แก่ ความเข้มข้นขาเข้าของก๊าซเป้าหมาย ร้อยละของออกซิเจนและความเข้มข้นของไอน้ำในกระแสก๊าซไนโตรเจน เพื่อให้เข้าใจผลกระทบซึ่งกันและกันระหว่างก๊าซเป้าหมาย การทดลองจะมีทั้งการกำจัดก๊าซเป้าหมายแต่ละชนิดโดดเดี่ยว ก๊าซเป้าหมาย 2 ชนิดพร้อมกัน และทั้ง 3 ชนิดพร้อมกันด้วย ผลการทดลองชี้ให้เห็นว่า ถ้าความเข้มข้นของก๊าซยิ่งต่ำ ประสิทธิภาพการกำจัดจะยิ่งสูงขึ้นโดยไม่ขึ้นกับอุณหภูมิการทดลอง อนึ่งการมีออกซิเจนผสมอยู่ในก๊าซไนโตรเจนจะช่วยเพิ่มประสิทธิภาพการกำจัดก๊าซเป้าหมายให้สูงขึ้นทั้งการกำจัดแบบโดดเดี่ยวและการกำจัดแบบ 2 และ 3 ชนิดพร้อมกัน ส่วนการมีไอน้ำจะช่วยเพิ่มประสิทธิภาพในการกำจัดก๊าซเป้าหมายจากก๊าซไนโตรเจนที่อุณหภูมิต่ำ แต่จะลดลงเล็กน้อยที่อุณหภูมิสูง อย่างไรก็ตามในกรณีที่มีไอน้ำในก๊าซผสมไนโตรเจนและออกซิเจน จะทำให้ประสิทธิภาพการกำจัดต่ำกว่ากรณีที่ไม่มีไอน้ำ

อนึ่งกรณีการศึกษาผลกระทบซึ่งกันและกันในการกำจัดก๊าซเป้าหมาย 2 และ 3 ชนิดพร้อมกัน พบว่าจำนวนโมเลกุลก๊าซอะเซทัลดีไฮด์ แอมโมเนียและไทรเมทีลอะมีนที่ถูกจับด้วยหนึ่งอิเล็กตรอนเมื่อกำจัดพร้อมกันทั้ง 3 ชนิด จะมากกว่าเมื่อเทียบกับกรณีกำจัดก๊าซเป้าหมาย 2 ชนิดพร้อมกัน นอกจากนี้เพื่อลดการเกิดผลิตภัณฑ์ที่ไม่ต้องการ การประยุกต์ใช้เครื่องปฏิกรณ์สองตัวต่ออนุกรม ซึ่งใช้เงื่อนไขในการทำงานที่แตกต่างกัน แสดงให้เห็นแนวโน้มที่ดีสำหรับการเพิ่มประสิทธิภาพในการกำจัดและการลดการเกิดขึ้นของผลิตภัณฑ์ที่ไม่ต้องการ โดยพบว่า NO_x ลดลงจาก 50 พีพีเอ็ม เหลือเพียง 20 พีพีเอ็ม และโอโซนถูกกำจัดได้ทั้งหมด

ภาควิชา..........วิศวกรรมเคมี....................... ลายมือชื่อนิสิต..
สาขาวิชา.........วิศวกรรมเคมี....................... ลายมือชื่ออาจารย์ที่ปรึกษา..
ปีการศึกษา 2545 ลายมือชื่ออาจารย์ที่ปรึกษาร่วม.....................................

4370248221 : MAJOR CHEMICAL ENGINEERING

KEY WORD: GASEOUS POLLUTANT / GAS PURIFICATION / ELECTRON ATTACHMENT / CORONA DICHARGE / HIGH TEMPERATURE

JINTAWAT CHAICHANAWONG : THESIS TITLE. (REMOVAL OF ACETALDEHYDE, AMMONIA AND TRIMETHYLAMINE GASES USING ELECTRON ATTACHMENT REACTION AT HIGH TEMPERATURE) THESIS ADVISOR : PROF. WIWUT TANTHAPANICHAKOON, Ph.D., THESIS COADVISOR : ASSOC. PROF. TAWATCHAI CHARINPANITKUL, D.Eng., 240 pp. ISBN 974-17-1960-4.

The main objective of this research is to investigate the effect of temperature on the removal of acetaldehyde, ammonia and trimethylamine gases from N_2 using electron attachment reactor. The target gases are malodorous gaseous components emitted at high temperature from a crematory furnace. Since the emitted gases from a crematory furnace consist of O_2 and water vapor, the factors investigated are inlet gas concentration of the target gases, percentage of coexisting O_2 and the concentration of water vapor in the N_2 gas stream. To understand the effect between the target gases, the experiments are carried out both for the separate removal of target gases and the simultaneous removal of 2 and 3 target gases. The experimental results reveal that, regardless of the temperature, the lower the inlet concentration, the higher the removal efficiency becomes. It is found that the presence of oxygen enhances the removal efficiency of the target gases both in the separate removal of target gases and the simultaneous removal of 2 and 3 target gases. The presence of water vapor enhances the removal efficiency of the target gases from N_2 at low temperature but slightly retards it at high temperature. However, the presence of water vapor in nitrogen and oxygen mixture has adverse effect on the removal efficiency.

The effects between the target gases on the simultaneous removal of 2 and 3 target gases are investigated. It is found that in the case of the simultaneous removal of 3 target gases, the number of acetaldehyde, ammonia and trimethylamine gas molecules captured by an electron are higher than in the case of simultaneous removal of these 2 target gases. Furthermore, the application of two independently operated corona-discharge reactors in series is shown to have a good promise for enhancing the removal efficiency and minimizing the generation of byproducts. It is found that the effluent NO_X is reduced from 50 ppm to 20 ppm and O_3 is removed completely.

Department................Chemical Engineering.......... Student's signature..
Field of study.............Chemical Engineering…….. Advisor's signature...
Academic year ….…2002.................................. CO-advisor's signature..

ACKNOWLEDGEMENTS

I am very grateful to my advisor, Prof. Wiwut Tanthapanichakoon, Department of Chemical Engineering, Chulalongkorn University, for his indispensable advice, and his encouragement to continue the course of this work. I am also grateful to Assoc. Prof. Tawatchai Charinpanitkul, Assist. Prof. Vichitra Chongvisal, Assist. Prof. Prasert Pavasant.and Ms. Nattaporn Tonanon for their stimulative comments and participation as the thesis committee.

I would like to acknowledge the Thailand-Japan Technology Transfer Project (TJTTP-JBIC) and the Thailand Research Fund (TRF). Dr. Noriaki Sano of Himeji Institute of Technology and Prof. Hajime Tamon of Kyoto University visited CU and brought research materials here as part of the TJTTP-JBIC. I would like to thank Dr. Sano for his on-the-job training, useful guidance, research assistance, and kindness. It has been a great experience learning a lot of things from him and Prof. Tamon.

The research work received research grant from Thailand Research Fund (High-Temperature Removal of Low-Concentration Multi-Component Air Pollutant Gases Using Electron Attachment Reaction Project). The Project is headed by Prof. Wiwut and I am one of the half-time research assistants.

I would like to thank my senior colleagues. Ms. Nantamas Dhattavorn and Mr. Sahat Chaiyo for their training and useful suggestions and Mr. Somchai Mahitthiroch of Bara, Windsor Co.Ltd. for his suggestion and information on the analytical instrument.

I would like to thank the Department of Chemical Engineering, Chulalongkorn University for allowing me to setup the experimental apparatus and using the accessories.

Thank you very much to all members of the Particle Technology and Material Processing Laboratory for their warm collaborations and kindness especially Ms. Kamarat Jermsirisakpong for her help and encouragement during the time of my study.

Finally it is my great wish to express my cordial and deep thanks to my parents for their love and encouragement.

CONTENS

CONTENS (CONTINUED)

CONTENS (CONTINUED)

CONTENS (CONTINUED)

LIST OF TABLES

LIST OF FIGURES

LIST OF FIGURES (CONTINUED)

LIST OF FIGURES (CONTINUED)

LIST OF FIGURES (CONTINUED)

NOMENCLATURE

C_{in} = inlet concentration [ppm]

$C_{out,0\ mA}$ = outlet concentration [ppm] when using zero current

$C_{out,Any\ mA}$ = outlet concentration [ppm] when using non-zero current

$[\ ]_{in}$ = inlet concentration [ppm]

$[\ ]_{out}$ = outlet concentration [ppm]

A = cross sectional area [m^2]

D_l = anode diameter [m]

D_o = cathode diameter [m]

E = electric field strength [$V\ m^{-1}$]

I = discharge current [mA]

N = gas density [$mol\ m^{-1}$]

N_r = number of gas molecules removed per time [s^{-1}]

N_{e0} = number of emitted electrons per time [s^{-1}]

$q_{out,\ 0\ mA}$ = the molar flow rate at reactor outlet without current [$mol\ s^{-1}$]

$q_{out\ at\ any\ mA}$ = the molar flow rate of at reactor outlet with current [$mol\ s^{-1}$]

p = total pressure [atm]

P = power consumption [W]

R = radial distance from the cylindrical axis [m]

R = gas constant [$0.082057\ dm^3\ atm\ K^{-1}\ mol^{-1}$]

T = temperature [^oC]

SV = space velocity [hr^{-1}]

V = discharge voltage [V]

V_r = effective volume of the corona discharge reactor [m^3]

θ = mean residence time [s]

$\langle \upsilon \rangle$ = superficial velocity [m/s]

ψ = apparent removal efficiency [-]

ψ' = removal efficiency excluding adsorption effect [-]

ψ'' = removal efficiency per unit residence time [-]

ψ_{elec} = electron-based efficiency [-]

ψ_{ener} = energy-based efficiency [$mol\ gas\ .J^{-1}$]

CHAPTER I

INTRODUCTION

Nowadays air pollution in Thailand poses a serious environmental issue. There are numerous sources of air pollutants in big cities such as heavy concentration of vehicles and traffic congestion. One severe public nuisance is emission gas from the crematorium during cremation rites. There are nearly 23,000 temples nationwide, including approximately 300 temples with crematory furnaces in Bangkok Metropolitan Area alone. During cremation, various malodorous gases and particulate are emitted without adequate treatment, causing frequent complaints from vicinal communities. Only a few rich temples have installed furnaces with efficient after-burning system to decompose the malodorous organic gaseous. However, the after-burning system is effective and economical only when the whole system is operated continuously but not suitable to the removal of impurity gases at low concentration levels. For this reason it is worthwhile to develop an alternative gas treatment method that achieves high efficiency at low energy consumption. In comparison to the conventional method, the new technology of electron attachment reaction is more suitable to treatment of occasional emission and the removal of impurity gases at low concentration levels.

Moreover the exhaust gas temperature from a well-operated furnace outlet may be as high as 800~900 ^{o}C whereas the stack temperature may range from 150~300 ^{o}C, there is insufficient report on the effect of high temperature. This research investigates the application of electron attachment to the removal of malodorous gases from room temperature up to 300 ^{o}C.

Table 1.1 lists the exhaust gas from one gas-fired crematory furnace in Japan. The list values are the average gaseous composition after 100-fold dilution with fresh air.

Table 1.1 Types and concentrations of gaseous components emitted from a crematory furnace in Japan after 100-fold dilution (Nishida K. 1981, 1988)

Type	Components	Concentration
Air	N_2	78 %
	O_2	20~21 %
Low-concentration components	CO_2	0.01~0.02 %
	H_2O	0.22 %
	NO_x	80 ppm (max)
	SO_x	5.8 ppm (max)
	Acetic acid	24 ppm
	Hydrocarbons	230 ppm (as propane)
Ultra-low-concentration malodorous components	Acetaldehyde	0.04 ppm
	Styrene	0.01 ppm
	Hydrogen sulfide	0.01 ppm
	Methyl mercaptan	0.001 ppm
	Dimethyl sulfide	0.0005 ppm
	Ammonia	0.37 ppm (max)
	Trimethyl amine	0.023 ppm (max)

1.1 Objective of research work

Investigate the effect of high temperature and coexisting gases on the removal efficiency of three malodorous gases from nitrogen using the deposition-type reactor.

1.2 Scope of research work

1.2.1 The malodorous gases investigated in this research are acetaldehyde, ammonia and trimethylamine

1.2.2 The coexisting gaseous components are oxygen (0-20%) and/ or water vapor (0-20,000 ppm)

1.2.3 The ranges of experimental conditions investigated are as follows:

- The reaction temperature ranges from room temperature to 300 ^{o}C
- Concentration of the malodorous gases are limited to the range of 100-1000 ppm
- Discharge current ranges between 0-3 mA
- Cathode diameter is 0.5 mm with 10 cm effective length
- Space velocity gas at room temperature is 55.8 hr^{-1}
- 2 reactors in series is used to improve the removal efficiency and/or reduce generation of by-products.

CHAPTER II

FUNDAMENTAL KNOWLEDGE

The self-sustaining discharge of electrons in a non-uniform electric field between a thin wire and a coaxial cylinder is called a corona discharge. This name is descriptive of the glowing light effects found when the applied voltage is several kilovolts. High vacuum is not always required and corona discharge can be generated at or near atmospheric pressure. The gas pressure needs not be low for the discharge to occur, but at low gas pressure the corona is not visible. The luminous part of the discharge is usually restricted to a region close to the wire surface, which may be positive or negative with respect to the cylinder. One distinguishes between positive and negative coronas by the applied positive or negative voltage of the central electrode.

Coronas are by no means only artificially produced. It is the natural phenomenon of the glow or corona surrounding the sun but is only visible during a total solar eclipse. In addition, nature produces them between and within electrically charged clouds. A theory on cloud electrification attributes this process to the corona on and around ice particles in the clouds. According to this theory, corona is not only the effect but also the cause of the appearance of charged clouds and therefore of lightning and thunderstorms.

In a corona discharge reactor, there are three regions in the void space between the anode and cathode as shown in **Figure 2.1**. In the high electron energy region, free electrons are emitted from the cathode surface and rapidly accelerated. Surrounding gas molecules will be ionized after collision with these free electrons and negative ions are produced. In the transient region, the electron energy is just enough to dissociate gas molecules to produce neutral radicals. In the vast region of low-energy electrons, electrons are prone to be captured after collision with gas molecules. Cluster formation and electron attachment reaction generally take place in this region.

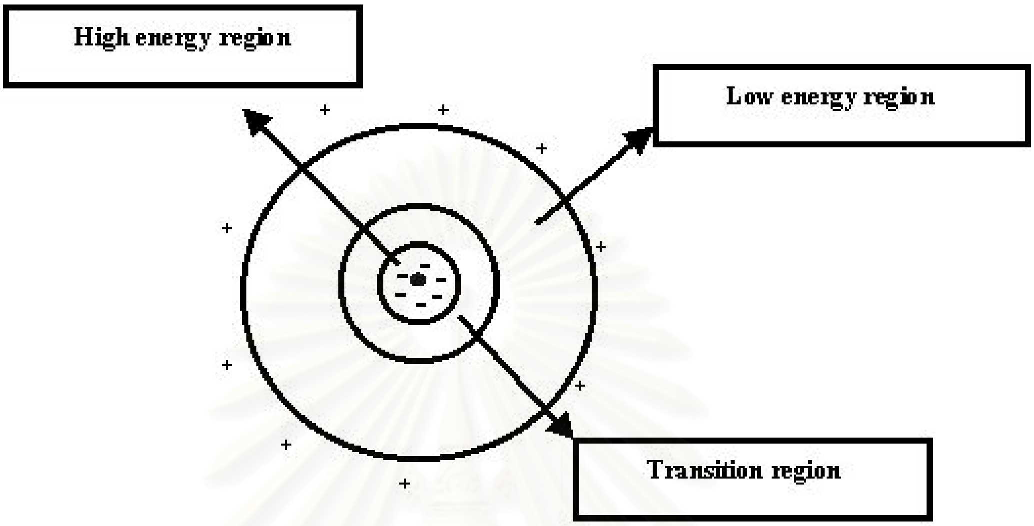

Figure 2.1 The regions of corona discharge reactor

2.1 Electron attachment reaction

When low-energy electrons collide with electronegative gas molecules, some electrons are captured by the gas molecules, and negative ions are formed. This phenomenon is called "electron attachment" (Massey, 1976). Electron attachment depends on the electron energy level, the structure of the gas molecule, and its electron affinity. There is a huge difference between the electron attachment probability of the gas molecules and that of the carrier gas. This high selectivity is reflected in the production of negative ions (Caledonia, 1975 and Massey, 1976, 1979). Therefore, electronegative impurities of very dilute concentration become negative ions by electron attachment, and they can effectively be separated from the neutral gas (for example, N_2) in an electric field.

In the case of excessively high-energy electron colliding with a gas molecule, the molecule would not only be negatively ionized but may be dissociated or be positively ionized due to the loss of one electron from the molecule itself. In contrast, if an electron whose energy is too low reaches the molecular orbital, the electron can not be captured by the molecule. It is necessary to take into account the moderate (appropriate) range of electron energy when the attachment probability is to be enhanced. A great deal of effort has been devoted to generate or utilize electrons with a variety of energy range via quite a number of gas-discharge devices. However, the appropriate range of electron energy contributing exclusively to electron attachment generated by such devices has not been clarified because of the limitation of measurement devices and/or techniques.

At the exact moment when an electron is captured by a gas molecule, the molecule would be placed at an excited state. To become stable, the molecule must release the excess energy in quanta, for example, by collision with another electron, by collision with another gas molecule, by being decomposed, or by radiation. Various processes for the electron attachment reaction have been reported (Moruzzi and Phelps, 1966) as shown by Eqs. (2.1), (2.2), and (2.3). A mixture of an electron-attaching gas, AB, and an appropriate third body, M, is considered in these processes.

Dissociative attachment: $e + AB \rightarrow A^- + B$ (2.1)

Three-body attachment: $e + AB + M \rightarrow AB^- + M$ (2.2)

Radiative attachment: $e + AB \rightarrow AB^- + h\nu$ (2.3)

Since the electron attachment probability of the gas molecule is also dependent upon its electron affinity, it is reasonable to expect that a molecule that contains one or more atoms with high electron affinity would have high probability of electron attachment. For example, in a comparison between SF_6 and N_2, the electron affinities of S, F, and N are 200 kJ/mol, 333 kJ/mol, and –

26 kJ/mol, respectively. So it is not surprising that the probability of electron attachment for SF_6 molecule is reportedly 10^{11} times that of N_2 molecule (Hickman and Fox, 1956). This huge difference in the electron attachment probability among various kinds of gas molecules results in high selectivity in the formation of the corresponding negative ions. Therefore, even a specific gas component whose concentration is extremely low can effectively be separated from the main (neutral) gas in an electric field by utilizing the electron attachment reaction. Also one can expect the method based on electron attachment to be one of the most efficient methods of gas purification.

Since most malodorous components in the crematory emission are highly electronegative gaseous components, electron attachment seems to be one highly effective way to remove them in an electric field. With further advancement of the technology and the use of multi-stage reactor, it is reasonable to aim at the simultaneous removal of both gaseous pollutants and fine particles since the basic principle of corona discharge and subsequent deposition on the anode is similar to that of an Electrostatic Precipitator (ESP) (White, 1960; Oglesby and Nichols, 1978; Ogawa, 1984). This is however beyond the scope of this work.

2.2 Principle of gas purification

Figure 2.2 illustrates the principle of gas purification by the removal of an impurity, AB, from an inert gas in a cylindrical corona-discharge reactor (Tamon et al., 1995). The corona discharge is employed here because it is an efficient method to supply a large number of low-energy electrons to the gas stream. The cathode is a wire stretched along the axis of the reactor and the outer cylinder acts as grounded anode. High DC voltage (-5~ -15kV) is applied to the cathode to induce corona discharge in the reactor. Electrons generated at the cathode drift to the anode along the applied electric field. During their drift to the anode, a portion of them collides with the gas molecules. Negative ions,

A^-, are thus selectively produced by electron attachment and they likewise drift to the anode as the electrons do.

In an ideal case, the number of electrons generated in the reactor is sufficient for all gaseous impurities to hitch up with the electrons and all negative ions thus generated are able to completely deposit on the anode surface. In other words, the outlet gas is devoid of unwanted impurities and complete removal is achieved. In reality, upon their arrival at the anode, certain kind of negative ions might simply discard their charges without depositing on its surface. In this case these gaseous impurities can not be separated using the simple deposition-type reactor. In any case, it is most desirable to capture most of the negative ions arriving at the anode surface. The idea of how to remove negative ions at the anode will be described later.

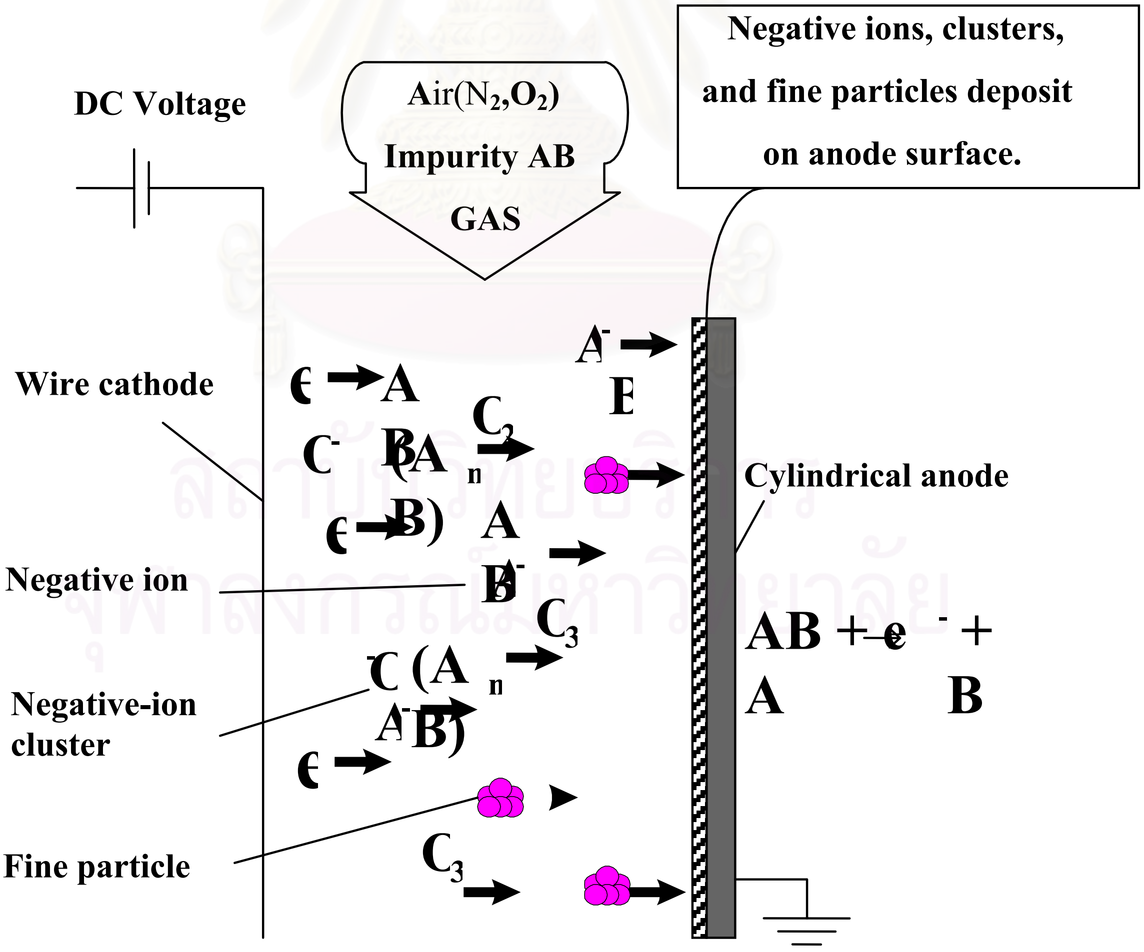

Figure 2.2 Principle of gas purification

Besides the above-mentioned removal mechanism associated with electron attachment reaction in the corona-discharge reactor, it is believed that other removal mechanisms may simultaneously contribute to the removal efficiency. When single negative ions are produced in the reactor, they may possibly interact with other adjacent gas molecules via their electrostatic forces and negative-ion clusters may be formed. Each cluster then contains multiple gas molecules targeted for removal. When the clusters drift to the anode and manage to deposit there, the removal efficiency is greatly enhanced.

Another possible mechanism contributing to the removal efficiency is the so-called radical reaction. When dissociative electron attachment also takes place in the reactor, not only negative ions but also reactive radicals are produced. In particular, the radicals may readily be produced in the immediate vicinity of the cathode surface where high electric field strength exists. It is logical to assume that the removal efficiency would be enhanced by radical reaction, which, however, often results in the generation of reaction by-products.

The reaction of targeted gas molecules with O_3 is frequently mentioned. Ozonation reaction usually takes place when oxygen coexists in the gas stream. High-energy electrons close to the cathode surface collide with O_2 molecules to dissociatively produce O^- radicals. O^- radicals can next react with O_2 molecules to produce O_3, which is reactive with various kinds of gases. Hence, ozonation reaction is expected to contribute to the oxidative destruction of a number of gaseous impurities in the gas stream, thus improving the removal efficiency while yielding by-products.

2.3 Types of reactor

As mentioned in section 2.2, in some cases certain kind of negative ions produced by electron attachment would drift towards but do not easily adhere to the anode surface. Thus they end up as uncaptured negatively charged or uncharged impurities at the outlet of the conventional deposition-type reactor, and cause a decrease in their removal efficiency. It is therefore essential to find out how to effectively remove such negative ions at the anode. This has motivated Tamon et al. to propose three types of reactor, as shown in **Figure 2.3**

2.3.1 Deposition-type reactor

Some negative ions readily adhere to the anode surface of the reactor after releasing their negative charges there. In this case they may form solid particles or react with the metallic anode. The solid particles form a thin deposition layer on the anode surface. Thus, the so-called deposition-type or (simple) reactor is adequate for the removal of these negative ions. Periodic cleaning of the anode surface or its replacement is often necessary to maintain high removal efficiency.

2.3.2 Sweep-out-type reactor

In some uncommon cases certain negative ions do not easily deposit on the anode surface but change back to the original uncharged molecules after releasing electrons at the anode surface. In such cases, the deposition-type reactor is not suitable because the original molecules of the gas impurities are not removed but diffuse back to the main gas stream. To solve this problem, the sweep-out-type reactor, which uses a porous pipe wall made of sintered metal as anode is recommended. A small portion of the carrier gas around the anode surface is swept out by suction through this pipe to restrict backward diffusion of the concentrated electronegative impurities so that the removal efficiency would be kept high. The swept-out stream with a much higher concentration of the gas impurities can then be treated using a suitable conventional method.

2.3.3 Wetted-wall reactor

Another option to remove negative ions at the anode surface is the wetted-wall reactor. Negative ions reaching the anode of the reactor can be absorbed into a down-flowing liquid film on the vertical anode surface. This absorption of the ions improves the removal efficiency. The most important advantage is the self-cleaning of the anode, which makes it suitable even for dirty gas streams containing both dust and gaseous pollutants. The major drawback is the need for a liquid (mostly water) treatment and recycle system. Anyway, the corona-discharge reactor to be investigated in this work will be limited to the deposition type because it is easier to construct and operate, and is applicable as a first step of the fundamental study in a laboratory.

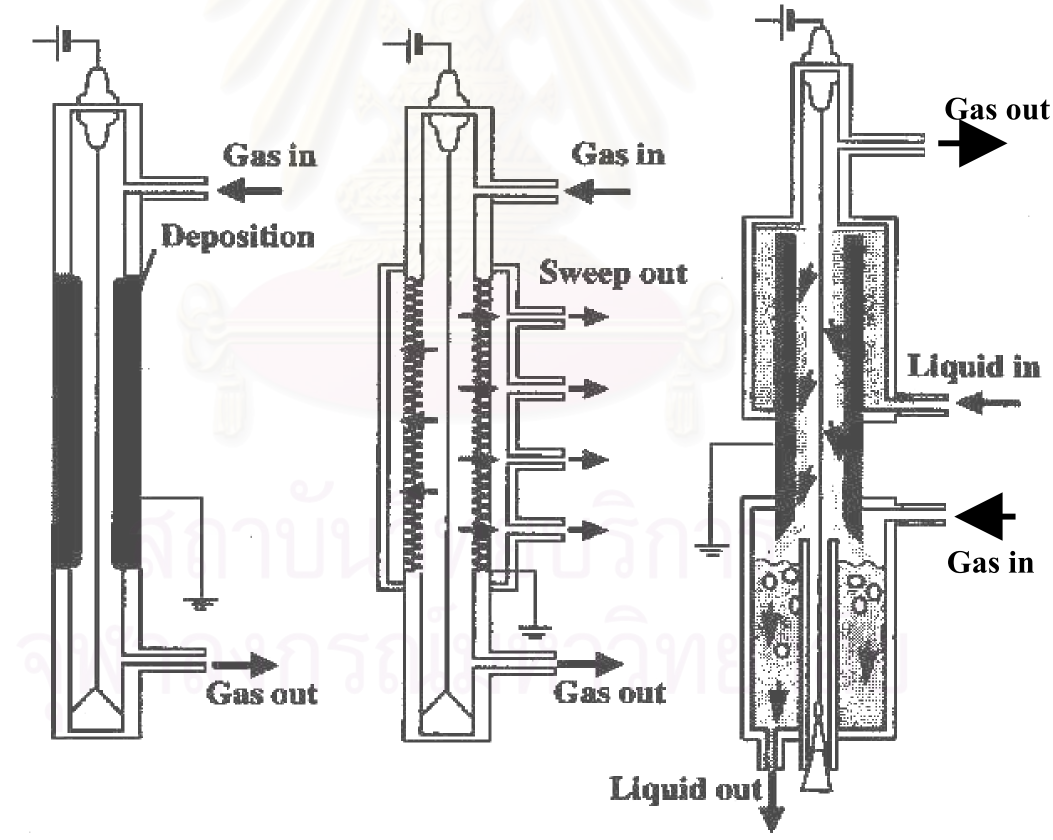

(a) Deposition-type (b) Sweep-out-type (c) Wetted-wall

Figure 2.3 Types of corona-discharge reactor

2.4 Effect of coexisting oxygen (ozone effect)

When O_2 is present in a gas mixture, it usually reacts with discharged electrons. Electron attachment on O_2 has been reported in the literature (Morruzzi and Phelps, 1966; Massay, 1976; Rapp and Briglia, 1976; Chantry and Schulz, 1967).

$$O_2 + e^- \longrightarrow O_2^- \qquad (2.4.)$$

$$O_2 + e^- \longrightarrow O + O^- \qquad (2.5)$$

Moruzzi and Phelps (1966) reported that the reaction in **Eq. (2.4)** occurs in the low electron energy range ($E/p < 1.5$ V.m^{-1}.Pa). In contrast, the reaction in **Eq. (2.5)** occurs in the higher electron energy range. Also in the corona-discharge reactor, the closer the electrons are to the cathode wire, the higher their energy level. When an O_2 molecule collides with a high-energy electron near the cathode wire in the corona-discharge reactor, production of O^- is expected as in **Eq. (2.5)**. Next O_3 is produced from the reaction of O^- with O_2 (Loiseau et al., 1994; Hadj-Zaine et al., 1992).

In short, some ozone (O_3) is produced. Since O_3 is very reactive, the ozonation reaction is used in some commercial devices for deodorization and sterilization. The same ozonation reaction is expected to contribute to the removal of gas impurities in the present corona discharge reactor.

2.5 Effect of negative-ion cluster

If a negative ion induces the formation of a cluster of multiple gas molecules, the removal efficiency of the impurities will be improved. This effect is significant because one negative ion and several gas molecules constitute a cluster that drifts to the anode and deposits on it.

2.6 Effect of temperature

The influence of gas or reactor temperature on the relationship between the voltage and the current has been confirmed (Sano et al., 1997). As expected, the higher the temperature, the lower the required voltage becomes. Reportedly, several factors may be considered as the reason for the temperature dependency of the voltage-current relationship. They are (1) the positive change in the frequency of the thermal electron emission from the cathode surface to initiate the corona discharge; (2) the positive change in the propagation rate of free electrons in the high electric field region around the wire cathode; (3) the positive change in the ionization rate of the gas molecules; (4) the positive change in the mobility of the ions.

As for the temperature effect on the dissociative electron attachment of O_2, it was reported that the dissociative electron attachment rate increased when the temperature increased. Thus it is logical to consider that the formation of clusters is inhibited by temperature elevation because the ion clusters are thought to be less stable at high temperature condition.

CHAPTER III

LITERATURE REVIEW

Gas purification involves the removal of vapor-phase impurities from a gas stream. Many methods for gas purification have been proposed, and the primary operation falls into one of the following three categories; 1) absorption into a liquid, 2) adsorption on a porous solid, 3) chemical conversion to another compound. In fact many research works to improve these processes are still going on.

Gas discharge technology is one promising method of achieving ultrahigh purification. Application of gas discharge processes with high-energy electrons has existed for over a hundred years, dating to the first electrostatic precipitator of Lodge (Oglesby and Nichols, 1978) and ozonizer of Simens (Horvath, 1980). The electrostatic precipitator (ESP) is a device-utilizing corona discharge for removing particulate pollutants in the form of either a solid (dust or fumes) or a liquid (mist) from a gas using the electrostatic force. One may realize that the corona-discharge reactor for the gaseous pollutant remover used in this work has the same working principle as ESP. Most information on ESP however focuses on the removal of particulate matter, whereas the reactor proposed in this work, utilizing low-energy electrons in gas discharge to induce electron attachment reaction, aims at separating gaseous impurities from a gas stream. Application of the electron attachment (a reaction of low-energy electrons and gas molecules to produce negative ions), first proposed by Tamon et al. (1989), is still innovative for gas separation processes nowadays.

Many publications on electron attachment and other reactions of electron with many kinds of gas molecules have appeared but most of them involve only the reaction kinetics (Moruzzi and Phelps, 1966, Caledonia, 1975 and Massey, 1976). In fact basic information on gas purification using electron attachment and the proposed use of the selectivity of electron to remove the electronegative gaseous molecules are still scarce.

Applications of gas discharge technology conducted to date are reviewed as follows.

Castle, Inculet, and Burgess (1969) discussed briefly about surface oxidation of discharge electrodes used in a wire-tube electrostatic precipitator. The rate of ozone generation in the precipitator with both stainless steel and copper wires was clarified. The reaction rate of ozone depended on the intensity of electron flux through the gas. The concentration of ozone generated was a linear function of current but decreased as the gas temperature increased.

Dorsey and Davidson (1994) reported an assessment of the contribution of contaminated wires and plates to ozone production in electrostatic air cleaners. It was found that runaway ozone generation due to contamination of electrode surfaces was a limiting factor in the long-term (7 weeks) effectiveness of electrostatic air cleaners. The corona discharge degraded to streamers after only two weeks, causing increased ozone levels. Wire contamination alone can increase ozone generation. These findings have serious implications for the safe operation of electrostatic air cleaners.

Chemical Vapor Decomposition (CVD) occurring on a discharge wire of an electrostatic air cleaner causes the corona current to decrease more than 95% at the same voltage (after 180 hrs operation). This phenomenon was shown by Jan H. Davidson et al. (1998). Neither current drop nor deposition occurred when operated with clean or dry air (after 2 days).

Several types of DC energized point-electrode reactors have been developed and tested for gas chemistry applications. Although designed with different purposes in mind, the configurations could be put to other uses.

Castle, Kanter, Lee, and Kline (1984) tested a narrow-gap, multipoint-to-plane geometry device in which the gas passed through a corona discharge at high velocity (approximately 100 m/s). The upper multipoint electrode (cathode) was separated from the lower flat electrode (anode) by acrylic spacers that electrically isolated the electrodes and allowed visual observation of the corona. The narrow gap spacing ensured that the inter-electrode space was filled with corona induced plasma. However, the lateral spacing of the pins allowed major fractions of the gas flow to bypass the corona zones. A DC current was applied to the multipoint pins through current limiting resistors.

An experimental investigation has been conducted by Chang, Jen-Shih et al. (1988) to obtain electrode surface temperature profiles of cylindrical hollow electrodes under corona discharges. The result show that a slight temperature increases (about 5 Kelvin within the 10 W input for discharge power level) occurs near the edge of the cylindrical hollow electrodes. Thus, the corona discharge still can be categorized as a cold discharge region.

The pulsed electron technology has also been shown to be capable of generating ozone and active radicals and decomposing several unwanted gases as well as aerosol particles.

Higashi, Sugaya, and Ueki (1985) and Weiss (1985) conducted the reduction of CO_2 the in exhaust gas from a diesel engine vehicle. It was shown that CO_2 concentration in a N_2-CO_2 or even pure CO_2 gas could be reduced by DC and pulsed corona discharges, respectively. Further experiments for soot elimination and NO_x and SO_x reduction in a diesel-engine exhaust by a combination of discharge plasma and oil dynamics have been investigated by Higashi, Uchida, Suzuki, and Fujii (1991, 1992).

Chang (1989) and Chakrabarti et al. (1995) found that the removal of NO_x, SO_x, and aerosol particles could be achieved when NH_3 or H_2O was introduced into a pulsed streamer corona reactor. The pulsed electrons have been shown to cause reactions between oxidizing radicals such as OH, O, and O_3 on the one hand and NO_x and SO_x on the other hand at the concentrations found in flue gases to form several acidic aerosol particles with NH_3 or H_2O injections.

Recent experimental study done by Helfritch (1993) led to the conclusion that H_2S decomposition to hydrogen and sulfur could be directly achieved electronically. A wire-in-tube pulsed corona reactor was energized by short voltage spikes to decompose small concentrations of H_2S contained in nitrogen. Some parameters including the reactor geometry, H_2S concentration, corona power, and the nature of the products were investigated.

Mizuno, Clements, and Davis (1986) compared the performance of the pulsed streamer corona, DC corona, and electron-beam processes. It was found that a pulsed streamer corona discharge produced the radicals instead of a high-energy electron beam. A positive pulsed streamer corona discharge in a non-uniform electrode geometry showed better energy efficiency and higher removal performance than a DC corona discharge. Based on the delivered power, the pulsed streamer corona process removed more than 90% of SO_2 with at least two times better power efficiency than the energetic electron-beam process.

Masuda, Sato, and Seki (1984) developed a high-efficiency ozonizer using traveling wave pulse voltage. The test results relating to the pulse-induced ozone generation showed a great enhancing effect on the speed of reactions by positive pulse corona producing streamers bridging across the entire electrode gap. It was believed that the ozone generated in a corona discharge was a two step process: generation of oxygen free radicals by ionic processes and generation of ozone by free radical reactions. It was found that the ozone generation processes were substantially reduced by increasing the gas temperature, while the ozone loss processes were significantly enhanced by increasing the gas temperature. It was therefore recommended to operate an ozonizer in lower temperature conditions.

High-voltage pulser was used in a pulse-induced plasma chemical processing unit (PPCP unit). This pulser comprised a synchronous rotary spark gap that produced a very sharp negative pulse voltage. High electron energies could be achieved by both units since higher electric fields were allowed in surface-corona and pulse-corona systems than in direct-current systems because of the breakdown limits of the discharge.

Eliasson, Hirth, and Kogelschatz (1987) applied a dielectric-barrier discharge for ozone generation from oxygen. The resulting efficiency of the generation was reported. A value of 1200 g/kWh was the theoretical ozone generation efficiency calculated by thermochemical theory. He also estimated the maximum ozone generation efficiency of 400 g/kWh for pure oxygen by analyzing a Boltzmann equation. The actual ozone generation efficiency was approximately 200 g/kWh for pure oxygen, which was very low compared to the theoretical values. It was because the discharge energy was consumed not only in producing the ozone but was also dissipated in heating the test gas and the electrodes of the ozonizer. Also some of the ozone produced was destroyed by the heat.

After the work of Eliasson et al., there has been attempt to improve the ozone generation efficiency. Ito, Ehara, Sakai, and Miyata (1990) reported that the efficiency in the silent discharge showed a rise of 3-6% by the radiation of ultra-violet ray from the discharge in nitrogen gas. Later, Hattori, Ito, Ehara, and Miyata (1992) reported the superposition effect of two types of discharge in the same discharge space, silent and surface discharges, on ozone generation. Their ozonizer had two power sources with a variable-phase shifter. A 22-30% increase in the efficiency was observed in their ozonizer.

Yamamoto et al.(1996) demonstrated a new concept-single-stage, catalysis-assisted packed-bed plasma technology, to decompose CCl_4, one of the ozone-depleting substances. The objective of the concept was twofold: to enhance the decomposition efficiency catalytically, and to selectively reduce the by-products. Either $BaTiO_3$ or $SrTiO_3$ pellets were packed in the ferroelectric packed-bed reactor employing an AC power supply. The configuration employed a unique one-stage catalysis/plasma process in which the $BaTiO_3$ pellets were coated or impregnated by active catalysts such as Co, Cu, Cr, Ni, and V. Enhancement of the CCl_4 destruction and the conversion of by-product CO to CO_2 were demonstrated using Ni catalyst in the one-stage plasma reactor.

The so-called non-thermal plasma including corona discharge has been widely studied

A non-thermal plasma chemical process with an AC powered ferroelectric packed-bed reactor was again tested by Zhang, Yamamoto, and Bundy (1996). In this work, the targeted gases to be decomposed were ammonia and odorous compounds gathered from animal houses. The plasma reactor packed with $BaTiO_3$ pellets produced high energy free electrons and radicals, which in turn, decomposed the targeted compounds. Four important parameters affecting the reactor performance were investigated: gas residence time, power voltage, power frequency and initial ammonia concentration.

Tamon, Sano, and Okazaki (1989) proposed a novel method of gas separation based on electron attachment. Two kinds of separation devices using either photocathode or glow discharge as electron source were constructed. They reported high efficiency for the removal from nitrogen of SF_6 at very low concentrations. Recently, Tamon et al. (1995) used two types of corona-discharge reactors, deposition-type and sweep-out-type reactors, to remove from nitrogen dilute sulfur compounds, dilute iodine and oxygen. They also discussed the purification mechanism and presented simulation models for predicting the removal efficiency. Subsequently, Tamon, Sano, and Okazaki (1996) investigated the influence of coexisting oxygen and water vapor on the removal of six sulfur compounds from nitrogen. They discovered that the presence of oxygen and water vapor increased the removal efficiency.

Sano et al. (1996) used a new type of corona-discharge reactor, the wetted-wall reactor, and the conventional deposition-type reactor to remove iodine and methyl iodide from nitrogen. The removal mechanism of I_2 and CH_3I in the reactor was also discussed.

Kittisak Larpsuriyakul et al. (1996) and Wiwut Tanthapanichakoon et al. (1998) reported experimental results regarding the influence of the structure of the corona-discharge reactor on the removal of dilute gases. The effects of the reactor structure, namely the cathode diameter, the anode shape, and the number of cathodes, were investigated. The results revealed that the thicker the cathode diameter, the higher the removal efficiency. In contrast, the smaller the reactor diameter among three equivolume reactors, the higher the removal efficiency. As for the number of cathodes in a single reactor vessel, the single-cathode reactor always exhibited a higher removal efficiency than the 5-cathode one.

Paisarn Khongphasarnkaln (1998) investigated the application of electron attachment to the removal of dilute gaseous pollutants using a corona-discharge deposition-type reactor. It has been found that the presence of O_2 enhanced the removal efficiency of each impurity gas. The enhancement was experimentally shown to be attributable to the ozone reaction in the removal of $(CH_3)_3N$ from O_2-N_2 mixed gas. Water vapor also enhanced the removal efficiency of $(CH_3)_3N$ and CH_3CHO. Furthermore, The high selectivity of electron attachment to electronegative gas molecules was utilized in the simultaneous removal of dilute $(CH_3)_3N$-CH_3CHO, NH_3-CH_3CHO, SO_2-$(CH_3)_3N$, SO_2-CH_3CHO, NO_2-CH_3CHO and CO_2-CH_3CHO from the air in the single reactor. Compared to single impurity removal, it has been shown that the presence of SO_2 enhanced the removal efficiency but retarded that of CH_3CHO in the single reactor. Some reaction by-products generated could be avoided by using two independently operated reactors in series. In the case of coexisting of NO_2, it was noted that the lower the inlet NO_2 concentration, the lower the discharge current that still yielded beneficial effect. At higher discharge currents, the retarding effect of CO_2 on CH_3CHO removal was obviously significant.

Han S. Uhm (1999) investigated the influence of the chamber temperature on the properties of the corona discharge system. It was found that the critical voltage V_c required for the corona discharge breakdown was inversely proportional to the chamber temperature T. The electrical energy w_c required for corona discharge breakdown was inversely proportional to the square of the chamber temperature T. Thus, the electrical energy consumption for the corona discharge system decreased significantly as the temperature increased. The plasma generation by corona discharge in a hot chamber was much more efficient than that in a cold chamber.

Wiwut Tanthapanichakoon et al. (2001) investigated the common gas species emitted during cremation. Even ultra-low concentrations of some organic compounds can still cause malodor. They summarized past and recent experimental results on the removal of sulfur compounds, nitrogen compounds and organics compounds, which indicated that the presence of oxygen and/or water vapor in N_2 gas contribute to an increase in the removal efficiency in the removal efficiency in many cases. Conversely, temperature elevation negatively affected the removal of SO_2.

Recently, Sano et al. (2001). applied a reactor using DC corona discharge of negative polarity to remove sulfur dioxide from an oxygen-nitrogen mixture in the presence or absence of water vapor for temperatures ranging from room temperature to 350 ^{o}C. It was observed that increasing the reactor temperature cause a decrease in the removal efficiency. Mixing water vapor with the process gas resulted in an increase of the removal efficiency. The effect of the presence of water vapor on improving the removal efficiency was significant under low temperature conditions, while it was relatively moderate under high temperature conditions.

CHAPTER IV

EXPERIMENTAL

4.1 Test materials and chemicals

Table 4.1 The specifications of test materials and chemicals

Type	Use	Company	Purity / Grade
Acetaldehyde(g)	Sample gas	TIG*	Acetaldehyde 2000 ppm balanced with N_2
Ammonia(g)	Sample gas	TIG	Ammonia 2000 ppm balanced with N_2
Trimethylamine(g)	Sample gas	TIG	Trimethylamine 2000 ppm balanced with N_2
Distilled Water	For preparing water vapor	-	-
Oxygen	Coexisting gas	TIG	Industrial grade
Nitrogen (g)	Carrier and diluent gas to reactor	TIG	UHP 99.999 % min
Nitrogen (g)	Carrier gas for GC (FID detector)	TIG	UHP 99.999 % min
Hydrogen	For flame ignition	TIG	HP, 99.99%
Air Zero	For flame ignition	TIG	N/A
Helium	Carrier gas for GC (TCD detector)	TIG	UHP, 99.999%

* Thai Industrial Gases Co., Ltd.

4.2 Experimental setup

Figure 4.1 shows the actual arrangement of the experimental apparatus of the gaseous pollutant remover used in the present work. **Figure 4.2** presents its schematic diagram.

Figure 4.1 Arrangement of present experimental apparatus

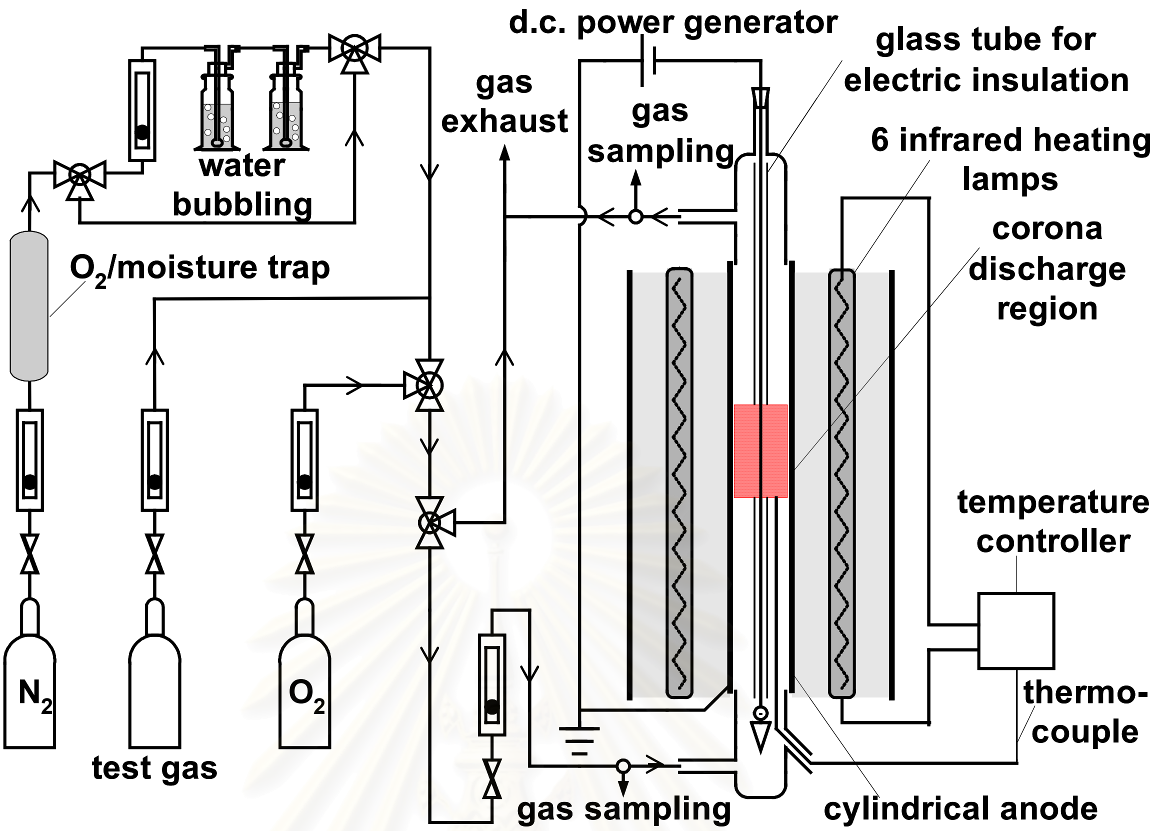

Figure 4.2 Schematic diagram of experimental apparatus

4.2.1 Details of the experimental apparatus

Figure 4.1 and **Figure 4.2** show the photograph and the schematic diagram of the experimental setup which consists of a deposition-type corona-discharge reactor, a high-voltage DC generator, a temperature controller and a test gas mixing system.

The deposition-type corona-discharge reactor is shown in **Figure 4.3**. It consists of a SUS tube, 3.7 cm. inner diameter and 80 cm. length, as the anode. The cathode is a 0.5-mm stainless-steel wire suspended from a silicone plug at the top of the reactor and straightened along the axis of the vertical anode by a small weight. The reactor cathode is connected to a high-voltage DC generator (Matsusada, HAR-30N5). The high-voltage DC generator whose maximum allowable voltage is 50 kV is utilized to supply a steady stream of low-energy electrons to the corona-discharge reactor. **Figure 4.4** shows the high-voltage DC generator adopted in this work. A slim pyrex glass tube is used to sheath either end of the cathode in order to limit the corona discharge zone to an effective length of 10 cm in the middle section of the reactor. In this way the discharge zone is restricted to the region from 10-20 cm above the mid-length of the reactor to utilize a more nearly uniform axial temperature distribution within the discharge zone. A type-K thermocouple is inserted into the reactor to measure the gas temperature in the discharge zone. To control the reactor temperature, 6 infrared heating lamps (200V, 700W each) are installed lengthwise around the outside perimeter of the reactor. The temperature control unit consists of a temperature controller (FENWAL, AR-24L) and a thyrister power regulator (Shimaden, PAC15C003081-NO).

The desired concentrations of acetaldehyde, ammonia, trimethylamine and/or coexisting O_2 are adjusted by diluting standard gases with pure N_2 carrier gas. An additional O_2/moisture trap is installed on the N_2 gas line to ensure the removal of trace O_2 and moisture in the carrier and diluent gas. To study the influence of water vapor on the removal efficiency, the desired concentration of water vapor is achieved by bubbling nitrogen gas through distilled water in the bottle placed in temperature-controlled bath.

Figure 4.3 Deposition-type corona discharge reactor

Figure 4.4 High-voltage DC generator

4.2.2 Analytical Instrument

Inlet and outlet concentrations of styrene, acetaldehyde (CH_3CHO) and trimethylamine in gas mixture are analyzed using a gas chromatograph (Shimadzu Corp., GC 9A) equipped with a flame ionization detector (FID). The packed material in the GC column used for separating the peak of acetaldehyde and trimethylamine is Polydivinylbenzene (Millopor Corp., Porapak Q) with 60/80 mesh size and usable at maximum temperature of 250º C. A calibration curve between the FID peak area of the GC and the concentration of acetaldehyde (CH_3CHO) and trimethylamine is obtained as shown in the Appendix A.

Figure 4.5 FID-Gas chromatograph

Concentrations of NH_3 are analyzed using another gas chromatograph (Shimadzu Corp., GC 14B) equipped with a thermal conductivity detector (TCD). The packed material in the GC column is Chromosorb 103 with 80/100 mesh size and usable at maximum temperature of 230 °C. A calibration curve between the TCD peak area of the GC and the concentration of ammonia is obtained as shown in the Appendix A.

Figure 4.6 TCD-Gas chromatograph

The concentrations of byproduct O_3 and/or NO_x can separately be detected with appropriate gas detector tubes (GASTEC Co., Ltd. and Kitagawa Co., Ltd.). NH_3 can also be detected and double-checked by detector tubes. Compare to the GC method, the detector-tube measurements were found to differ by less 12%.

Table 4.2 Operating conditions of FID gas chromatograph

Sample gas	Column temperature (^oC)	Injection temperature (^oC)	Detector temperature (^oC)	Retention time (min)
CH_3CHO	190	200	200	2.3
$(CH_3)_3N$	190	200	200	5.4

Table 4.3 Operating conditions of TCD gas chromatograph

Sample gas	Column temperature (^oC)	Injection temperature (^oC)	Detector temperature (^oC)	TCD temperature (^oC)	Retention time (min)
NH_3	50	100	100	110	2.3

4.3 Experimental procedure

To carry out the gaseous pollutant removal experiments, the following implementation steps must be carried out carefully because of the high risk of physical injury caused by the high voltage supplied to the reactor.

a. Ensure that the reactor is securely grounded and each unit of the experimental apparatus is also securely connected.
b. Check the gas line for the experiment (feed gas balance nitrogen, O_2 and N_2 for water bubbling)
c. Mix the above streams in the gas mixing device and measure the total flow rate with the soap film flow meter.
d. Feed the gas mixture to the inlet of the reactor and wait until its inlet and outlet concentrations become stable at the reactor temperature of interest.
e. Take gas samples at the reactor inlet and outlet to analyze their concentrations during blank test (zero discharge current).

f. Turn on the high-voltage DC generator, adjust the discharge current as desired, and then keep the current stable throughout each experimental run.
g. Take gas samples at the inlet and outlet of the reactor and analyze their concentrations. Shut off the current after the finish of the experimental run.
h. To study the effect of the reactor temperature, reset the temperature as desired and wait until it becomes stable. Return to step (e) until all reactor temperatures have been investigated.
i. Wait for the reactor temperature to cool down sufficiently, stop the flow of the gas mixture and turn off the DC generator after the completion of the experiment. Be careful that high voltage does not remain in the reactor.

CHAPTER V

RESULTS AND DISCUSSION

5.1 Definition of removal efficiency

This section describes the various definitions of the removal efficiency.

5.1.1 Apparent removal efficiency

$$\psi = \frac{(C_{in} - C_{out,anymA})}{C_{in}} \quad [-] \qquad (5.1)$$

5.1.2 Removal efficiency (by discharge effect only)

$$\psi' = \frac{(C_{out,0\,mA} - C_{out\ at\ any\ mA})}{C_{out,0\,mA}} \quad [-] \qquad (5.2)$$

In this definition, ψ represents the sole effect of corona discharge and excludes any effect of possible low-temperature adsorption and thermal decomposition inside the reactor system.

5.1.3 Removal efficiency per unit residence time

$$\psi'' = \frac{\psi' \times residence\ \ time\ \ at\ 25\ {}^{0}C}{residence\ \ time\ \ at\ T\ {}^{0}C} \qquad (5.3)$$

At steady state, the equation of continuity requires that $\rho_1 \langle \upsilon_1 \rangle A_1 = \rho_2 \langle \upsilon_2 \rangle A_2$. Since $A_1 = A_2$ and ρ is a function of the gas temperature, the gas velocity at temperature T_2 will be faster than its velocity at room temperature T_1. Thus the mean residence time $\theta_2 = \frac{V_r}{\langle \upsilon_2 \rangle A_2}$ of this gas at T_2 is shorter than $\theta_1 = \frac{V_r}{\langle \upsilon_1 \rangle A_1}$ at room temperature. Here V_r is the effective volume of the corona discharge reactor. The removal efficiency per unit residence time is defined so as to take into account the effect of shortened residence time on the observed removal efficiency as the reactor temperature is increased.

5.1.3 Electron-based efficiency

$$\psi_{elec} = \frac{N_r}{N_{e0}} \tag{5.4}$$

The electron-based efficiency ψ_{elec} (-) is defined as the number of gas molecules removed by one discharged electron.

5.1.4 Energy-based efficiency

The energy-based efficiency ψ_{ener} (mol gas .J^{-1}) is defined as the mole of gas removed per energy consumption (J), as in Eq.(5.5).

$$\psi_{ener} = \frac{(q_{out,0\,mA} - q_{out\ at\ any\ mA})}{P} \tag{5.5}$$

where $q_{out,\ 0\ mA}$, $q_{out\ at\ any\ mA}$, P are the molar flow rate of the target gases at the reactor outlet when using zero current, the molar flow rate of the target gases at the reactor outlet when using non-zero current and the power consumption, respectively.

5.2 Influence of temperature

5.2.1 Influence of temperature on electron energy

The voltages required to generate corona discharge are measured at different gas temperatures. From the experimental results, the voltages required to generate 0.5 mA in the removal of 600 ppm CH_3CHO, 400 ppm NH_3, and 400 ppm $(CH_3)_3N$ from N_2 are, respectively, 14.3, 9.2 and 10.1 kV at room temperature, and these voltages decrease to 5.3 , 4.6 and 5.1 kV, respectively, as temperature rises to 300°C. These voltages are approximately 30% higher when the target gases are removed from N_2-O_2 mixture. Their values correspond to the profile changes in the electric field strength, E, inside the reactor. Meanwhile the gas temperature also affects the gas density, N. Thus it is important to note that the electron energy corresponds to the electric field strength divided by the gas density, E/N. To approximate E/N, the electric field strength described as Eq. (5.6) is used.

$$E = V / \{ r \ln (D_1/D_o) \} \tag{5.6}$$

V, r, D_1, D_o are the applied voltage, radial distance from the cylindrical axis, inner diameter of the cylindrical anode, and diameter of the wire cathode, respectively. Thus, the mean E/N is approximated by Eq. (5.7) (Tanthapanichakoon et al. 1998).

$$\langle E/N \rangle = \frac{\int_{D_0/2}^{D_1/2} (2\pi r)(E/N)\, \mathrm{d}r}{\pi \left((D_1/2)^2 - (D_0/2)^2 \right)} = \frac{4V}{N(D_1 + D_0)\ln(D_1/D_0)} \tag{5.7}$$

N is calculated as $p/\{\mathrm{R}(273+T)\}$, where p, R, T are total pressure, gas constant, and gas temperature, respectively. From this correlation, the average

<*E*/*N*> in our case is 7.0 kV m^2 mol^{-1} and 5.8 kV m^2 mol^{-1} at room temperature and 300 °C, respectively. *E* positively affects the electron energy because the electrons emitted by the corona discharge are accelerated by *E*. On the other hand, *N* negatively affects the electron energy because the frequency of collisions between electrons and gas molecules becomes higher as *N* increases. In the case of toluene removal at high temperatures, there exists a general tendency that <*E*/*N*>, the averaged value of E/N across a cross section of the reactor, in both N_2 and air decreases with temperature in the high temperature range (Dhattavorn, 2000). A similar tendency is also observed for the present cases of CH_3CHO, NH_3 and $(CH_3)_3N$. This is primarily caused by a decrease in the required voltage associated with the temperature elevation. This voltage drop associated with temperature elevation may be explained as follows: (1) The voltage required for 'corona discharge breakdown' which initiates ionization around the cathode is inversely proportional to the reactor temperature (Uhm, 1999). (2) Gas heating leads to more frequent electron detachment and decomposition of ion clusters that release the electron component so that the effective mobility of negative charges in the gas becomes high (Mnatsakanyan et al., 1987). (3) Gas expansion results in a longer mean free path of charged particles (Uhm, 1999). In spite of the voltage drop associated with the temperature elevation, if the negative thinning effect of gas expansion on *N* is relatively more significant than that of the temperature-induced voltage drop, the temperature dependency of <*E*/*N*> may become reversed. This phenomenon is often observed when *T* is below 200°C in N_2.

Since the electric field strength decreases only slightly when the temperature is elevated, the electron energy at 300 °C turns out to be approximately 17% lower than at room temperature. Generally, the electron energy level should affect the reaction mechanism. For example, electron attachment tends to occur when electron energy is relatively low (Massey, 1976; Moruzzi, 1966; Caledonia, 1975), while formation of radicals may take place when electron energy is very high.

5.2.2 Influence of temperature on removal mechanism

Rigorously speaking, the relevant reactions contributing to the removal of CH_3CHO, NH_3 and $(CH_3)_3N$ are affected not only by the change in electron energy level but also by other effects of the elevated temperature. To consider the reaction mechanism, one must take byproduct formation into account. As for the gaseous byproducts, O_3 and NO_x were respectively detected mainly in the low and high temperature ranges. In fact, the measurements of O_3 concentration during the removal of toluene from N_2-O_2 mixture reveal that O_3 is produced up to 1370 ppm at room temperature but it rapidly drops down to 430 ppm at 100 ^{o}C. When T is further increased above 300 ^{o}C, O_3 concentration becomes negligible (Dhattavorn, 2000). This is because O_3 is unstable at high temperature (Peyrous, Pignolet and Held, 1989; Devins, 1956). Therefore, oxidation by O_3 should play a negligible role in the high temperature range.

Contrary to O_3 formation, it is known that production of NO_x by the discharge process is favored at high temperature. This is also confirmed in our experiments. While the outlet concentration of NO_x was negligible at room temperature, its concentration gradually increased with temperature and reached 300 ppm at 400 ^{o}C. Since NO_x formation can be attributed to the reaction of discharge-induced N radicals with O_2 (Lowke and Morrow, 1995; Mukkavilli et al., 1988), N radicals should also contribute to the removal of styrene and/or NH_3 from both N_2 and air at high temperatures. In addition, in the removal from air, there should be the extra effect of O radicals produced by electron impact to O_2 and by O_3 decomposition (Peyrous et al., 1989; Loiseau et al., 1966; Hadj-Ziane et al.,1990). Therefore, the removal efficiency from air at high temperatures should be enhanced by O radicals, though O_3 oxidation is not effective. In fact Peyrous et al. (1989) simulated the concentrations of O_3 and O radicals in pulsed corona discharge in the presence of O_2, and showed that temperature elevation brings about higher O radical concentration and lower O_3.

When H_2O is present in the gas stream, H^-, OH^- and a few O^- anions are expected to be produced by dissociative electron attachment to H_2O molecules at low temperature (Massey, 1976; Moruzzi and Phelps, 1966). The selectivity for these ionic products should depend on the gas temperature and electron energy. At high temperature, electron detachment would become significant so that radicals of O, H, and OH may play a more important role than their anionic counterparts. These radicals are also expected to contribute to the removal of the target gases. More specifically, OH is believed to dissociate NH_3 to produce an aminogen radical (NH_2) and H_2O (Bityurin, Potapkin and Demisky, 2000).

In non-thermal corona discharge in the air at room temperature, electrons are sometimes captured by O_2 to form negative ions, O^-, O_2^-, O_3^-, and clusters via electron attachment. The reversed electron detachment process, however, becomes significant at high temperature, causing ion clusters to become unstable (Mnatsakanyan, Naydis and Solozobov, 1987). The previous articles indicate that the corona discharge reactor plays host to electron attachment reactions and relevant ion cluster formation at room temperature (Sano et al., 1997; Tamon, Sano and Okasaki, 1996). However, because of high temperature effects such as electron detachment and radical formation, electron attachment and ion clustering would be less and less important as the temperature rises.

In the case of NH_3 removal, the removed NH_3 was converted to needle-like bright crystal, which was observed inside the reactor and the gas line after it. It is reported (Sugimitsu, 1998) that NH_3 does not react with O_3 to directly form NH_4NO_3. Instead the following consecutive reactions are mentioned: $2\ NH_3 + 4\ O_3 = NH_4NO_2 + H_2O_2 + 4\ O_2$; $NH_4NO_2 + H_2O_2 = NH_4NO_3 + H_2O$. Our result is also consistent with published reports that NH_4NO_3 solid is produced by corona treatment of humid air containing NH_3 (Bityurin et al., 2000; Kanasawa et al., 1998; Urashima, Kim and Chang, 1999). The mechanism for NH_4NO_3 formation in the high temperature range is not clear but it may be considered that NH_3, H_2O and NO_x as well as N and H radicals could react to form NH_4NO_3.

5.3 Substantiation of ozone effect

When O_2 is present in N_2 or a gas mixture, it readily reacts with electrons of sufficient energy level. Electron attachment on O_2 has been reported in the literature (Morruzzi and Phelps, 1966; Massey, 1976; Rapp and Briglia, 1976; Chantry and Schulz, 1967)

$$O_2 + e^- \longrightarrow O_2^- \qquad (a)$$

$$O_2 + e^- \longrightarrow O + O^- \qquad (b)$$

Moruzzi and Phelps (1966) report that the reaction in Equation (a) occurs in the low electron energy range ($E/p < 1.5$ V.m^{-1}.Pa^{-1}). In contrast, the reaction in Equation (b) occurs in the higher electron energy range. Also in a corona-discharge reactor, the closer the electrons are to the cathode wire, the higher their energy level. When O_2 collides with a high-energy electron near the cathode wire in the corona-discharge reactor, production of O^- is expected as in Equation (b). Next O_3 is produced from the reaction of O^- with O_2 (Loiseau et al., 1994; Hadj-Zaine et al., 1992).

In short, not only O_2^- and O^- radicals but some ozone (O_3) is also produced. Since O_3 is very reactive, the ozonation reaction is used in some commercial devices for deodorization and sterilization. The same ozonation reaction as well as the oxidation reaction with O^- radicals is expected to contribute to the decomposition and removal of gas impurities in the present corona discharge reactor. The O^- radicals is also expected to contribute to the formation of ionic clusters and removal of the gas impurities.

To substantiate the role of the ozonation, two identical reactors are connected serially. **Figure 5.1** shows the experimental setup used to confirm the O_3 effect. N_2-O_2 mixture is supplied to the first reactor to produce O_3 by corona discharge. Then a gas impurity is mixed into the effluent stream from the first reactor, and the resulting mixture is introduced to the second reactor. No voltage is supplied to the second reactor, so there is no corona discharge in the second reactor, which only provides space for the reaction of ozone with the impurity. Then the change in the concentration of the impurity at the outlet of the second reactor is measured. The decrease in the outlet concentration from the second reactor gives the O_3 effect.

In the experiment shows the formation of O_3 from N_2-O_2 mixed gas (N_2 65 cc/min and O_2 5 cc/min.). In the first reactor, N_2-O_2 mixed gas is carried out at the discharge current 0.20 mA and the effluent stream is mixed with N_2 20 cc/min before feeding to the second reactor without discharge current. $[O_3]_{in}$ and $[O_3]_{out}$ of the second reactor are 700 ppm and 650 ppm, respectively. Next CH_3CHO (2000 ppm balanced with N_2) at 30 cc/min is mixed with N_2 70 cc/min before feeding in the second reactor. $[CH_3CHO]_{in}$ and $[CH_3CHO]_{out}$ are 600 ppm and 583 ppm, respectively. In contrast, when CH_3CHO (2000 ppm balanced with N_2) at 30cc/min is mixed with the N_2-O_2 effluent stream (N_2 65 cc/min and O_2 5 cc/min) from the first reactor at the discharge current 0.20 mA, the outlet concentration of CH_3CHO at the outlet of the second reactor is reduced from 600 ppm to 380 ppm. It can be confirmed that O_3 has an important role on CH_3CHO removal efficiency.

In addition, the effect of O_3 on the removal of $(CH_3)_3N$ also investigated as shown in appendix K. The results were the same as in the case of CH_3CHO. In the case of NH_3, O_3 also has an important role on the removal efficiency (Chaiyo, 2001).

5.4 Blank test for the investigation of the effect of temperature on acetaldehyde, ammonia and trimethylamine removal

The experimental results in the Appendix D-J show the result of the blank test for the investigation of temperature effect on acetaldehyde, ammonia and trimethylamine removal. Here the concentration of the target gases at the reactor outlet was measured at various temperatures in the absence of the discharge current. **Figure 5.2** shows the results of blank test for investigation of temperature effect on acetaldehyde (CH_3CHO) in N_2-O_2 mixture. It is found that the outlet concentration of CH_3CHO slightly decreases at 300 ^{o}C via the thermal decomposition. **Figure 5.3** shows the results of blank test for investigation of temperature effect on ammonia (NH_3) in N_2-O_2 mixture. There appeared a slight concentration drop at room temperature, which is considered to be due to physical adsorption inside the reactor. At moderate temperature**,** the effect of adsorption inside the reactor slightly increased as the reactor temperature increased. However, the outlet concentration of NH_3 again decreased at 300 ^{o}C**.** The reverse effect at this highest temperature may be attributed to the thermal decomposition. **Figure 5.4** shows the results of blank test for investigation of temperature effect on trimethylamine $(CH_3)_3N$ in N_2-O_2 mixture. It is found that the outlet concentration of $(CH_3)_3N$ decreases above 200 ^{o}C. The extraneous peaks were observed in the gas chromatogram of the effluent stream which is confirmed that thermal decomposition of $(CH_3)_3N$ may occur.

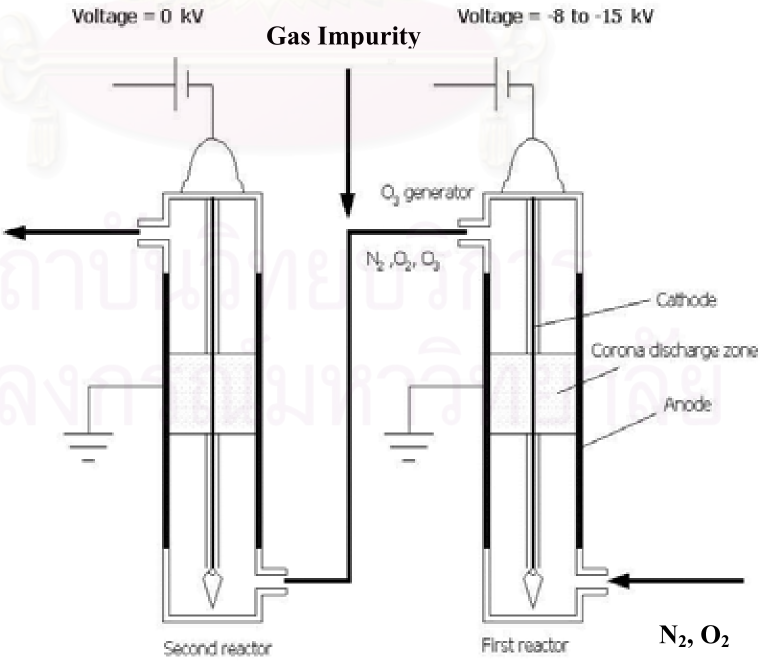

Figure 5.1 Apparatus to substantiate O_3 effect

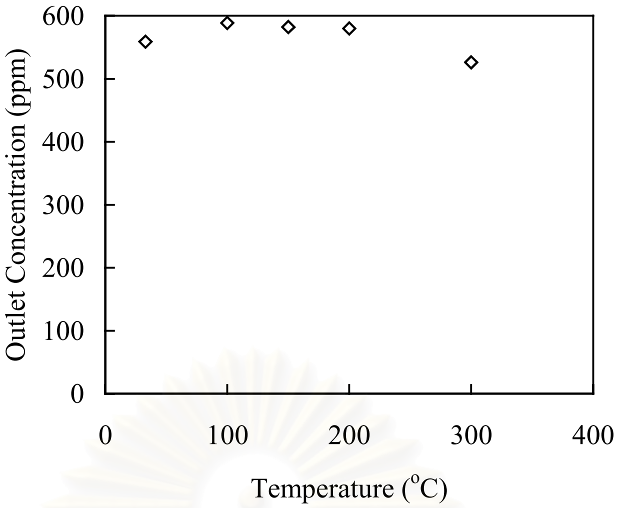

Figure 5.2 Blank test for the removal of CH_3CHO 600 ppm from N_2-O_2(10%)

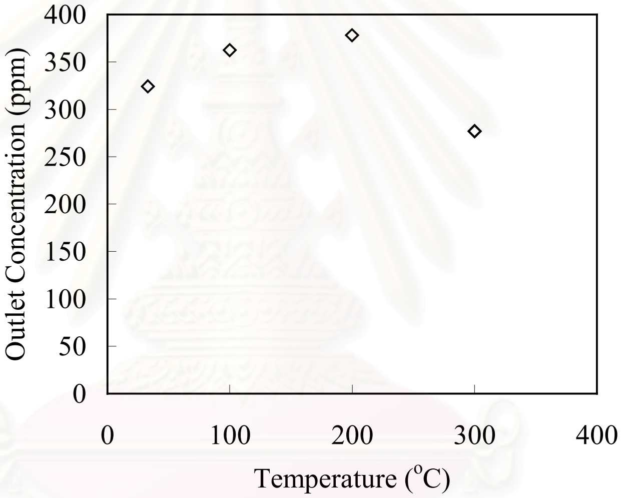

Figure 5.3 Blank test for the removal of NH_3 400 ppm from N_2-O_2(10%)

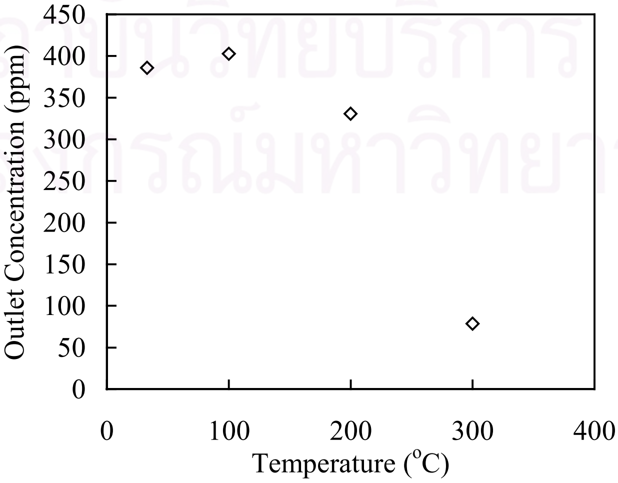

Figure 5.4 Blank test for the removal of $(CH_3)_3N$ 400 ppm from N_2-O_2(10%)

5.5 Removal of acetaldehyde (CH_3CHO)

5.5.1 Effect of temperature and inlet concentration on removal of CH_3CHO from N_2

Figure 5.5 shows the two kinds of the removal efficiency of CH_3CHO from pure N_2 at elevated temperatures. From **Figure 5.5(a),** we see that, as the temperature increases, the removal efficiency ψ' decreases starting from room temperature up to 200 °C, then the tendency reverses up to 300 °C because the mean residence time of the gas mixture inside the reactor decreases as the reactor temperature rises. This phenomenon is attributable to the fact that the gas mixture flows upward more quickly as its volume expands. **Figure 5.5(b)** reveals that when the negative effect of reduced residence time is taken in account, the value of ψ'' increases with temperature up to 150 °C.

At room temperature, ψ_{elec} of CH_3CHO at 200, 400, 600 ppm are 6.5, 12.5, 17.7, respectively. At 100, 200, 300 °C. the corresponding set of ψ_{elec} are (5.2, 9.6, 13.7), and (1.2, 1.7, 2.7), and (1.6, 2.3, 3.0). Interestingly, ψ_{elec} at 200 °C become lower than at 300 °C, thus indicating the possible existence of an optimal temperature. The high values of ψ_{elec} at low temperature reveal that the ion clusters may produce and these clusters increase when the inlet concentration increases. It has been reported that dissociative electron attachment of CH_3CHO may produce O^-, C_2O^-, HC_2O^-, CH_3CO^-, or CH_3^- (Dressler and Allan, 1985). The selectivity to produce these ions depends on the level of electron energy. However, at high temperature, electron detachment would become significant so that the positive effect of these ions is negated. Moreover, at high temperature, the rate of detachment of attached CH_3CHO molecules on the reactor wall is sufficiently enhanced by the lowered adsorption equilibrium to overcome the effect of electrostatic attraction, thus significantly reducing the net rate of CH_3CHO deposition on the wall.

Tamon et al. (1995) have found that the removal efficiency via electron attachment tends to decrease when the inlet concentration is increased. As expected, the present experimental results also exhibit the same tendency. The more dilute the inlet concentration, the higher the removal efficiency becomes because, when the discharged current is kept constant, the number ratio of the discharge electrons to the CH_3CHO molecules increases. The ratios of the discharge electrons to the molecules of CH_3CHO at 600, 400, 200 ppm at I=0.2 mA are, respectively, 0.05, 0.08 and 0.15 at room temperature which is consistent with the fact that the more dilute the inlet concentration, the higher the number ratio of the discharge electrons to the CH_3CHO molecules increases becomes.

5.5.2 Effect of temperature and coexisting O_2 on removal of CH_3CHO from N_2

In most actual applications of gas purification, other kinds of gas components often coexist. Therefore it is necessary to study the influence of common coexisting gases on the removal efficiency.

Figure 5.6 and **5.7** show the removal efficiency ψ' of CH_3CHO from N_2–O_2 when the acetaldehyde inlet concentration is 600 ppm. **Figure 5.6** shows the removal efficiency ψ' of CH_3CHO from N_2–O_2 at 0.2 mA, as temperature increases, the CH_3CHO removal efficiency ψ' remains nearly 100% from room temperature to 300 ^oC, except at 5% O_2 and 300^oC. To elucidate the effect of temperature, the discharge current is deliberately set at 0.05 mA as shown in **Figure 5.7.** It is found that the CH_3CHO removal efficiency ψ' increases with temperature up to 150 ^oC, at 5% O_2, and 200 ^oC, at 10% and 20% O_2, above which the tendency reverses up to 300 ^oC. This can be attributed to the fact that O_3 is produced from O_2 by the corona discharge reaction and is quite stable at room temperature. At room to moderate temperatures, electron attachment reactions contribute to, and relevant ion cluster formation enhances, the removal of numerous electro-negative compounds (Sano et al., 1997; Bityurin; 2000). Considered to be applicable to the removal of CH_3CHO, this mechanism is consistent with the observation that the biggest effect of coexisting O_2 is found at the highest concentration of 20% O_2. Contrary to O_3 formation, it is known that production of NO_x by the discharge process is favored at high temperature. This is also confirmed in our experiments. While the outlet concentration of NO_x was negligible at room temperature, its concentration gradually increased with temperature and reached 80 ppm at 300 ^{o}C. Since NO_x formation can be attributed to the reaction of discharge-induced N radicals with O_2 (Lowke and Morrow, 1995; Mukkavilli et al., 1988), N radicals should also contribute to the removal of CH_3CHO from both N_2 and air at high temperatures. In addition, in the removal from air, there should be the extra effect of O radicals produced by electron impact to O_2 and by O_3 decomposition (Peyrous, Pignolet and Held, 1989; Loiseau et al. 1994; Hadj-Ziane, 1990). Therefore, the CH_3CHO removal efficiency ψ' at high temperatures should be enhanced by O radicals though O_3 oxidation is not effective.

5.5.3 Effect of temperature and H_2O on removal of CH_3CHO from N_2

Figure 5.8 shows the removal efficiency ψ'' versus temperature. The values of ψ'' increases up to 200 ^{o}C, above which the tendency reverses up to 300 ^{o}C. **Figure 5.9** shows the removal efficiency ψ'' versus the concentration of H_2O. At low temperature, the effect of H_2O on the removal efficiency is not significant. At 200 ^{o}C, the presence of H_2O enhances the removal efficiency because, when H_2O is present in the gas stream, H^-, OH^- and a few O^- anions are expected to be produce by dissociative electron attachment to H_2O molecules (Massey 1976, Moruzzi and Phelps 1966). The selectivity for these ionic products should depend on the gas temperature and electron energy. At high temperature, electron detachment would become significant so that radicals of O, H, and OH may play a more important role than their anionic counterparts. These radicals are also expected to contribute to the removal of the target gases. As mentioned previously, NO_x formation can be attributed to the reaction of discharge-induced N radicals with O_2 (Lowke and Morrow, 1995; Mukkavilli et al., 1988), N radicals should also contribute to the removal of CH_3CHO from both N_2 and air at high temperatures. Since N radicals are consumed by their reaction with H_2O at high temperatures, the CH_3CHO removal efficiency at high temperatures decreases in the presence of H_2O.

5.5.4 Effect of temperature, coexisting O_2 and H_2O on removal of CH_3CHO from N_2

Experiments were carried out to observe the combined effect of O_2 and H_2O on the removal of CH_3CHO from N_2. **Figure 5.10** shows the two types of the removal efficiency ψ' and ψ'' of CH_3CHO from N_2-O_2 at various concentrations of H_2O. Again note that the discharge current in the case of pure N_2 is 4 times the case of N_2-O_2 mixture. When the reaction temperature is increased, the removal efficiency is found to increase starting from room temperature up to 200 ^{o}C, above which the tendency reverses up to 300 ^{o}C because less O_3 is generated from O_2 as temperature increases. As for the effect of H_2O, the presence of H_2O slightly retards the removal efficiency of CH_3CHO from N_2-O_2(20%) from room temperature to 300 ^{o}C because N radicals are consumed by their reaction with H_2O at high temperatures, the CH_3CHO removal efficiency at high temperatures decreases in the presence of H_2O.

5.5.5 Preliminary summary

Generally, two other types of removal efficiency are reported for a corona-discharge system. The electron-based efficiency ψ_{elec} (-) is defined as the number of gas molecules removed by one discharged electron, and the energy-based efficiency ψ_{ener} (mol gas .J^{-1}) is defined as the mole of gas removed per energy consumption (J). At 33, 100, 150, 200 and 300 °C, the experimental values of ψ_{elec} and ψ_{ener} of the CH_3CHO 600 ppm removal are as follows:

Pure N_2 (I = 0.2 mA) :

ψ_{elec} = 17.7, 13.7, 11.5, 2.6; 3.0 $\psi_{\text{ener}} \times 10^{-9}$ = 14.6, 14.3, 13.8, 3.9, 6.8

$N_2 – 20\% O_2$ (I = 0.05 mA):

ψ_{elec} = 50.3, 53.0, 48.7, 45.6, 29.5; $\psi_{\text{ener}} \times 10^{-9}$ = 47.9, 57.3, 58.7, 59.8, 46.4

N_2 – 21800 ppm H_2O (I = 0.2 mA):

ψ_{elec} = 18.7, 15.1, 12.7, 11.3, 2.8; $\psi_{\text{ener}} \times 10^{-9}$ = 15.1, 14.7, 14.3, 14.3, 7.0

N_2 – 21800 ppm H_2O – 20% O_2 (I = 0.2 mA):

ψ_{elec} = 53.9, 54.4, 51.3, 44.9, 25.7; $\psi_{\text{ener}} \times 10^{-9}$ = 50.8, 58.8, 61.1, 58.2, 41.0

In the absence of O_2, ψ_{elec} ranges from 17.7 at room temperature to 3.0 at 300 °C while ψ_{ener} ranges from 14.6×10^{-9} to 6.8×10^{-9}. In the presence of 20% O_2, ψ_{elec} and ψ_{ener} increases 2.8 - 9.8 folds and 3.3 – 6.8 folds, respectively, despite a 4-fold reduction in the discharge current compared to the case of pure N_2. The remarkable enhancement effect of O_2 can be attributed to the effect of O_3 and O^- anion at low temperatures and N and O radicals at high temperatures. Generally ψ_{elec} and ψ_{ener} tends to decrease as the gas temperature increases. This trend may be ascribed to the combined effect of reduced residence time and the shift in removal mechanism. Interestingly, in the case of pure N_2, ψ_{elec} and ψ_{ener} at 200 °C become lower than at 300 °C, thus indicating the possible existence of an optimal temperature.

In actual applications of gas purification, it is importance to consider the energy-based efficiency ψ_{ener}. From the above results, it is recommended to operate from 100 to 200 °C for minimizing the operating cost when air is purified because the values of ψ_{ener} are high.

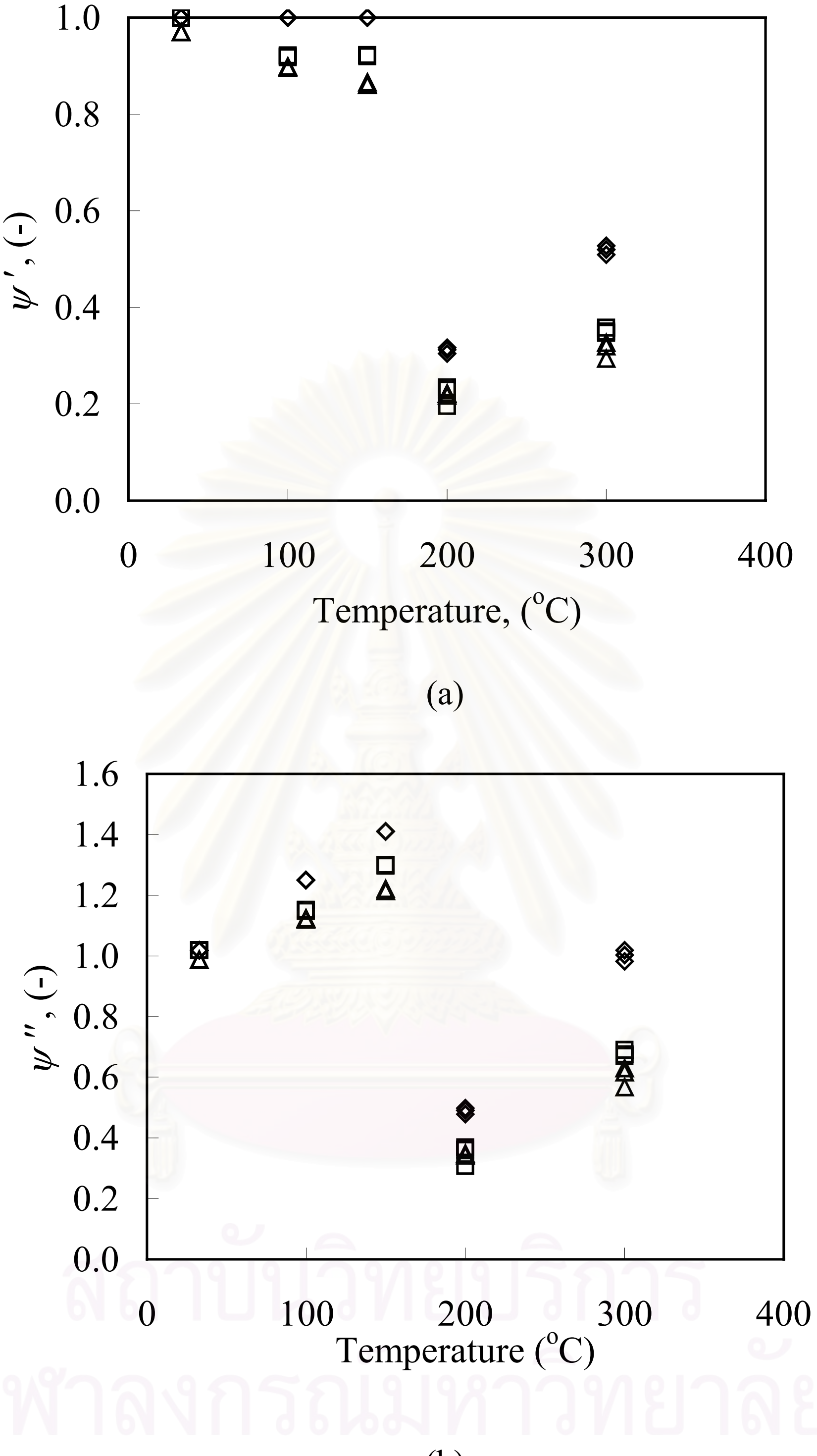

(a)

(b)

Figure 5.5 Effect of inlet concentration on the removal of CH_3CHO from N_2; I = 0.2 mA, SV = 55.8 hr^{-1} at room temperature : (◊) CH_3CHO 200 ppm, (□) CH_3CHO 400 ppm, (Δ) CH_3CHO 600 ppm

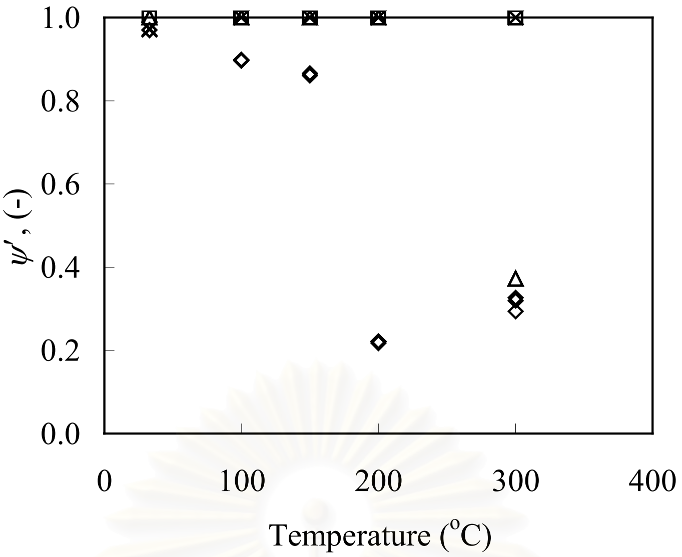

Figure 5.6 Effect of coexisting O_2 on the removal of CH_3CHO from N_2; $C_{in,\ acetaldehyde}$= 600 ppm, I = 0.2 mA, SV = 55.8 hr^{-1} at room temperature : (◊) O_2 0%, (Δ) O_2 5%, (□) O_2 10%, (×) O_2 20%

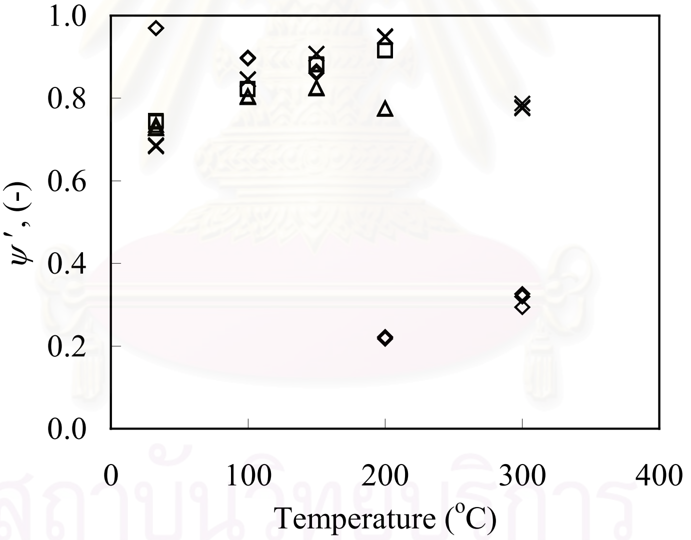

Figure 5.7 Effect of coexisting O_2 on the removal of CH_3CHO from N_2; $C_{in,\ acetaldehyde}$= 600 ppm, I = 0.05 mA, SV = 55.8 hr^{-1} at room temperature: (◊) O_2 0% I=0.2 mA, (Δ) O_2 5%, (□) O_2 10%, (×) O_2 20%

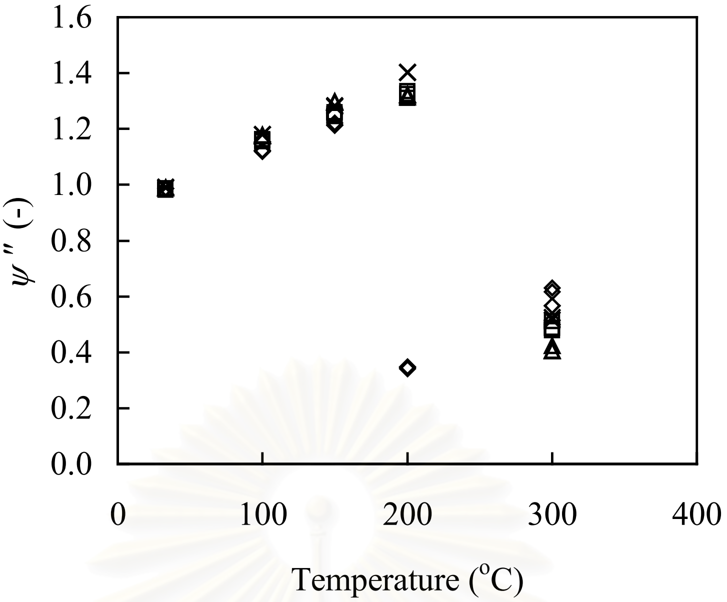

Figure 5.8 Effect of H_2O on the removal CH_3CHO from N_2; $C_{in,\ acetaldehyde}$= 600 ppm, I = 0.2 mA, SV = 55.8 hr^{-1} at room temperature: (◊) H_2O 0 ppm, (□) H_2O 5250 ppm, (Δ) H_2O 10500 ppm, (×) H_2O 21800 ppm

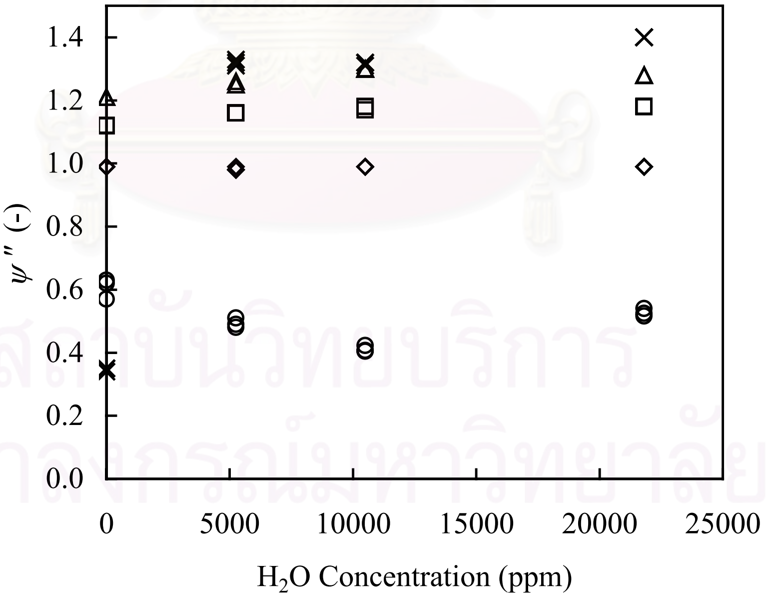

Figure 5.9 Effect of temperature on the removal CH_3CHO from N_2-H_2O; $C_{in,\ acetaldehyde}$= 600 ppm, I = 0.2 mA, SV = 55.8 hr^{-1} at room temperature: (◊) 33 °C, (□) 100 °C, (Δ)150 °C, (×)200 °C, (o)300 °C

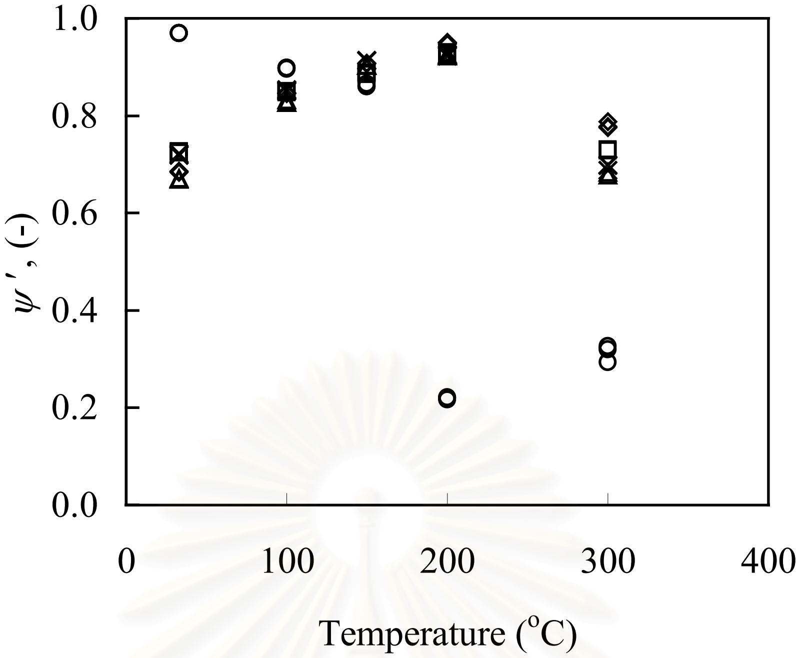

(a)

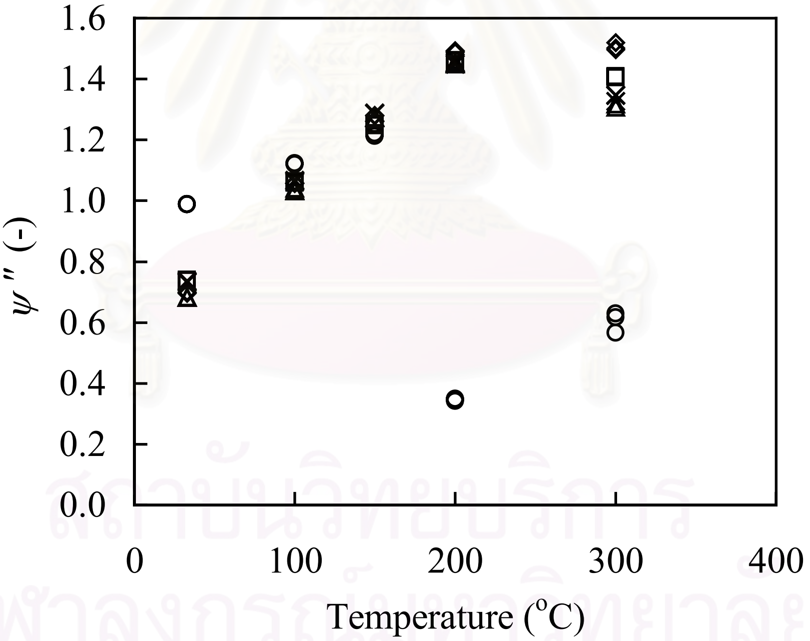

(b)

Figure 5.10 Effect of H_2O on the removal CH_3CHO from N_2-O_2(20%); $C_{in,\ acetaldehyde}$= 600 ppm, I = 0.05 mA, SV = 55.8 hr^{-1} at room temperature: (◊) H_2O 0 ppm, (□) H_2O 5250 ppm, (Δ) H_2O 10500 ppm, (×) H_2O 21800 ppm, (o) Pure N_2 I=0.2 mA

5.6 Removal of ammonia (NH_3)

5.6.1 Effect of temperature and inlet concentration on removal of NH_3 from N_2

Figure 5.11 shows the two kinds of the removal efficiency of NH_3 from pure N_2 at elevated temperatures. From **Figure 5.11(a)**, we see that, as the temperature increases, the removal efficiency ψ' increases monotonically from room temperature to 300 °C. **Figure 5.11(b)** reveals that when the negative effect of reduced residence time is taken in account, the value of ψ'' still increases with temperature. As mentioned in section 5.5, the present experimental results also exhibit the same tendency. The ratios of the discharge electrons to the molecules of NH_3 at 1000, 400, 250 ppm at I=0.5 mA are, respectively, 0.08, 0.19 and 0.31 at room temperature which is consistent with the fact that the more dilute the inlet concentration, the higher the removal efficiency becomes because, when the discharged current is kept constant, the number ratio of the discharge electrons to the NH_3 molecules increases (Tamon et al,1995).

5.6.2 Effect of temperature and coexisting O_2 on removal of NH_3 from N_2

Figure 5.12 shows the removal efficiency of NH_3 from N_2 at various concentrations of coexisting O_2 when the NH_3 inlet concentration is 400 ppm. As in the case of CH_3CHO, the presence of O_2 in N_2 greatly enhances the NH_3 removal efficiency despite the fact that the discharge current has been reduced fivefold to 0.1 mA, compare to the case of pure N_2 in the same figure. The effect of elevated temperature on ψ' and ψ'' is not straightforward but appears to depend on O_2 concentration. When the O_2 concentration is high at 10% and 20%, both ψ' and ψ'' are increases with temperature up to 100 and 200 °C, respectively, above which the tendency reverse up to 300 °C because of the unstable of O_3 at high temperature. In contrast, the NH_3 removal efficiency at lower O_2 concentration (5%) decreases with the temperature up to 300 ^{o}C because of less O_3 generated from O_2 compared to the cases of higher O_2 concentration. Moreover, the positive effect of various radicals at high temperature is negated by much reduced residence time.

5.6.3 Effect of temperature and H_2O on removal of NH_3 from N_2

Figure 5.13 shows the NH_3 removal efficiency from N_2 versus temperature at various concentrations of H_2O. From **Figure 5.13(a)**, we see that, as the temperature increases, the removal efficiency ψ' increases monotonically from room temperature to 300 ^{o}C. **Figure 5.13(b)** reveals that when the negative effect of reduced residence time is taken in account, the value of ψ'' still increases with temperature. At low to moderate temperatures, the presence of H_2O has slightly enhanced the removal efficiency because, when H_2O is present in the gas stream, H^-, OH^- and a few O^- anions are expected to be produced by dissociative electron attachment to H_2O molecules at low temperature (Massey 1976, Moruzzi and Phelps 1966). At 200 ^{o}C or more, electron detachment would become significant so that radicals of O, H, and OH may play a more important role than their anionic counterparts. More specifically, OH radical is believed to dissociate NH_3 to produce an aminogen radical (NH_2) and H_2O (Bityurin, Potapkin and Deminsky, 2000). This reversible reaction is, however, retarded by a big excess of the reaction product H_2O. Similarly, N and H radicals are produced from NH_3, especially at 300 ^{o}C. Since N and H radicals are considered to contribute more to the formation of NH_4NO_3, the high consumption of N radicals at 300 ^{o}C to form NO_x leads to the observed retardation effect. At 200 ^{o}C, fewer N radicals are consumed to form NO_x and, without excessive H_2O, the combined effect of N, H and OH radicals leads to the observed efficiency enhancement.

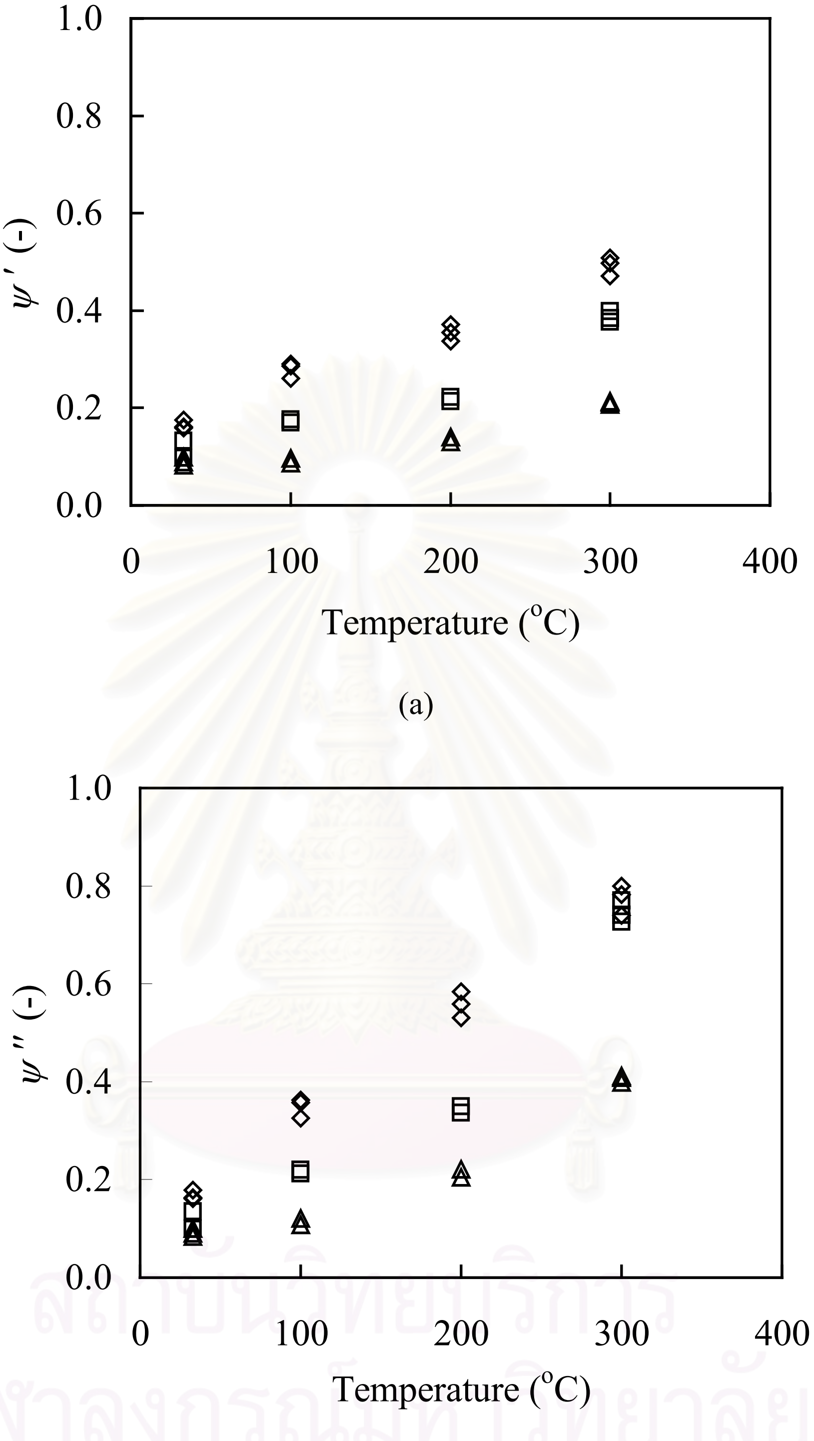

(a)

(b)

Figure 5.11 Effect of inlet concentration on the removal of NH_3 from N_2; I = 0.5 mA, SV = 55.8 hr^{-1} at room temperature: (◇) NH_3 250 ppm, (□) NH_3 400 ppm, (Δ) NH_3 1000 ppm

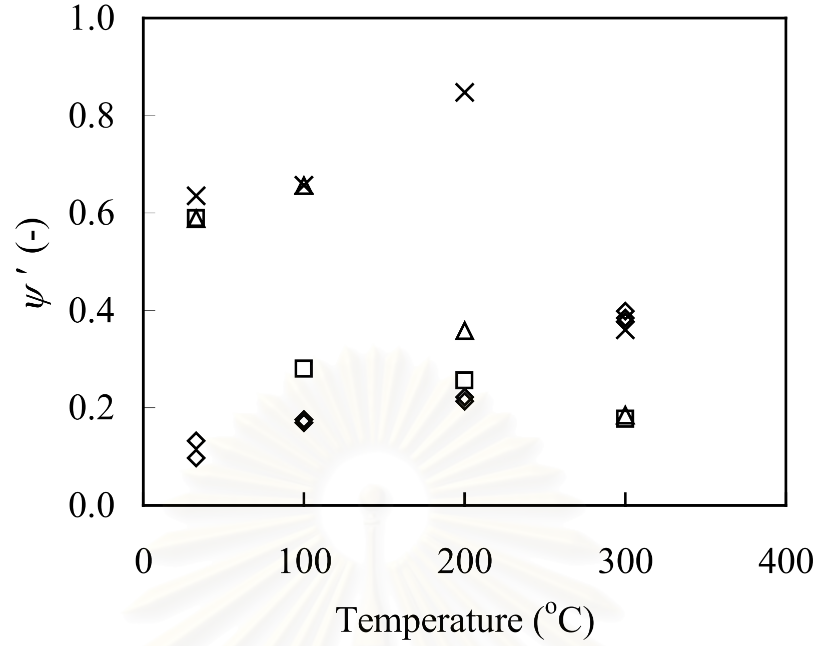

(a)

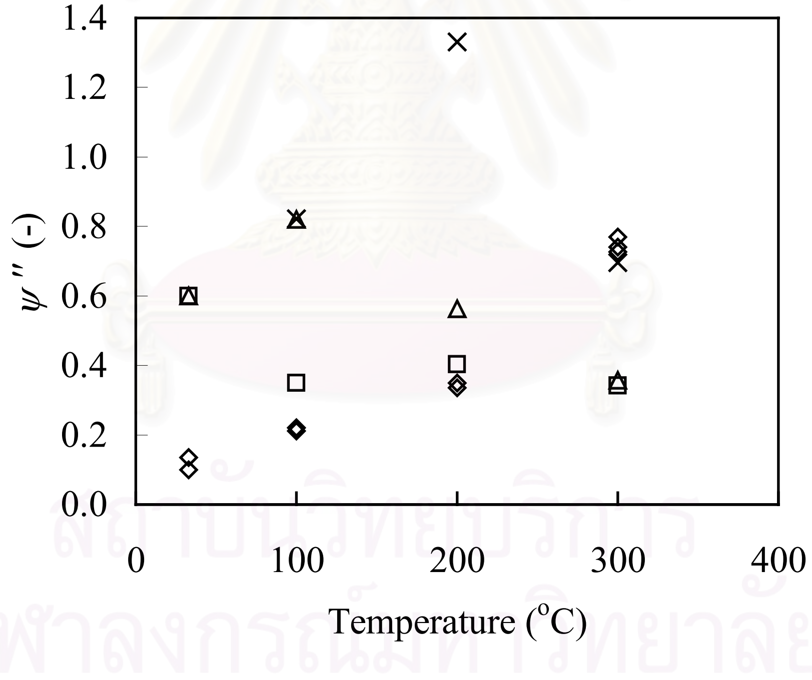

(b)

Figure 5.12 Effect of coexisting O_2 the removal of NH_3 from N_2; $C_{in,\ ammonia}$= 400 ppm, I = 0.1 mA, SV = 55.8 hr^{-1} at room temperature: (◇) O_2 0% I=0.5 mA, (□) O_2 5%, (Δ) O_2 10%, (×) O_2 20%

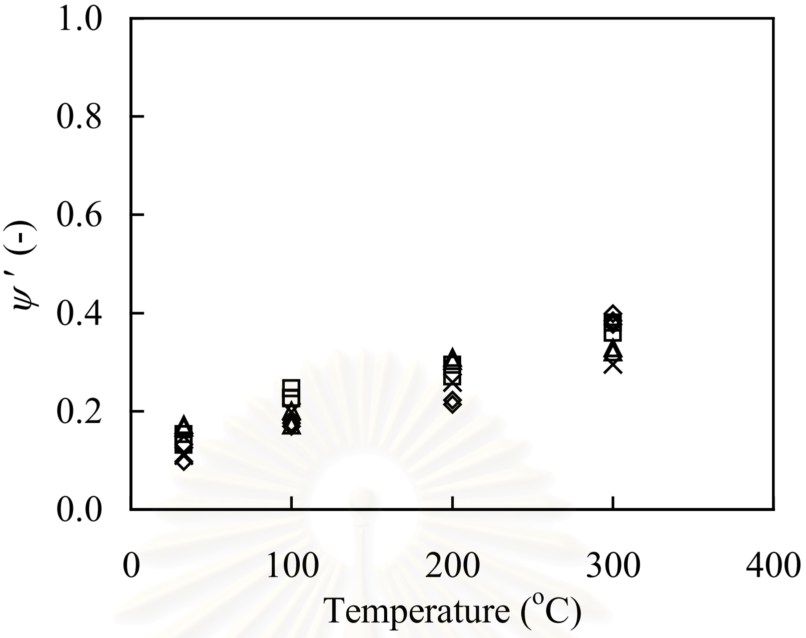

(a)

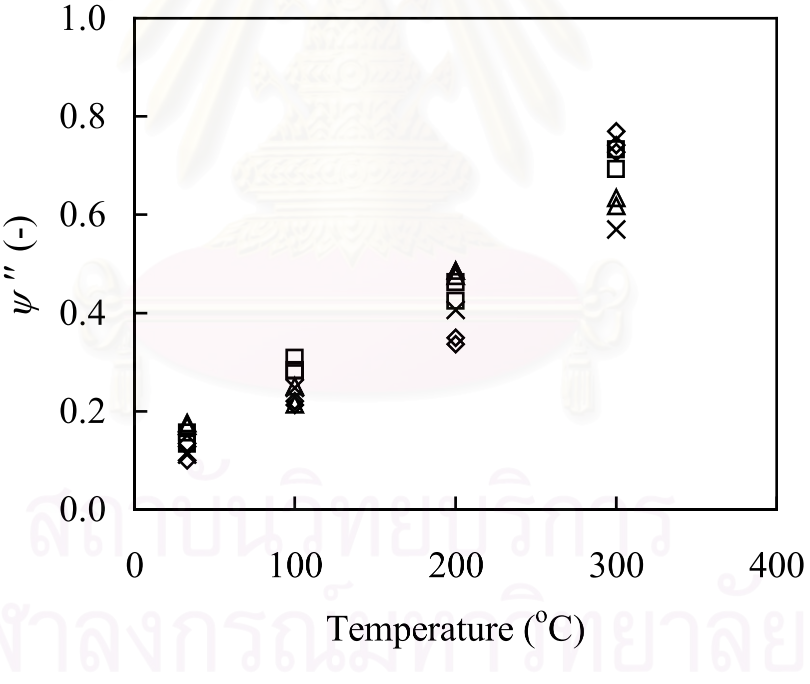

(b)

Figure 5.13 Effect of H_2O on the removal NH_3 from N_2; $C_{in,\ ammonia}$= 400 ppm, I = 0.5 mA, SV = 55.8 hr^{-1} at room temperature: : (◇) H_2O 0 ppm, (□) H_2O 5250 ppm, (Δ) H_2O 10500 ppm, (×) H_2O 21800 ppm

5.6.4 Effect of temperature and H_2O on removal of NH_3 from N_2-O_2

Figure 5.14 shows the two types of the removal efficiency ψ' and ψ'' of NH_3 from N_2-O_2 at various concentrations of H_2O. When the reaction temperature is increased, the removal efficiency is found to increase starting from room temperature up to 200 ^{o}C, above which the tendency reverses up to 300 ^{o}C because less O_3 is generated from O_2 as temperature increases. As for the effect of H_2O, H^-, OH^- and a few O^- anions should contribute to the removal of NH_3 from air at low to moderate temperatures. At 300 ^{o}C, the presence of H_2O slightly retards the removal efficiency of NH_3 from N_2-O_2 because at low discharge current, the relatively much smaller number of electrons tends to attach mostly to H_2O. In addition, N radicals are consumed by their reaction with H_2O at high temperatures.

5.6.5 Preliminary summary

Generally, two other types of removal efficiency are reported for a corona-discharge system. The electron-based efficiency ψ_{elec} (-) is defined as the number of gas molecules removed by one discharged electron, and the energy-based efficiency ψ_{ener} (mol gas .J^{-1}) is defined as the mole of gas removed per energy consumption (J). At 33, 100, 200 and 300 ^{o}C, the experimental values of ψ_{elec} and ψ_{ener} of the NH_3 400 ppm removal are as follows:

Pure N_2 (I = 0.5 mA) :

ψ_{elec} = 0.5, 0.7, 0.7, 1.0; $\psi_{\text{ener}} \times 10^{-9}$ = 0.5, 0.9, 1.1, 2.3

N_2 – 20% O_2 (I = 0.1 mA):

ψ_{elec} = 14.0, 12.6, 12.6, 4.2; $\psi_{\text{ener}} \times 10^{-9}$ = 12.8, 12.9, 15.6, 6.9

N_2 – 21800 ppm H_2O (I = 0.5 mA):

ψ_{elec} = 0.5, 0.8, 0.8, 0.7; $\psi_{\text{ener}} \times 10^{-9}$ = 0.5, 0.9, 1.3, 1.3

N_2 – 21800 ppm H_2O – 20% O_2 (I = 0.1 mA):

ψ_{elec} = 13.2, 15.3, 14.1, 4.5; ψ_{ener} x 10^{-9} = 11.9, 15.5, 17.0, 6.6

In the absence of O_2 , ψ_{elec} ranges from 0.5 at room temperature to 1.0 at 300 °C while ψ_{ener} ranges from 0.5 x 10^{-9} to 2.3 x 10^{-9}. In the presence of 20% O_2, ψ_{elec} and ψ_{ener} increases 28 – 4.2 folds and 25.6 – 3 folds, respectively, despite a 5-fold reduction in the discharge current compared to the case of pure N_2. The remarkable enhancement effect of O_2 can be attributed to the effect of O_3 and O^- anion at low temperatures and N and O radicals at high temperatures. Generally ψ_{elec} and ψ_{ener} tends to decrease as the gas temperature increases. This trend may be ascribed to the combined effect of reduced residence time and the shift in removal mechanism. Interestingly, in the case of pure N_2, ψ_{elec} and ψ_{ener} at 300 °C become higher than at room temperature. Moreover, in the case of pure N_2, the value of E/N at 300 °C is approximately 17% higher than at room temperature thus indicating the higher electron energy level should affect the reaction mechanism. For example, the formation of radicals may take place.

In actual applications of gas purification, it is importance to consider the energy-based efficiency ψ_{ener}. From the above results, it is recommended to operate at 200 °C for minimizing the operating cost when air is purified because the value of ψ_{ener} is highest. Compare to the case of the removal of CH_3CHO from air, ψ_{ener} of NH_3 at 200 °C is approximately 70% lower than in the case of CH_3CHO thus indicating the operating cost of the removal of NH_3 from air are lower than CH_3CHO.

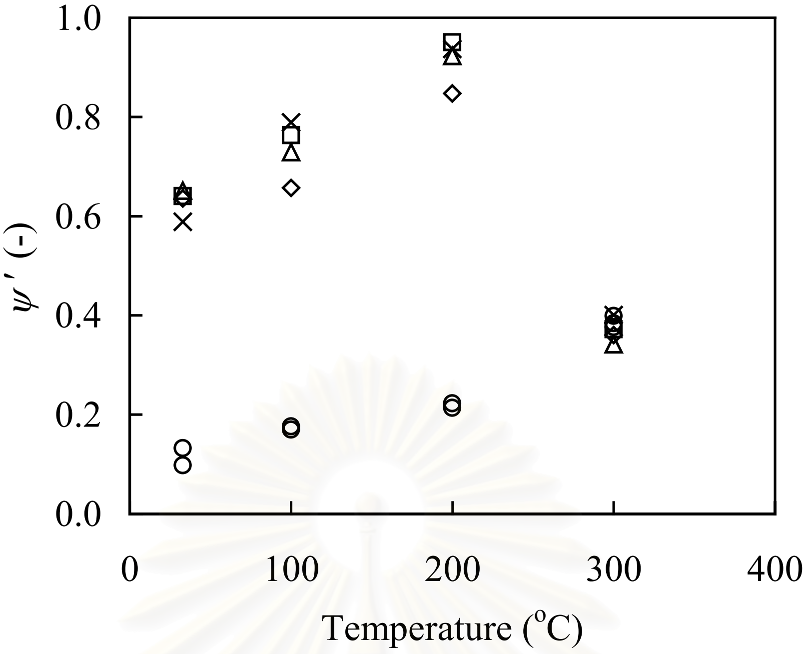

(a)

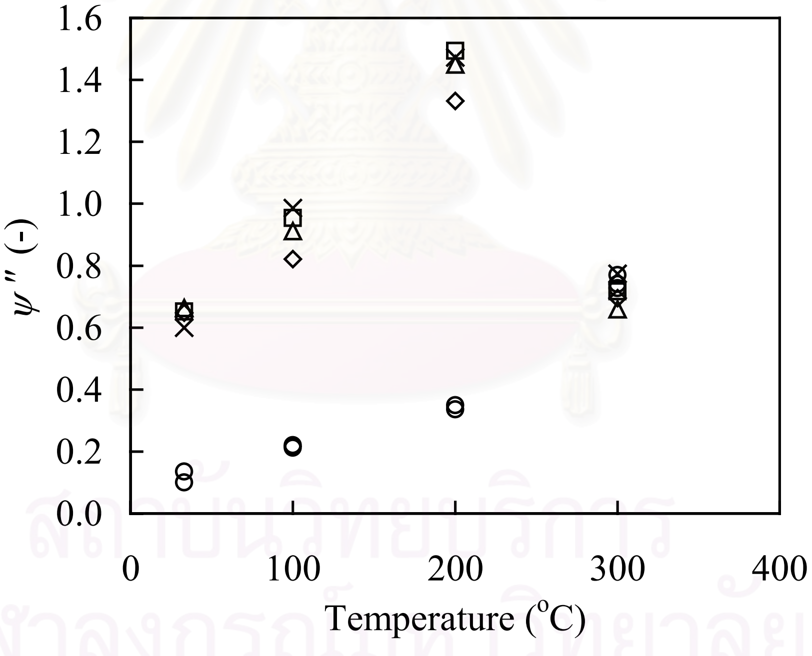

(b)

Figure 5.14 Effect of H_2O on the removal NH_3 from N_2-O_2(20%); $C_{in,\ ammonia}$= 400 ppm, I = 0.1 mA, SV = 55.8 hr^{-1} at room temperature: (◇) H_2O 0 ppm, (□) H_2O 5250 ppm, (Δ) H_2O 10500 ppm, (×) H_2O 21800 ppm, (o) Pure N_2

5.7 Removal of trimethylamine [$(CH_3)_3N$]

5.7.1 Effect of temperature and inlet concentration on removal of $(CH_3)_3N$ from N_2

Figure 5.15 shows the two kinds of the removal efficiency of $(CH_3)_3N$ from pure N_2 at elevated temperatures. From **Figure 5.15(a)**, we see that, as the temperature increases, the removal efficiency ψ' increases starting from room temperature up to 200 ^oC, then the tendency reverses up to 300 ^oC because the mean residence time of the gas mixture inside the reactor decreases as the reactor temperature rises. **Figure 5.15(b)** reveals that when the negative effect of reduced residence time is taken in account. The value of ψ'' increases monotonically with temperature.

As mentioned in section 5.5, the present experimental results also exhibit the same tendency. The ratios of the discharge electrons to the molecules of $(CH_3)_3N$ at 600, 400, 200 ppm at I=0.2 mA are, respectively, 0.05, 0.08 and 0.15 at room temperature which is consistent with the fact that the more dilute the inlet concentration, the higher the removal efficiency becomes because, when the discharged current is kept constant, the number ratio of the discharge electrons to the $(CH_3)_3N$ molecules increases (Tamon et al.,1995).

5.7.2 Effect of temperature and coexisting O_2 on removal of $(CH_3)_3N$ from N_2

Figure 5.16 shows the two kinds of the removal efficiency of CH_3CHO from N_2–O_2 when the $(CH_3)_3N$ inlet concentration is 400 ppm. It is found that the present of O_2 in N_2 always enhances the $(CH_3)_3N$ removal efficiency. When the reaction temperature is increased, the removal efficiency is found to increase starting from room temperature to 300 ^oC. As mentioned previously, the improved removal efficiency for $(CH_3)_3N$ can be attributed to effect of O_3

and O^- anion at low temperatures and various radicals at high temperatures. In addition, the reduction of $(CH_3)_3N$ concentration via the thermal decomposition about 80% at 300 ^oC may contribute to enhance the removal efficiency of $(CH_3)_3N$ because the number ratio of the discharge electrons to the $(CH_3)_3N$ molecules increases.

5.7.3 Effect of temperature and H_2O on removal of $(CH_3)_3N$ from N_2

Figure 5.17 shows the $(CH_3)_3N$ removal efficiency from N_2 versus temperature at various concentrations of H_2O. It is found that as the temperature increases, the values of ψ' and ψ'' increases starting from room temperature to 100 ^oC, then the tendency reverses up to 200 ^oC. Both ψ' and ψ'' increase again at 300 ^oC. For the effect of H_2O, H^-, OH^- and a few O^- anions should contribute to the removal of $(CH_3)_3N$ at low to moderate temperatures. At 200 ^oC, the presence of H_2O slightly retards the removal efficiency of $(CH_3)_3N$ because at low discharge current, the relatively much smaller number of electrons tend to attach mostly to H_2O. In addition, N radicals are consumed by their reaction with H_2O at high temperatures.

5.7.4 Effect of temperature and H_2O on removal of $(CH_3)_3N$ from N_2-O_2

Figure 5.18 shows the two types of the removal efficiency ψ' and ψ'' of $(CH_3)_3N$ from N_2-O_2(10%) at various concentrations of H_2O. It is found that the presence of O_2 and H_2O enhance the removal of $(CH_3)_3N$ from N_2. When the reaction temperature is increased, the removal efficiency is found to increase starting from room temperature up to 300 ^oC. As mentioned previously, the effect of H_2O, H^-, OH^- and a few O^- anions at low temperatures and various radicals at high temperatures should contribute to the removal of $(CH_3)_3N$. In addition, the reduction of $(CH_3)_3N$ concentration via the thermal decomposition at 300 °C may contribute to enhance the removal efficiency of $(CH_3)_3N$.

5.7.5 Preliminary summary

Generally, two other types of removal efficiency are reported for a corona-discharge system. The electron-based efficiency ψ_{elec} (-) is defined as the number of gas molecules removed by one discharged electron, and the energy-based efficiency ψ_{ener} (mol gas $.J^{-1}$) is defined as the mole of gas removed per energy consumption (J). At 33, 100, 200 and 300 °C, the experimental values of ψ_{elec} and ψ_{ener} of the $(CH_3)_3N$ 400 ppm removal are as follows:

Pure N_2 ($I = 0.2$ mA) :

ψ_{elec} = 2.3, 2.7, 4.3, 2.6; $\psi_{ener} \times 10^{-9}$ = 2.6, 3.3, 7.4, 5.5

N_2 – 20% O_2 ($I = 0.2$ mA):

ψ_{elec} = 11.5, 9.6, 6.2, 1.1; $\psi_{ener} \times 10^{-9}$ = 9.4, 9.0, 6.8, 1.6

N_2 – 21800 ppm H_2O ($I = 0.2$ mA):

ψ_{elec} = 2.4, 6.8, 2.4, 1.9; $\psi_{ener} \times 10^{-9}$ = 2.7, 7.6, 4.1, 4.5

N_2 – 21800 ppm H_2O – 20% O_2 ($I = 0.2$ mA):

ψ_{elec} = 7.8, 4.8, 4.1, 6.8 ; $\psi_{ener} \times 10^{-9}$ = 6.5, 4.4, 4.6, 9.8

Generally ψ_{elec} and ψ_{ener} tends to decrease as the gas temperature increases. This trend may be ascribed to the combined effect of reduced residence time and the shift in removal mechanism. Interestingly, in the presence of H_2O, ψ_{elec} and ψ_{ener} increases starting from room temperature up to 100 °C, then the tendency reverses up to 300 °C thus indicating the higher electron energy level should affect the reaction mechanism.

In actual applications of gas purification, it is importance to consider the energy-based efficiency ψ_{ener}. From the above results, it is recommended to operate at 300 ^{o}C for minimizing the operating cost when air is purified because the value of ψ_{ener} is highest. Compare to the case of the separately removal of CH_3CHO and NH_3 from air, the mean valueψ_{ener} of $(CH3)_3N$ is lower than in the case of CH_3CHO and NH_3 thus indicating the operating cost of the removal of $(CH3)_3N$ from air are lower than CH_3CHO and NH_3.

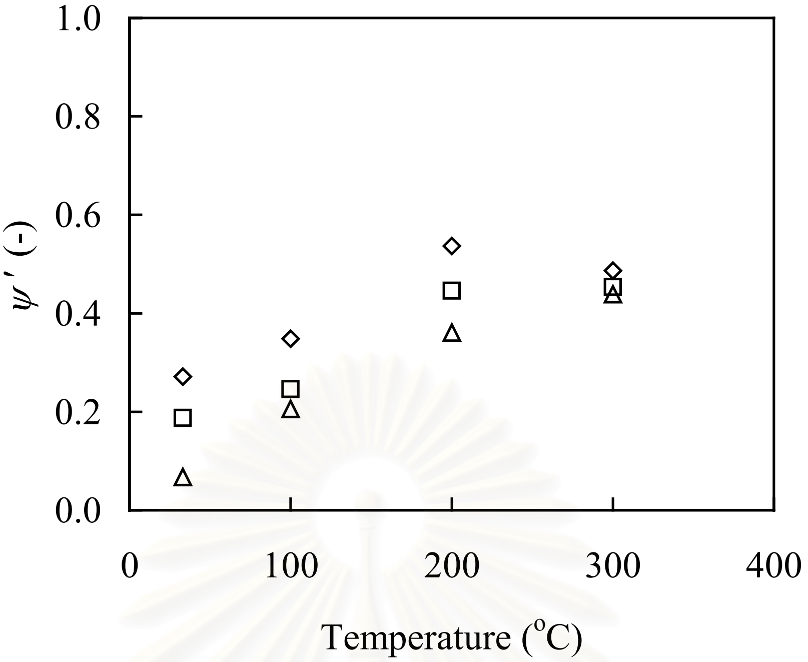

(a)

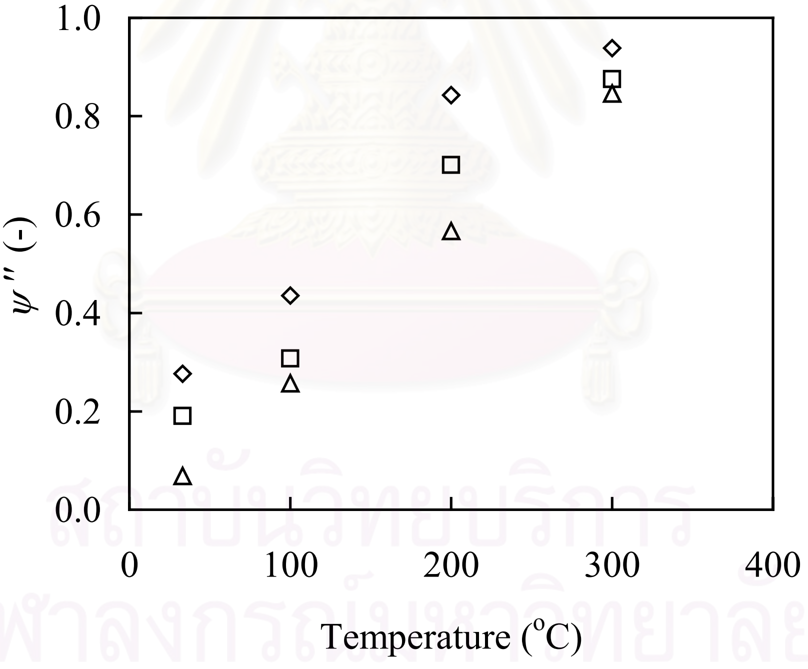

(b)

Figure 5.15 Effect of inlet concentration on the removal of $(CH_3)_3N$ from N_2; I = 0.2 mA, SV = 55.8 hr^{-1} at room temperature: (◇) $(CH_3)_3N$ 200 ppm, (□) $(CH_3)_3N$ 400 ppm, (Δ) $(CH_3)_3N$ 600 ppm

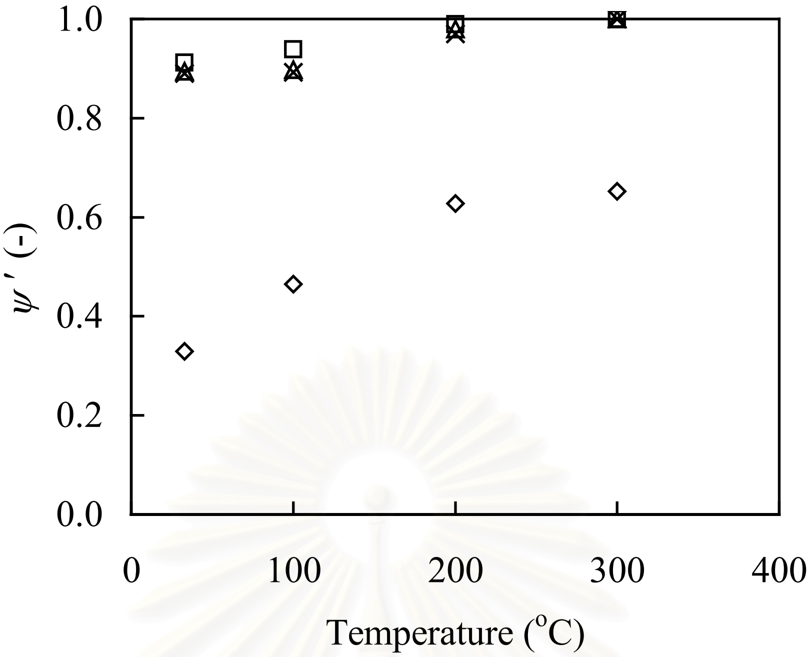

(a)

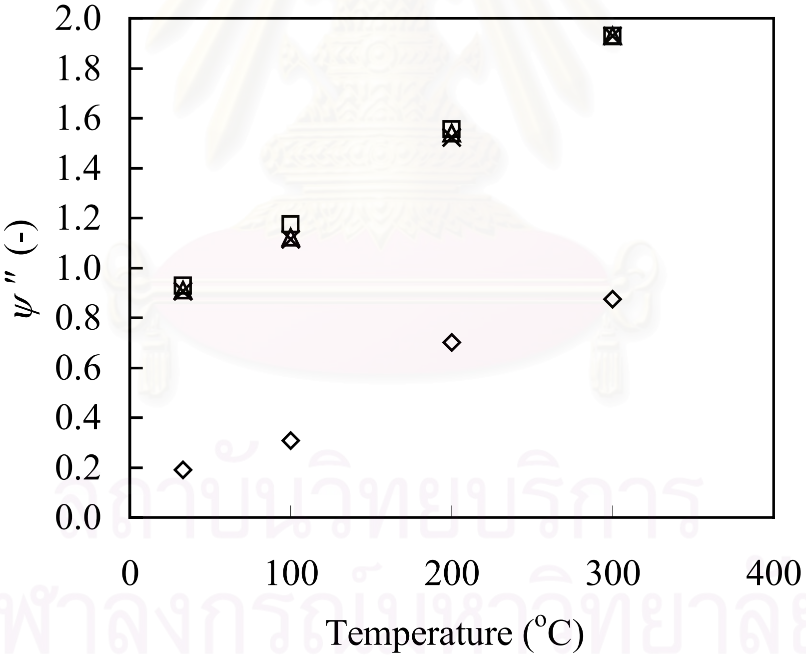

(b)

Figure 5.16 Effect of coexisting O_2 on the removal of $(CH_3)_3N$ from N_2; $C_{in,\ trimethylamine}$= 400 ppm, I = 0.2 mA, SV = 55.8 hr^{-1} at room temperature: (◇) O_2 0%, (□) O_2 10%, (Δ) O_2 15%, (×) O_2 20%

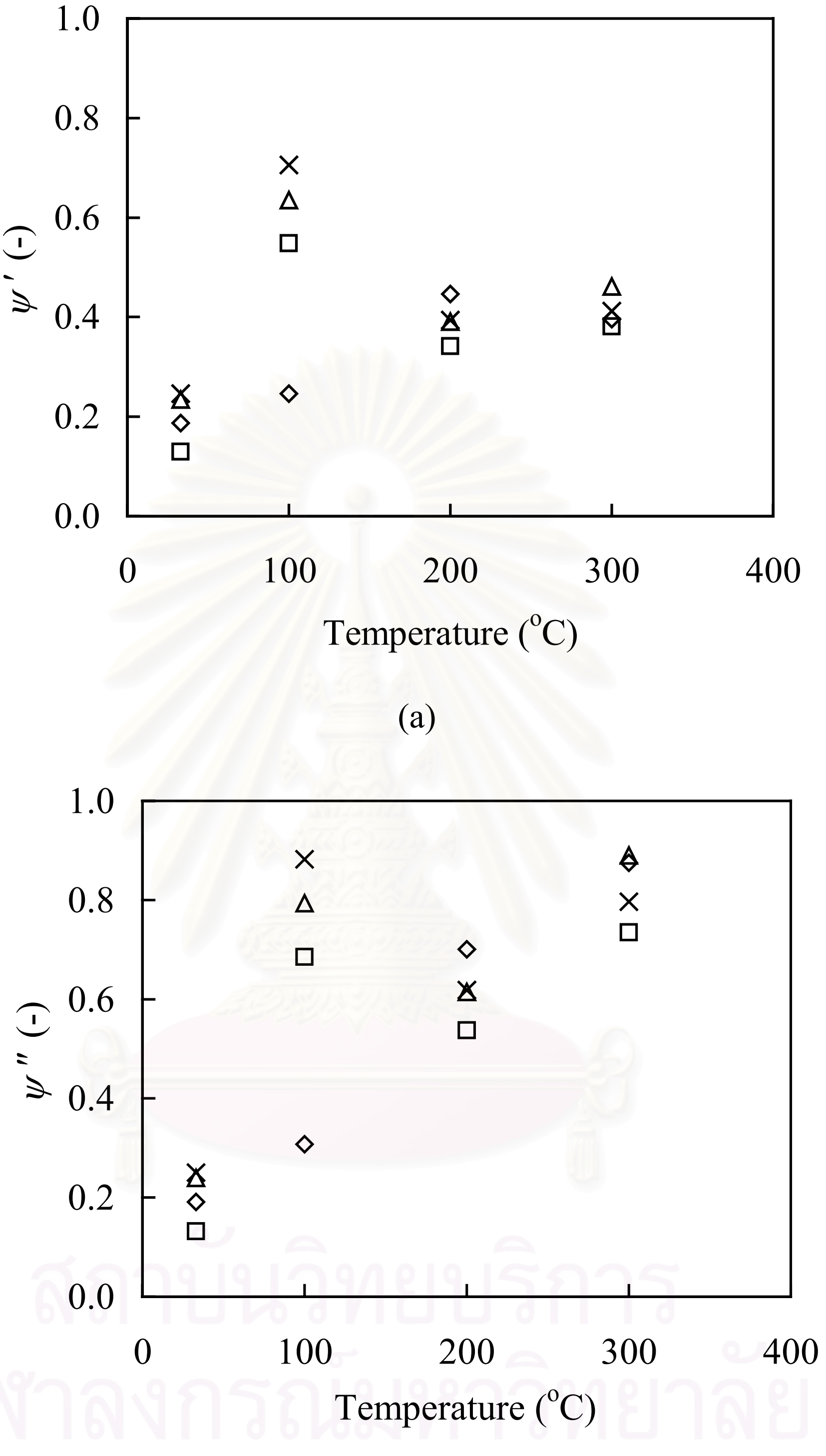

Figure 5.17 Effect of H_2O on the removal $(CH_3)_3N$ from N_2; $C_{in,\ trimethylamine}$= 400 ppm, I = 0.2 mA, SV = 55.8 hr^{-1} at room temperature: (◇) H_2O 0 ppm, (□) H_2O 5250 ppm, (Δ) H_2O 10500 ppm, (×) H_2O 21800 ppm

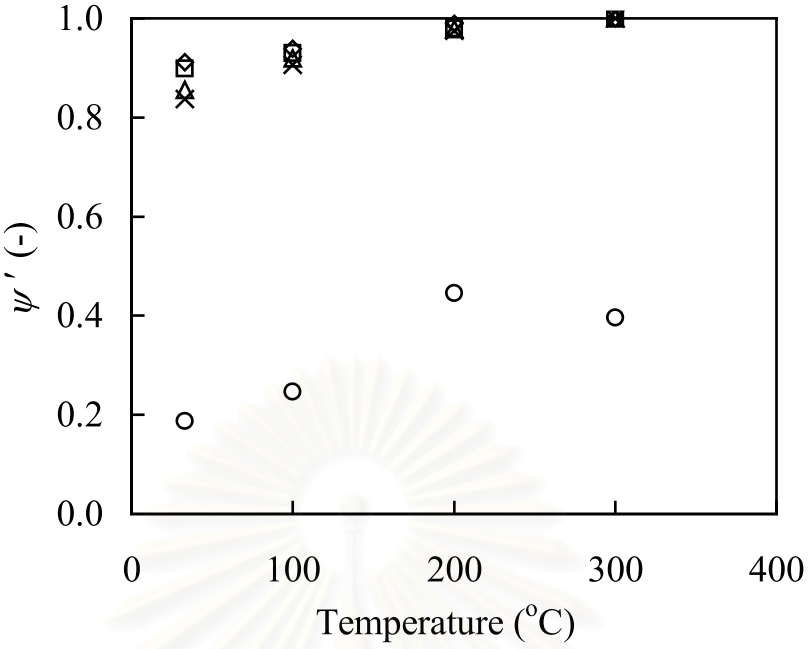

(a)

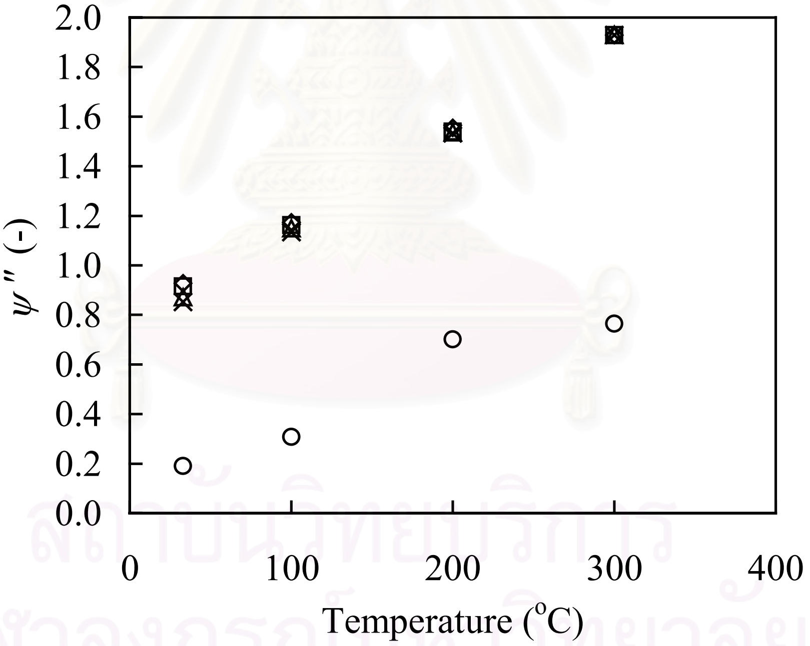

(b)

Figure 5.18 Effect of H_2O on the removal $(CH_3)_3N$ from N_2-O_2(10%); $C_{in,\ trimethylamine}$= 400 ppm, I = 0.2 mA, SV = 55.8 hr^{-1} at room temperature: (◇) H_2O 0 ppm, (□) H_2O 5250 ppm, (Δ) H_2O 10500 ppm, (×) H_2O 21800 ppm, (o) Pure N_2

5.8 Simultaneous removal of acetaldehyde and ammonia

5.8.1 Effect of temperature and coexisting O_2 on the simultaneous removal of CH_3CHO and NH_3 from N_2

Figure 5.19 shows the effect of O_2 on the simultaneous removal efficiency of CH_3CHO and NH_3 from N_2. The inlet concentration of CH_3CHO and NH_3 are 150 ppm and 1000 ppm, respectively, while the current is 0.3 mA. It is found that the presence of O_2 has a significant enhancement effect on the simultaneous CH_3CHO removal efficiency ψ' in **Figure 5.19(a)**. As temperature increases, the CH_3CHO removal efficiency remains nearly 100% from room temperature to 200 ^oC, above which the CH_3CHO removal efficiency tends to significantly decrease because of less O_3 generated from O_2 and reduction of the mean residence time of the gas mixture inside the reactor at high temperature. In **Figure 15.9(b),** at 20% O_2, the NH_3 removal efficiency increases with temperature up to 200 ^oC then dramatically decreases up to 300^oC. In contrast, the NH_3 removal efficiency at lower O_2 concentration (10%) decreases with the temperature up to 300 ^oC because of less O_3 generated from O_2 compared to the cases of higher O_2 concentration.

5.8.2 Effect of temperature and H_2O on the simultaneous removal of CH_3CHO and NH_3 from N_2-O_2

Figure 5.20 shows the combined effect of O_2 and H_2O on the simultaneous removal efficiency ψ' of CH_3CHO and NH_3. Compare to the case of only coexisting O_2, the simultaneous removal efficiency of both CH_3CHO and NH_3 is enhanced by the presence of H_2O. At high temperature, O_3 generated from O_2 and H^-, OH^- and a few O^- anions from H_2O are unstable. Couple with the negative effect of reduced residence time, the simultaneous removal efficiency of both CH_3CHO and NH_3 decreases significantly at 300 ^oC.

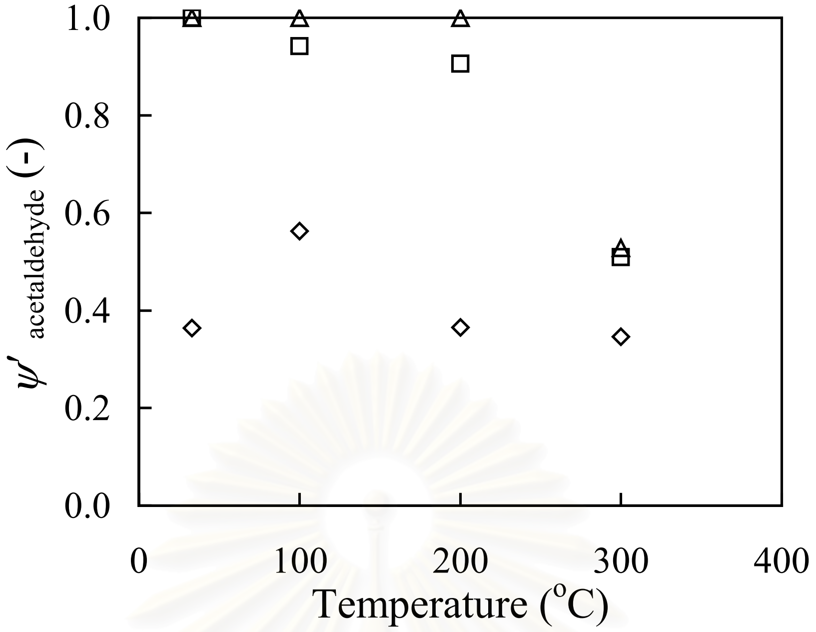

(a)

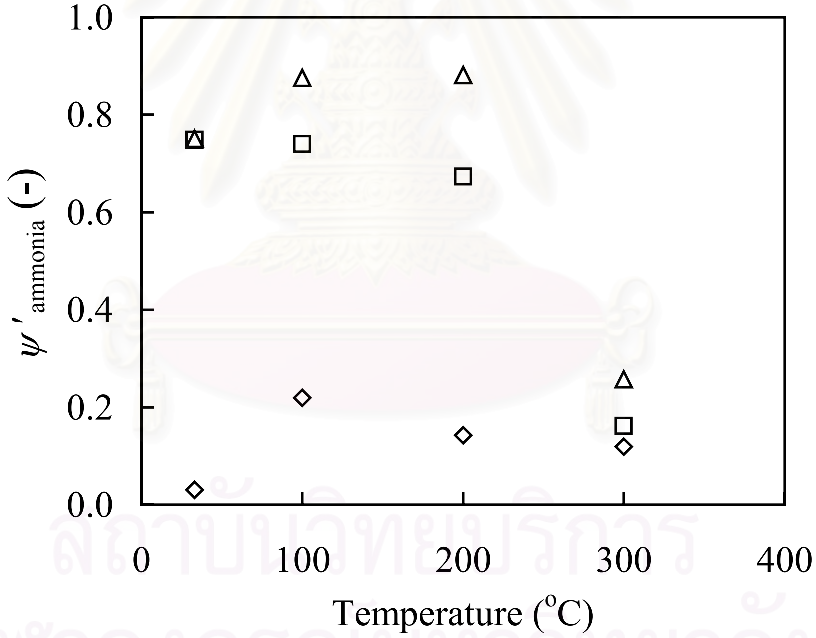

(b)

Figure 5.19 Effect of coexisting O_2 on the simultaneous removal of CH_3CHO and NH_3 from N_2; $C_{in,\ acetaldehyde}$= 150 ppm, $C_{in,\ ammonia}$ = 1000 ppm, I = 0.3 mA, SV = 55.8 hr^{-1} at room temperature: (◇) O_2 0%, (□) O_2 10%, (Δ) O_2 20%

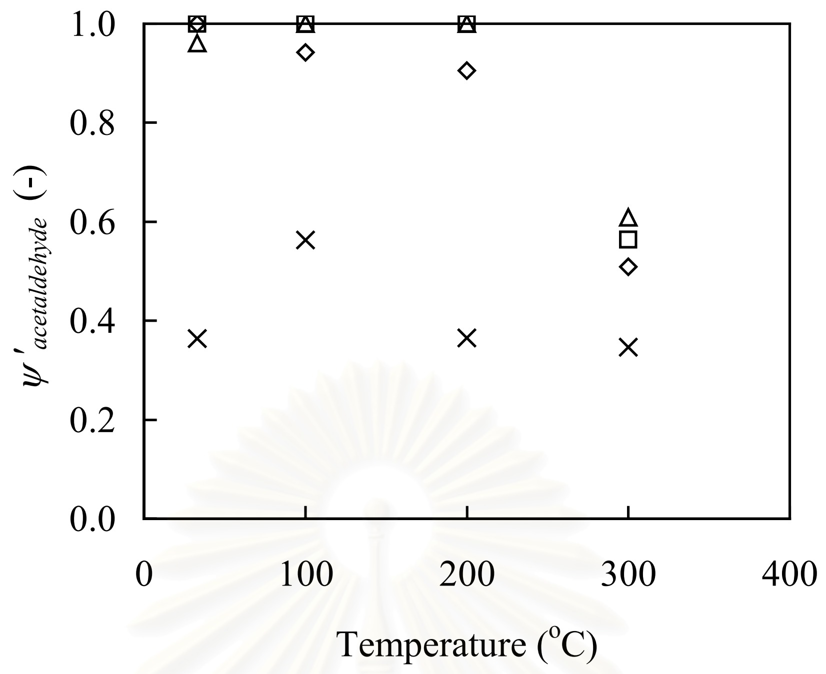

(a)

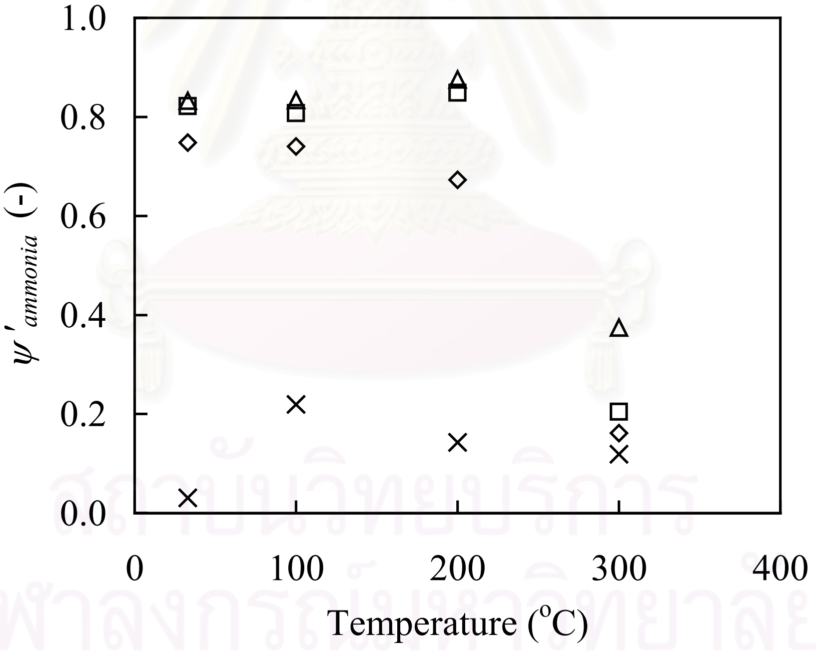

(b)

Figure 5.20 Effect of H_2O on the simultaneous removal of CH_3CHO and NH_3 from N_2-O_2(10%); $C_{in,\ acetaldehyde}$= 150 ppm, $C_{in,\ ammonia}$ = 1000 ppm, I = 0.3 mA, SV = 55.8 hr^{-1} at room temperature: (◇) H_2O 0 ppm, (□) H_2O 5250 ppm, (Δ) H_2O 10500 ppm, (×) Pure N_2

5.9 Simultaneous removal of acetaldehyde and trimethylamine

5.9.1 Effect temperature and coexisting O_2 on the simultaneous removal of CH_3CHO and $(CH_3)_3N$ from N_2

Figure 5.21 shows the effect of O_2 on the simultaneous removal efficiency of CH_3CHO and $(CH_3)_3N$ from N_2. The inlet concentration of CH_3CHO and $(CH_3)_3N$ are 150 ppm and 100 ppm, respectively, while the current is 0.3 mA. It is found that the presence of O_2 has a significant enhancement effect on the simultaneous CH_3CHO removal efficiency ψ' in **Figure 5.21(a).** As temperature increases, the CH_3CHO removal efficiency remains at 100% from room temperature to 100 ^oC, above which the CH_3CHO removal efficiency tends to significantly decrease because the mean residence time of the gas mixture inside the reactor decreases as the reactor temperature rises. As expected, the presence of O_2 also has a significant effect on the simultaneous $(CH_3)_3N$ removal efficiency in **Figure 5.21(b).** As mentioned previously, the improved removal efficiency for both CH_3CHO and $(CH_3)_3N$ can be attributed to effect of O_3 and O^- anion at low temperatures and various radicals at high temperatures.

5.9.2 Effect of temperature and H_2O on removal of CH_3CHO and $(CH_3)_3N$ from N_2-O_2

Figure 5.22 shows the combined effect of O_2 and H_2O on the simultaneous removal efficiency of CH_3CHO and $(CH_3)_3N$ from N_2. In **Figure 5.22(a)**, as temperature increases, the CH_3CHO removal efficiency remains at 100% from room temperature to 200 ^oC, above which the CH_3CHO removal efficiency tends to significantly decrease. In **Figure 5.22(b)**, the simultaneous $(CH_3)_3N$ removal efficiency increases from room temperature to 300 ^oC. Compare to the case of only coexisting O_2, the simultaneous removal efficiency of $(CH_3)_3N$ is retarded by the presence of H_2O because at low discharge current, the relatively much smaller number of electrons tend to attach mostly to H_2O.

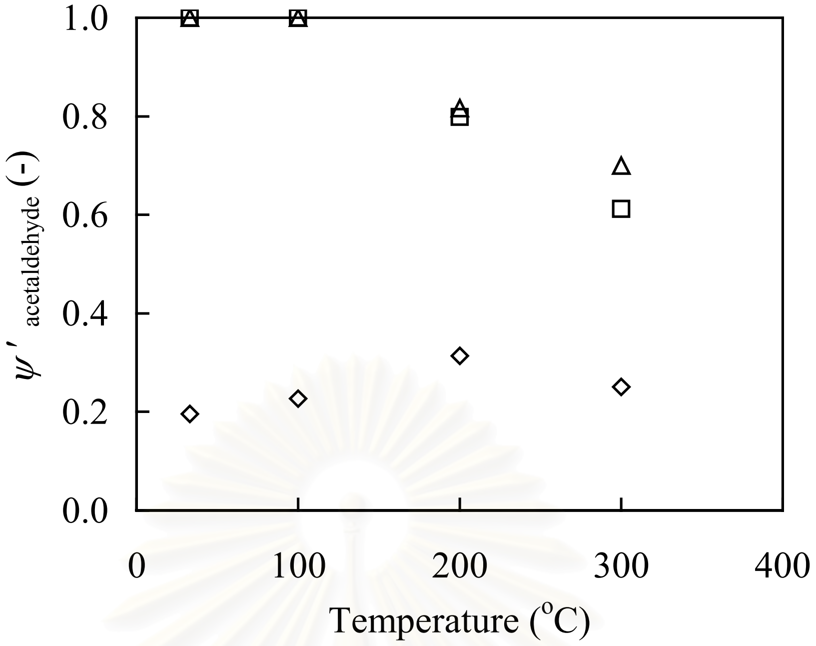

(a)

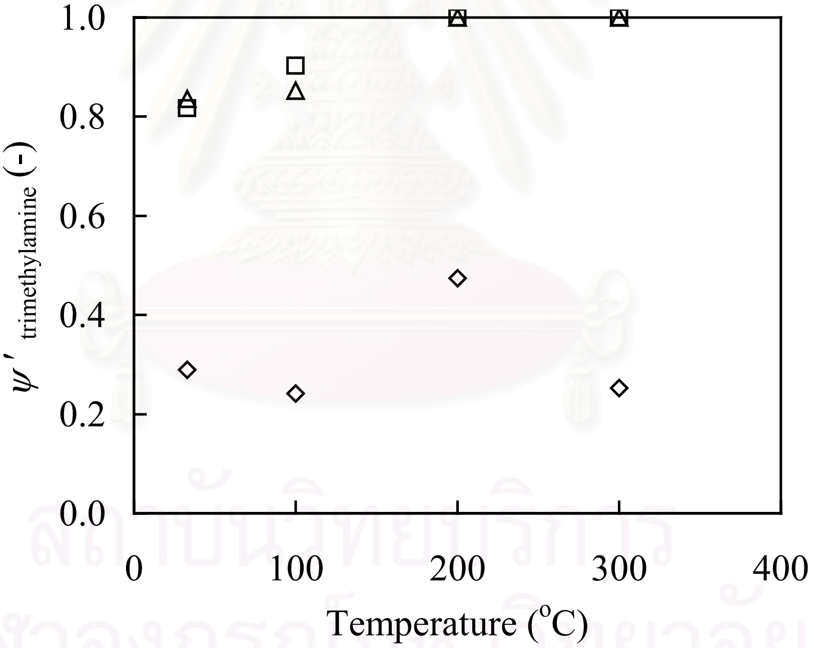

(b)

Figure 5.21 Effect of coexisting O_2 on the simultaneous removal of CH_3CHO and $(CH_3)_3N$ from N_2; $C_{in,\ acetaldehyde}$= 150 ppm, $C_{in,\ trimethylamine}$= 100 ppm, I = 0.3 mA, SV = 55.8 hr^{-1} at room temperature: (◇) O_2 0%, (□) O_2 10%, (Δ) O_2 20%

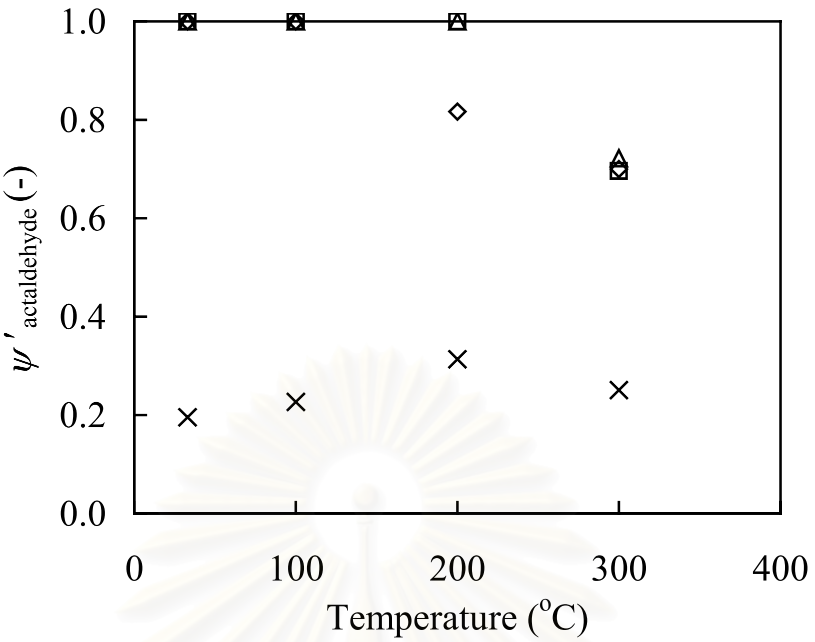

(a)

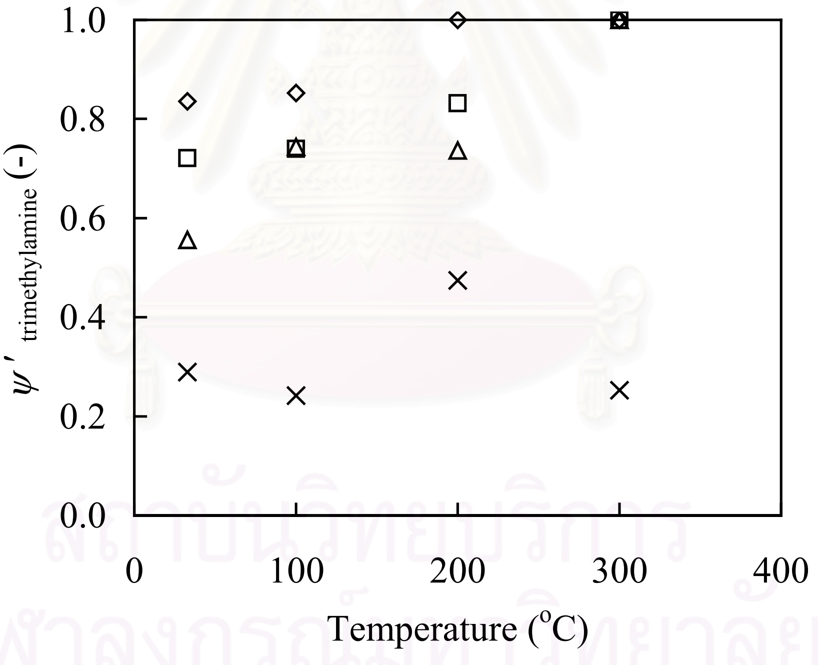

(b)

Figure 5.22 Effect of H_2O on the simultaneous removal of CH_3CHO and $(CH_3)_3N$ from N_2-O_2(20%); $C_{in, acetaldehyde}$= 150 ppm, $C_{in, trimethylamine}$= 100 ppm, I = 0.3 mA, SV = 55.8 hr^{-1} at room temperature: (◇) H_2O 0 ppm, (□) H_2O 5250 ppm, (Δ) H_2O 10500 ppm, (×) Pure N_2

5.10 Simultaneous removal of ammonia and trimethylamine

5.10.1 Effect temperature and coexisting O_2 on removal of NH_3 and $(CH_3)_3N$ from N_2

Figure 5.23 shows the effect of O_2 on the simultaneous removal efficiency of NH_3 and $(CH_3)_3N$ from N_2. The inlet concentration of NH_3 and $(CH_3)_3N$ are 1000 ppm and 150 ppm, respectively, while the current is 0.3 mA. It is found that the presence of O_2 has a significant enhancement effect on the simultaneous NH_3 removal efficiency ψ' in **Figure 5.23(a)**. As temperature increases, the NH_3 removal efficiency increases from room temperature to 200 ^oC, above which the NH_3 removal efficiency tends to significantly decrease because of less O_3 generated from O_2 and reduction of the mean residence time of the gas mixture inside the reactor at high temperature. In **Figure 5.23(b)**, when the reaction temperature is increased, the removal efficiency is found to increase starting from room temperature to 300 ^oC. As mentioned previously, the improved removal efficiency for $(CH_3)_3N$ can be attributed to effect of O_3 and O^- anion at low temperatures and various radicals at high temperatures. In addition, the reduction of $(CH_3)_3N$ concentration via the thermal decomposition high temperature may contribute to enhance the removal efficiency of $(CH_3)_3N$.

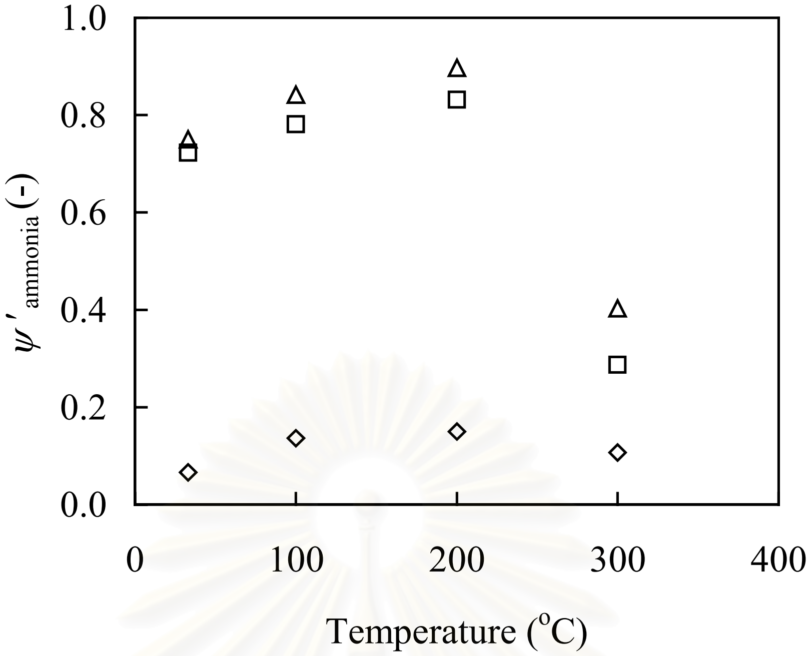

(a)

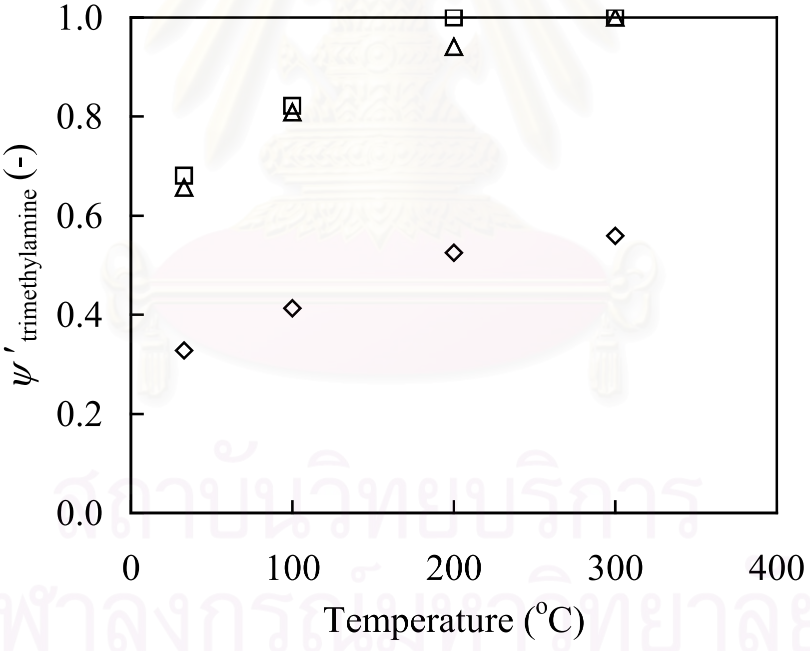

(b)

Figure 5.23 Effect of coexisting O_2 on the simultaneous removal of NH_3 and $(CH_3)_3N$ from N_2-O_2; $C_{in,\ ammonia}$ = 1000 ppm, $C_{in,\ trimethylamine}$= 100 ppm, I = 0.3 mA, SV = 55.8 hr^{-1} at room temperature: (◇) O_2 0%, (□) O_2 10%, (Δ) O_2 20%

5.10.2 Effect of temperature and H_2O on the simultaneous removal of NH_3 and $(CH_3)_3N$ from N_2-O_2

Figure 5.24 shows the combined effect of O_2 and H_2O on the simultaneous removal efficiency ψ' of NH_3 and $(CH_3)_3N$ from N_2. In **Figure 5.24(a)**, the NH_3 removal efficiency increases with temperature up to 200 °C, above which the tendency reverses up to 300 °C. Compared to the case of only coexisting O_2, the simultaneous removal efficiency of NH_3 is enhanced by the presence of H_2O because the effect of H^-, OH^- and a few O^- anions should contribute to the removal of NH_3 at low to moderate temperatures. At high temperature, O_3 generated from O_2 and H^-, OH^- and a few O^- anions from H_2O are unstable. Couple with the negative effect of reduced residence time, the simultaneous removal efficiency of NH_3 decreases significantly at 300 °C. **Figure 24(b)** shows the removal efficiency ψ' of $(CH_3)_3N$ versus temperature. When the reaction temperature is increased, the removal efficiency is found to increase starting from room temperature up to 300 °C. As mentioned previously, the effect of H_2O, H^-, OH^- and a few O^- anions at low temperatures and various radicals at high temperatures should contribute to the removal of $(CH_3)_3N$. In addition, the reduction of $(CH_3)_3N$ concentration via the thermal decomposition at high temperature may contribute to enhance the removal efficiency. Compare to the case of only coexisting O_2, the presence of H_2O slightly retards the removal efficiency of $(CH_3)_3N$ because at low discharge current, the relatively much smaller number of electrons tend to attach mostly to H_2O.

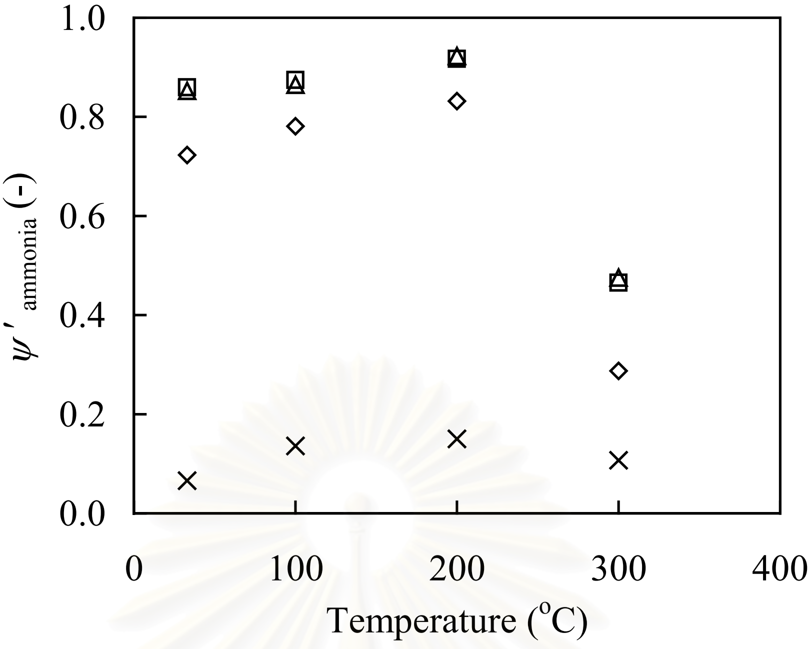

(a)

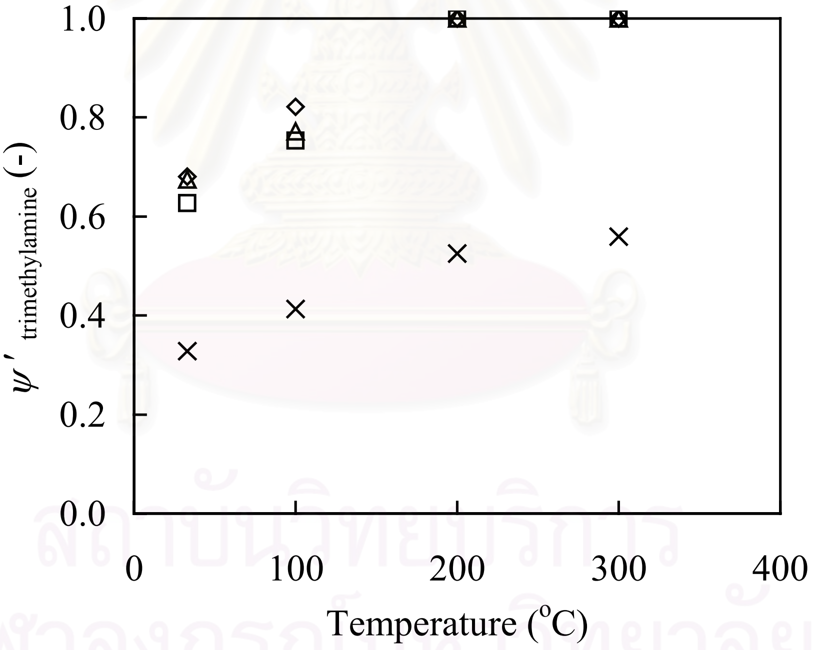

(b)

Figure 5.24 Effect of H_2O on the simultaneous removal of NH_3 and $(CH_3)_3N$ from N_2-O_2(10%); $C_{in,\ ammonia} = 1000$ ppm, $C_{in,\ trimethylamine} = 100$ ppm, I = 0.3 mA, SV = 55.8 hr^{-1} at room temperature: (◇) H_2O 0 ppm, (□) H_2O 5250 ppm, (Δ) H_2O 10500 ppm, (×) Pure N_2

5.11 Simultaneous removal of acetaldehyde, ammonia and trimethylamine

5.10.3 Effect temperature and coexisting O_2 on the simultaneous removal of CH_3CHO, NH_3 and $(CH_3)_3N$ from N_2

To investigate possible interaction between CH_3CHO, NH_3 and $(CH_3)_3N$, three of the reported crematory gas components, several experiments to simultaneously remove CH_3CHO, NH_3 and $(CH_3)_3N$ from N_2-O_2 have been carried out. The inlet concentration of CH_3CHO, NH_3 and $(CH_3)_3N$ are 150 ppm, 1000 ppm and 100 ppm, respectively, while the current is 0.3 mA.

Figure 5.25 shows the simultaneous removal efficiency ψ' of CH_3CHO, NH_3 and $(CH_3)_3N$ from N_2-O_2. **Figure 5.25(a)** shows the removal efficiency ψ' of CH_3CHO versus temperature. Obviously, the presence of O_2 has a significant effect on the acetaldehyde removal efficiency. As temperature increases, the CH_3CHO removal efficiency above 200 °C tends to significantly decrease. **Figure 5.25(b)** shows the removal efficiency ψ' of NH_3 versus temperature. Obviously, the presence of O_2 has a significant effect on the NH_3 removal efficiency. As the temperature increases, the NH_3 removal efficiency increases starting from room temperature up to 200 °C, then the tendency reverses up to 300 °C. **Figure 5.25(c)** shows the removal efficiency ψ' of $(CH_3)_3N$ versus temperature. It is found that the presence of O_2 in N_2 always enhances the $(CH_3)_3N$ removal efficiency. When the reaction temperature is increased, the removal efficiency is found to increase starting from room temperature up to 300 °C.

The removal efficiency enhancement is found to depend on the concentration of coexisting O_2. As mentioned previously, the improved removal efficiency of CH_3CHO, NH_3, $(CH_3)_3N$ can be attributed to effect of O_3 and O^- anion at low temperatures and various radicals at high temperatures. In addition, the reduction of $(CH_3)_3N$ concentration via the thermal decomposition may contribute to enhance the removal efficiency of $(CH_3)_3N$ at high temperature.

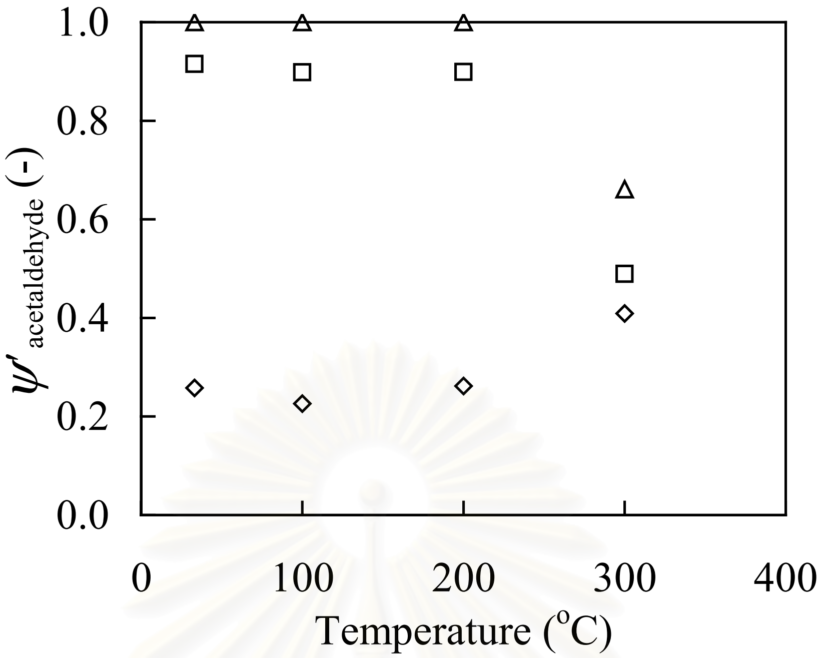

(a)

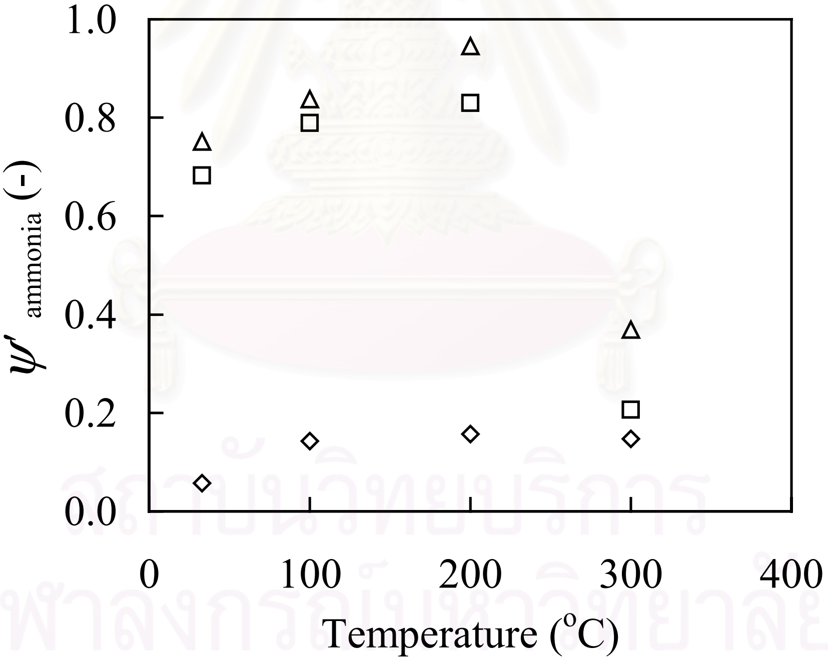

(b)

Figure 5.25 Effect of O_2 on simultaneous removal of CH_3CHO, NH_3 and $(CH_3)_3N$ from N_2; $C_{in,\ acetaldehyde} = 150$ ppm, $C_{in,\ ammonia} = 1000$ ppm, $C_{in,\ trimethylamine} = 100$ ppm, I = 0.3 mA, SV = 55.8 hr^{-1} at room temperature: (◇) O_2 0%, (□) O_2 10%, (Δ) O_2 20%

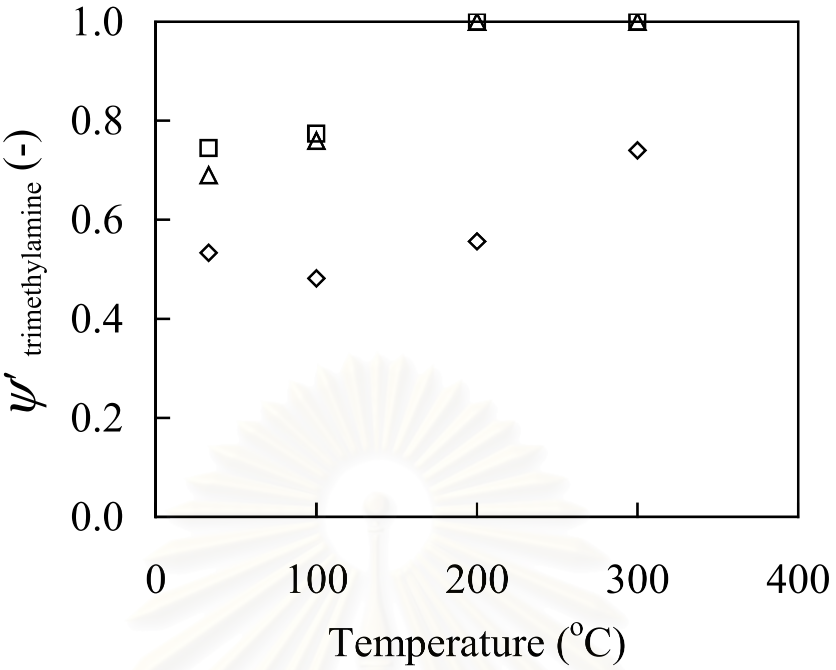

(c)

Figure 5.25 Effect of O_2 on simultaneous removal of CH_3CHO, NH_3 and $(CH_3)_3N$ from N_2; $C_{in,\ acetaldehyde}$ = 150 ppm, $C_{in,\ ammonia}$ = 1000 ppm, $C_{in,\ trimethylamine}$ = 100 ppm, I = 0.3 mA, SV = 55.8 hr^{-1} at room temperature: (◇) O_2 0%, (□) O_2 10%, (Δ) O_2 20%

5.11.2 Effect of temperature and H_2O on the simultaneous removal of CH_3CHO, NH_3 and $(CH_3)_3N$ from N_2-O_2

Figure 5.26 shows the combined effect of O_2 and H_2O on the simultaneous removal efficiency ψ' of CH_3CHO, NH_3 and $(CH_3)_3N$ from N_2. In **Figure 5.26(a)**, as temperature increases, the CH_3CHO removal efficiency slightly decreases from room temperature to 300 ^oC. In **Figure 5.26(b)**, as the temperature increases, the NH_3 removal efficiency increases starting from room temperature up to 200 ^oC, above which the NH_3 removal efficiency tends to significantly decrease because of less O_3 generated from O_2. As for the effect of H_2O, H^-, OH^- and a few O^- anions should contribute to the removal of CH_3CHO, NH_3 at low to moderate temperatures. In **Figure 5.26(c)**, the simultaneous $(CH_3)_3N$ removal efficiency decreases from room temperature to 100 ^oC, above which the tendency reverses up to 300 ^oC. Compared to the case of no H_2O, the removal efficiency of $(CH_3)_3N$ is slightly retarded by the presence of H_2O at low to moderate temperatures. At high temperature, the reduction of $(CH_3)_3N$ concentration via the thermal decomposition may contribute to enhance the removal efficiency of $(CH_3)_3N$.

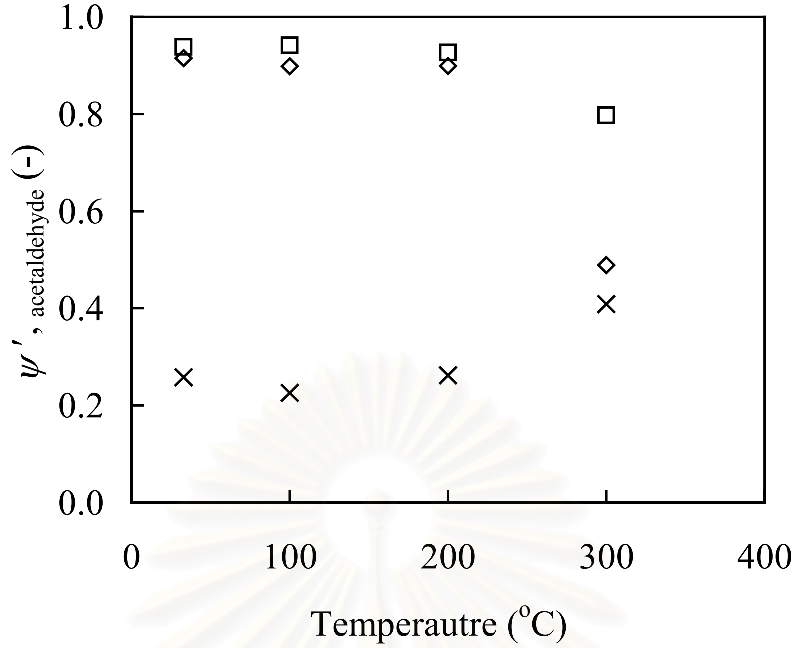

(a)

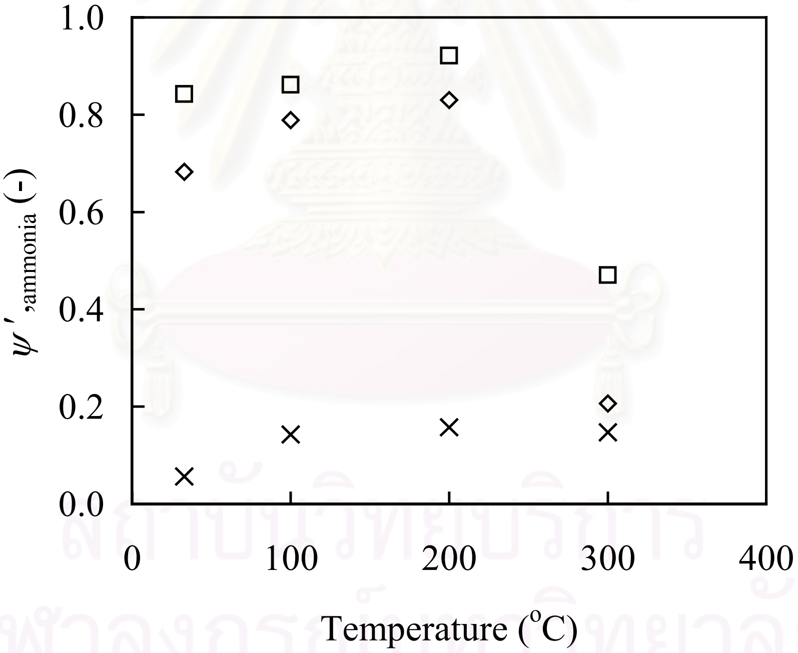

(b)

Figure 5.26 Effect of H_2O on simultaneous removal of CH_3CHO, NH_3 and $(CH_3)_3N$ from N_2-O_2(10%); $C_{in,\ acetaldehyde} = 150$ ppm, $C_{in,\ ammonia} = 1000$ ppm, $C_{in,\ trimethylamine} = 100$ ppm, I = 0.3 mA, SV = 55.8 hr^{-1} at room temperature: (◇) H_2O 0 ppm, (□) H_2O 5250 ppm, (×) Pure N_2

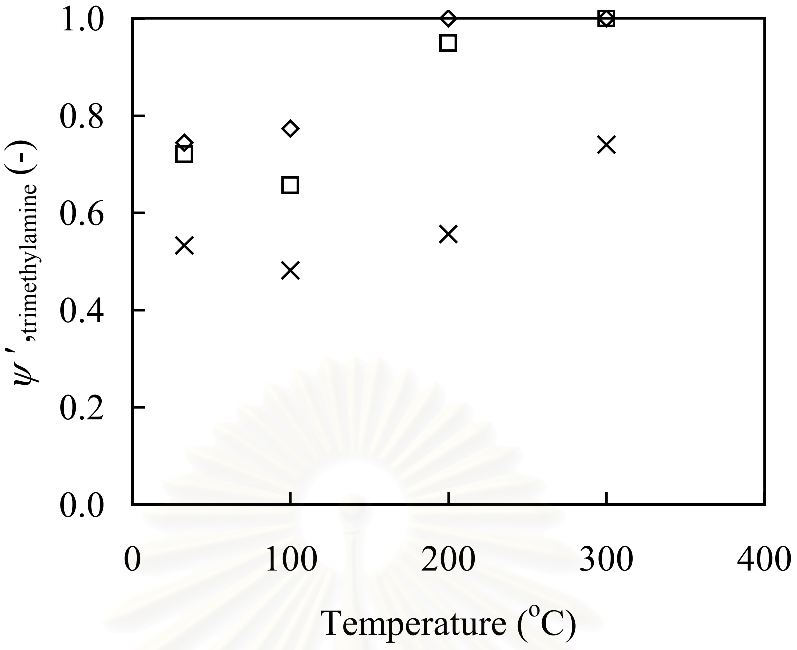

(c)

Figure 5.26 Effect of H_2O on simultaneous removal of CH_3CHO, NH_3 and $(CH_3)_3N$ from N_2-O_2(10%); $C_{in,\ acetaldehyde} = 150$ ppm, $C_{in,\ ammonia} = 1000$ ppm, $C_{in,\ trimethylamine} = 100$ ppm, I = 0.3 mA, SV = 55.8 hr^{-1} at room temperature: (◇) H_2O 0 ppm, (□) H_2O 5250 ppm, (×) Pure N_2

5.11.3 Simultaneous removal of CH_3CHO, NH_3 and $(CH_3)_3N$ from N_2-O_2-H_2O using two reactors in series

The experiments for simultaneous removal of CH_3CHO, NH_3 and $(CH_3)_3N$ from N_2-O_2(10%)-H_2O(5250 ppm) were studied using two reactors in series to decrease byproducts and/or increase the removal efficiency.

According to the past experiments, it was found that $(CH_3)_3N$ was removed completely and the removal efficiency of CH_3CHO was nearly complete by using the single reactor at 300°C and 0.3 mA. Therefore, the temperature and the current discharge of the first reactor were kept constantly at these conditions. As the expected result, $(CH_3)_3N$ was removed completely but the concentration of CH_3CHO still remained about 14 ppm. In addition, the concentration of NH_3 was 440 ppm. Moreover, there was NO_x 50 ppm as a byproduct and extraneous peaks were observed in the gas chromatograms of the effluent stream.

Then the second reactor was added in series with the first reactor in order to decrease byproducts and/or increase the removal efficiency. The experiments were divided into two cases. In the first case, the temperature of the second reactor was room temperature. It revealed that the target gases were removed completely at 0.3 mA. Additionally, NO_x and extraneous peaks were disappeared, however, O_3 was increased more than 400 ppm when the current discharge increased from 0.1 to 0.3 mA. In the second case, the temperature of the second reactor was set at 200 °C. The results showed that the target gases were removed completely at 0.3 mA. Besides, O_3 and extraneous peaks were disappeared, NO_x was decreased to 20 ppm.

5.11.4 Preliminary summary

Generally, two other types of removal efficiency are reported for a corona-discharge system. The electron-based efficiency ψ_{elec} (-) is defined as the number of gas molecules removed by one discharged electron, and the energy-based efficiency ψ_{ener} (mol gas $.J^{-1}$) is defined as the mole of gas removed per energy consumption (J). From the experimental results, in the case of the simultaneous removal of CH_3CHO, NH_3 and $(CH_3)_3N$ from air, the values of ψ_{elec} of CH_3CHO at room temperature increase, respectively, 1.5 and 1.3 folds compared to the case of simultaneous removal of CH_3CHO with NH_3 and the case of simultaneous removal of CH_3CHO with $(CH_3)_3N$. The values of ψ_{elec} of NH_3 at room temperature increase, respectively, 1.7 and 1.5 folds compared to the case of simultaneous removal of $NH_3$with CH_3CHO and the case of simultaneous removal of NH_3 with $(CH_3)_3N$. The values of ψ_{elec} of $(CH_3)_3N$ at room temperature increase, respectively, 1.5 and 2.1 folds compared to the case of simultaneous removal of $(CH_3)_3N$ with CH_3CHO and the case of simultaneous removal of $(CH_3)_3N$ with NH_3.

In actual applications of gas purification, it is importance to consider the energy-based efficiency ψ_{ener}. In the case of in the case of the simultaneous removal of CH_3CHO, NH_3 and $(CH_3)_3N$ from air, it is recommended to operate at room temperature for minimizing the operating cost when air is purified because the values of ψ_{ener} of CH_3CHO, NH_3 and $(CH_3)_3N$ are highest at 5.4, 39.9 and 2.6 (x 10^{-9} mol gas $.J^{-1}$), respectively.

CHAPTER VI

CONCLUSIONS AND RECOMMENDATION

6.1 Conclusions

The main purpose of the present research is to investigate the effect of high temperature and coexisting gases on the removal efficiency of acetaldehyde (CH_3CHO), ammonia (NH_3) and trimethylamine [$(CH_3)_3N$] from N_2 using electron attachment reaction. The additional factors investigated are the inlet concentration, coexisting oxygen gas, water vapor and simultaneous removal of acetaldehyde, ammonia and trimethylamine. From the results, it can be concluded as follows:

6.1.1 Effect of inlet concentration on the removal efficiency

In the separate removal of target gases, CH_3CHO, (NH_3) and $(CH_3)_3N$, from nitrogen, the more dilute the inlet concentration, the higher the removal efficiency becomes.

6.1.2 Effect of O_2 coexisting gas on separate and simultaneous CH_3CHO, (NH_3) and $(CH_3)_3N$ removal

The presence of O_2 substantially enhances the removal efficiency of CH_3CHO, (NH_3) and $(CH_3)_3N$ because of O_3 and O^- anion at low temperatures and N, O radicals at high temperatures.

6.1.3 Effect of H_2O on the removal of separate and simultaneous CH_3CHO, (NH_3) and $(CH_3)_3N$ removal

The presence of H_2O in N_2 slightly enhances the removal efficiency of CH_3CHO, (NH_3) and $(CH_3)_3N$ at low to moderate temperature because of H^-, OH^- and a few O^- anions but slightly retards at high temperature because at low discharge current, the relatively much smaller number of electrons tend to attach mostly to H_2O. The presence of water vapor in N_2-O_2 mixed gas generally has adverse effect on the removal efficiency of CH_3CHO, NH_3 and $(CH_3)_3N$.

6.1.4 Two corona-discharge reactors in series for minimizing generation of byproducts and/or enhancing removal efficiency

Two independently operated corona-discharge reactors in series have shown a good promise for minimizing generation of byproducts and enhancing removal efficiency. The first reactor was aimed at complete removal of $(CH_3)_3N$ at 300°C, then the second was aimed at complete removal of CH_3CHO and NH_3 while minimizing the generation of byproduct NO_x and O_3 to 20 ppm and 0 ppm, respectively, at 200 °C.

6.2 Recommendation for future work

From the experimental results, NO_x is still detected at high temperature and its concentration generally increases with temperature. More investigation of the applications of two independently operated corona-discharge reactors in series for minimizing generation of NO_x and other byproducts should be carried out. For minimizing the operating cost, the temperature and current discharge which affect on the value of energy-based efficiency ψ_{ener} should be considered.

REFERENCES

Bityurin, V.A., Potapkin, B.V., Deminsky, M.A. Chemical activity of discharges, electrical discharges for environmental purposes, edited by E.M. Van Veldhuizen. New York: Nova Science Publishers, 2000. pp. 49-117.

Caledonia, G. E. A survey of the gas-phase negative ion kinetics of inorganic molecules - Electron Attachment Reactions. Chem. Rev. 75 (1975): 333-351.

Castle, G. S. P., Inculet, I. I., and Burgess, K. I. Ozone generation in positive corona electrostatic precipitators. IEEE Trans. Ind. and Gen. Appl. IGA-5 (1969): 489-496.

Castle, P. M., Kanter, I. E., Lee, P. K., and Kline, L. E. Corona glow detoxification study. Final Rep., Westinghouse Co., Contract No. DAAA 09-82-C-5396, 1984.

Chaiyo, S. Removal of dilute mixture of styrene and ammonia using corona discharge reactor at various temperatures. Master's degree thesis. Chulalongkorn University 2001.

Chakarbarti, A., et al. Gas cleaning with semi-wet type plasma reactor. IEEE Trans. Ind. Appl. 31 (1995): 500-506.

Chang, J. S., and Masuda S. Mechanism of pulse corona induced plasma chemical processes for removal of NO_x and SO_x from combustion gases. Conf. Rec. IEEE/IAS 1988 Meeting (1988): 1599-1635.

Chang, J. S., and Maezono I. The electrode surface temperature profile in a corona discharge. J. Phys. D: Appl. Phys. 21 (1988): 1023-1024.

Chantry, P.J. and G.J. Schulz, Phys. Rev., 156 (1967): 134.

Davidson, J.H. and Mckinney, P.J. Chemical vapor deposition in the corona discharge of electrostatic air cleaners. Aerosol Science and Technology. 29(2) 1998.

Devins, J. C. Mechanism of ozone formation in the silent electric discharge. J. Electroche. Soc. 103(1956): 460-466.

Dhattavorn, N. Effect of temperature on the removal of toluene vapor using the electron attachment reaction. Master's degree thesis. Chulalongkorn University 2000.

Dorsey, J. A., and Davidson, J. H. Ozone production in electrostatic air cleaners with contaminated electrodes. IEEE Trans. Ind. Appl. 30 (1994): 370-376.

Dressler, R. and M. Allan, Chem. Phys. Lett., 118, 93 (1985)

Eliasson, B., Hirth, M., and Kogelschatz, U. Ozone synthesis from oxygen in dielectric barrier discharges. J. Phys. D: Applied Phys. 20 (1987): 1421-1437.

Hadj-Ziane, S., Held, B., Pignolet, P., Peyrous, R., Benas, J.M., Coste, C. Ozone production in an oxygen-fed wire to cylindrical ozonizer. J. Phys. D: Appl. Phys. 23 (1990): 1390-1395.

Hadj-Ziane, S., B. Held, P. Pignolet, R. Peyrous and C. Coste. J. Phys. D: Appl. Phys. 25 (1992): 677.

Hattori, H., Ito, T., Ehara, Y., and Miyata, Y. Superposition effect on ozone synthesis by two types of discharges. Trans. IEE Japan 112A (1992): 41-46.

Helfritch, D. J. Pulsed corona discharge for hydrogen sulfide decomposition. IEEE Trans. Ind. Appl. 29, 1993.

Higashi, M., Sugaya, M., Ueki, K., and Fujii, K. Plasma processing of exhaust gas from a diesel engine vehicle. Proc. Int. Conf. on Plasma Chem. 2 (1985): 366-371.

Higashi, M., Uchida, S., Suzuki, N., and Fujii, K. Simultaneous reduction of soot and NO_x in a diesel engine exhaust by discharge plasma. Trans. IEEE Japan III-A (1991): 457-473.

Higashi, M. Soot elimination and NO_x and SO_x reduction in diesel engine exhaust by a combination of discharge plasma and oil dynamics. IEEE Trans. Plasma Sci. 20 (1992): 1-12.

Horvath, M. Ozone. Amsterdam, The Netherlands: Elsevier Sci., 1980.

Ito, T., Ehara, Y., Sakai, T., and Miyata, Y. Superposition effect on ozone synthesis by discharge. J. Jpn. Res. Group Elec. Discharges. 127 (1990): 113-118.

Khongphasarnkaln, P. Removal of trimethylamine acetaldehyde and ammonia using electron attachment reaction. Master's degree thesis. Chulalongkorn University, 1998.

Kanasawa, K., Chang, J. S., Round, G. F., Sheng, G. F., Ohkubo, T., Nomoto, Y., Adachi, T. Reduction of NO_X from flue gas by corona discharge activated ammonia radical showers. Combust. Sci. Technol. 133(1998): 93-105.

Larpsuriyakul, K., Sano, N., Tamon, H., Tanthapanichakoon, W., and Okazaki, M. Influence of structure of corona-discharge reactor on removal of dilute gases using electron attachment. Proc. Himeji Conf. Soc. Chem. Engrs. Japan (1996): 270-271.

Loiseau, J.F., F. Lacassie, C. Monge, R. Peyrous, B. Held and C. Coste, J., Phys, D, 29 (1994): 63.

Lowke, J.J., Morrow, R. Theoretical analysis of removal oxides of sulfer and nitrogen in pulsed operation of electrostatic precipitation of electrostatic precipitators. IEEE Trans. Plasma. Sci. 23 (1995) 661-667.

Massey, S. H. Negative Ions. Cambridge, England: Cambridge Univ. Press, 1976.

Massey, S. H. Atomic and Molecular Collisions. London: Taylor & Francis, 1979.

Masuda, S., Sato, M., and Seki, T. High efficiency ozonizer using traveling wave pulse voltage. Conf. Rec. IEEE/IAS 1984 Ann. Meet. Chicago, IL, (1984): 978-985.

Mizuno, A., Clements, J. S., and Davis, R. H. A method for the removal of sulfur dioxide from exhaust gas utilizing pulsed streamer corona for electron energization. IEEE Trans. Ind. Appl. IA-22 (1986): 516-522.

Mnatsakanyan, A. K., Nadis, G. V., Solozobov,Y.M. Theory of a corona discharge in heated air. High Temperature. (1987): 771-776.

Moruzzi, J. L., and Phelps, A. V. Survey of negative-ion-molecule reactions in O_2, CO_2, H_2O, CO, and mixtures of these gases at high pressures. J. Chem. Phys. 45 (December 1966): 4617-4627.

Mukkavilli, S., Lee, C.K., Vaghese, K., Tavlarides, L.L. Modeling of the electrostatic corona discharge reactor. IEEE Trans. Plasma. Sci. 16 (1988): 652-660.

Nishida, K. Malodor at cremation Facility (Part I). PPM. 3(1988): 49-58. (in Japanese)

Nishida, K. Malodor at cremation Facility (Part II). PPM. 4(1988): 51-59. (in Japanese)

Nishida, K., Masuda,Y. Malodor of exhaust gas from crematory. J. of Odor Control. 10(1981): 1-11. (in Japanese)

Oda, T., et al. Decomposition of gaseous organic contaminants by surface discharge induced plasma chemical process-SPCP. IEEE Trans. Ind. Appl. 32 (1996): 118-124.

Oglesby, S., and Nichols, G. B. Electrostatic Precipitation. New York: Marcel Dekker, 1978.

Perry, R.H., and Green, D. W. Perry’s chemical engineers’ handbook. 7th ed. New York: McGraw-Hill, 1997.

Peyrous, R., Pignolet, P., Held, B. Kinetic simulation of gaseous spicies created by an electrical discharge in dry or humid oxygen J. Phys. D: Apply Phys. 22 (1989): 1658-1667.

Rapp, D. And D. D. Briglia, J. Chem. Phys. 43 (1965): 1480.

Sano, N., Nagamoto, T., Tamon, H., and Okazaki, M. Removal of iodine and methyl iodide in gas by wetted-wall reactor based on selective electron attachment. J. Chem. Eng. Japan 29 (1996): 59-64.

Sano, N., Nagamoto, T., Tamon, H., Suzuki, T.and Okazaki, M. Removal of acetaldehyde and skatole in gas by corona-discharge. Ind. Eng. Chem. Res. 36 (1997): 3783-3791.

Sano, N. Development of Gas Purification Technology by Selective Electron Attachment. Doctoral Dissertation, Kyoto Univ., Japan, 1997.

Sano, N, Nishimura, S., Kanki, T., Tamon, H., Tanthapanichakoon, W., Charinpanitkul, T. Influence of temperature of SO_2 removal enhanced by water vapor using a corona-discharge reactor. Chem. Eng. Technol. 24(2001): 1295-1299.

Sugimitsu, H. Ozone no kiso to ouyo (Fundamentals and application of ozone). Tokyo: Korin, 1998. (in Japanese)

Tamon, H., Yano, H., and Okazaki, M. A new method of gas mixture separation based on selective electron attachment. Kagaku Kogaku Ronbunshu 15 (1989): 663-668.

Tamon, H., Mizota, H., Sano, N., Schulze, S., Okazaki, M. New concept of gas purification by electron attachment. AIChE J. 41 (1995): 1701-1711.

Tamon, H., Sano, N., Okazaki, M. Influence of oxygen and water vapor on removal of sulfur compounds by electron attachment. AIChE J. 42 (1996): 1481-1486.

Tanthapanichakoon, W., Larpsuriyakul, K., Charinpanitkul, T., Sano, N., Tamon, H., and Okazaki, M. Effect of structure of corona-discharge reactor on removal of dilute gaseous pollutant using selective electron attachment. J. Chem. Eng. Japan. 31 (1998): 7-13.

Tanthapanichakoon, W., Dhattavorn, N., Chaiyo, S., Tamon, H., Sano, N. Development of odor control technology for crematory furnace using corona discharge reaction. J. Multidisciplinary Res. 14(2001): 34-41.

Uhm, H.S. Influence of chamber temperature on properties of the corona discharge system. Physics of Plasmas 6(2) 1999: 623-626.

Urashima, K., Kim, S. J., Chang, J. S. Characteristics of aerosol particles from corona discharge ammonia radical injection desulfurization and denitrification processes for flue gases cleanings. J. Aerosol Sci. 30(1999): S849-S850.

Weiss, H. R. Plasma induced dissociation of carbon dioxide. Proc. Int. Conf. on Plasma Chem. 2 (1985): 383-388.

White, H. J., and Cole, W. H. Design and performance of high-velocity, high-efficiency air cleaning precipitators. JAPCA 10 (1960): 239-245.

Yamamoto, T., et al. Catalysis-assisted plasma technology for carbon tetrachloride destruction. IEEE Trans. Ind. Appl. 32 (1996): 100-105.

Zhang, R., Yamamoto, T., and Bundy, D. S. Control of ammonia and odors in animal house by a ferroelectric plasma reactor. IEEE Trans. Ind. Appl. 32 (1996): 113-117.

APPENDICES

APPENDIX A

Calibration Curve

Calibration curve between GC peak area and concentration of acetaldehyde

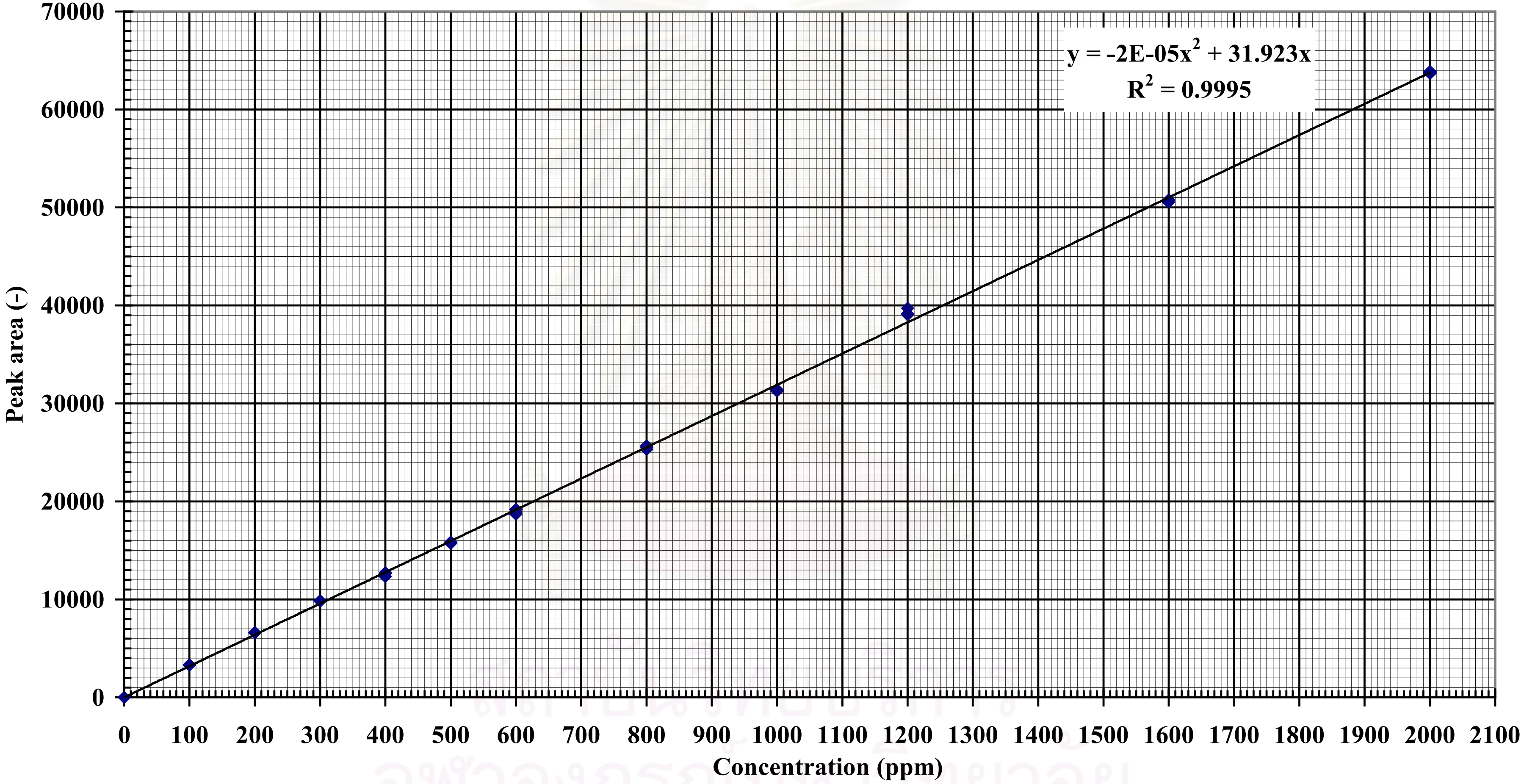

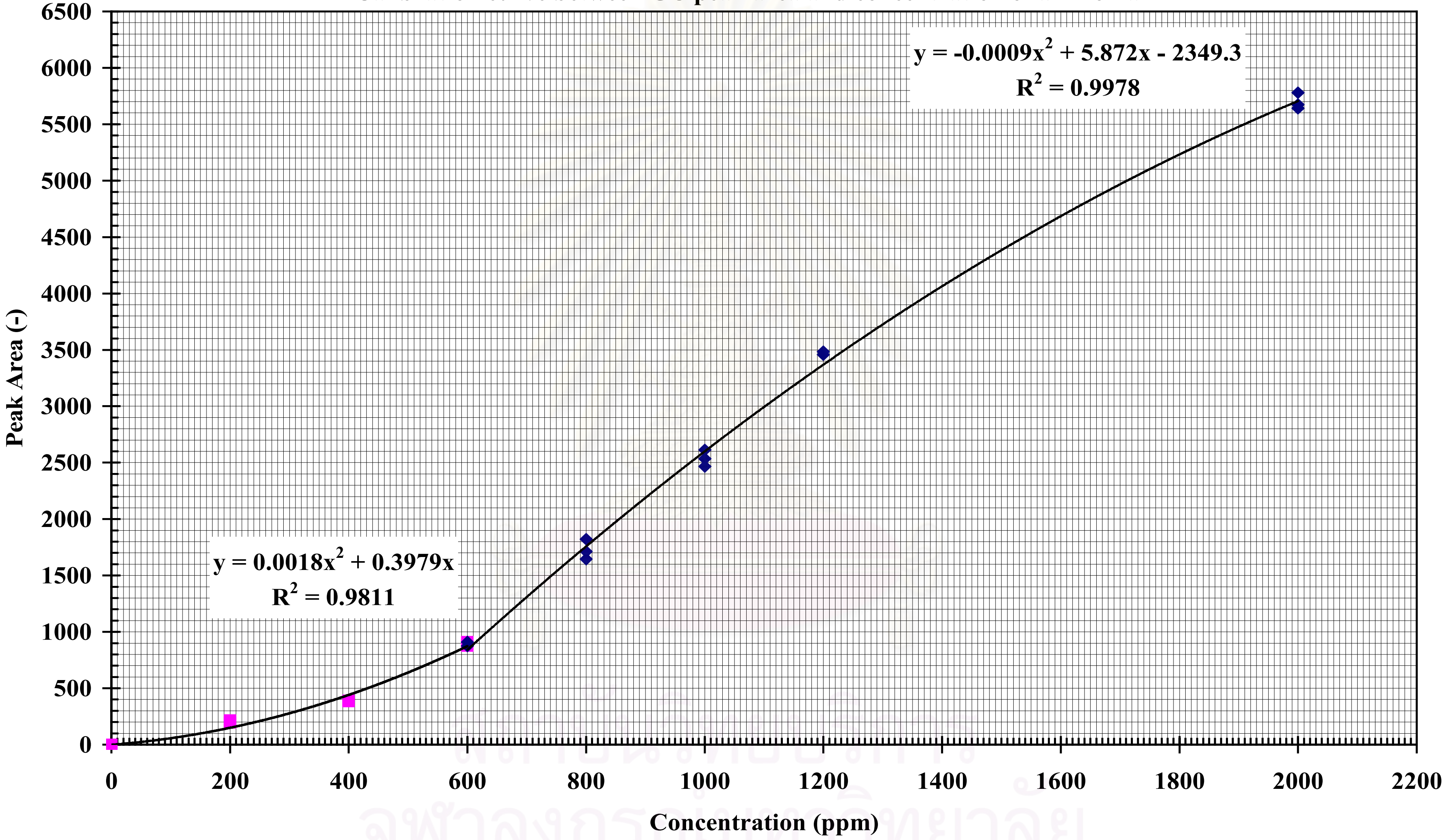

Calibration curve between GC peak area and concentration of ammonia

Calibration curve between GC peak area and concentration of trimethylamine

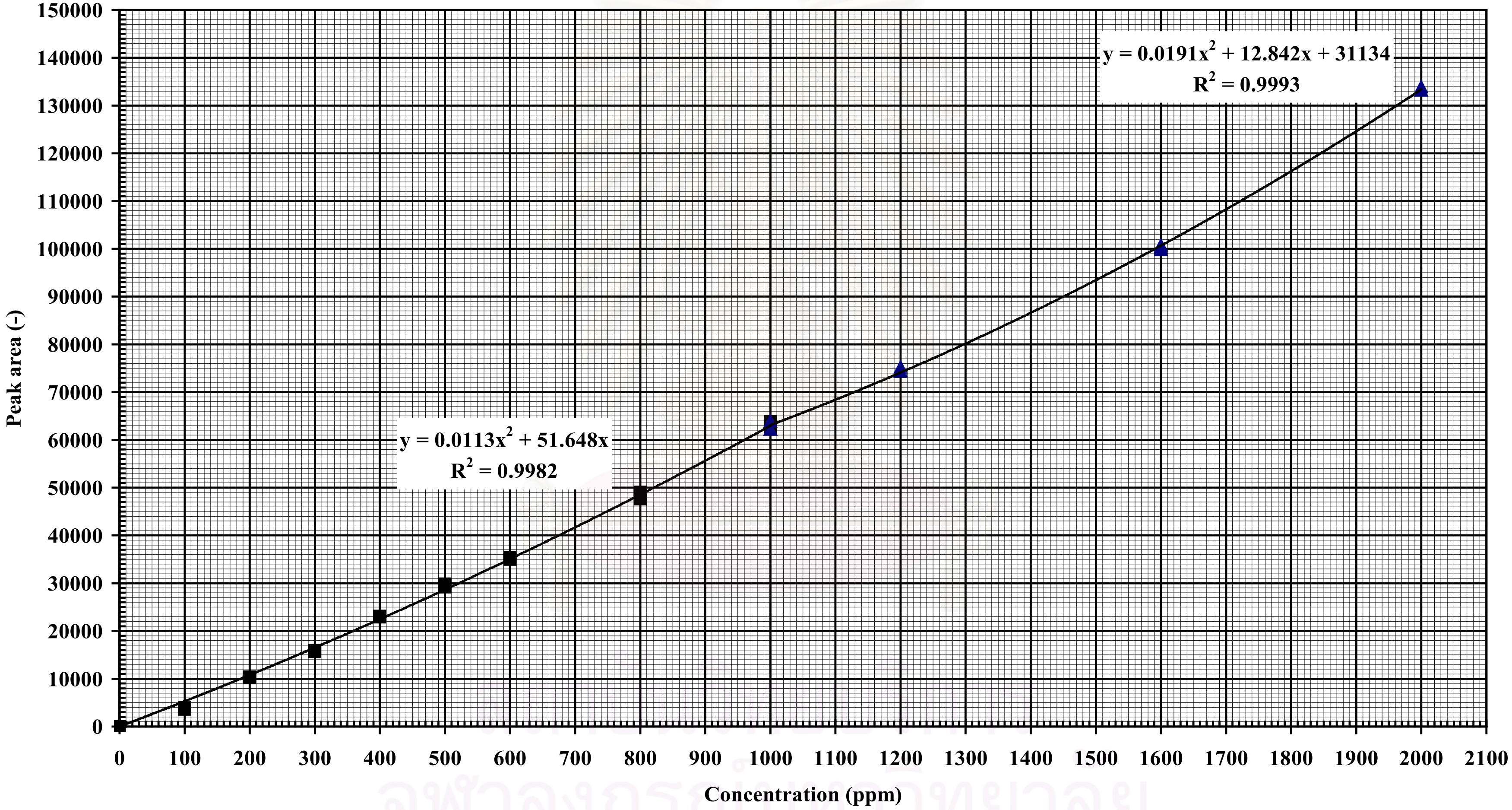

APPENDIX B

Calculation of Water Vapor Concentration

CALCULATION OF WATER VAPOR CONCENTRATION

Vapor pressure of liquid water from "PERRY'S CHEMICAL ENGINEER'S HANDBOOK" 7th Edition, Page 2-49

			N_2 bubbling water flow rate (cc/min) : total flow rate (cc/min)		
T(^oC)	Vapor pressure (mmHg)	conc. (ppm)	10/100	20/100	30/100
0	4.579	6025	603	1205	1808
2	5.294	6966	697	1393	2090
4	6.101	8028	803	1606	2408
6	7.013	9228	923	1846	2768
8	8.045	10586	1059	2117	3176
10	9.209	12117	1212	2423	3635
12	10.518	13839	1384	2768	4152
14	11.987	15772	1577	3154	4732
16	13.634	17939	1794	3588	5382
18	15.477	20364	2036	4073	6109
20	17.535	23072	2307	4614	6922
22	19.827	26088	2609	5218	7826
24	22.377	29443	2944	5889	8833
26	25.209	33170	3317	6634	9951
28	28.349	37301	3730	7460	11190
30	31.824	41874	4187	8375	12562
32	35.663	46925	4693	9385	14078
34	39.898	52497	5250	10499	15749
36	44.563	58636	5864	11727	17591
38	49.692	65384	6538	13077	19615
40	55.324	72795	7279	14559	21838
41	58.338	76761	7676	15352	23028

APPENDIX C

Calculation of Residence Time and Space Velocity

CALCULATION OF RESIDENCE TIME AND SPACE VELOCITY

$$\text{Effective residence time} = \frac{\text{Volume of corona discharge region}}{\text{Volumetric flow rate}}$$

Corona discharge region (i.d. 37 mm x 100 mm)

$= \pi \times 3.7^2 \times 10 / 4 = 107.535 \ \text{cm}^3$

Volumetric flow rate (at 33 ^{0}C)

$= 100 \ \text{cm}^3 / \text{min}$

Volumetric flow rate (at 100 ^{0}C)

From PV = nRT ; P,n,R constant

$= 100 \times (373/306) = 121.9 \ \text{cm}^3 / \text{min}$

Temperature (^{0}C)	Volumetric flow rate (cc/min)	Residence time (min)	Space velocity (hr^{-1})
25	97.39	1.10	54.34
33	100.00	1.08	55.80
100	121.90	0.88	68.01
200	154.58	0.70	86.25
300	187.25	0.57	104.48

APPENDIX D

Acetaldehyde Removal

Date : 22/3/2002

Subject : **Removal of CH_3CHO 200 ppm from N_2, I=0.15 mA**

Gas flow rate :	CH_3CHO (2000 ppm balance N_2)	10	cc/min
	N_2 dilute flow rate	90	cc/min
	Total flow rate	100	cc/min

Inlet concentration : 200 ppm **Current :** 0.15 mA

			Peak Area		Concentration(ppm)		Removal Efficiency		
T, ^{o}C	V(kV)	P(W)	Outlet(0 mA)(avg)	Outlet(0.15 mA)	Cout(0 mA)	Cout(0.15 mA)	ψ,(-)	ψ'',(-)	ψ'',(-)
33	12.0	1.80	7370	0	197	0	1.00	1.00	1.02
33	12.0	1.80	7370	0	197	0	1.00	1.00	1.02
33	12.0	1.80	7370	0	197	0	1.00	1.00	1.02
100	7.9	1.19	7323	5989	196	161	0.20	0.18	0.22
100	7.9	1.19	7323	5993	196	161	0.20	0.18	0.22
100	7.9	1.19	7323	6007	196	161	0.19	0.18	0.22
150	6.6	0.99	7364	5774	197	155	0.22	0.21	0.30
150	6.6	0.99	7364	5805	197	156	0.22	0.21	0.29
150	6.6	0.99	7364	5824	197	156	0.22	0.21	0.29
200	6.3	0.95	7303	5590	195	150	0.25	0.23	0.36
200	6.3	0.95	7303	5738	195	154	0.23	0.21	0.33
200	6.3	0.95	7303	5632	195	151	0.24	0.22	0.35
300	3.9	0.59	7336	4539	196	123	0.39	0.37	0.72
300	3.9	0.59	7336	4521	196	122	0.39	0.38	0.73
300	3.9	0.59	7336	4527	196	122	0.39	0.38	0.73

Date : 7/3/2002

Subject : **Removal of CH_3CHO 200 ppm from N_2, I=0.2 mA**

Gas flow rate : CH_3CHO (2000 ppm balance N_2) 10 cc/min

N_2 dilute flow rate 90 cc/min

Total flow rate 100 cc/min

Inlet concentration : 200 ppm **Current :** 0.2 mA

			Peak Area		Concentration(ppm)		Removal Efficiency		
T, °C	V(kV)	P(W)	Outlet(0 mA)(avg)	Outlet(0.2 mA)	Cout(0 mA)	Cout(0.2 mA)	ψ,(-)	ψ",(-)	ψ",(-)
33	12.3	2.46	7602	0	203	0	1.00	1.00	1.02
33	12.3	2.46	7602	0	203	0	1.00	1.00	1.02
33	12.3	2.46	7602	0	203	0	1.00	1.00	1.02
100	10.2	2.04	7382	0	197	0	1.00	1.00	1.25
100	10.2	2.04	7382	0	197	0	1.00	1.00	1.25
100	10.2	2.04	7382	0	197	0	1.00	1.00	1.25
150	8.9	1.78	7111	0	190	0	1.00	1.00	1.41
150	8.9	1.78	7111	0	190	0	1.00	1.00	1.41
150	8.9	1.78	7111	0	190	0	1.00	1.00	1.41
200	6.7	1.34	6916	4685	185	126	0.37	0.32	0.50
200	6.7	1.34	6916	4717	185	127	0.36	0.31	0.49
200	6.7	1.34	6916	4772	185	129	0.36	0.30	0.48
300	4	0.80	6570	3091	176	85	0.58	0.52	1.00
300	4	0.80	6570	3162	176	86	0.57	0.51	0.98
300	4	0.80	6570	3038	176	83	0.58	0.53	1.02

Date : 8/3/2002

Subject : **Removal of CH_3CHO 200 ppm from N_2, I=0.3 mA**

Gas flow rate : CH_3CHO (2000 ppm balance N_2) 10 cc/min
N_2 dilute flow rate 90 cc/min
Total flow rate 100 cc/min

Inlet concentration : 200 ppm **Current :** 0.3 mA

			Peak Area		Concentration(ppm)		Removal Efficiency		
T, °C	V(kV)	P(W)	Outlet(0 mA)(avg)	Outlet(0.3 mA)	Cout(0 mA)	Cout(0.3 mA)	ψ,(-)	ψ'',(-)	ψ'',(-)
33	13.3	3.99	7321	0	196	0	1.00	1.00	1.02
33	13.3	3.99	7321	0	196	0	1.00	1.00	1.02
33	13.3	3.99	7321	0	196	0	1.00	1.00	1.02
100	10.8	3.24	7588	0	203	0	1.00	1.00	1.25
100	10.8	3.24	7588	0	203	0	1.00	1.00	1.25
100	10.8	3.24	7588	0	203	0	1.00	1.00	1.25
150	9.0	2.70	7361	0	197	0	1.00	1.00	1.41
150	9.0	2.70	7361	0	197	0	1.00	1.00	1.41
150	9.0	2.70	7361	0	197	0	1.00	1.00	1.41
200	6.0	1.80	7388	4116	198	112	0.44	0.44	0.68
200	6.0	1.80	7388	4085	198	111	0.45	0.44	0.69
200	6.0	1.80	7388	4228	198	114	0.43	0.42	0.66
300	4.0	1.20	7123	3564	191	97	0.51	0.49	0.95
300	4.0	1.20	7123	3550	191	97	0.52	0.49	0.95
300	4.0	1.20	7123	3554	191	97	0.52	0.49	0.95

Date : 24/3/2002

Subject : **Removal of CH_3CHO 400 ppm from N_2, I=0.15 mA**

Gas flow rate :	CH_3CHO (2000 ppm balance N_2)	20	cc/min
	N_2 dilute flow rate	80	cc/min
	Total flow rate	100	cc/min

Inlet concentration : 400 ppm **Current :** 0.15 mA

			Peak Area		Concentration(ppm)		Removal Efficiency		
T, ^oC	V(kV)	P(W)	Outlet(0 mA)(avg)	Outlet(0.15 mA)	Cout(0 mA)	Cout(0.15 mA)	ψ,(-)	ψ",(-)	ψ",(-)
33	11.9	1.79	14100	505	374	17	0.96	0.96	0.97
33	11.9	1.79	14100	518	374	17	0.96	0.95	0.97
33	11.9	1.79	14100	520	374	17	0.96	0.95	0.97
100	8.3	1.25	15157	1545	402	44	0.89	0.89	1.11
100	8.3	1.25	15157	1513	402	43	0.89	0.89	1.12
100	8.3	1.25	15157	1526	402	43	0.89	0.89	1.11
150	7.3	1.10	14907	12072	395	321	0.20	0.19	0.27
150	7.3	1.10	14907	12067	395	321	0.20	0.19	0.27
150	7.3	1.10	14907	12024	395	319	0.20	0.19	0.27
200	6.0	0.90	14425	11586	383	308	0.23	0.20	0.31
200	6.0	0.90	14425	11370	383	302	0.24	0.21	0.33
200	6.0	0.90	14425	11387	383	303	0.24	0.21	0.33
300	3.6	0.54	13992	9991	371	266	0.33	0.28	0.55
300	3.6	0.54	13992	9906	371	264	0.34	0.29	0.56
300	3.6	0.54	13992	10102	371	269	0.33	0.28	0.53

Date : 12/3/2002

Subject : **Removal of CH_3CHO 400 ppm from N_2, I=0.2 mA**

Gas flow rate : CH_3CHO (2000 ppm balance N_2) 20 cc/min

N_2 dilute flow rate 80 cc/min

Total flow rate 100 cc/min

Inlet concentration : 400 ppm **Current :** 0.2 mA

			Peak Area		Concentration(ppm)		Removal Efficiency		
T, °C	V(kV)	P(W)	Outlet(0 mA)(avg)	Outlet(0.2 mA)	Cout(0 mA)	Cout(0.2 mA)	ψ,(-)	ψ'',(-)	ψ'',(-)
33	12.1	2.42	14799	0	392	0	1.00	1.00	1.02
33	12.1	2.42	14799	0	392	0	1.00	1.00	1.02
33	12.1	2.42	14799	0	392	0	1.00	1.00	1.02
100	9.8	1.96	14909	1059	395	31	0.92	0.92	1.15
100	9.8	1.96	14909	1088	395	32	0.92	0.92	1.15
100	9.8	1.96	14909	1111	395	33	0.92	0.92	1.15
150	9.0	1.80	14907	1082	395	32	0.92	0.92	1.30
150	7.7	1.54	14907	1055	395	31	0.92	0.92	1.30
150	7.7	1.54	14907	1048	395	31	0.92	0.92	1.30
200	6.5	1.30	14454	11035	383	293	0.27	0.23	0.37
200	6.5	1.30	14454	11103	383	295	0.26	0.23	0.36
200	6.5	1.30	14454	11602	383	308	0.23	0.20	0.31
300	4.2	0.84	14089	9116	374	243	0.39	0.35	0.68
300	4.2	0.84	14089	9003	374	240	0.40	0.36	0.69
300	4.2	0.84	14089	9153	374	244	0.39	0.35	0.67

Date : 10/3/2002

Subject : **Removal of CH_3CHO 400 ppm from N_2, I=0.3 mA**

Gas flow rate : CH_3CHO (2000 ppm balance N_2) 20 cc/min

N_2 dilute flow rate 80 cc/min

Total flow rate 100 cc/min

Inlet concentration : 400 ppm **Current :** 0.3 mA

			Peak Area		Concentration(ppm)		Removal Efficiency		
T, °C	V(kV)	P(W)	Outlet(0 mA)(avg)	Outlet(0.3 mA)	Cout(0 mA)	Cout(0.3 mA)	ψ,(-)	ψ'',(-)	ψ'',(-)
33	13.2	3.96	14157	0	376	0	1.00	1.00	1.02
33	13.2	3.96	14157	0	376	0	1.00	1.00	1.02
33	13.2	3.96	14157	0	376	0	1.00	1.00	1.02
100	10.4	3.12	14189	0	376	0	1.00	1.00	1.25
100	10.4	3.12	14189	0	376	0	1.00	1.00	1.25
100	10.4	3.12	14189	0	376	0	1.00	1.00	1.25
150	9.0	2.70	13761	619	365	20	0.95	0.95	1.33
150	9.0	2.70	13761	648	365	20	0.95	0.94	1.33
150	9.0	2.70	13761	619	365	20	0.95	0.95	1.33
200	7.2	2.16	13696	8366	363	223	0.44	0.39	0.61
200	7.2	2.16	13696	8326	363	222	0.44	0.39	0.61
200	7.2	2.16	13696	8235	363	220	0.45	0.40	0.62
300	5.5	1.65	13384	6647	355	178	0.55	0.50	0.96
300	5.5	1.65	13384	6392	355	171	0.57	0.52	1.00
300	5.5	1.65	13384	6505	355	174	0.56	0.51	0.98

Date : 26/3/2002

Subject : **Removal of CH_3CHO 400 ppm from N_2-O_2 5%, I=0.3 mA**

Gas flow rate :

CH_3CHO (2000 ppm balance N_2)	20	cc/min
O_2	5	cc/min
N_2 dilute flow rate	75	cc/min
Total flow rate	100	cc/min

Inlet concentration : 400 ppm **Current :** 0.3 mA

			Peak Area		Concentration(ppm)		Removal Efficiency		
T, ^oC	V(kV)	P(W)	Outlet(0 mA)(avg)	Outlet(0.3 mA)	Cout(0 mA)	Cout(0.3 mA)	ψ,(-)	ψ'',(-)	ψ'',(-)
33	13.9	4.17	14081	0	374	0	1.00	1.00	1.02
33	13.9	4.17	14081	0	374	0	1.00	1.00	1.02
33	13.9	4.17	14081	0	374	0	1.00	1.00	1.02
100	12.1	3.63	14101	0	374	0	1.00	1.00	1.25
100	12.1	3.63	14101	0	374	0	1.00	1.00	1.25
100	12.1	3.63	14101	0	374	0	1.00	1.00	1.25
150	10.8	3.24	13296	0	353	0	1.00	1.00	1.41
150	10.8	3.24	13296	0	353	0	1.00	1.00	1.41
200	9.9	2.97	13527	0	359	0	1.00	1.00	1.57
200	9.9	2.97	13527	0	359	0	1.00	1.00	1.57
200	9.9	2.97	13527	0	359	0	1.00	1.00	1.57
300	5.7	1.71	12605	5759	335	155	0.61	0.54	1.04
300	5.7	1.71	12605	5522	335	149	0.63	0.56	1.07
300	5.7	1.71	12605	5176	335	139	0.65	0.58	1.13

Date : 25/4/2002

Subject : **Removal of CH_3CHO 600 ppm from N_2-O_2(5%)-H_2O 5250 ppm, I=0.05 mA**

Gas flow rate :

CH_3CHO (2000 ppm balance N_2)	30	cc/min
O_2	5	cc/min
N_2 bubbling flow rate(water)	10	cc/min (water bath 34 °C)
N_2 dilute flow rate	55	cc/min
Total flow rate	100	cc/min

Inlet concentration : 600 ppm **Current :** 0.05 mA

			Peak Area		Concentration(ppm)		Removal Efficiency		
T, °C	V(kV)	P(W)	Outlet(0 mA)(avg)	Outlet(0.05 mA)	Cout(0 mA)	Cout(0.05 mA)	ψ,(-)	ψ",(-)	ψ",(-)
33	11.2	0.56	21321	6412	564	172	0.71	0.70	0.71
33	11.2	0.56	21321	6339	564	170	0.72	0.70	0.71
33	11.2	0.56	21321	6388	564	171	0.71	0.70	0.71
100	9.7	0.49	21939	5344	580	144	0.76	0.75	0.94
100	9.7	0.49	21939	5326	580	143	0.76	0.75	0.94
100	9.7	0.49	21939	5334	580	144	0.76	0.75	0.94
150	8.6	0.43	22389	5092	592	137	0.77	0.77	1.08
150	8.6	0.43	22389	5094	592	137	0.77	0.77	1.08
150	8.6	0.43	22389	5116	592	138	0.77	0.77	1.08
200	7.8	0.39	22144	6525	586	175	0.71	0.70	1.10
200	7.8	0.39	22144	6489	586	174	0.71	0.70	1.10
200	7.8	0.39	22144	6424	586	172	0.71	0.71	1.11
300	unstable		20521	-	543	-	-	-	-

Date : 22/4/2002

Subject : **Removal of CH_3CHO 600 ppm from N_2-O_2(5%)-H2O 10499 ppm, I=0.05 mA**

CH_3CHO (2000 ppm balance

Gas flow rate :

N_2) 30 cc/min

O_2 5 cc/min

N_2 bubbling flow rate(water) 20 cc/min (water bath 34 °C)

N_2 dilute flow rate 45 cc/min

Total flow rate 100 cc/min

Inlet concentration : 600 ppm **Current :** 0.05 mA

			Peak Area		Concentration(ppm)		Removal Efficiency		
T, °C	V(kV)	P(W)	Outlet(0 mA)(avg)	Outlet(0.05 mA)	Cout(0 mA)	Cout(0.05 mA)	ψ,(-)	ψ'',(-)	ψ'',(-)
33	11.1	0.56	22626	5316	598	143	0.76	0.76	0.77
33	11.1	0.56	22626	5566	598	150	0.75	0.75	0.76
33	11.1	0.56	22626	5622	598	151	0.75	0.75	0.76
100	9.7	0.49	22716	5351	601	144	0.76	0.76	0.95
100	9.7	0.49	22716	5464	601	147	0.76	0.76	0.94
100	9.7	0.49	22716	5527	601	149	0.75	0.75	0.94
150	8.7	0.44	22513	4830	595	130	0.78	0.78	1.10
150	8.7	0.44	22513	4769	595	129	0.79	0.78	1.11
150	8.7	0.44	22513	4814	595	130	0.78	0.78	1.10
200	7.9	0.40	22514	5491	595	148	0.75	0.75	1.18
200	7.9	0.40	22514	5596	595	150	0.75	0.75	1.17
200	7.9	0.40	22514	5464	595	147	0.76	0.75	1.18
300	unstable		20726	-	548	-	-	-	-

Date : 23/4/2002

Subject : **Removal of CH_3CHO 600 ppm from N_2-O_2(5%)-H_2O 21838 ppm, I=0.05 mA**

CH_3CHO (2000 ppm balance

Gas flow rate :

N_2)	30	cc/min
O_2	5	cc/min
N_2 bubbling flow rate(water)	30	cc/min (water bath 40 °C)
N_2 dilute flow rate	35	cc/min
Total flow rate	100	cc/min

Inlet concentration : 600 ppm **Current :** 0.05 mA

			Peak Area		Concentration(ppm)		Removal Efficiency		
T, °C	V(kV)	P(W)	Outlet(0 mA)(avg)	Outlet(0.05 mA)	Cout(0 mA)	Cout(0.05 mA)	ψ,(-)	ψ",(-)	ψ",(-)
33	11.2	0.56	21464	5172	568	139	0.77	0.75	0.77
33	11.2	0.56	21464	5330	568	143	0.76	0.75	0.76
33	11.2	0.56	21464	5604	568	151	0.75	0.73	0.75
100	9.8	0.49	22459	4648	594	126	0.79	0.79	0.99
100	9.8	0.49	22459	4657	594	126	0.79	0.79	0.99
100	9.8	0.49	22459	4672	594	126	0.79	0.79	0.98
150	8.8	0.44	21773	3984	576	108	0.82	0.81	1.15
150	8.8	0.44	21773	3966	576	108	0.82	0.81	1.15
150	8.8	0.44	21773	4007	576	109	0.82	0.81	1.14
200	7.9	0.40	21879	4965	579	134	0.78	0.77	1.21
200	7.9	0.40	21879	5076	579	137	0.77	0.76	1.20
200	7.9	0.40	21879	4956	579	134	0.78	0.77	1.21
300	unstable		21091	-	558	-	-	-	-

Date : 21/4/2002

Subject : **Removal of CH_3CHO 600 ppm from N_2-O_2(5%)-H_2O 5250 ppm, I=0.2 mA**

Gas flow rate :

CH_3CHO (2000 ppm balance	30	cc/min
O_2	5	cc/min
N_2 bubbling flow rate(water)	10	cc/min (water bath 34 °C)
N_2 dilute flow rate	55	cc/min
Total flow rate	100	cc/min

Inlet concentration : 600 ppm **Current :** 0.2 mA

			Peak Area		Concentration(ppm)		Removal Efficiency		
T, °C	V(kV)	P(W)	Outlet(0 mA)(avg)	Outlet(0.2 mA)	Cout(0 mA)	Cout(0.2 mA)	ψ,(-)	ψ'',(-)	ψ'',(-)
33	13.0	2.60	22417	0	593	0	1.00	1.00	1.02
33	13.0	2.60	22417	0	593	0	1.00	1.00	1.02
33	13.0	2.60	22417	0	593	0	1.00	1.00	1.02
100	11.4	2.28	22394	0	592	0	1.00	1.00	1.25
100	11.4	2.28	22394	0	592	0	1.00	1.00	1.25
100	11.4	2.28	22394	0	592	0	1.00	1.00	1.25
150	10.3	2.06	22485	0	595	0	1.00	1.00	1.41
150	10.3	2.06	22485	0	595	0	1.00	1.00	1.41
150	10.3	2.06	22485	0	595	0	1.00	1.00	1.41
200	9.3	1.86	22603	0	598	0	1.00	1.00	1.57
200	9.3	1.86	22603	0	598	0	1.00	1.00	1.57
200	9.3	1.86	22603	0	598	0	1.00	1.00	1.57
300	5.9	1.18	20745	12398	549	329	0.45	0.40	0.70
300	5.9	1.18	20745	12458	549	331	0.45	0.40	0.70
300	4.1	0.82	20745	12542	549	333	0.44	0.39	0.69

Date : 22/4/2002

Subject : **Removal of CH_3CHO 600 ppm from N_2-O_2(5%)-H_2O 10499 ppm, I=0.2 mA**

Gas flow rate :

CH_3CHO (2000 ppm balance	30	cc/min
O_2	5	cc/min
N_2 bubbling flow rate(water)	20	cc/min (water bath 34 °C)
N_2 dilute flow rate	45	cc/min
Total flow rate	100	cc/min

Inlet concentration : 600 ppm **Current :** 0.2 mA

			Peak Area		Concentration(ppm)		Removal Efficiency		
T, °C	V(kV)	P(W)	Outlet(0 mA)(avg)	Outlet(0.2 mA)	Cout(0 mA)	Cout(0.2 mA)	ψ,(-)	ψ'',(-)	ψ'',(-)
33	13.1	2.62	22626	0	598	0	1.00	1.00	1.02
33	13.1	2.62	22626	0	598	0	1.00	1.00	1.02
33	13.1	2.62	22626	0	598	0	1.00	1.00	1.02
100	11.4	2.28	22716	0	601	0	1.00	1.00	1.25
100	11.4	2.28	22716	0	601	0	1.00	1.00	1.25
100	11.4	2.28	22716	0	601	0	1.00	1.00	1.25
150	10.5	2.10	22513	0	595	0	1.00	1.00	1.41
150	10.5	2.10	22513	0	595	0	1.00	1.00	1.41
150	10.5	2.10	22513	0	595	0	1.00	1.00	1.41
200	9.4	1.88	22514	0	595	0	1.00	1.00	1.57
200	9.4	1.88	22514	0	595	0	1.00	1.00	1.57
200	9.4	1.88	22514	0	595	0	1.00	1.00	1.57
300	6.1	1.22	20726	12070	548	321	0.47	0.42	0.80
300	6.1	1.22	20726	12194	548	324	0.46	0.41	0.79
300	6.1	1.22	20726	12324	548	327	0.45	0.40	0.78

Date : 23/4/2002

Subject : **Removal of CH_3CHO 600 ppm from N_2-O_2(5%)-H_2O 21838 ppm, I=0.2 mA**

Gas flow rate :	CH_3CHO (2000 ppm balance N_2)	30 cc/min
	O_2	5 cc/min
	N_2 bubbling flow rate(water)	30 cc/min (water bath 40 °C)
	N_2 dilute flow rate	35 cc/min
	Total flow rate	100 cc/min

Inlet concentration : 600 ppm **Current :** 0.2 mA

			Peak Area		Concentration(ppm)		Removal Efficiency		
T, °C	V(kV)	P(W)	Outlet(0 mA)(avg)	Outlet(0.2 mA)	Cout(0 mA)	Cout(0.2 mA)	ψ,(-)	ψ'',(-)	ψ'',(-)
33	13.1	2.62	21464	0	568	0	1.00	1.00	1.02
33	13.1	2.62	21464	0	568	0	1.00	1.00	1.02
33	13.1	2.62	21464	0	568	0	1.00	1.00	1.02
100	11.5	2.30	22459	0	594	0	1.00	1.00	1.25
100	11.5	2.30	22459	0	594	0	1.00	1.00	1.25
100	11.5	2.30	22459	0	594	0	1.00	1.00	1.25
150	10.4	2.08	21773	0	576	0	1.00	1.00	1.41
150	10.4	2.08	21773	0	576	0	1.00	1.00	1.41
150	10.4	2.08	21773	0	576	0	1.00	1.00	1.41
200	9.4	1.88	21879	0	579	0	1.00	1.00	1.57
200	9.4	1.88	21879	0	579	0	1.00	1.00	1.57
200	9.4	1.88	21879	0	579	0	1.00	1.00	1.57
300	6.3	1.26	21091	11968	558	318	0.47	0.43	0.83
300	6.3	1.26	21091	12109	558	322	0.46	0.42	0.82
300	6.3	1.26	21091	12019	558	319	0.47	0.43	0.83

Date : **30/3/2002**

Subject Removal of CH_3CHO 600 ppm form N_2-O_2 5%, I=0.2 mA

Gas flow rate :	CH_3CHO (2000 ppm balance N_2)	30	cc/min
	O_2	5	cc/min
	N_2 dilute flow rate	65	cc/min
	Total flow rate	100	cc/min
Inlet concentration	600 ppm	**Current :**	0.2 mA

			Peak Area		Concentration(ppm)		Removal Efficiency		
T, ^oC	V(kV)	P(W)	Outlet(0 mA)(avg)	Outlet(0.2	Cout(0 mA)	Cout(0.2 mA)	ψ,(-)	ψ",(-)	ψ",(-)
33	13.2	2.64	21298	0	563	0	1.00	1.00	1.02
33	13.2	2.64	21298	0	563	0	1.00	1.00	1.02
33	13.2	2.64	21298	0	563	0	1.00	1.00	1.02
100	11.4	2.28	21969	0	581	0	1.00	1.00	1.25
100	11.4	2.28	21969	0	581	0	1.00	1.00	1.25
100	11.4	2.28	21969	0	581	0	1.00	1.00	1.25
150	10.3	2.06	21367	0	565	0	1.00	1.00	1.41
150	10.3	2.06	21367	0	565	0	1.00	1.00	1.41
150	10.3	2.06	21367	0	565	0	1.00	1.00	1.41
200	9.5	1.90	21949	0	580	0	1.00	1.00	1.57
200	9.5	1.90	21949	0	580	0	1.00	1.00	1.57
200	9.5	1.90	21949	0	580	0	1.00	1.00	1.57
300	6	1.20	20090	12561	532	334	0.44	0.37	0.72
300	6	1.20	20090	12561	532	334	0.44	0.37	0.72
300	6	1.20	20090	12561	532	334	0.44	0.37	0.72

Date : 1/4/2002

Subject : Removal of $CH3CHO$ 600 ppm form N2-O2 10%, I=0.2 mA

Gas flow rate :	CH_3CHO (2000 ppm balance N_2)	30	cc/min
	O_2	10	cc/min
	N_2 dilute flow rate	60	cc/min
	Total flow rate	100	cc/min

Inlet concentration : 600 ppm **Current :** 0.2 mA

			Peak Area		Concentration(ppm)		Removal Efficiency		
T, ^oC	V(kV)	P(W)	Outlet(0 mA)(avg)	Outlet(0.2 mA)	Cout(0 mA)	Cout(0.2 mA)	ψ,(-)	ψ",(-)	ψ",(-)
33	13.1	2.62	21129	0	559	0	1.00	1.00	1.02
33	13.1	2.62	21129	0	559	0	1.00	1.00	1.02
33	13.1	2.62	21129	0	559	0	1.00	1.00	1.02
100	11.4	2.28	22262	0	589	0	1.00	1.00	1.25
100	11.4	2.28	22262	0	589	0	1.00	1.00	1.25
100	11.4	2.28	22262	0	589	0	1.00	1.00	1.25
150	10.3	2.06	22011	0	582	0	1.00	1.00	1.41
150	10.3	2.06	22011	0	582	0	1.00	1.00	1.41
200	9.4	1.88	21929	0	580	0	1.00	1.00	1.57
200	9.4	1.88	21929	0	580	0	1.00	1.00	1.57
200	9.4	1.88	21929	0	580	0	1.00	1.00	1.57
300	7.7	1.54	19883	0	526	0	1.00	1.00	1.93
300	7.7	1.54	19883	0	526	0	1.00	1.00	1.93
300	7.7	1.54	19883	0	526	0	1.00	1.00	1.93

Date : 1/4/2002

Subject : **Removal of CH_3CHO 600 ppm form N_2-O_2 (20%), I=0.2 mA**

Gas flow rate :	CH_3CHO (2000 ppm balance N_2)	30	cc/min
	O_2	20	cc/min
	N_2 dilute flow rate	50	cc/min
	Total flow rate	100	cc/min

Inlet concentration : 600 ppm **Current :** 0.2 mA

			Peak Area		Concentration(ppm)		Removal Efficiency		
T, °C	V(kV)	P(W)	Outlet(0 mA)(avg)	Outlet(0.2 mA)	Cout(0 mA)	Cout(0.2 mA)	ψ,(-)	ψ",(-)	ψ",(-)
33	12.9	2.58	21591	496	571	16	0.97	0.97	0.99
33	12.9	2.58	21591	497	571	16	0.97	0.97	0.99
33	12.9	2.58	21591	439	571	15	0.98	0.97	0.99
100	11.2	2.24	22466	0	594	0	1.00	1.00	1.25
100	11.2	2.24	22466	0	594	0	1.00	1.00	1.25
100	11.2	2.24	22466	0	594	0	1.00	1.00	1.25
150	10.2	2.04	21037	0	556	0	1.00	1.00	1.41
150	10.2	2.04	21037	0	556	0	1.00	1.00	1.41
200	9.2	1.84	21831	0	577	0	1.00	1.00	1.57
200	9.2	1.84	21831	0	577	0	1.00	1.00	1.57
200	9.2	1.84	21831	0	577	0	1.00	1.00	1.57
300	7.8	1.56	20301	0	537	0	1.00	1.00	1.93
300	7.8	1.56	20301	0	537	0	1.00	1.00	1.93
300	7.8	1.56	20301	0	537	0	1.00	1.00	1.93

Date : 30/4/2002

Subject : **Removal of CH_3CHO 600 ppm form N_2-O_2 (20%), I=0.05 mA**

Gas flow rate :
CH_3CHO (2000 ppm balance N_2) 30 cc/min
O_2 20 cc/min
N_2 dilute flow rate cc/min
Total flow rate 100 cc/min

Inlet concentration : 600 ppm **Current :** 0.05 mA

			Peak Area		Concentration(ppm)		Removal Efficiency		
T, ^oC	V(kV)	P(W)	Outlet(0 mA)(avg)	Outlet(0.2 mA)	Cout(0 mA)	Cout(0.2 mA)	ψ,(-)	ψ",(-)	ψ",(-)
33	10.9	0.55	21688	6721	574	180	0.70	0.69	0.70
33	10.9	0.55	21688	6790	574	182	0.70	0.68	0.70
33	10.9	0.55	21688	6727	574	180	0.70	0.69	0.70
100	9.6	0.48	22593	3394	597	93	0.85	0.85	1.06
100	9.6	0.48	22593	3370	597	92	0.85	0.85	1.06
100	9.6	0.48	22593	3387	597	92	0.85	0.85	1.06
150	8.6	0.43	21900	1905	579	53	0.91	0.91	1.28
150	8.6	0.43	21900	1922	579	54	0.91	0.91	1.28
150	8.6	0.43	21900	1916	579	54	0.91	0.91	1.28
200	7.9	0.40	21937	1036	580	31	0.95	0.95	1.49
200	7.9	0.40	21937	965	580	29	0.95	0.95	1.49
200	7.9	0.40	21937	994	580	29	0.95	0.95	1.49
300	6.6	0.33	20915	4602	553	124	0.79	0.78	1.50
300	6.6	0.33	20915	4353	553	118	0.80	0.79	1.52
300	6.6	0.33	20915	4545	553	123	0.80	0.78	1.50

Date : 29/4/2002

Subject : **Removal of CH_3CHO 600 ppm from N_2-O_2 (10%), I=0.05 mA**

Gas flow rate : CH_3CHO (2000 ppm balance N_2) 30 cc/min
O_2 10 cc/min
N_2 dilute flow rate 60 cc/min
Total flow rate 100 cc/min

Inlet concentration : 600 ppm **Current :** 0.05 mA

			Peak Area		Concentration(ppm)		Removal Efficiency		
T, ^oC	V(kV)	P(W)	Outlet(0 mA)(avg)	Outlet(0.2 mA)	Cout(0 mA)	Cout(0.2 mA)	ψ,(-)	ψ",(-)	ψ",(-)
33	11.1	0.56	21987	5574	581	150	0.75	0.74	0.76
33	11.1	0.56	21987	5502	581	148	0.75	0.75	0.76
33	11.1	0.56	21987	5501	581	148	0.75	0.75	0.76
100	9.7	0.49	22321	3894	590	106	0.82	0.82	1.03
100	9.7	0.49	22321	3875	590	105	0.82	0.82	1.03
100	9.7	0.49	22321	3840	590	104	0.83	0.82	1.03
150	8.7	0.44	22569	2582	597	71	0.88	0.88	1.24
150	8.7	0.44	22569	2561	597	71	0.88	0.88	1.24
150	8.7	0.44	22569	2531	597	70	0.88	0.88	1.25
200	8.0	0.40	21756	1736	575	49	0.92	0.91	1.44
200	8.0	0.40	21756	1722	575	49	0.92	0.92	1.44
200	8.0	0.40	21756	1704	575	48	0.92	0.92	1.44
300	unstable		20251	-	-	-	-	-	-

Date : 28/4/2002

Subject : **Removal of CH_3CHO 600 ppm from N_2-O_2 (5%), I=0.05 mA**

Gas flow rate :

CH_3CHO (2000 ppm balance N_2)	30	cc/min
O_2	5	cc/min
N_2 dilute flow rate	65	cc/min
Total flow rate	100	cc/min

Inlet concentration : 600 ppm **Current :** 0.05 mA

			Peak Area		Concentration(ppm)		Removal Efficiency		
T, ^oC	V(kV)	P(W)	Outlet(0 mA)(avg)	Outlet(0.2 mA)	Cout(0 mA)	Cout(0.2 mA)	ψ,(-)	ψ",(-)	ψ",(-)
33	11.2	0.56	22924	6172	606	166	0.72	0.73	0.74
33	11.2	0.56	22924	6103	606	164	0.73	0.73	0.74
33	11.2	0.56	22924	5976	606	160	0.73	0.74	0.75
100	9.7	0.49	23020	4445	609	120	0.80	0.80	1.00
100	9.7	0.49	23020	4415	609	119	0.80	0.80	1.00
100	9.7	0.49	23020	4383	609	119	0.80	0.81	1.01
150	8.6	0.43	22339	3822	591	104	0.83	0.82	1.16
150	8.6	0.43	22339	3830	591	104	0.83	0.82	1.16
150	8.6	0.43	22339	3770	591	102	0.83	0.83	1.17
200	7.8	0.39	22525	4945	596	133	0.78	0.78	1.22
200	7.8	0.39	22525	4981	596	134	0.78	0.77	1.22
200	7.8	0.39	22525	4991	596	135	0.78	0.77	1.22
300	unstable		20906	-	553	-	-	-	-

Date : 10/9/2002

Subject : **Removal of CH_3CHO 1000 ppm from N_2, I=0.2 mA**

Gas flow rate : CH_3CHO (2000 ppm balance N_2) 50 cc/min

N_2 dilute flow rate 50 cc/min

Total flow rate 100 cc/min

Inlet concentration : 1000 ppm **Current :** 0.2 mA

			Peak Area		Concentration(ppm)		Removal Efficiency		
T, °C	V(kV)	P(W)	Outlet(0 mA)(avg)	Outlet(0.2 mA)	Cout(0 mA)	Cout(0.2 mA)	ψ,(-)	ψ'',(-)	ψ'',(-)
33	12.3	2.46	30861	1559	963	49	0.95	0.95	0.97
33	12.3	2.46	30861	1461	963	46	0.95	0.95	0.97
33	12.3	2.46	30861	1460	963	46	0.95	0.95	0.97
100	10.1	2.02	31091	5514	970	172	0.83	0.82	1.03
100	10.1	2.02	31091	5529	970	172	0.83	0.82	1.03
100	10.1	2.02	31091	5351	970	167	0.83	0.83	1.03
200	7.0	1.40	31283	15357	976	479	0.52	0.51	0.80
200	7.0	1.40	31283	15060	976	470	0.53	0.52	0.81
200	7.0	1.40	31283	15721	976	490	0.51	0.50	0.78
300	4.4	0.88	31874	25124	994	784	0.22	0.21	0.41
300	4.4	0.88	31874	25314	994	790	0.21	0.21	0.40
300	4.4	0.88	31874	25162	994	785	0.22	0.21	0.41

Date : 8/4/2002

Subject : **Removal of CH3CHO 600 ppm form N2-H2O 5250 ppm, I=0.2 mA**

Gas flow rate :	CH_3CHO (2000 ppm)	30	cc/min
	N_2 bubbling flow rate (water)	10	cc/min (water bath 34 °C)
	N_2 dilute flow rate	60	cc/min
	Total flow rate	100	cc/min

Inlet concentration : 600 ppm **Current :** 0.2 mA

			Peak Area		Concentration(ppm)		Removal Efficiency		
T, °C	V(kV)	P(W)	Outlet(0 mA)(avg)	Outlet(0.2 mA)	Cout(0 mA)	Cout(0.2 mA)	ψ,(-)	ψ'',(-)	ψ'',(-)
33	12.8	2.56	20465	530	541	17	0.97	0.97	0.99
33	12.8	2.56	20465	554	541	18	0.97	0.97	0.98
33	12.8	2.56	20465	613	541	19	0.97	0.96	0.98
100	10.3	2.06	20270	1344	536	39	0.94	0.93	1.16
100	10.3	2.06	20270	1420	536	41	0.93	0.92	1.16
100	10.3	2.06	20270	1311	536	38	0.94	0.93	1.16
150	9.0	1.80	20898	2226	553	62	0.90	0.89	1.25
150	9.0	1.80	20898	2323	553	64	0.89	0.88	1.25
150	9.0	1.80	20898	2130	553	59	0.90	0.89	1.26
200	8.0	1.60	20774	3161	550	86	0.86	0.84	1.32
200	8.0	1.60	20774	3332	550	91	0.85	0.83	1.31
200	8.0	1.60	20774	3031	550	83	0.86	0.85	1.33
300	3.9	0.78	20185	15056	534	399	0.33	0.25	0.49
300	3.9	0.78	20185	15144	534	401	0.33	0.25	0.48
300	3.9	0.78	20185	14798	534	392	0.35	0.27	0.51

Date : 9/4/2002

Subject : **Removal of CH3CHO 600 ppm form N_2-H_2O (10499 ppm), I=0.2 mA**

Gas flow rate :	CH_3CHO (2000 ppm)	30	cc/min
	N_2 bubbling flow rate(water)	20	cc/min (water bath 34 C)
	N_2 dilute flow rate	60	cc/min
	Total flow rate	100	cc/min
Inlet concentration :	600 ppm	**Current :**	0.2 mA

			Peak Area		Concentration(ppm)		Removal Efficiency		
T, ^{o}C	V(kV)	P(W)	Outlet(0 mA)(avg)	Outlet(0.2 mA)	Cout(0 mA)	Cout(0.2 mA)	ψ,(-)	ψ'',(-)	ψ'',(-)
33	12.7	2.54	21034	504	556	17	0.97	0.97	0.99
33	12.7	2.54	21034	485	556	16	0.97	0.97	0.99
33	12.7	2.54	21034	491	556	16	0.97	0.97	0.99
100	10.5	2.10	21588	1145	571	33	0.94	0.94	1.18
100	10.5	2.10	21588	1198	571	35	0.94	0.94	1.17
100	10.5	2.10	21588	1119	571	33	0.95	0.94	1.18
150	9.2	1.84	20636	1525	546	43	0.93	0.92	1.30
150	9.2	1.84	20636	1560	546	44	0.93	0.92	1.30
150	9.2	1.84	20636	1556	546	44	0.93	0.92	1.30
200	8.0	1.60	21202	3252	561	89	0.85	0.84	1.32
200	8.0	1.60	21202	3268	561	89	0.85	0.84	1.32
200	8.0	1.60	21202	3366	561	92	0.85	0.84	1.31
300	3.9	0.78	20541	16011	543	424	0.29	0.22	0.42
300	3.9	0.78	20541	16209	543	429	0.28	0.21	0.40
300	3.9	0.78	20541	16182	543	429	0.29	0.21	0.41

Date : 20/4/2002

Subject : **Removal of CH_3CHO 600 ppm form N_2-H_2O (21838 ppm), I=0.2 mA**

Gas flow rate :	CH_3CHO (2000 ppm)	30	cc/min
	N_2 bubbling flow rate(water)	30	cc/min (water bath 40 °C)
	N_2 dilute flow rate	40	cc/min
	Total flow rate	100	cc/min
Inlet concentration :	600 ppm	**Current :**	0.2 mA

			Peak Area		Concentration(ppm)		Removal Efficiency		
T, °C	V(kV)	P(W)	Outlet(0 mA)(avg)	Outlet(0.2 mA)	Cout(0 mA)	Cout(0.2 mA)	ψ,(-)	ψ'',(-)	ψ'',(-)
33	12.8	2.56	22709	490	600	16	0.97	0.97	0.99
33	12.8	2.56	22709	480	600	16	0.97	0.97	0.99
33	12.8	2.56	22709	531	600	17	0.97	0.97	0.99
100	10.6	2.12	23010	1160	608	34	0.94	0.94	1.18
100	10.6	2.12	23010	1172	608	34	0.94	0.94	1.18
100	10.6	2.12	23010	1184	608	34	0.94	0.94	1.18
150	9.2	1.84	22752	1924	602	54	0.91	0.91	1.28
150	9.2	1.84	22752	1979	602	55	0.91	0.91	1.28
150	9.2	1.84	22752	1939	602	54	0.91	0.91	1.28
200	8.2	1.64	23193	2352	613	65	0.89	0.89	1.40
200	8.2	1.64	23193	2394	613	66	0.89	0.89	1.40
200	8.2	1.64	23193	2396	613	66	0.89	0.89	1.40
300	4.1	0.82	22512	16357	595	433	0.28	0.27	0.52
300	4.1	0.82	22512	16174	595	429	0.29	0.28	0.54
300	4.1	0.82	22512	16460	595	436	0.27	0.27	0.52

Date : 10/9/2002

Subject : **Removal of CH_3CHO 1000 ppm from N_2, I=0.3 mA**

Gas flow rate : CH_3CHO (2000 ppm balance N_2) 50 cc/min

N_2 dilute flow rate 50 cc/min

Total flow rate 100 cc/min

Inlet concentration : 600 ppm **Current :** 0.3 mA

			Peak Area		Concentration(ppm)		Removal Efficiency		
T, °C	V(kV)	P(W)	Outlet(0 mA)(avg)	Outlet(0.3 mA)	Cout(0 mA)	Cout(0.3 mA)	ψ,(-)	ψ'',(-)	ψ'',(-)
33	13	3.90	30861	655	963	20	0.98	0.98	1.00
33	13	3.90	30861	639	963	20	0.98	0.98	1.00
33	13	3.90	30861	645	963	20	0.98	0.98	1.00
100	10.6	3.18	31091	3695	970	115	0.88	0.88	1.10
100	10.6	3.18	31091	3766	970	117	0.88	0.88	1.10
100	10.6	3.18	31091	3793	970	118	0.88	0.88	1.10
200	6.7	2.01	31283	21544	976	672	0.33	0.31	0.49
200	6.7	2.01	31283	21891	976	683	0.32	0.30	0.47
200	6.7	2.01	31283	21730	976	678	0.32	0.31	0.48
300	4.8	1.44	31874	22592	994	705	0.30	0.29	0.56
300	4.8	1.44	31874	22527	994	703	0.30	0.29	0.57
300	4.8	1.44	31874	22396	994	699	0.30	0.30	0.57

Date: 10/9/2002

Subject : **Removal of CH3CHO 1000 ppm from N2, I=0.5 mA**

Gas flow rate :

CH_3CHO (2000 ppm balance N_2)	50	cc/min
N_2 dilute flow rate	50	cc/min
Total flow rate	100	cc/min

Inlet concentration : 1000 ppm **Current :** 0.5 mA

			Peak Area		Concentration(ppm)		Removal Efficiency		
T, °C	V(kV)	P(W)	Outlet(0 mA)(avg)	Outlet(0.5 mA)	Cout(0 mA)	Cout(0.5 mA)	ψ,(-)	ψ'',(-)	ψ'',(-)
33	14.1	7.05	30861	286	963	9	0.99	0.99	1.01
33	14.1	7.05	30861	249	963	8	0.99	0.99	1.01
33	14.1	7.05	30861	232	963	7	0.99	0.99	1.01
100	11.4	5.70	31091	1265	970	39	0.96	0.96	0.98
100	11.4	5.70	31091	1280	970	40	0.96	0.96	0.98
100	11.4	5.70	31091	1296	970	40	0.96	0.96	0.98
200	8.3	4.15	31283	4984	976	155	0.84	0.84	0.86
200	8.3	4.15	31283	5102	976	159	0.84	0.84	0.85
200	8.3	4.15	31283	5032	976	157	0.84	0.84	0.85
300	5.6	2.80	31874	17845	994	557	0.44	0.44	0.45
300	5.6	2.80	31874	17717	994	553	0.45	0.44	0.45
300	5.6	2.80	31874	17867	994	557	0.44	0.44	0.45

APPENDIX E

Ammonia Removal

Date : 18/9/2002

Subject : **Removal of NH_3 250 ppm from N_2,I=0.3 mA**

Gas flow rate : NH_3 (2000 ppm balance N_2) 12.5 cc/min

N2 dilute flow rate 87.5 cc/min

Total flow rate 100 cc/min

Inlet concentration : 250 ppm **Current :** 0.3 mA

			Peak Area		Concentration(ppm)		Removal Efficiency		
T, °C	V(kV)	P(W)	Outlet(0 mA)(avg)	Outlet(0.3 mA)	Cout(0 mA)	Cout(0.3 mA)	ψ,(-)	ψ',(-)	ψ'',(-)
33	8.4	2.52	354	250	211	161	0.35	0.23	0.24
33	8.4	2.52	354	262	211	167	0.33	0.20	0.21
33	8.4	2.52	354	275	211	174	0.30	0.17	0.18
100	7.3	2.19	379	283	221	178	0.29	0.20	0.25
100	7.3	2.19	379	296	221	184	0.26	0.17	0.21
100	7.3	2.19	379	280	221	176	0.30	0.20	0.26
200	6.0	1.80	415	191	237	130	0.48	0.45	0.71
200	6.0	1.80	415	189	237	129	0.48	0.45	0.71
200	6.0	1.80	415	176	237	122	0.51	0.48	0.76
300	4.5	1.35	328	220	199	146	0.42	0.27	0.42
300	4.5	1.35	328	222	199	147	0.41	0.26	0.41

Date : 22/9/2002

Subject : **Removal of NH3 250 ppm from N_2,I=0.5 mA**

Gas flow rate : NH_3 (2000 ppm balance N_2) 12.5 cc/min

N_2 dilute flow rate 87.5 cc/min

Total flow rate 100 cc/min

Inlet concentration : 250 ppm Current : 0.5 mA

			Peak Area		Concentration(ppm)		Removal Efficiency		
T, °C	V(kV)	P(W)	Outlet(0 mA)(avg)	Outlet(0.5 mA)	Cout(0 mA)	Cout(0.5 mA)	ψ,(-)	ψ',(-)	ψ'',(-)
33	9	4.50	336	268	202	170	0.32	0.16	0.16
33	9	4.50	336	267	202	170	0.32	0.16	0.16
33	9	4.50	336	261	202	167	0.33	0.18	0.18
100	8.1	4.05	378	254	221	163	0.35	0.26	0.33
100	8.1	4.05	378	243	221	158	0.37	0.29	0.36
100	8.1	4.05	378	241	221	157	0.37	0.29	0.36
200	6.3	3.15	448	242	250	157	0.37	0.37	0.58
200	6.3	3.15	448	259	250	166	0.34	0.34	0.53
200	6.3	3.15	448	250	250	161	0.35	0.36	0.56
300	4.5	2.25	443	176	248	122	0.51	0.51	0.80
300	4.5	2.25	443	193	248	131	0.47	0.47	0.74
300	4.5	2.25	443	181	248	125	0.50	0.50	0.78

Date : 19/9/2002

Subject : **Removal of NH3 400 ppm from N_2,I=0.5 mA**

Gas flow rate : NH_3 (2000 ppm balance N_2) 20cc/min

N_2 dilute flow rate 80cc/min

Total flow rate 100cc/min

Inlet concentration : 400 ppm **Current :** 0.5 mA

			Peak Area		Concentration(ppm)		Removal Efficiency		
T, ^oC	V(kV)	P(W)	Outlet(0 mA)(avg)	Outlet(0.5 mA)	Cout(0 mA)	Cout(0.5 mA)	ψ,(-)	ψ',(-)	ψ'',(-)
33	9.2	4.60	776	668	368	332	0.17	0.10	0.10
33	9.2	4.60	776	631	368	319	0.20	0.13	0.14
100	8.3	4.15	809	610	379	312	0.22	0.18	0.22
100	8.3	4.15	809	617	379	314	0.21	0.17	0.21
200	6.5	3.25	824	581	383	301	0.25	0.21	0.34
200	6.5	3.25	824	572	383	298	0.25	0.22	0.35
300	4.6	2.30	853	434	393	245	0.39	0.38	0.73
300	4.6	2.30	853	427	393	242	0.40	0.38	0.74
300	4.6	2.30	853	413	393	236	0.41	0.40	0.77

Date : 21/9/2002

Subject : **Removal of NH3 1000 ppm from N_2,I=0.5 mA**

Gas flow rate : NH_3 (2000 ppm balance N_2) 50cc/min

N2 dilute flow rate 50cc/min

Total flow rate 100cc/min

Inlet concentration : 1000 ppm **Current :** 0.5 mA

			Peak Area		Concentration(ppm)		Removal Efficiency		
T, ^oC	V(kV)	P(W)	Outlet(0 mA)(avg)	Outlet(0.5 mA)	Cout(0 mA)	Cout(0.5 mA)	ψ,(-)	ψ',(-)	ψ'',(-)
33	8.9	4.45	3743	3150	969	874	0.13	0.10	0.10
33	8.9	4.45	3743	3211	969	884	0.12	0.09	0.09
33	8.9	4.45	3743	3248	969	889	0.11	0.08	0.08
100	7.7	3.85	3841	3320	986	901	0.10	0.09	0.11
100	7.7	3.85	3841	3255	986	891	0.11	0.10	0.12
200	5.6	2.80	3909	3041	997	857	0.14	0.14	0.22
200	5.6	2.80	3909	3107	997	867	0.13	0.13	0.20
300	4.4	2.20	3785	2473	976	770	0.23	0.21	0.41
300	4.4	2.20	3785	2461	976	768	0.23	0.21	0.41
300	4.4	2.20	3785	2505	976	775	0.23	0.21	0.40

Date : 2/10/2002

Subject : **Removal of NH3 400 ppm from N_2-O2(20%) ,I=0.1 mA**

Gas flow rate :	NH_3 (2000 ppm balance N_2)	20 cc/min
	O2	20 cc/min
	N2 dilute flow rate	60 cc/min
	Total flow rate	100 cc/min

Inlet concentration : 400 ppm **Current :** 0.1 mA

			Peak Area		Concentration(ppm)		Removal Efficiency		
T, °C	V(kV)	P(W)	Outlet(0 mA)(avg)	Outlet(0.1 mA)	Cout(0 mA)	Cout(0.1 mA)	ψ,(-)	ψ',(-)	ψ'',(-)
33	11.3	1.13	700	-	343	125	0.69	0.64	0.65
100	10.1	1.01	764	-	364	125	0.69	0.66	0.82
200	8.4	0.84	752	-	360	55	0.86	0.85	1.33
300	6.3	0.63	689	369	339	217	0.46	0.36	0.70

Date : 4/10/2002

Subject : **Removal of NH3 400 ppm from N_2-O2(10%) ,I=0.1 mA**

Gas flow rate :	NH_3 (2000 ppm balance N_2)	20cc/min
	O2	10cc/min
	N2 dilute flow rate	70cc/min
	Total flow rate	100cc/min

Inlet concentration : 400 ppm **Current :** 0.1 mA

			Peak Area		Concentration(ppm)		Removal Efficiency		
T, ^{o}C	V(kV)	P(W)	Outlet(0 mA)(avg)	Outlet(0.1 mA)	Cout(0 mA)	Cout(0.1 mA)	ψ,(-)	ψ',(-)	ψ'',(-)
33	11.4	1.14	763	-	364	150	0.63	0.59	0.60
100	10.0	1.00	718	-	349	120	0.70	0.66	0.82
200	7.8	0.78	732	392	354	227	0.43	0.36	0.56
300	6.0	0.60	554	417	292	238	0.41	0.18	0.36

Date : 5/10/2002

Subject : **Removal of NH3 400 ppm from N_2-O_2(5%) ,I=0.1 mA**

Gas flow rate :

NH_3 (2000 ppm balance N_2)	20	cc/min
O_2	5	cc/min
N_2 dilute flow rate	75	cc/min
Total flow rate	100	cc/min

Inlet concentration : 400 ppm **Current :** 0.1 mA

			Peak Area		Concentration(ppm)		Removal Efficiency		
T, °C	V(kV)	P(W)	Outlet(0 mA)(avg)	Outlet(0.1 mA)	Cout(0 mA)	Cout(0.1 mA)	ψ,(-)	ψ',(-)	ψ'',(-)
33	11.3	1.13	671	-	333	137	0.66	0.59	0.60
100	8.9	0.89	807	503	378	272	0.32	0.28	0.35
200	6.9	0.69	878	570	400	297	0.26	0.26	0.40
300	5.2	0.52	593	451	306	252	0.37	0.18	0.34

Date : 28/9/2002

Subject : **Removal of NH_3 400 ppm from N_2-O_2(20%) ,I=0.5 mA**

Gas flow rate :
NH_3 (2000 ppm balance N_2) 20 cc/min
O_2 20 cc/min
N_2 dilute flow rate 60 cc/min
Total flow rate 100 cc/min

Inlet concentration : 400 ppm Current : 0.5 mA

			Peak Area		Concentration(ppm)		Removal Efficiency		
T, °C	V(kV)	P(W)	Outlet(0 mA)(avg)	Outlet(0.5 mA)	Cout(0 mA)	Cout(0.5 mA)	ψ,(-)	ψ',(-)	ψ'',(-)
33	13.6	6.80	626	-	318	3	0.99	0.99	1.01
33	13.6	6.80	626	-	318	3	0.99	0.99	1.01
100	13.0	6.50	727	-	352	0	1.00	1.00	1.25
100	13.0	6.50	727	-	352	0	1.00	1.00	1.25
200	11.6	5.80	771	-	367	0	1.00	1.00	1.57
200	11.6	5.80	771	-	367	0	1.00	1.00	1.57
300	8.7	4.35	526	-	281	68	0.83	0.76	1.46
300	8.7	4.35	526	-	281	61	0.85	0.78	1.51

Date : 1/10/2002

Subject : **Removal of NH3 400 ppm from N_2-O_2(10%) ,I=0.5 mA**

Gas flow rate : NH_3 (2000 ppm balance N_2) 20cc/min

O_2 10cc/min

N_2 dilute flow rate 70cc/min

Total flow rate 100cc/min

Inlet concentration : 400 ppm Current : 0.5 mA

			Peak Area		Concentration(ppm)		Removal Efficiency		
T, ^oC	V(kV)	P(W)	Outlet(0 mA)(avg)	Outlet(0.5 mA)	Cout(0 mA)	Cout(0.5 mA)	ψ,(-)	ψ',(-)	ψ'',(-)
33	13.9	6.95	645	-	324	9	0.98	0.97	0.99
100	13.0	6.50	758	-	362	2	1.00	0.99	1.24
200	11.6	5.80	807	-	378	0	1.00	1.00	1.57
300	6.9	3.45	515	248	277	160	0.60	0.42	0.81
300	6.9	3.45	515	227	277	150	0.63	0.46	0.89

Date : 29/10/2002

Subject : **Removal of NH_3 400 ppm from N_2-O_2(5%)-H_2O(5250 ppm) ,I=0.1 mA**

Gas flow rate :	NH_3 (2000 ppm balance N_2)	20 cc/min	
	O_2	5 cc/min	
	N_2 (bubbling)	10 cc/min	(water bath 34 °C)
	N_2 (dilute flow rate)	65 cc/min	
	Total flow rate	100 cc/min	

Inlet concentration : 400 ppm **Current :** 0.1 mA

			Peak Area		Concentration(ppm)		Removal Efficiency		
T, °C	V(kV)	P(W)	Outlet(0 mA)(avg)	Outlet(0.1 mA)	Cout(0 mA)	Cout(0.1 mA)	ψ,(-)	ψ',(-)	ψ'',(-)
33	13.5	1.35	340	-	338	181	0.55	0.46	0.47
100	11.9	1.19	345	290	341	306	0.24	0.10	0.13
200	10.6	1.06	350	280	344	299	0.25	0.13	0.21
300	5.4	0.54	320	220	325	256	0.36	0.21	0.41

Date : 2/11/2002

Subject : **Removal of NH_3 400 ppm from N_2-O_2(5%)-H_2O(10499 ppm) ,I=0.1 mA**

Gas flow rate :	NH_3 (2000 ppm balance N_2)	20cc/min	
	O_2	5cc/min	
	N_2 (bubbling)	20cc/min	(water bath 34 °C)
	N_2 (dilute flow rate)	55cc/min	
	Total flow rate	100cc/min	392

Inlet concentration : 400 ppm **Current :** 0.1 mA

			Peak Area		Concentration(ppm)		Removal Efficiency		
T, °C	V(kV)	P(W)	Outlet(0 mA)(avg)	Outlet(0.1 mA)	Cout(0 mA)	Cout(0.1 mA)	ψ,(-)	ψ',(-)	ψ'',(-)
33	10.3	1.03	350	281	344	300	0.25	0.13	0.13
100	8.9	0.89	392	310	369	319	0.20	0.14	0.17
200	7.1	0.71	403	329	375	331	0.17	0.12	0.19
300	5.4	0.54	329	281	331	300	0.25	0.09	0.18

Date : 4/11/2002

Subject : **Removal of NH_3 400 ppm from N_2-O_2(5%)-H_2O(21838 ppm) ,I=0.1 mA**

Gas flow rate:	NH_3 (2000 ppm balance N_2)	20cc/min
	O_2	5cc/min
	N_2 (bubbling)	30cc/min (water bath 40 °C)
	$_{N2}$ (dilute flow rate)	45cc/min
	Total flow rate	100cc/min

Inlet concentration : 400 ppm **Current :** 0.1 mA

			Peak Area		Concentration(ppm)		Removal Efficiency		
T, °C	V(kV)	P(W)	Outlet(0 mA)(avg)	Outlet(0.1 mA)	Cout(0 mA)	Cout(0.1 mA)	ψ,(-)	ψ',(-)	ψ'',(-)
33	10.2	1.02	350	229	344	263	0.34	0.24	0.24
100	8.9	0.89	369	290	356	306	0.24	0.14	0.17
200	6.9	0.69	369	301	356	313	0.22	0.12	0.19
300	5.3	0.53	340	273	338	294	0.26	0.13	0.25

Date : 11/11/2002

Subject : **Removal of NH_3 400 ppm from N_2-O_2(10%)-H_2O(5250 ppm) ,I=0.1 mA**

Gas flow rate :	NH_3 (2000 ppm balance N_2)	20 cc/min	
	O_2	10 cc/min	
	N_2 (bubbling)	10 cc/min	(water bath 34 °C)
	N_2 (dilute flow rate)	60 cc/min	
	Total flow rate	100 cc/min	

Inlet concentration : 400 ppm **Current :** 0.1 mA

			Peak Area		Concentration(ppm)		Removal Efficiency		
T, °C	V(kV)	P(W)	Outlet(0 mA)(avg)	Outlet(0.1 mA)	Cout(0 mA)	Cout(0.1 mA)	ψ,(-)	ψ',(-)	ψ'',(-)
33	11.5	1.15	304	-	315	110	0.73	0.65	0.66
100	9.8	0.98	304	-	315	130	0.68	0.59	0.73
200	8.0	0.80	336	-	335	200	0.50	0.40	0.63
300	6.0	0.60	288	-	304	230	0.43	0.24	0.47

Date : 7/11/2002

Subject : **Removal of NH_3 400 ppm from N_2-O2(20%)-H_2O(10499 ppm) ,I=0.1 mA**

Gas flow rate :	NH_3 (2000 ppm balance N_2)	20 cc/min	
	O_2	10 cc/min	
	N_2 (bubbling)	20 cc/min	(water bath 34 °C)
	N_2 (dilute flow rate)	50 cc/min	
	Total flow rate	100 cc/min	

Inlet concentration : 400 ppm **Current :** 0.1 mA

			Peak Area		Concentration(ppm)		Removal Efficiency		
T, °C	V(kV)	P(W)	Outlet(0 mA)(avg)	Outlet(0.1 mA)	Cout(0 mA)	Cout(0.1 mA)	ψ,(-)	ψ',(-)	ψ'',(-)
33	11.6	1.16	274	-	295	105	0.74	0.64	0.66
100	10.0	1.00	281	-	300	110	0.73	0.63	0.79
200	8.2	0.82	281	-	300	175	0.56	0.42	0.65
300	6.0	0.60	260	-	285	210	0.48	0.26	0.51

Date : 5/11/2002

Subject : **Removal of NH_3 400 ppm from N_2-O_2(10%)-H_2O(21838 ppm) ,I=0.1 mA**

Gas flow rate :	NH_3 (2000 ppm balance N_2)	20 cc/min	
	O_2	10 cc/min	
	N_2 (bubbling)	30 cc/min	(water bath 40 °C)
	N_2 (dilute flow rate)	40 cc/min	
	Total flow rate	100 cc/min	

Inlet concentration : 400 ppm **Current :** 0.1 mA

			Peak Area		Concentration(ppm)		Removal Efficiency		
T, °C	V(kV)	P(W)	Outlet(0 mA)(avg)	Outlet(0.1 mA)	Cout(0 mA)	Cout(0.1 mA)	ψ,(-)	ψ',(-)	ψ'',(-)
33	11.5	1.15	328	-	330	150	0.63	0.55	0.56
100	10.2	1.02	260	-	285	110	0.73	0.61	0.77
200	8.6	0.86	328	-	330	165	0.59	0.50	0.79
300	7.0	0.70	312	187	320	230	0.42	0.28	0.54

Date : 6/11/2002

Subject : **Removal of NH_3 400 ppm from N_2-O_2(20%)-H_2O(5250 ppm) ,I=0.1 mA**

Gas flow rate :	NH_3 (2000 ppm balance N_2)	20 cc/min	
	O_2	20 cc/min	
	N_2 (bubbling)	10 cc/min	(water bath 34 °C)
	N_2 (dilute flow rate)	65 cc/min	
	Total flow rate	100 cc/min	

Inlet concentration : 400 ppm **Current :** 0.1 mA

			Peak Area		Concentration(ppm)		Removal Efficiency		
T, °C	V(kV)	P(W)	Outlet(0 mA)(avg)	Outlet(0.1 mA)	Cout(0 mA)	Cout(0.1 mA)	ψ,(-)	ψ',(-)	ψ'',(-)
33	11.4	1.14	311	-	320	115	0.71	0.64	0.65
100	10.2	1.02	340	-	338	80	0.80	0.76	0.95
200	8.7	0.87	350	-	344	17	0.96	0.95	1.49
300	6.7	0.67	309	-	318	200	0.50	0.37	0.72

Date : 7/11/2002

Subject : **Removal of NH_3 400 ppm from N_2-O2(20%)-H_2O(10499 ppm) ,I=0.1 mA**

Gas flow rate :
NH_3 (2000 ppm balance N_2) 20 cc/min
O2 20 cc/min
N_2 (bubbling) 20 cc/min (water bath 34 °C)
N_2 (dilute flow rate) 40 cc/min
Total flow rate 100 cc/min

Inlet concentration : 400 ppm **Current :** 0.1 mA

			Peak Area		Concentration(ppm)		Removal Efficiency		
T, °C	V(kV)	P(W)	Outlet(0 mA)(avg)	Outlet(0.1 mA)	Cout(0 mA)	Cout(0.1 mA)	ψ,(-)	ψ',(-)	ψ'',(-)
33	11.5	1.15	350	-	344	120	0.70	0.65	0.66
100	10.1	1.01	392	-	369	100	0.75	0.73	0.91
200	8.6	0.86	403	-	375	29	0.93	0.92	1.45
300	6.7	0.67	329	-	331	218	0.46	0.34	0.66

Date : 5/11/2002

Subject : **Removal of NH_3 400 ppm from N_2-O_2(20%)-H_2O(21838 ppm) ,I=0.1 mA**

Gas flow rate :	NH_3 (2000 ppm balance N_2)	20 cc/min	
	O_2	20 cc/min	
	N_2 (bubbling)	30 cc/min	(water bath 40 °C)
	N_2 (dilute flow rate)	30 cc/min	
	Total flow rate	100 cc/min	

Inlet concentration : 400 ppm **Current :** 0.1 mA

			Peak Area		Concentration(ppm)		Removal Efficiency		
T, °C	V(kV)	P(W)	Outlet(0 mA)(avg)	Outlet(0.1 mA)	Cout(0 mA)	Cout(0.1 mA)	ψ,(-)	ψ',(-)	ψ'',(-)
33	11.5	1.15	360	-	350	144	0.64	0.59	0.60
100	10.2	1.02	392	-	369	78	0.81	0.79	0.99
200	8.6	0.86	382	-	363	23	0.94	0.94	1.47
300	7.0	0.70	320	146	325	195	0.51	0.40	0.77

Date : 25/9/2002

Subject : **Removal of NH_3 400 ppm from N_2-H_2O(5250 ppm) ,I=0.5 mA**

Gas flow rate :

NH_3 (2000 ppm balance N_2)	20	cc/min	
N_2 (bubbling)	10	cc/min	(water bath 40 °C)
N_2 (dilute flow rate)	70	cc/min	
Total flow rate	100	cc/min	

Inlet concentration : 400 ppm **Current :** 0.5 mA

			Peak Area		Concentration(ppm)		Removal Efficiency		
T, °C	V(kV)	P(W)	Outlet(0 mA)(avg)	Outlet(0.5 mA)	Cout(0 mA)	Cout(0.5 mA)	ψ,(-)	ψ',(-)	ψ'',(-)
33	8.8	4.40	758	618	362	315	0.21	0.13	0.13
33	8.8	4.40	758	596	362	307	0.23	0.15	0.16
100	8.2	4.10	773	515	367	277	0.31	0.25	0.31
100	8.2	4.10	773	535	367	284	0.29	0.23	0.28
100	8.2	4.10	773	534	367	284	0.29	0.23	0.28
200	6.1	3.05	791	480	373	263	0.34	0.29	0.46
200	6.1	3.05	791	503	373	272	0.32	0.27	0.42
300	4.4	2.20	816	414	381	236	0.41	0.38	0.73
300	4.4	2.20	816	433	381	244	0.39	0.36	0.69

Date : 25/10/2002

Subject : **Removal of NH_3 400 ppm from N_2-H_2O(10499 ppm) ,I=0.5 mA**

Gas flow rate : NH_3 (2000 ppm balance N_2) 20 cc/min
N_2 (bubbling) 20 cc/min (water bath 34 °C)
N_2 (dilute flow rate) 60 cc/min
Total flow rate 100 cc/min

Inlet concentration : 400 ppm **Current :** 0.5 mA

			Peak Area		Concentration(ppm)		Removal Efficiency		
T, °C	V(kV)	P(W)	Outlet(0 mA)(avg)	Outlet(0.5 mA)	Cout(0 mA)	Cout(0.5 mA)	ψ,(-)	ψ',(-)	ψ'',(-)
33	9.3	4.65	700	534	343	284	0.29	0.17	0.18
33	9.3	4.65	700	539	343	286	0.29	0.17	0.17
100	8.9	4.45	715	546	348	289	0.28	0.17	0.21
100	8.9	4.45	715	519	348	278	0.30	0.20	0.25
200	6.3	3.15	707	419	346	238	0.40	0.31	0.49
200	6.3	3.15	707	425	346	241	0.40	0.30	0.48
300	5.1	2.55	810	458	379	254	0.36	0.33	0.63
300	5.1	2.55	810	466	379	258	0.36	0.32	0.62

Date : 26/10/2002

Subject : **Removal of NH_3 400 ppm from N_2-H_2O(21838 ppm) ,I=0.5 mA**

Gas flow rate :

NH_3 (2000 ppm balance N_2)	20	cc/min	
N_2 (bubbling)	30	cc/min	(water bath 40 ^oC)
N_2 (dilute flow rate)	50	cc/min	
Total flow rate	100	cc/min	

Inlet concentration : 400 ppm **Current :** 0.5 mA

			Peak Area		Concentration(ppm)		Removal Efficiency		
T, ^oC	V(kV)	P(W)	Outlet(0 mA)(avg)	Outlet(0.5 mA)	Cout(0 mA)	Cout(0.5 mA)	ψ,(-)	ψ',(-)	ψ'',(-)
33	9.5	4.75	-	-	327	291	0.27	0.11	0.11
100	8.8	4.40	-	-	363	291	0.27	0.20	0.25
200	6.3	3.15	-	-	375	278	0.31	0.26	0.41
300	5.8	2.90	-	-	359	253	0.37	0.30	0.57

APPENDIX F

Trimethylamine Removal

Date : 22/12/02

Subject : **Removal of $(CH_3)_3N$ 200 ppm from N_2,I=0.2 mA**

Gas flow rate : $(CH_3)_3N$ (2000 ppm balance N_2) 10cc/min

N_2 dilute flow rate 90cc/min

Total flow rate 100cc/min

Inlet concentration : 200 ppm **Current :** 0.2 mA

			Peak Area		Concentration(ppm)		Removal Efficiency		
T, ^{o}C	V(kV)	P(W)	Outlet(0 mA)(avg)	Outlet(0.2 mA)	Cout(0 mA)	Cout(0.2 mA)	ψ,(-)	ψ',(-)	ψ'',(-)
33	9.4	1.88	9245	6672	172	126	0.37	0.27	0.28
100	8.6	1.72	10695	6869	198	129	0.35	0.35	0.44
200	5.9	1.18	11136	5041	206	96	0.52	0.54	0.84
300	5.0	1.00	7498	3795	141	72	0.64	0.49	0.94

Date : 21/12/02

Subject : **Removal of $(CH_3)_3N$ 400 ppm from N_2,I=0.2 mA**

Gas flow rate :		
	$(CH_3)_3N$ (2000 ppm balance N_2)	20 cc/min
	N_2 dilute flow rate	90 cc/min
	Total flow rate	100 cc/min

Inlet concentration : 400 ppm **Current :** 0.2 mA

			Peak Area		Concentration(ppm)		Removal Efficiency		
T, °C	V(kV)	P(W)	Outlet(0 mA)(avg)	Outlet(0.2 mA)	Cout(0 mA)	Cout(0.2 mA)	ψ,(-)	ψ',(-)	ψ'',(-)
33	9.4	1.88	21960	17579	392	318	0.20	0.19	0.19
100	8.7	1.74	23841	17600	423	319	0.20	0.25	0.31
200	6.1	1.22	26741	14196	470	260	0.35	0.45	0.70
300	4.9	0.98	18440	9765	333	182	0.55	0.45	0.88

Date : 24/12/02

Subject : **Removal of $(CH_3)_3N$ 400 ppm from N_2,I=0.3 mA**

Gas flow rate : $(CH_3)_3N$ (2000 ppm balance N_2) 20cc/min

N_2 dilute flow rate 90cc/min

Total flow rate 100cc/min

Inlet concentration : 400 ppm **Current :** 0.3 mA

			Peak Area		Concentration(ppm)		Removal Efficiency		
T, °C	V(kV)	P(W)	Outlet(0 mA)(avg)	Outlet(0.3 mA)	Cout(0 mA)	Cout(0.3 mA)	ψ,(-)	ψ',(-)	ψ'',(-)
33	9.1	2.73	21960	16700	392	303	0.24	0.23	0.23
100	8.1	2.43	23841	14479	423	265	0.34	0.37	0.47
200	6.2	1.86	26741	12938	470	238	0.40	0.49	0.77
300	5.3	1.59	18440	9523	333	177	0.56	0.47	0.90

Date : 24/12/02

Subject : **Removal of $(CH_3)_3N$ 400 ppm from N_2,I=0.5 mA**

Gas flow rate :	$(CH_3)_3N$ (2000 ppm balance N_2)	20 cc/min
	N_2 dilute flow rate	90 cc/min
	Total flow rate	100 cc/min

Inlet concentration : 400 ppm **Current :** 0.3 mA

			Peak Area		Concentration(ppm)		Removal Efficiency		
T, ^oC	V(kV)	P(W)	Outlet(0 mA)(avg)	Outlet(0.3 mA)	Cout(0 mA)	Cout(0.3 mA)	ψ,(-)	ψ',(-)	ψ'',(-)
33	10.1	5.05	21960	14332	392	262	0.34	0.33	0.34
100	10.4	5.20	23841	12255	423	226	0.43	0.46	0.58
200	7.5	3.75	26741	9389	470	175	0.56	0.63	0.99
300	5.1	2.55	18440	6118	333	116	0.71	0.65	1.26

Date : 22/12/02

Subject : **Removal of $(CH_3)_3N$ 200 ppm from N_2,I=0.2 mA**

Gas flow rate :	$(CH_3)_3N$ (2000 ppm balance N_2)	10 cc/min
	N_2 dilute flow rate	90 cc/min
	Total flow rate	100 cc/min

Inlet concentration : 200 ppm **Current :** 0.2 mA

			Peak Area		Concentration(ppm)		Removal Efficiency		
T, °C	V(kV)	P(W)	Outlet(0 mA)(avg)	Outlet(0.2 mA)	Cout(0 mA)	Cout(0.2 mA)	ψ,(-)	ψ',(-)	ψ'',(-)
33	9.0	1.80	34151	31597	586	546	0.09	0.07	0.07
100	7.2	1.44	31867	24751	551	437	0.27	0.21	0.26
200	6.3	1.26	38345	23414	650	416	0.31	0.36	0.57
300	5.4	1.08	31692	16961	548	308	0.49	0.44	0.85

Date : 26/12/02

Subject : **Removal of $(CH_3)_3N$ 400 ppm from N_2-O_2(10%),I=0.2 mA**

Gas flow rate :		
	$(CH_3)_3N$ (2000 ppm balance N_2)	20cc/min
	O_2	10cc/min
	N_2 dilute flow rate	70cc/min
	Total flow rate	100cc/min

Inlet concentration : 400 ppm **Current :** 0.2 mA

			Peak Area		Concentration(ppm)		Removal Efficiency		
T, °C	V(kV)	P(W)	Outlet(0 mA)(avg)	Outlet(0.2 mA)	Cout(0 mA)	Cout(0.2 mA)	ψ,(-)	ψ',(-)	ψ'',(-)
33	12.6	2.52	21608	1779	386	34	0.91	0.91	0.93
100	11.0	2.20	22630	1281	403	25	0.94	0.94	1.17
200	9.5	1.90	18311	182	331	4	0.99	0.99	1.55
300	7.0	1.40	4129	0	79	0	1.00	1.00	1.93

Date : 29/12/02

Subject : **Removal of $(CH_3)_3N$ 400 ppm from N_2-O_2(15%),I=0.2 mA**

Gas flow rate :	$(CH_3)_3N$ (2000 ppm balance N_2)	20 cc/min
	O_2	15 cc/min
	N_2 dilute flow rate	65 cc/min
	Total flow rate	100 cc/min

Inlet concentration : 400 ppm **Current :** 0.2 mA

			Peak Area		Concentration(ppm)		Removal Efficiency		
T, °C	V(kV)	P(W)	Outlet(0 mA)(avg)	Outlet(0.2 mA)	Cout(0 mA)	Cout(0.2 mA)	ψ,(-)	ψ',(-)	ψ'',(-)
33	12.6	2.52	21003	2071	376	40	0.90	0.89	0.91
100	11.0	2.20	17740	1710	321	33	0.92	0.90	1.12
200	9.4	1.88	20727	389	371	8	0.98	0.98	1.54
300	7.1	1.42	4549	0	86	0	1.00	1.00	1.93

Date : 28/12/02

Subject : **Removal of $(CH_3)_3N$ 400 ppm from N_2-O_2(20%),I=0.2 mA**

Gas flow rate :	$(CH_3)_3N$ (2000 ppm balance N_2)	20cc/min
	O_2	20cc/min
	N_2 dilute flow rate	60cc/min
	Total flow rate	100cc/min

Inlet concentration : 400 ppm **Current :** 0.2 mA

			Peak Area		Concentration(ppm)		Removal Efficiency		
T, ^{o}C	V(kV)	P(W)	Outlet(0 mA)(avg)	Outlet(0.2 mA)	Cout(0 mA)	Cout(0.2 mA)	ψ,(-)	ψ',(-)	ψ'',(-)
33	12.6	2.52	22631	2309	403	44	0.89	0.89	0.91
100	11.0	2.20	23057	2304	410	44	0.89	0.89	1.12
200	9.5	1.90	17127	485	311	9	0.98	0.97	1.52
300	7.0	1.40	3383	0	65	0	1.00	1.00	1.93

Date : 3/1/03

Subject : **Removal of $(CH_3)_3N$ 400 ppm from N_2-H_2O(5250 ppm),I=0.2 mA**

Gas flow rate : $(CH_3)_3N$ (2000 ppm balance N_2) 20cc/min

N_2 (bubbling) 10cc/min (water bath 34 ^{o}C)

N_2 (dilute flow rate) 70cc/min

Total flow rate 100cc/min

Inlet concentration : 400 ppm **Current :** 0.2 mA

			Peak Area		Concentration(ppm)		Removal Efficiency		
T, ^{o}C	V(kV)	P(W)	Outlet(0 mA)(avg)	Outlet(0.2 mA)	Cout(0 mA)	Cout(0.2 mA)	ψ,(-)	ψ',(-)	ψ'',(-)
33	8.8	1.76	19384	16715	349	303	0.24	0.13	0.13
100	9.1	1.82	22815	9843	406	183	0.54	0.55	0.69
200	5.8	1.16	17462	11240	316	208	0.48	0.34	0.54
300	4.4	0.88	13343	8103	245	152	0.62	0.38	0.73

Date : 4/1/03

Subject : **Removal of $(CH_3)_3N$ 400 ppm from N_2-H_2O(10500 ppm),I=0.2 mA**

Gas flow rate :	$(CH_3)_3N$ (2000 ppm balance N_2)	20cc/min
	N_2 (bubbling)	20cc/min (water bath 34 °C)
	N_2 (dilute flow rate)	60cc/min
	Total flow rate	100cc/min

Inlet concentration : 400 ppm **Current :** 0.2 mA

			Peak Area		Concentration(ppm)		Removal Efficiency		
T, C	V(kV)	P(W)	Outlet(0 mA)(avg)	Outlet(0.2 mA)	Cout(0 mA)	Cout(0.2 mA)	ψ,(-)	ψ',(-)	ψ'',(-)
33	9.1	1.82	17903	13486	324	248	0.38	0.23	0.24
100	9.3	1.86	19441	6785	350	128	0.68	0.63	0.79
200	6.2	1.24	19632	11621	353	215	0.46	0.39	0.61
300	4.4	0.88	15990	8380	291	157	0.61	0.46	0.89

Date : 3/1/03

Subject : **Removal of $(CH_3)_3N$ 400 ppm from N_2-H_2O(21800 ppm),I=0.2 mA**

Gas flow rate :	$(CH_3)_3N$ (2000 ppm balance N_2)	20 cc/min
	N_2 (bubbling)	30 cc/min (water bath 40 °C)
	N_2 (dilute flow rate)	50 cc/min
	Total flow rate	100 cc/min

Inlet concentration : 400 ppm **Current :** 0.2 mA

			Peak Area		Concentration(ppm)		Removal Efficiency		
T, °C	V(kV)	P(W)	Outlet(0 mA)(avg)	Outlet(0.2 mA)	Cout(0 mA)	Cout(0.2 mA)	ψ,(-)	ψ',(-)	ψ'',(-)
33	9.3	1.86	17095	12690	310	234	0.42	0.25	0.25
100	9.3	1.86	20555	5733	368	108	0.73	0.71	0.88
200	6.1	1.22	16088	9524	293	178	0.56	0.39	0.62
300	4.4	0.88	14735	8455	269	158	0.60	0.41	0.80

Date : 9/1/03

Subject : **Removal of $(CH_3)_3N$ 400 ppm from N_2-O_2(10%)-H_2O(5250 ppm),I=0.2 mA**

Gas flow rate :

$(CH_3)_3N$ (2000 ppm balance N_2)	20cc/min
O_2	10
N_2 (bubbling)	10cc/min (water bath 34 °C)
N_2 (dilute flow rate)	60cc/min
Total flow rate	100cc/min

Inlet concentration : 400 ppm **Current :** 0.2 mA

			Peak Area		Concentration(ppm)		Removal Efficiency		
T, °C	V(kV)	P(W)	Outlet(0 mA)(avg)	Outlet(0.2 mA)	Cout(0 mA)	Cout(0.2 mA)	ψ,(-)	ψ',(-)	ψ'',(-)
33	12.6	2.52	17821	1701	322	33	0.92	0.90	0.92
100	10.9	2.18	16057	1067	292	21	0.95	0.93	1.16
200	9.3	1.86	10359	206	192	4	0.99	0.98	1.54
300	7.0	1.40	0	0	0	0	1.00	1.00	1.93

Date : 14/1/03

Subject : **Removal of $(CH_3)_3N$ 400 ppm from N_2-O_2(10%)-H_2O(10500 ppm),I=0.2 mA**

Gas flow rate :	$(CH_3)_3N$ (2000 ppm balance N_2)	20cc/min
	O_2	10
	N_2 (bubbling)	20cc/min (water bath 34 °C)
	N_2 (dilute flow rate)	50cc/min
	Total flow rate	100cc/min

Inlet concentration : 400 ppm **Current :** 0.2 mA

			Peak Area		Concentration(ppm)		Removal Efficiency		
T, °C	V(kV)	P(W)	Outlet(0 mA)(avg)	Outlet(0.2 mA)	Cout(0 mA)	Cout(0.2 mA)	ψ,(-)	ψ',(-)	ψ'',(-)
33	12.6	2.52	13681	1889	251	36	0.91	0.86	0.87
100	11.0	2.20	16495	1260	300	24	0.94	0.92	1.15
200	9.3	1.86	10950	230	203	4	0.99	0.98	1.54
300	7.0	1.40	0	0	0	0	1.00	1.00	1.93

Date : 16/1/03

Subject : **Removal of $(CH_3)_3N$ 400 ppm from N_2-O_2(10%)-H_2O(21800 ppm),I=0.2 mA**

Gas flow rate :

$(CH_3)_3N$ (2000 ppm balance N_2)	20	cc/min
O_2	10	
N_2 (bubbling)	30	cc/min (water bath 40 °C)
N_2 (dilute flow rate)	40	cc/min
Total flow rate	100	cc/min

Inlet concentration : 400 ppm **Current :** 0.2 mA

			Peak Area		Concentration(ppm)		Removal Efficiency		
T, °C	V(kV)	P(W)	Outlet(0 mA)(avg)	Outlet(0.2 mA)	Cout(0 mA)	Cout(0.2 mA)	ψ,(-)	ψ',(-)	ψ'',(-)
33	12.5	2.50	12318	1929	227	37	0.91	0.84	0.85
100	10.9	2.18	12373	1104	228	21	0.95	0.91	1.13
200	9.3	1.86	9982	239	186	5	0.99	0.98	1.53
300	6.9	1.38	0	0	0	0	1.00	1.00	1.93

Date : 10/1/03

Subject : **Removal of $(CH_3)_3N$ 400 ppm from N_2-O_2(20%)-H_2O(5250 ppm),I=0.2 mA**

Gas flow rate :	$(CH_3)_3N$ (2000 ppm balance N_2)	20cc/min
	O_2	20
	N_2 (bubbling)	10cc/min (water bath 34 ^oC)
	N_2 (dilute flow rate)	50cc/min
	Total flow rate	100cc/min

Inlet concentration : 400 ppm **Current :** 0.2 mA

			Peak Area		Concentration(ppm)		Removal Efficiency		
T, ^oC	V(kV)	P(W)	Outlet(0 mA)(avg)	Outlet(0.2 mA)	Cout(0 mA)	Cout(0.2 mA)	ψ,(-)	ψ',(-)	ψ'',(-)
33	12.6	2.52	15304	2145	279	41	0.90	0.85	0.87
100	11.1	2.22	14697	1674	269	32	0.92	0.88	1.10
200	9.4	1.88	13520	378	248	7	0.98	0.97	1.53
300	7.2	1.44	0	0	0	0	1.00	1.00	1.93

Date : 15/1/03

Subject : **Removal of $(CH_3)_3N$ 400 ppm from N_2-O_2(20%)-H_2O(10500 ppm),I=0.2 mA**

Gas flow rate :	$(CH_3)_3N$ (2000 ppm balance N_2)	20cc/min
	O_2	20
	N_2 (bubbling)	20cc/min (water bath 34 °C)
	N_2 (dilute flow rate)	40cc/min
	Total flow rate	100cc/min

Inlet concentration : 400 ppm **Current :** 0.2 mA

			Peak Area		Concentration(ppm)		Removal Efficiency		
T, °C	V(kV)	P(W)	Outlet(0 mA)(avg)	Outlet(0.2 mA)	Cout(0 mA)	Cout(0.2 mA)	ψ,(-)	ψ',(-)	ψ'',(-)
33	12.6	2.52	15867	2256	289	43	0.89	0.85	0.87
100	11.1	2.22	11211	1828	208	35	0.91	0.83	1.04
200	9.5	1.90	5025	505	95	10	0.98	0.90	1.41
300	7.3	1.46	0	0	0	0	1.00	1.00	1.93

Date : 16/1/03

Subject : **Removal of $(CH_3)_3N$ 400 ppm from N_2-O_2(20%)-H_2O(21800 ppm),I=0.2 mA**

Gas flow rate :	$(CH_3)_3N$ (2000 ppm balance N_2)	20cc/min
	O_2	20
	N_2 (bubbling)	30cc/min (water bath 40 °C)
	N_2 (dilute flow rate)	30cc/min
	Total flow rate	100cc/min

Inlet concentration : 400 ppm **Current :** 0.2 mA

			Peak Area		Concentration(ppm)		Removal Efficiency		
T, °C	V(kV)	P(W)	Outlet(0 mA)(avg)	Outlet(0.2 mA)	Cout(0 mA)	Cout(0.2 mA)	ψ,(-)	ψ',(-)	ψ'',(-)
33	12.5	2.50	16246	2642	295	51	0.87	0.83	0.84
100	11.3	2.26	11873	1857	219	36	0.91	0.84	1.05
200	9.4	1.88	11251	454	208	9	0.98	0.96	1.51
300	7.2	1.44	0	0	0	0	1.00	1.00	1.93

APPENDIX G

Simultaneous Removal of Acetaldehyde and Ammonia

Date: 2/2/2003

Subject: **Removal of CH_3CHO(150 ppm)-NH_3 1000 ppm from N_2, I=0.3 mA**

Gas flow rate:		
	CH_3CHO	7.5 cc/min
	NH_3	50 cc/min
	N_2 (dilute flow rate)	42.5 cc/min
	Total flow rate	100 cc/min

			CH_3CHO							NH_3						
			Peak Area		Concentration(ppm)		Removal Efficiency			Peak Area		Concentration(ppm)		Removal Efficiency		
T, C	V(kV)	P(W)	Outlet (0 mA)	Outlet (0.3 mA)	Cout (0 mA)	Cout (0.3 mA)	ψ,(-)	ψ',(-)	ψ'',(-)	Outlet (0 mA)	Outlet (0.3 mA)	Cout (0 mA)	Cout (0.3 mA)	ψ,(-)	ψ',(-)	ψ'',(-)
33	9.6	2.88	3319	2111	104	66	0.56	0.36	0.37	1930	1816	836	810	0.19	0.03	0.03
100	9.3	2.79	3540	1547	111	48	0.68	0.56	0.70	1496	827	738	576	0.42	0.22	0.27
200	6.1	1.83	3322	2108	104	66	0.56	0.37	0.57	2203	1642	899	771	0.23	0.14	0.22
300	4.1	1.23	2356	1540	74	48	0.68	0.35	0.67	2057	1603	865	762	0.24	0.12	0.23

Date: 3/2/2003

Subject: **Removal of CH_3CHO(150 ppm)-NH_3 1000 ppm from N_2-O_2(10%) I=0.3 mA**

Gas flow rate:	CH_3CHO	7.5	cc/min
	NH_3	50	cc/min
	O_2	10	cc/min
	N_2 (dilute flow rate)	32.5	cc/min
	Total flow rate	100	cc/min

			CH_3CHO							NH_3						
			Peak Area		Concentration(ppm)		Removal Efficiency			Peak Area		Concentration(ppm)		Removal Efficiency		
T, C	V(kV)	P(W)	Outlet (0 mA)	Outlet (0.3 mA)	Cout (0 mA)	Cout (0.3 mA)	ψ,(-)	ψ',(-)	ψ'',(-)	Outlet (0 mA)	Outlet (0.3 mA)	Cout (0 mA)	Cout (0.3 mA)	ψ,(-)	ψ',(-)	ψ'',(-)
33	12.4	3.72	4585	0	144	0	1.00	1.00	1.02	1479	135	735	185	0.82	0.75	0.76
100	10.8	3.24	4660	271	146	8	0.94	0.94	1.18	1983	175	848	220	0.78	0.74	0.93
200	9.0	2.70	3619	342	113	11	0.93	0.91	1.42	2190	271	896	293	0.71	0.67	1.06
300	5.8	1.74	2991	1469	94	46	0.69	0.51	0.98	1755	1168	796	667	0.33	0.16	0.31

Date: 3/2/2003

Subject: **Removal of CH_3CHO(150 ppm)-NH_3 1000 ppm from N_2-O_2(20%) I=0.3 mA**

Gas flow rate:	CH_3CHO	7.5 cc/min
	NH_3	50 cc/min
	O_2	20 cc/min
	N_2 (dilute flow rate)	22.5 cc/min
	Total flow rate	100 cc/min

			CH_3CHO							NH_3						
			Peak Area		Concentration(ppm)		Removal Efficiency			Peak Area		Concentration(ppm)		Removal Efficiency		
T, C	V(kV)	P(W)	Outlet (0 mA)	Outlet (0.3 mA)	Cout (0 mA)	Cout (0.3 mA)	ψ,(-)	ψ',(-)	ψ'',(-)	Outlet (0 mA)	Outlet (0.3 mA)	Cout (0 mA)	Cout (0.3 mA)	ψ,(-)	ψ',(-)	ψ'',(-)
33	10.8	3.24	5122	0	160	0	1.00	1.00	1.02	1851	156	818	204	0.80	0.75	0.76
100	12.2	3.66	5181	0	162	0	1.00	1.00	1.25	1788	0	804	100	0.90	0.88	1.09
200	9.4	2.82	5388	0	169	0	1.00	1.00	1.57	2334	0	930	110	0.89	0.88	1.39
300	6.5	1.95	3099	1463	97	46	0.69	0.53	1.02	1607	803	763	566	0.43	0.26	0.50

Date: 28/2/2003

Subject: **Removal of CH_3CHO(150 ppm)-NH_3 1000 ppm from N_2-H_2O(5250 ppm) I=0.3 mA**

Gas flow rate:

CH_3CHO	7.5	cc/min	
NH_3	50	cc/min	
N2(bubbling)	10	cc/min	(water bath 34°C)
N_2 (dilute flow rate)	32.5	cc/min	
Total flow rate	100	cc/min	

			CH_3CHO							NH_3						
			Peak Area		Concentration(ppm)		Removal Efficiency			Peak Area		Concentration(ppm)		Removal Efficiency		
T, C	V(kV)	P(W)	Outlet (0 mA)	Outlet (0.3 mA)	Cout (0 mA)	Cout (0.3 mA)	ψ,(-)	ψ',(-)	ψ'',(-)	Outlet (0 mA)	Outlet (0.3 mA)	Cout (0 mA)	Cout (0.3 mA)	ψ,(-)	ψ',(-)	ψ'',(-)
33	9.1	2.73	3541	2496	111	78	0.48	0.30	0.30	1973	1724	846	789	0.21	0.07	0.07
100	8.7	2.61	3747	2420	117	76	0.49	0.35	0.44	2035	1728	860	790	0.21	0.08	0.10
200	7.9	2.37	3794	1228	119	38	0.74	0.68	1.06	2304	1045	923	641	0.36	0.31	0.48
300	5.1	1.53	2317	1567	73	49	0.67	0.32	0.62	2356	1659	935	775	0.23	0.17	0.33

Date: 3/2/2003

Subject: **Removal of CH_3CHO(150 ppm)-NH_3 1000 ppm from N_2-H_2O(10500 ppm) I=0.3 mA**

Gas flow rate:			
	CH_3CHO	7.5 cc/min	
	NH_3	50 cc/min	
	N_2(bubbling)	10 cc/min	(water bath 34°C)
	N_2 (dilute flow rate)	32.5 cc/min	
	Total flow rate	100 cc/min	

			CH_3CHO							NH_3						
			Peak Area		Concentration(ppm)		Removal Efficiency			Peak Area		Concentration(ppm)		Removal Efficiency		
T, C	V(kV)	P(W)	Outlet (0 mA)	Outlet (0.3 mA)	Cout (0 mA)	Cout (0.3 mA)	ψ,(-)	ψ',(-)	ψ'',(-)	Outlet (0 mA)	Outlet (0.3 mA)	Cout (0 mA)	Cout (0.3 mA)	ψ,(-)	ψ',(-)	ψ'',(-)
33	8.9	2.67	3325	2484	104	78	0.48	0.25	0.26	1991	1885	850	826	0.17	0.03	0.03
100	8.5	2.55	3618	2498	113	78	0.48	0.31	0.39	2204	1780	899	802	0.20	0.11	0.14
200	6.7	2.01	3516	2466	110	77	0.48	0.30	0.47	2057	1550	865	750	0.25	0.13	0.21
300	4.9	1.47	2892	1896	91	59	0.60	0.34	0.66	1875	1724	823	789	0.21	0.04	0.08

Date: 1/3/2003

Subject: **Removal of CH_3CHO(150 ppm)-NH_3 1000 ppm from N_2-O_2(10%)-H_2O(5250 ppm) I=0.3 mA**

Gas flow rate:			
	CH_3CHO	7.5 cc/min	
	NH_3	50 cc/min	
	O_2	10 cc/min	
	N_2 (bubbling)	10 cc/min	(water bath 34°C)
	N_2 (dilute flow rate)	22.5 cc/min	
	Total flow rate	100 cc/min	

			CH_3CHO							NH_3						
			Peak Area		Concentration(ppm)		Removal Efficiency			Peak Area		Concentration(ppm)		Removal Efficiency		
T, C	V(kV)	P(W)	Outlet (0 mA)	Outlet (0.3 mA)	Cout (0 mA)	Cout (0.3 mA)	ψ,(-)	ψ',(-)	ψ'',(-)	Outlet (0 mA)	Outlet (0.3 mA)	Cout (0 mA)	Cout (0.3 mA)	ψ,(-)	ψ',(-)	ψ'',(-)
33	13.2	3.96	3486	0	109	0	1.00	1.00	1.02	2078	-	870	155	0.85	0.82	0.84
100	11.8	3.54	3881	0	122	0	1.00	1.00	1.25	1912	-	832	160	0.84	0.81	1.01
200	10.3	3.09	3745	0	117	0	1.00	1.00	1.57	2035	-	860	130	0.87	0.85	1.33
300	6.5	1.95	2149	938	67	29	0.80	0.56	1.09	1945	1168	839	667	0.33	0.20	0.40

Date: 2/3/2003

Subject: **Removal of CH_3CHO(150 ppm)-NH_3 1000 ppm from N_2-O_2(10%)-H_2O(10500 ppm) I=0.3 mA**

Gas flow rate:			
CH_3CHO	7.5	cc/min	
NH_3	50	cc/min	
O_2	10	cc/min	
N_2 (bubbling)	20	cc/min	(water bath 34°C)
N_2 (dilute flow rate)	12.5	cc/min	
Total flow rate	100	cc/min	

			CH_3CHO							NH_3						
			Peak Area		Concentration(ppm)		Removal Efficiency			Peak Area		Concentration(ppm)		Removal Efficiency		
T, C	V(kV)	P(W)	Outlet (0 mA)	Outlet (0.3 mA)	Cout (0 mA)	Cout (0.3 mA)	ψ,(-)	ψ',(-)	ψ'',(-)	Outlet (0 mA)	Outlet (0.3 mA)	Cout (0 mA)	Cout (0.3 mA)	ψ,(-)	ψ',(-)	ψ'',(-)
33	13.2	3.96	4316	169	135	5	0.96	0.96	0.98	1798	-	806	135	0.87	0.83	0.85
100	11.8	3.54	4280	0	134	0	1.00	1.00	1.25	2097	-	874	145	0.86	0.83	1.04
200	10.3	3.09	4486	0	141	0	1.00	1.00	1.57	1784	-	803	100	0.90	0.88	1.38
300	6.8	2.04	1286	503	40	16	0.89	0.61	1.18	1774	650	800	500	0.50	0.37	0.72

Date: 1/3/2003

Subject: **Removal of CH_3CHO(150 ppm)-NH_3 1000 ppm form N_2-O_2(20%)-H_2O(5250 ppm) I=0.3 mA**

Gas flow rate:			
	CH_3CHO	7.5 cc/min	
	NH_3	50 cc/min	
	O_2	20 cc/min	
	N_2 (bubbling)	10 cc/min	(water bath 34°C)
	N_2 (dilute flow rate)	12.5 cc/min	
	Total flow rate	100 cc/min	

			CH_3CHO							NH_3						
			Peak Area		Concentration(ppm)		Removal Efficiency			Peak Area		Concentration(ppm)		Removal Efficiency		
T, C	V(kV)	P(W)	Outlet (0 mA)	Outlet (0.3 mA)	Cout (0 mA)	Cout (0.3 mA)	ψ,(-)	ψ',(-)	ψ'',(-)	Outlet (0 mA)	Outlet (0.3 mA)	Cout (0 mA)	Cout (0.3 mA)	ψ,(-)	ψ',(-)	ψ'',(-)
33	13.1	3.93	3970	0	124	0	1.00	1.00	1.02	1731	-	791	145	0.86	0.82	0.83
100	11.6	3.48	4215	0	132	0	1.00	1.00	1.25	1852	-	818	115	0.89	0.86	1.07
200	10.4	3.12	3796	0	119	0	1.00	1.00	1.57	2114	-	878	70	0.93	0.92	1.45
300	7.6	2.28	2064	406	65	13	0.92	0.80	1.55	1748	444	795	398	0.60	0.50	0.96

APPENDIX H

Simultaneous Removal of Acetaldehyde and Trimethylamine

Date: 25/1/2003

Subject: **Removal of CH_3CHO(150 ppm)-$(CH_3)_3N$ 100 ppm from N_2 , I=0.3 mA**

Gas flow rate:		
	CH_3CHO	7.5 cc/min
	$(CH_3)_3N$	5 cc/min
	N_2 (dilute flow rate)	87.5 cc/min
	Total flow rate	100 cc/min

			CH_3CHO									$(CH_3)_3N$								
			Peak Area		Concentration(ppm)		Removal Efficiency			Peak Area		Concentration(ppm)		Removal Efficiency		
T, C	V(kV)	P(W)	Outlet (0 mA)	Outlet (0.2 mA)	Cout (0 mA)	Cout (0.2 mA)	ψ,(-)	ψ',(-)	ψ'',(-)	Outlet (0 mA)	Outlet (0.2 mA)	Cout (0 mA)	Cout (0.2 mA)	ψ,(-)	ψ',(-)	ψ'',(-)
33	9.3	2.79	4291	3450	134	108	0.28	0.20	0.20	6182	4360	117	83	0.17	0.29	0.29
100	8.2	2.46	4159	3215	130	101	0.33	0.23	0.28	5675	4280	107	81	0.19	0.24	0.30
200	6.1	1.83	4186	2874	131	90	0.40	0.31	0.49	5847	3040	111	58	0.42	0.47	0.75
300	4.2	1.26	3419	2561	107	80	0.47	0.25	0.48	6337	4707	120	89	0.11	0.25	0.49

Date: 26/1/2003

Subject: **Removal of CH_3CHO(150 ppm)-$(CH_3)_3N$ 100 ppm from N_2-O_2(10%), I=0.3 mA**

Gas flow rate:		
	CH_3CHO	7.5 cc/min
	$(CH_3)_3N$	5 cc/min
	O_2	10 cc/min
	N_2 (dilute flow rate)	77.5 cc/min
	Total flow rate	100 cc/min

			CH_3CHO							$(CH_3)_3N$						
			Peak Area		Concentration(ppm)		Removal Efficiency			Peak Area		Concentration(ppm)		Removal Efficiency		
T, C	V(kV)	P(W)	Outlet (0 mA)	Outlet (0.2 mA)	Cout (0 mA)	Cout (0.2 mA)	ψ,(-)	ψ',(-)	ψ'',(-)	Outlet (0 mA)	Outlet (0.2 mA)	Cout (0 mA)	Cout (0.2 mA)	ψ,(-)	ψ',(-)	ψ'',(-)
33	12.6	3.78	4953	0	155	0	1.00	1.00	1.02	3865	698	74	13	0.87	0.82	0.83
100	10.4	3.12	4999	0	157	0	1.00	1.00	1.25	4108	394	78	8	0.92	0.90	1.13
200	7.5	2.25	4528	912	142	29	0.81	0.80	1.25	3969	0	76	0	1.00	1.00	1.57
300	6.1	1.83	3092	1201	97	38	0.75	0.61	1.18	1424	0	27	0	1.00	1.00	1.93

Date: 24/1/2003

Subject: **Removal of CH_3CHO(150 ppm)-$(CH_3)_3N$ 100 ppm from N_2-O_2(20%), I=0.3 mA**

Gas flow rate:		
	CH_3CHO	7.5 cc/min
	$(CH_3)_3N$	5 cc/min
	O_2	20 cc/min
	N_2 (dilute flow rate)	77.5 cc/min
	Total flow rate	100 cc/min

			CH_3CHO							$(CH_3)_3N$						
			Peak Area		Concentration(ppm)		Removal Efficiency			Peak Area		Concentration(ppm)		Removal Efficiency		
T, C	V(kV)	P(W)	Outlet (0 mA)	Outlet (0.2 mA)	Cout (0 mA)	Cout (0.2 mA)	ψ,(-)	ψ',(-)	ψ'',(-)	Outlet (0 mA)	Outlet (0.2 mA)	Cout (0 mA)	Cout (0.2 mA)	ψ,(-)	ψ',(-)	ψ'',(-)
33	12.4	3.72	4012	0	126	0	1.00	1.00	1.02	4957	801	94	15	0.85	0.84	0.85
100	10.8	3.24	4107	0	129	0	1.00	1.00	1.25	4740	687	90	13	0.87	0.85	1.07
200	7.9	2.37	4421	812	139	25	0.83	0.82	1.28	2905	0	56	0	1.00	1.00	1.93
300	5.8	1.74	4135	1241	130	39	0.74	0.70	1.35	0	0	0	0	1.00	1.00	1.57

Date: 19/2/2003

Subject: **Removal of CH_3CHO(150 ppm)-$(CH_3)_3N$ 100 ppm from N_2-H_2O(5250 ppm), I=0.3 mA**

Gas flow rate:			
	CH_3CHO	7.5 cc/min	
	$(CH_3)_3N$	5 cc/min	
	N_2 (bubling)	10 cc/min	(water bath 34°C)
	N_2 (dilute flow rate)	77.5 cc/min	
	Total flow rate	100 cc/min	

			CH_3CHO							$(CH_3)_3N$						
			Peak Area		Concentration(ppm)		Removal Efficiency			Peak Area		Concentration(ppm)		Removal Efficiency		
T, C	V(kV)	P(W)	Outlet (0 mA)	Outlet (0.2 mA)	Cout (0 mA)	Cout (0.2 mA)	ψ,(-)	ψ',(-)	ψ'',(-)	Outlet (0 mA)	Outlet (0.2 mA)	Cout (0 mA)	Cout (0.2 mA)	ψ,(-)	ψ',(-)	ψ'',(-)
33	11.4	3.42	4073	633	128	20	0.87	0.84	0.86	4918	144	93	3	0.97	0.97	0.99
100	10.8	3.24	4017	321	126	10	0.93	0.92	1.15	5460	985	103	19	0.81	0.82	1.02
200	8.9	2.67	3981	429	125	13	0.91	0.89	1.40	5751	1078	109	21	0.79	0.81	1.27
300	5.4	1.62	3761	2230	118	70	0.53	0.41	0.79	5489	1544	104	30	0.70	0.71	1.38

Date: 19/2/2003

Subject: **Removal of CH_3CHO(150 ppm)-$(CH_3)_3N$ 100 ppm from N_2-H_2O(10500 ppm), I=0.3 mA**

Gas flow rate:			
CH_3CHO	7.5	cc/min	
$(CH_3)_3N$	5	cc/min	
N_2 (bubling)	20	cc/min	(water bath 34°C)
N_2 (dilute flow rate)	67.5	cc/min	
Total flow rate	100	cc/min	

			CH_3CHO							$(CH_3)_3N$						
			Peak Area		Concentration(ppm)		Removal Efficiency			Peak Area		Concentration(ppm)		Removal Efficiency		
T, C	V(kV)	P(W)	Outlet (0 mA)	Outlet (0.2 mA)	Cout (0 mA)	Cout (0.2 mA)	ψ,(-)	ψ',(-)	ψ'',(-)	Outlet (0 mA)	Outlet (0.2 mA)	Cout (0 mA)	Cout (0.2 mA)	ψ,(-)	ψ',(-)	ψ'',(-)
33	11.5	3.45	4050	463	127	15	0.90	0.89	0.90	4847	145	92	3	0.97	0.97	0.99
100	10.8	3.24	4013	263	126	8	0.95	0.93	1.17	5048	941	96	18	0.82	0.81	1.01
200	9.0	2.70	4019	345	126	11	0.93	0.91	1.44	5241	954	99	18	0.82	0.81	1.28
300	4.9	1.47	3737	2341	117	73	0.51	0.37	0.72	5014	1745	95	34	0.66	0.65	1.25

Date: 20/2/2003

Subject: **Removal of CH_3CHO(150 ppm)-$(CH_3)_3N$ 100 ppm from N_2-O_2(10%)-H_2O(5250 ppm), I=0.3 mA**

Gas flow rate:	CH_3CHO	7.5 cc/min	
	$(CH_3)_3N$	5 cc/min	
	O_2	10 cc/min	
	N_2 (bubling)	10 cc/min	(water bath 34°C)
	N_2 (dilute flow rate)	67.5 cc/min	
	Total flow rate	100 cc/min	

			CH_3CHO							$(CH_3)_3N$						
			Peak Area		Concentration(ppm)		Removal Efficiency			Peak Area		Concentration(ppm)		Removal Efficiency		
T, C	V(kV)	P(W)	Outlet (0 mA)	Outlet (0.2 mA)	Cout (0 mA)	Cout (0.2 mA)	ψ,(-)	ψ',(-)	ψ'',(-)	Outlet (0 mA)	Outlet (0.2 mA)	Cout (0 mA)	Cout (0.2 mA)	ψ,(-)	ψ',(-)	ψ'',(-)
33	13.6	4.08	4048	0	127	0	1.00	1.00	1.02	3668	938	70	18	0.82	0.74	0.76
100	12.4	3.72	4259	0	133	0	1.00	1.00	1.25	5413	715	103	14	0.86	0.87	1.08
200	10.3	3.09	4246	394	133	12	0.92	0.91	1.43	0	0	0	0	1.00	1.00	1.57
300	6.6	1.98	2919	1151	91	36	0.76	0.61	1.17	0	0	0	0	1.00	1.00	1.93

Date: 22/2/2003

Subject: **Removal of CH_3CHO(150 ppm)-$(CH_3)_3N$ 100 ppm from N_2-O_2(10%)-H_2O(10500 ppm), I=0.3 mA**

Gas flow rate:			
	CH_3CHO	7.5 cc/min	
	$(CH_3)_3N$	5 cc/min	
	O_2	10 cc/min	
	N_2 (bubling)	20 cc/min	(water bath 34°C)
	N_2 (dilute flow rate)	57.5 cc/min	
	Total flow rate	100 cc/min	

			CH_3CHO							$(CH_3)_3N$						
			Peak Area		Concentration(ppm)		Removal Efficiency			Peak Area		Concentration(ppm)		Removal Efficiency		
T, C	V(kV)	P(W)	Outlet (0 mA)	Outlet (0.2 mA)	Cout (0 mA)	Cout (0.2 mA)	ψ,(-)	ψ',(-)	ψ'',(-)	Outlet (0 mA)	Outlet (0.2 mA)	Cout (0 mA)	Cout (0.2 mA)	ψ,(-)	ψ',(-)	ψ'',(-)
33	13.1	3.93	4366	0	137	0	1.00	1.00	1.02	3545	622	68	12	0.88	0.82	0.84
100	11.8	3.54	4325	0	135	0	1.00	1.00	1.25	3689	573	70	11	0.89	0.84	1.05
200	10.2	3.06	4413	327	138	10	0.93	0.93	1.45	3379	211	65	4	0.96	0.94	1.47
300	7.2	2.16	2777	586	87	18	0.88	0.79	1.52	1393	0	27	0	1.00	1.00	1.93

Date: 21/2/2003

Subject: **Removal of CH_3CHO(150 ppm)-$(CH_3)_3N$ 100 ppm from N_2-O_2(20%)-H_2O(5250 ppm), I=0.3 mA**

Gas flow rate:			
CH_3CHO	7.5	cc/min	
$(CH_3)_3N$	5	cc/min	
O_2	20	cc/min	
N_2 (bubling)	10	cc/min	(water bath 34°C)
N_2 (dilute flow rate)	57.5	cc/min	
Total flow rate	100	cc/min	

			CH_3CHO							$(CH_3)_3N$						
			Peak Area		Concentration(ppm)		Removal Efficiency			Peak Area		Concentration(ppm)		Removal Efficiency		
T, C	V(kV)	P(W)	Outlet (0 mA)	Outlet (0.2 mA)	Cout (0 mA)	Cout (0.2 mA)	ψ,(-)	ψ',(-)	ψ'',(-)	Outlet (0 mA)	Outlet (0.2 mA)	Cout (0 mA)	Cout (0.2 mA)	ψ,(-)	ψ',(-)	ψ'',(-)
33	13.2	3.96	4453	0	140	0	1.00	1.00	1.02	3678	1016	70	20	0.80	0.72	0.73
100	12.3	3.69	4819	0	151	0	1.00	1.00	1.25	4690	1203	89	23	0.77	0.74	0.92
200	10.2	3.06	4842	0	152	0	1.00	1.00	1.57	2950	492	56	10	0.90	0.83	1.31
300	7.2	2.16	3409	1037	107	32	0.78	0.70	1.34	0	0	0	0	1.00	1.00	1.93

Date: 22/2/2003

Subject: **Removal of CH_3CHO(150 ppm)-$(CH_3)_3N$ 100 ppm from N_2-O_2(20%)-H_2O(10500 ppm), I=0.3 mA**

Gas flow rate:			
	CH_3CHO	7.5 cc/min	
	$(CH_3)_3N$	5 cc/min	
	O_2	20 cc/min	
	N_2 (bubling)	20 cc/min	(water bath 34°C)
	N_2 (dilute flow rate)	47.5 cc/min	
	Total flow rate	100 cc/min	

			CH_3CHO							$(CH_3)_3N$						
			Peak Area		Concentration(ppm)		Removal Efficiency			Peak Area		Concentration(ppm)		Removal Efficiency		
T, C	V(kV)	P(W)	Outlet (0 mA)	Outlet (0.2 mA)	Cout (0 mA)	Cout (0.2 mA)	ψ,(-)	ψ',(-)	ψ'',(-)	Outlet (0 mA)	Outlet (0.2 mA)	Cout (0 mA)	Cout (0.2 mA)	ψ,(-)	ψ',(-)	ψ'',(-)
33	13.4	4.02	4305	0	135	0	1.00	1.00	1.02	2370	1047	45	20	0.80	0.56	0.57
100	12.5	3.75	4761	0	149	0	1.00	1.00	1.25	3696	936	70	18	0.82	0.74	0.93
200	10.3	3.09	4627	0	145	0	1.00	1.00	1.57	1596	419	31	8	0.92	0.74	1.16
300	7.7	2.31	3267	909	102	28	0.81	0.72	1.39	0	0	0	0	1.00	1.00	1.93

APPENDIX I

Simultaneous Removal of Ammonia and Trimethylamine

Date: 1/2/2003

Subject: **Removal of NH_3(1000 ppm)-(CH3)$_3$N (100 ppm) from N_2, I=0.3 mA**

NH_3	50 cc/min
$(CH_3)_3N$	5 cc/min
N_2 (dilute flow rate)	45 cc/min
Total flow rate	100 cc/min

			NH_3							$(CH_3)_3N$						
			Peak Area		Concentration(ppm)		Removal Efficiency			Peak Area		Concentration(ppm)		Removal Efficiency		
T, C	V(kV)	P(W)	Outlet (0 mA)	Outlet (0.3 mA)	Cout (0 mA)	Cout (0.3 mA)	ψ,(-)	ψ',(-)	ψ'',(-)	Outlet (0 mA)	Outlet (0.3 mA)	Cout (0 mA)	Cout (0.3 mA)	ψ,(-)	ψ',(-)	ψ'',(-)
33	9.0	2.70	2477	2210	964	901	0.10	0.07	0.07	4018	2685	77	51	0.49	0.33	0.33
100	8.0	2.40	2582	2014	990	855	0.14	0.14	0.17	4406	2568	84	49	0.51	0.41	0.52
200	6.0	1.80	2607	1978	996	847	0.15	0.15	0.24	4687	2203	89	42	0.58	0.53	0.83
300	4.6	1.38	2298	1874	922	823	0.18	0.11	0.21	3914	1710	75	33	0.67	0.56	1.08

Date: 31/1/2003

Subject: **Removal of NH_3(1000 ppm)-$(CH3)_3N$ (100 ppm) from N_2-O_2(10%), I=0.3 mA**

NH_3	50	cc/min
$(CH_3)_3N$	5	cc/min
O_2	10	cc/min
N_2 (dilute flow rate)	35	cc/min
Total flow rate	100	cc/min

			NH_3							$(CH_3)_3N$						
			Peak Area		Concentration(ppm)		Removal Efficiency			Peak Area		Concentration(ppm)		Removal Efficiency		
T, C	V(kV)	P(W)	Outlet (0 mA)	Outlet (0.3 mA)	Cout (0 mA)	Cout (0.3 mA)	ψ,(-)	ψ',(-)	ψ'',(-)	Outlet (0 mA)	Outlet (0.3 mA)	Cout (0 mA)	Cout (0.3 mA)	ψ,(-)	ψ',(-)	ψ'',(-)
33	11.9	3.57	2241	214	908	252	0.75	0.72	0.74	4256	1345	81	26	0.74	0.68	0.69
100	10.5	3.15	2356	157	935	205	0.80	0.78	0.98	4997	878	95	17	0.83	0.82	1.03
200	9.0	2.70	2424	0	952	160	0.84	0.83	1.31	6197	0	117	0	1.00	1.00	1.57
300	6.5	1.95	2324	1141	928	661	0.34	0.29	0.55	1616	0	31	0	1.00	1.00	1.93

Date: 31/1/2003

Subject: **Removal of NH_3(1000 ppm)-$(CH3)_3N$ (100 ppm) from N_2-O_2(20%), I=0.3 mA**

NH_3	50	cc/min
$(CH_3)_3N$	5	cc/min
O_2	20	cc/min
N_2 (dilute flow rate)	25	cc/min
Total flow rate	100	cc/min

			NH_3							$(CH_3)_3N$						
			Peak Area		Concentration(ppm)		Removal Efficiency			Peak Area		Concentration(ppm)		Removal Efficiency		
T, C	V(kV)	P(W)	Outlet (0 mA)	Outlet (0.3 mA)	Cout (0 mA)	Cout (0.3 mA)	ψ,(-)	ψ',(-)	ψ'',(-)	Outlet (0 mA)	Outlet (0.3 mA)	Cout (0 mA)	Cout (0.3 mA)	ψ,(-)	ψ',(-)	ψ'',(-)
33	12.0	3.60	2206	180	900	224	0.78	0.75	0.76	5181	1754	98	34	0.66	0.66	0.67
100	10.6	3.18	2412	0	949	150	0.85	0.84	1.05	5613	1054	106	20	0.80	0.81	1.01
200	9.2	2.76	2497	0	969	100	0.90	0.90	1.41	3667	215	70	4	0.96	0.94	1.48
300	6.7	2.01	2297	764	921	550	0.45	0.40	0.78	0	0	0	0	1.00	1.00	1.93

Date: 25/2/2003

Subject: **Removal of NH_3(1000 ppm)-$(CH3)_3N$ (100 ppm) from N_2-H_2O(5250 ppm), I=0.3 mA**

NH_3	50 cc/min	
$(CH_3)_3N$	5 cc/min	
N_2 (bubling)	10 cc/min	(water bath 34°C)
N_2 (dilute flow rate)	35 cc/min	
Total flow rate	100 cc/min	

			NH_3							$(CH_3)_3N$						
			Peak Area		Concentration(ppm)		Removal Efficiency			Peak Area		Concentration(ppm)		Removal Efficiency		
T, C	V(kV)	P(W)	Outlet (0 mA)	Outlet (0.3 mA)	Cout (0 mA)	Cout (0.3 mA)	ψ,(-)	ψ',(-)	ψ'',(-)	Outlet (0 mA)	Outlet (0.3 mA)	Cout (0 mA)	Cout (0.3 mA)	ψ,(-)	ψ',(-)	ψ'',(-)
33	8.6	2.58	2521	2291	975	920	0.08	0.06	0.06	3734	1245	71	24	0.76	0.66	0.68
100	7.8	2.34	2601	2175	995	893	0.11	0.10	0.13	3201	1337	61	26	0.74	0.58	0.72
200	6.7	2.01	2641	2154	1004	888	0.11	0.12	0.18	3539	1396	68	27	0.73	0.60	0.95
300	4.7	1.41	2465	2293	962	920	0.08	0.04	0.08	1567	854	30	16	0.84	0.45	0.87

Date: 26/2/2003

Subject: **Removal of NH_3(1000 ppm)-(CH3)$_3$N (100 ppm) from N_2-H_2O(10500 ppm), I=0.3 mA**

NH_3	50 cc/min	
$(CH_3)_3N$	5 cc/min	
N_2 (bubling)	20 cc/min	(water bath 34°C)
N_2 (dilute flow rate)	25 cc/min	
Total flow rate	100 cc/min	

			NH_3							$(CH_3)_3N$						
			Peak Area		Concentration(ppm)		Removal Efficiency			Peak Area		Concentration(ppm)		Removal Efficiency		
T, C	V(kV)	P(W)	Outlet (0 mA)	Outlet (0.3 mA)	Cout (0 mA)	Cout (0.3 mA)	ψ,(-)	ψ',(-)	ψ'',(-)	Outlet (0 mA)	Outlet (0.3 mA)	Cout (0 mA)	Cout (0.3 mA)	ψ,(-)	ψ',(-)	ψ'',(-)
33	8.6	2.58	2534	2002	978	852	0.15	0.13	0.13	3503	1256	67	24	0.76	0.64	0.65
100	7.8	2.34	2589	2068	992	868	0.13	0.13	0.16	3681	1452	70	28	0.72	0.60	0.75
200	6.7	2.01	2690	1981	1017	848	0.15	0.17	0.26	3798	1437	72	28	0.72	0.62	0.97
300	4.7	1.41	2389	1754	943	796	0.20	0.16	0.30	1999	857	38	17	0.83	0.57	1.10

Date: 27/2/2003

Subject: **Removal of NH_3(1000 ppm)-$(CH3)_3N$ (100 ppm) from N_2-O_2(10%)-H_2O(5250 ppm), I=0.3 mA**

NH_3	50 cc/min	
$(CH_3)_3N$	5 cc/min	
O_2	10 cc/min	
N_2 (bubling)	10 cc/min	(water bath 34°C)
N_2 (dilute flow rate)	25 cc/min	
Total flow rate	100 cc/min	

			NH_3							$(CH_3)_3N$						
			Peak Area		Concentration(ppm)		Removal Efficiency			Peak Area		Concentration(ppm)		Removal Efficiency		
T, C	V(kV)	P(W)	Outlet (0 mA)	Outlet (0.3 mA)	Cout (0 mA)	Cout (0.3 mA)	ψ,(-)	ψ',(-)	ψ'',(-)	Outlet (0 mA)	Outlet (0.3 mA)	Cout (0 mA)	Cout (0.3 mA)	ψ,(-)	ψ',(-)	ψ'',(-)
33	13.0	3.90	2463	0	961	135	0.87	0.86	0.88	3287	1215	63	23	0.77	0.63	0.64
100	11.8	3.54	2610	0	997	125	0.88	0.87	1.09	3688	899	70	17	0.83	0.75	0.94
200	10.4	3.12	2475	0	964	80	0.92	0.92	1.44	2072	0	40	0	1.00	1.00	1.57
300	7.2	2.16	2215	611	902	482	0.52	0.47	0.90	0	0	0	0	1.00	1.00	1.93

Date: 26/2/2003

Subject: **Removal of NH_3(1000 ppm)-(CH3)$_3$N (100 ppm) from N_2-O_2(10%)-H_2O(10500 ppm), I=0.3 mA**

NH_3	50 cc/min	
$(CH_3)_3N$	5 cc/min	
O_2	10 cc/min	
N_2 (bubling)	20 cc/min	(water bath 34°C)
N_2 (dilute flow rate)	15 cc/min	
Total flow rate	100 cc/min	

			NH_3							$(CH_3)_3N$						
			Peak Area		Concentration(ppm)		Removal Efficiency			Peak Area		Concentration(ppm)		Removal Efficiency		
T, C	V(kV)	P(W)	Outlet (0 mA)	Outlet (0.3 mA)	Cout (0 mA)	Cout (0.3 mA)	ψ,(-)	ψ',(-)	ψ'',(-)	Outlet (0 mA)	Outlet (0.3 mA)	Cout (0 mA)	Cout (0.3 mA)	ψ,(-)	ψ',(-)	ψ'',(-)
33	13.1	3.93	2548	0	982	145	0.86	0.85	0.87	3370	1087	64	21	0.79	0.67	0.69
100	11.8	3.54	2612	0	997	135	0.87	0.86	1.08	3871	873	74	17	0.83	0.77	0.96
200	10.4	3.12	2754	0	1032	80	0.92	0.92	1.45	1531	0	29	0	1.00	1.00	1.57
300	7.2	2.16	2540	680	980	514	0.49	0.48	0.92	0	0	0	0	1.00	1.00	1.93

APPENDIX J

Simultaneous Removal of Acetaldehyde, Ammonia and Trimethylamine

Date: 11/2/03

Subject: **Removal of CH_3CHO(150 ppm)-NH_3(1000 ppm)-$(CH3)_3N$ (100 ppm) from N_2, I=0.3 mA**

Gas flow rate:

CH_3CHO	7.5	cc/min
NH_3	50	cc/min
$(CH_3)_3N$	5	cc/min
N_2 (dilute flow rate)	37.5	cc/min
Total flow rate	100	cc/min

			CH_3CHO								$(CH_3)_3N$							
			Peak Area		Concentration(ppm)		Removal Efficiency			Peak Area		Concentration(ppm)		Removal Efficiency		
T, C	V(kV)	P(W)	Outlet (0 mA)	Outlet (0.3 mA)	Cout (0 mA)	Cout (0.3 mA)	ψ,(-)	ψ',(-)	ψ'',(-)	Outlet (0 mA)	Outlet (0.3 mA)	Cout (0 mA)	Cout (0.3 mA)	ψ,(-)	ψ',(-)	ψ'',(-)
33	8.8	2.64	3956	2935	124	92	0.39	0.26	0.26	3918	1814	75	35	0.65	0.53	0.54
100	8.1	2.43	3862	2989	121	94	0.38	0.23	0.28	4302	2210	82	42	0.58	0.48	0.60
200	6.0	1.80	3586	2647	112	83	0.45	0.26	0.41	4504	1978	86	38	0.62	0.56	0.87
300	4.5	1.35	2994	1770	94	55	0.63	0.41	0.79	3727	957	71	18	0.82	0.74	1.43

	NH_3						
	Peak Area		Concentration(ppm)		Removal Efficiency		
T, C	Outlet (0 mA)	Outlet (0.3 mA)	Cout (0 mA)	Cout (0.3 mA)	ψ,(-)	ψ',(-)	ψ'',(-)
33	1760	1557	797	752	0.25	0.06	0.06
100	1986	1447	849	728	0.27	0.14	0.18
200	2612	1950	997	840	0.16	0.16	0.25
300	1665	1142	776	662	0.34	0.15	0.28

Date: 12/2/03

Subject: **Removal of CH_3CHO(150 ppm)-NH_3(1000 ppm)-$(CH3)_3N$ (100 ppm) from N_2-O_2(10%), I=0.3 mA**

Gas flow rate:		
	CH_3CHO (2000 ppm balance N_2)	7.5 cc/min
	NH_3 (2000 ppm balance N_2)	50 cc/min
	$(CH_3)_3N$(2000 ppm balance N_2)	5 cc/min
	O_2	10 cc/min
	N_2 (dilute flow rate)	27.5 cc/min
	Total flow rate	100 cc/min

			CH_3CHO							$(CH_3)_3N$						
			Peak Area		Concentration(ppm)		Removal Efficiency			Peak Area		Concentration(ppm)		Removal Efficiency		
T, C	V(kV)	P(W)	Outlet (0 mA)	Outlet (0.3 mA)	Cout (0 mA)	Cout (0.3 mA)	ψ,(-)	ψ',(-)	ψ'',(-)	Outlet (0 mA)	Outlet (0.3 mA)	Cout (0 mA)	Cout (0.3 mA)	ψ,(-)	ψ',(-)	ψ'',(-)
33	12.5	3.75	4363	370	137	12	0.92	0.92	0.93	4181	1055	80	20	0.80	0.74	0.76
100	10.8	3.24	4549	463	143	15	0.90	0.90	1.12	3733	835	71	16	0.84	0.77	0.97
200	9.3	2.79	4603	465	144	15	0.90	0.90	1.41	2556	-	49	0	1.00	1.00	1.57
300	6.2	1.86	2535	1295	79	41	0.73	0.49	0.94	-	-	0	0	1.00	1.00	1.93

	NH_3						
	Peak Area		Concentration(ppm)		Removal Efficiency		
T, C	Outlet (0 mA)	Outlet (0.3 mA)	Cout (0 mA)	Cout (0.3 mA)	ψ,(-)	ψ',(-)	ψ'',(-)
33	1648	-	772	245	0.76	0.68	0.70
100	2008	-	854	180	0.82	0.79	0.99
200	2253	-	911	155	0.85	0.83	1.30
300	1873	1101	823	653	0.35	0.21	0.40

Date: 13/2/03

Subject: **Removal of CH_3CHO(150 ppm)-NH_3(1000 ppm)-$(CH3)_3N$ (100 ppm) from N_2-O_2(20%), I=0.3 mA**

Gas flow rate:		
	CH_3CHO (2000 ppm balance N_2)	7.5 cc/min
	NH_3 (2000 ppm balance N_2)	50 cc/min
	$(CH_3)_3N$(2000 ppm balance N_2)	5 cc/min
	O_2	20 cc/min
	N_2 (dilute flow rate)	17.5 cc/min
	Total flow rate	100 cc/min

			CH_3CHO							$(CH_3)_3N$						
			Peak Area		Concentration(ppm)		Removal Efficiency			Peak Area		Concentration(ppm)		Removal Efficiency		
T, C	V(kV)	P(W)	Outlet (0 mA)	Outlet (0.3 mA)	Cout (0 mA)	Cout (0.3 mA)	ψ,(-)	ψ',(-)	ψ'',(-)	Outlet (0 mA)	Outlet (0.3 mA)	Cout (0 mA)	Cout (0.3 mA)	ψ,(-)	ψ',(-)	ψ'',(-)
33	12.3	3.69	4753	0	149	0	1.00	1.00	1.02	3629	1115	69	21	0.79	0.69	0.70
100	10.9	3.27	5751	0	180	0	1.00	1.00	1.25	3980	945	76	18	0.82	0.76	0.95
200	9.5	2.85	5261	0	165	0	1.00	1.00	1.57	1363	0	26	0	1.00	1.00	1.57
300	6.5	1.95	4110	1393	129	44	0.71	0.66	1.28	-	-	0	0	1.00	1.00	1.93

	NH_3						
	Peak Area		Concentration(ppm)		Removal Efficiency		
T, C	Outlet (0 mA)	Outlet (0.3 mA)	Cout (0 mA)	Cout (0.3 mA)	ψ,(-)	ψ',(-)	ψ'',(-)
33	1792	-	804	200	0.80	0.75	0.77
100	1918	-	833	135	0.87	0.84	1.05
200	2271	-	915	50	0.95	0.95	1.49
300	1669	627	777	490	0.51	0.37	0.71

Date: 3/3/2003

Subject: **Removal of CH_3CHO(150 ppm)-NH_3(1000 ppm)-$(CH3)_3N$ (100 ppm) from N_2-H_2O(5250 ppm), I=0.3 mA**

Gas flow rate:

CH_3CHO (2000 ppm balance N_2)	7.5	cc/min	
NH_3 (2000 ppm balance N_2)	50	cc/min	
$(CH_3)_3N$(2000 ppm balance N_2)	5	cc/min	
N2 (bubling)	10	cc/min	(water bath 34°C)
N_2 (dilute flow rate)	27.5	cc/min	
Total flow rate	100	cc/min	

			CH_3CHO							$(CH_3)_3N$						
			Peak Area		Concentration(ppm)		Removal Efficiency			Peak Area		Concentration(ppm)		Removal Efficiency		
T, C	V(kV)	P(W)	Outlet (0 mA)	Outlet (0.3 mA)	Cout (0 mA)	Cout (0.3 mA)	ψ,(-)	ψ',(-)	ψ'',(-)	Outlet (0 mA)	Outlet (0.3 mA)	Cout (0 mA)	Cout (0.3 mA)	ψ,(-)	ψ',(-)	ψ'',(-)
33	9.4	2.82	3063	2480	96	78	0.48	0.19	0.19	3764	2736	72	52	0.87	0.27	0.28
100	8.7	2.61	3895	2985	122	94	0.38	0.23	0.29	3864	1853	74	36	0.91	0.52	0.65
200	6.5	1.95	4052	2882	127	90	0.40	0.29	0.45	3458	1702	66	33	0.92	0.50	0.79
300	4.7	1.41	2679	1911	84	60	0.60	0.29	0.55	1216	400	23	8	0.98	0.67	1.29

	NH_3						
	Peak Area		Concentration(ppm)		Removal Efficiency		
T, C	Outlet (0 mA)	Outlet (0.3 mA)	Cout (0 mA)	Cout (0.3 mA)	ψ,(-)	ψ',(-)	ψ'',(-)
33	2315	1905	926	830	0.17	0.10	0.11
100	2596	1926	993	835	0.17	0.16	0.20
200	2415	1963	950	843	0.16	0.11	0.18
300	2119	1884	880	825	0.17	0.06	0.12

Date: 3/3/2003

Subject: **Removal of CH_3CHO(150 ppm)-NH_3(1000 ppm)-(CH3)$_3$N (100 ppm) from N_2-H_2O(10500 ppm), I=0.3 mA**

Gas flow rate:			
	CH_3CHO (2000 ppm balance N_2)	7.5 cc/min	
	NH_3 (2000 ppm balance N_2)	50 cc/min	
	$(CH_3)_3N$(2000 ppm balance N_2)	5 cc/min	
	N_2 (bubling)	20 cc/min	(water bath 34°C)
	N_2 (dilute flow rate)	17.5 cc/min	
	Total flow rate	100 cc/min	

			CH_3CHO							$(CH_3)_3N$						
			Peak Area		Concentration(ppm)		Removal Efficiency			Peak Area		Concentration(ppm)		Removal Efficiency		
T, C	V(kV)	P(W)	Outlet (0 mA)	Outlet (0.3 mA)	Cout (0 mA)	Cout (0.3 mA)	ψ,(-)	ψ',(-)	ψ'',(-)	Outlet (0 mA)	Outlet (0.3 mA)	Cout (0 mA)	Cout (0.3 mA)	ψ,(-)	ψ',(-)	ψ'',(-)
33	9.4	2.82	3737	2883	117	90	0.40	0.23	0.23	4362	2495	83	48	0.52	0.42	0.43
100	8.4	2.52	3996	2982	125	93	0.38	0.25	0.32	4935	2498	94	48	0.52	0.49	0.61
200	6.8	2.04	4268	3006	134	94	0.37	0.30	0.46	4208	2921	80	56	0.44	0.30	0.47
300	4.8	1.44	3091	2055	97	64	0.57	0.34	0.65	2503	1228	48	24	0.76	0.51	0.98

	NH_3						
	Peak Area		Concentration(ppm)		Removal Efficiency		
T, C	Outlet (0 mA)	Outlet (0.3 mA)	Cout (0 mA)	Cout (0.3 mA)	ψ,(-)	ψ',(-)	ψ'',(-)
33	2526	2068	976	868	0.13	0.11	0.11
100	2601	2162	995	890	0.11	0.11	0.13
200	3054	2295	1109	921	0.08	0.17	0.27
300	2119	1884	880	825	0.17	0.06	0.12

Date: 4/3/2003

Subject: **Removal of CH_3CHO(150 ppm)-NH_3(1000 ppm)-(CH3)$_3$N (100 ppm) from N_2-O_2(10%)H_2O(5250 ppm), I=0.3 mA**

Gas flow rate:			
	CH_3CHO (2000 ppm balance N_2)	7.5 cc/min	
	NH_3 (2000 ppm balance N_2)	50 cc/min	
	$(CH_3)_3N$(2000 ppm balance N_2)	5 cc/min	
	O_2	10 cc/min	
	N_2 (bubling)	10 cc/min	(water bath 34°C)
	N_2 (dilute flow rate)	17.5 cc/min	
	Total flow rate	100 cc/min	

			CH_3CHO							$(CH_3)_3N$						
			Peak Area		Concentration(ppm)		Removal Efficiency			Peak Area		Concentration(ppm)		Removal Efficiency		
T, C	V(kV)	P(W)	Outlet (0 mA)	Outlet (0.3 mA)	Cout (0 mA)	Cout (0.3 mA)	ψ,(-)	ψ',(-)	ψ'',(-)	Outlet (0 mA)	Outlet (0.3 mA)	Cout (0 mA)	Cout (0.3 mA)	ψ,(-)	ψ',(-)	ψ'',(-)
33	13.3	3.99	3672	226	115	7	0.95	0.94	0.96	3838	1060	73	20	0.80	0.72	0.73
100	11.8	3.54	3512	205	110	6	0.96	0.94	1.18	3611	1228	69	24	0.76	0.66	0.82
200	10.4	3.12	3526	259	110	8	0.95	0.93	1.46	2849	143	55	3	0.97	0.95	1.49
300	7.2	2.16	2663	540	83	17	0.89	0.80	1.54	-	-	-	-	1.00	1.00	1.93

	NH_3						
	Peak Area		Concentration(ppm)		Removal Efficiency		
T, C	Outlet (0 mA)	Outlet (0.3 mA)	Cout (0 mA)	Cout (0.3 mA)	ψ,(-)	ψ',(-)	ψ'',(-)
33	2415	-	950	150	0.85	0.84	0.86
100	2521	-	975	135	0.87	0.86	1.08
200	2705	-	1020	80	0.92	0.92	1.45
300	2455	401	959	508	0.49	0.47	0.91

APPENDIX K

Simultaneous Removal of Acetaldehyde, Ammonia and Trimethylamine using two serial reactors

Date: 6/3/03

Subject: **Simultaneous removal of CH_3CHO(150)-NH_3(1000ppm)-$(CH_3)_3N$ (100ppm) from N_2-O_2 (10%)-H_2O(5250ppm) using two reactors in series**

Gas flow rate:

CH_3CHO (balanced N_2 2000 ppm)	7.5	cc/min
NH_3(balanced N_2 2000 ppm)	50	cc/min
$(CH_3)_3N$(balanced N_2 2000 ppm)	5	cc/min
O_2	10	cc/min
N_2 (bubbling)	10	cc/min(34 ^oC)
N_2 (dilute)	17.5	cc/min
total flow rate	100	cc/min

1.First reactor

Inlet concentration			
	CH_3CHO	150	ppm
	NH3	1000	ppm
	$(CH_3)_3N$	100	ppm

Temperature: 300 ^0C Cuurent: 0.3 mA

I (mA)	V (kV)	Cout, CH_3CHO (ppm)	Cout, NH_3 (ppm)	Cout, $(CH_3)_3N$(ppm)	Reaction by products
0.3	7.4	14	440	0	NOx-50 ppm

2. Second reactor (33 ^oC)

I (mA)	V (kV)	Cout, CH_3CHO (ppm)	Cout, NH_3 (ppm)	Cout, $(CH_3)_3N$(ppm)	Reaction by products
0	0	16	400	0	NOx-35 ppm,O_3-0 ppm
0.01	10.6	0	390	0	NOx-0 ppm, O_3-60 ppm
0.03	10.8	0	230	0	NOx-0 ppm, O_3-170ppm
0.1	11.7	0	45	0	NOx-0 ppm, O_3>400 ppm
0.2	12.7	0	20	0	NOx-0 ppm, O_3>400 ppm
0.3	13.3	0	0	0	NOx-0 ppm, O_3>400 ppm

3. Second reactor (200 ^oC)

I (mA)	V (kV)	Cout, CH_3CHO (ppm)	Cout, NH_3 (ppm)	Cout, $(CH_3)_3N$(ppm)	Reaction by products
0	0	16	460	0	NOx-30 ppm
0.1	8.3	0	255	0	NOx-0 ppm
0.2	9.3	0	45	0	NOx-20 ppm
0.3	10.1	0	0	0	NOx-20 ppm
0.4	10.7	0	0	0	NOx-35 ppm

Date: 15/5/02

Subject: Substantiation of ozone effect on the CH_3CHO removal

1) Ozone disappear in second reactor

1) Gas flow rate:	**First reactor**			**Second reactor**					
	N_2 flow rate	65	cc/min	Flow rate from first reactor	70	cc/min			
	O_2 flow rate	5	cc/min	add N_2 flow rate	30	cc/min			
	total flow rate	70	cc/min	total flow rate	100	cc/min			
Current 0.2 mA	Voltage	12.8	kV	Current	0	mA	Voltage	0	kV
				Cin, O_3	700	ppm	Cout, O_3	650	ppm

2) CH_3CHO disappear in second reactor

2) Gas flow rate:	**First reactor**			**Second reactor**					
	N_2 flow rate	0	cc/min	N_2 flow rate	70	cc/min			
	CH_3CHO balanced N2	0	cc/min	CH_3CHO balanced N_2	30	cc/min			
	total flow rate	0	cc/min	total flow rate	100	cc/min			
Current 0 mA	Voltage	0	kV	Current	0	mA	Voltage	0	kV
				Cin, CH_3CHO	600	ppm	Cout, CH_3CHO	583	ppm

3)Ozone effect on CH_3CHO

3) Gas flow rate:	**First reactor**			**Second reactor**					
	N_2 flow rate	75	cc/min	Flow rate from first reactor	70	cc/min			
	O_2 flow rate	5	cc/min	add CH_3CHO balanced N_2	30	cc/min			
	total flow rate	80	cc/min	total flow rate	100	cc/min			
Current 0.2 mA	Voltage	12.8	kV	Current	0	mA	Voltage	0	kV
				Cin, O_3	700	ppm	Cout, O_3	460	ppm
				Cin, CH_3CHO	600	ppm	Cout, CH_3CHO	380	ppm

Date: 14/12/02

Subject: Substantiation of ozone effect on the $(CH_3)_3N$ removal

1) Ozone disappear in second reactor

1) Gas flow rate:	**First reactor**			**Second reactor**					
	N_2 flow rate	70	cc/min	Flow rate from first reactor	80	cc/min			
	O_2 flow rate	10	cc/min	add N_2 flow rate	20	cc/min			
	total flow rate	80	cc/min	total flow rate	100	cc/min			
Current 0.02 mA	Voltage	11.0	kV	Current	0	mA	Voltage	0	kV
				Cin, O_3	860	ppm	Cout, O_3	720	ppm

2) CH_3CHO disappear in second reactor

2) Gas flow rate:	**First reactor**			**Second reactor**					
	N_2 flow rate	0	cc/min	N_2 flow rate	80	cc/min			
	$(CH_3)_3N$ balanced N_2	0	cc/min	$(CH_3)_3N$ balanced N_2	20	cc/min			
	total flow rate	0	cc/min	total flow rate	100	cc/min			
Current 0 mA	Voltage	0	kV	Current	0	mA	Voltage	0	kV
				Cin, $(CH_3)_3N$	400	ppm	Cout, $(CH_3)_3N$	313	ppm

3)Ozone effect on $(CH_3)_3N$

3) Gas flow rate:	**First reactor**			**Second reactor**					
	N_2 flow rate	75	cc/min	Flow rate from first reactor	80	cc/min			
	O_2 flow rate	5	cc/min	add $(CH_3)_3N$ balanced N_2	20	cc/min			
	total flow rate	80	cc/min	total flow rate	100	cc/min			
Current 0.02 mA	Voltage	11.0	kV	Current	0	mA	Voltage	0	kV
				Cin, O_3	860	ppm	Cout, O_3	10	ppm
				Cin, $(CH_3)_3N$	400	ppm	Cout, $(CH_3)_3N$	222	ppm

APPENDIX L

Publications Co-authored by J.Chaichanawong

1. Tanthapanichakoon, W., Charinpanitkul, T., **Chaichanawong, J.,** Sano, N., Tamon, H., "High-Temperature Removal of Acetaldehyde in a Corona Discharge Reactor" accepted for publication in The Fourth Asia Pacific Conference on Sustainable Energy and Energy and Environmental Technologies (4th APCSEET), May 8-10, 2003.

2. Tanthapanichakoon, W., Charinpanitkul, T., Chaiyo, S., Dhattavorn, N., **Chaichanawong, J.**, Sano, N., Tamon, H., "Effect of Oxygen and Water Vapor on the Removal of Styrene and Ammonia from Nitrogen by Non-pulse Corona Discharge at Elevated Temperatures", submit for publication in Chemical Engineering Journal.

High-Temperature Removal of Acetaldehyde in a Corona Discharge Reactor

WIWUT TANTHAPANICHAKOON*, TAWATCHAI CHARINPANITKUL AND
JINTAWAT CHAICHANAWONG

Department of Chemical Engineering, Chulalongkorn University
Payathai Road, Pathumwan, Bangkok 10330 Thailand
E-mail: fchwtt@eng.chula.ac.th
NORIAKI SANO

Department of Chemical Engineering, Himeji Institute of Technology
2167 Shosha, Himeji, Hyogo 671-2201, Japan
HAJIME TAMON

Department of Chemical Engineering, Kyoto university
Yoshida-Honmachi, Sakyo-ku, Kyoto 606-8501, Japan.

Acetaldehyde is one of the malodorous gaseous components emitted at high temperature from a crematory furnace. In this study a corona discharge reactor is employed to remove acetaldehyde (CH_3CHO) from N_2 and air from room temperature up to 300 °C. First the effect of acetaldehyde inlet concentration (200 ,400 and 600 ppm) is investigated. In contrast to conventional separation processes, the more dilute the inlet concentration, the higher the removal efficiency becomes because, when the discharged current is kept constant, the number ratio of discharge electrons to acetaldehyde molecules increases. Next the effect of oxygen and/or water vapor in the emission gas is investigated. Interestingly the presence of either oxygen or water vapor always enhances the removal of acetaldehyde from N_2. When the reaction temperature is increased, the removal efficiency is found to increase starting from room temperature up to 200 °C, above which the tendency reverses up to 300 °C. It is found that the smallest discharge current required for complete removal of 600 ppm of acetaldehyde from the air is only 0.2 mA at room temperature. To elucidate the effect of temperature, the discharge current is deliberately set at 0.05 mA in some experiments.

1 Introduction

Air pollution is an important public issue in Thailand. One major cause of air pollution is the emission of toxic and malodorous gases from many sources such as industrial plants and automobile. Recently, a latent source of public nuisance has become prominent. It is the emission of gases and particulate from the crematory furnace in a temple. There are nearly 23,000 temples in Thailand. The majority of them have crematory furnaces, most of which release the exhaust gas from the stacks to the atmosphere without any effective treatment. Although the concentration levels of malodorous gases are very low in the ppm or ppb orders, they not only pose serious public nuisance but may also be detrimental to public health. Only a few rich temples in Bangkok have installed furnaces with efficient after-burning systems to decompose the malodorous organic gaseous components. The outlet gas temperature from a well-operated furnace may be as high as 800~900 °C whereas the stack temperature may range from 150~300 °C.

In 1995, a novel gas purification method using electron attachment was proposed [1]. The gas impurities are ionized by collisions with electrons produced, for example, in a corona discharge between a wire cathode and a cylindrical anode. The resulting negative ions drift to the anode and deposit on it. Previous studies have revealed that gases of high electron affinity, for example sulfur compounds, halogens, malodorous gases, VOCs and CFCs are selectively removed by the proposed method [1-8]. Though acetaldehyde is emitted at high temperature from a crematory furnace, there is insufficient report on the effect of high temperature [9-11]. In this study a corona discharge reactor is employed to remove acetaldehyde (CH_3CHO) from N_2 and air from room temperature up to 300 ^oC.

2 Experimental Setup

Figure 1 shows a schematic diagram of the experimental apparatus. The deposition-type reactor consists of a SUS pipe, 3.7 cm inner diameter and 80 cm length, as the anode. The cathode is a 0.5-mm stainless-steel wire suspended from a silicone plug at the top of the reactor and straightened along the axis of the vertical anode by a small weight. A high-voltage DC generator (Matsusada, HAR-30N5) is utilized to supply a steady stream of low-energy electrons to the corona-discharge reactor. To control the reactor temperature, 6 infrared heating lamps (200V, 700W each) are installed lengthwise around the outside perimeter of the reactor. The temperature control unit consists of a temperature controller (FENWAL, AR-24L) and a thyrister power regulator (Shimaden, PAC15C003081-NO). The desired concentrations of acetaldehyde and coexisting oxygen are adjusted by diluting standard gases with pure nitrogen. The inlet concentrations of acetaldehyde investigated are 200, 400 and 600 ppm. Similarly, the concentrations of coexisting O_2 and H_2O are varied from 0-20% and 0-23000 ppm, respectively. Inlet and outlet concentrations of acetaldehyde are analyzed using a gas chromatograph (Shimadzu Corp., GC 9A) equipped with a flame ionization detector (FID). The concentration of byproduct ozone is separately detected with appropriate gas detector tubes (GASTEC Co., Ltd. and Kitagawa Co., Ltd.).

The inlet concentrations of acetaldehyde are deliberately set higher than their reported values of ca. 4 ppm in crematory emission for two reasons. First, our present and previous investigations have conclusively shown that, as the inlet concentration of an impurity gas rises, its removal efficiency always drops because the ratio of its absolute number of molecules to the number of discharged electrons decreases. Thus the experimental results represent conservative values. Second, if the concentration is too low (a few ppm order or less), there will be high uncertainty in the measurement values obtained by the gas chromatographs.

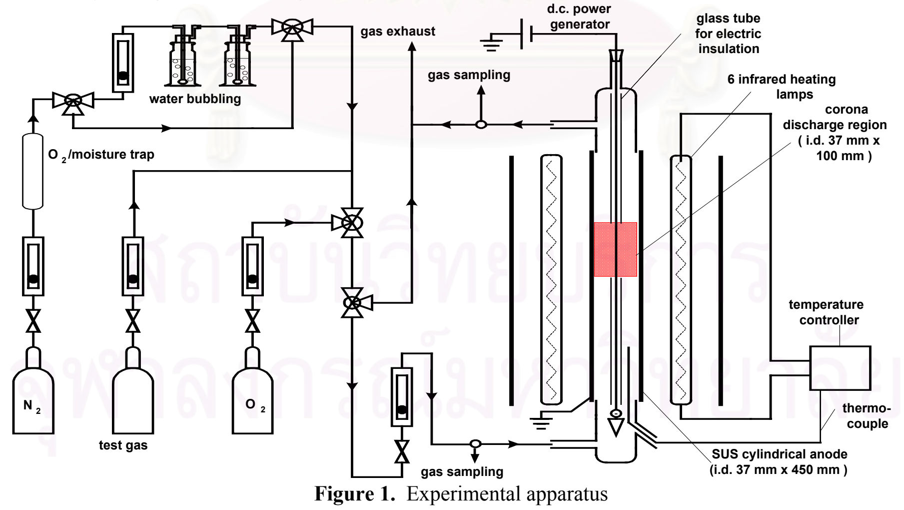

Figure 1. Experimental apparatus

3 Results and Discussion

3.1 *Definitions of removal efficiency*

To exclude any possible effect of adsorption at low temperature and thermal decomposition at high temperature, the removal efficiency ψ is defined as Eq.1

$$\psi = \frac{(C_{out,0mA} - C_{out,any\ mA})}{C_{out,0mA}} \quad [-] \qquad (1)$$

Here, $C_{out,0\ mA}$ (ppm) and $C_{out,\ any\ mA}$ (ppm) are the outlet concentrations of the impurity gas without and with discharge current.

The removal efficiency per unit residence time, ψ', in Eq. 2 takes into account the actual shorter residence time of the hot gas in the reactor even though the inlet gas flow rate (mole basis) remains unchanged before and after the reactor temperature is elevated.

$$\psi' = \frac{\psi \times residence\ \ time\ \ at\ \ 25\ \ {}^0C}{residence\ \ time\ \ at\ \ T\ \ {}^0C} \quad [-] \qquad (2)$$

At steady state, the equation of continuity requires that $\rho_1\langle\upsilon_1\rangle A_1 = \rho_2\langle\upsilon_2\rangle A_2$. Since $A_1 = A_2$ and ρ is a function of the gas temperature, the gas velocity at an elevated temperature T_2 will be faster than its velocity at room temperature T_1. Thus the mean residence time $\theta_2 = \frac{V}{\langle\upsilon_2\rangle}$ of this gas at T_2 is shorter than $\theta_1 = \frac{V}{\langle\upsilon_1\rangle}$ at room temperature. Here V is the effective volume of the reactor.

3.2 Effect of temperature and inlet concentration on the removal of acetaldehyde from N_2

Figure 2 shows the two kinds of the removal efficiency of acetaldehyde from pure N_2 at elevated temperatures. From Figure 2(a), we see that, as the temperature increase, the removal efficiency ψ decrease starting from room temperature up to 200 °C, then the tendency reverses up to 300 °C. Figure 2(b) reveals that when the negative effect of reduced resident time is taken in account, the value of ψ' increases with temperature up to 150 °C. Tamon et al.[1] have found that the removal efficiency via electron attachment tends to decrease when the inlet concentration is increased. As expected, the present experimental results also exhibit the same tendency. The more dilute the inlet concentration, the higher the removal efficiency becomes because, when the discharged current is kept constant, the number ratio of the discharge electrons to the acetaldehyde molecules increases.

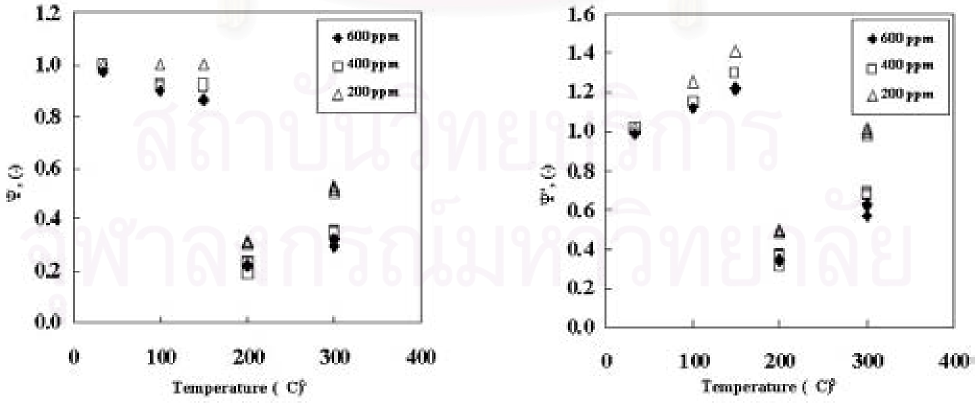

(a) (b)

Figure 2. Effect of temperature and inlet concentration on the removal of acetaldehyde from N_2; I=0.2 mA, SV=55.8 hr^{-1} at room temperature.

3.3 Effect of coexisting O_2 and water vapor on the removal of acetaldehyde from N_2

Experiments were carried out to observe the combined effect of O_2 and H_2O on the removal of acetaldehyde from N_2. Figure 3 shows the two types of the removal efficiency ψ and ψ' of acetaldehyde from N_2-O_2 at various concentrations of water vapor. It is found that the presence of either oxygen or water vapor always enhances the removal of acetaldehyde from N_2. When the reaction temperature is increased, the removal efficiency is found to increase starting from room temperature up to 200 ^oC, above which the tendency reverses up to 300 ^oC because less ozone is generated from O_2 as temperature increases. As for the effect of H_2O, the presence of H_2O slightly retards the removal efficiency of acetaldehyde from N_2-O_2(20%) from room temperature to 300 ^{o} C because at low discharge current, the relatively much smaller number of electrons tend to attach mostly to H_2O. In addition, it is found that the smallest discharge current required for complete removal of 600 ppm of acetaldehyde from the air is only 0.2 mA at room temperature.

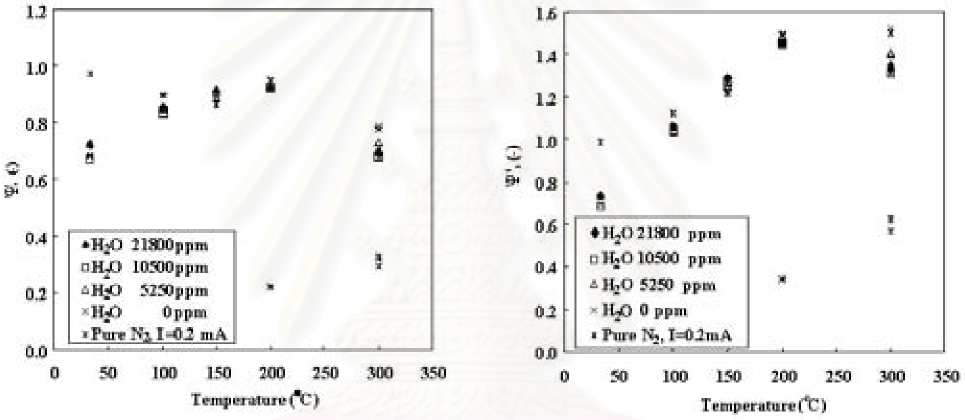

(a) (b)

Figure 3. Combined effect of oxygen and water vapor on the removal efficiency of acetaldehyde from N_2 at 20% O_2; [acetaldehyde]= 600 ppm, I=0.05 mA, SV=55.8 hr^{-1} at room temperature

4 Conclusion

High-temperature removal of acetaldehyde in a corona dicharge reactor was investigated. As expected, the more dilute the inlet concentration, the higher the removal efficiency becomes because, when the discharged current is kept constant, the number ratio of the discharge electrons to the acetaldehyde molecules increases. The presence of either oxygen or water vapor always enhances the removal of acetaldehyde from N_2 because of the ozone effect. In addition, it is found that the smallest discharge current required for complete removal of 600 ppm of acetaldehyde from the air is only 0.2 mA at room temperature.

5 Acknowledgement

W.T., T.C., and J.C. received research grant and financial support from Thailand Research Fund (High-Temperature Removal of Low-Concentration Multi-Component Air Pollutant Gases Using Electron Attachment Reaction Project and Team Research Buildup Program). H.T. and N.S. received support from TJTTP-JBIC Project of Chulalongkorn University to carry out research collaboration at C.U.

Notation

C = concentration, ppm
ψ = removal efficiency excluding adsorption and thermal decomposition effect, (-)
ψ' = removal efficiency per unit residence time, (-)
SV = space velocity, hr^{-1}
θ = mean residence time, (min)
V = effective volume of the corona discharge reactor, (ml)
A = cross sectional area, (cm^2)
$\langle \upsilon \rangle$ = superficial velocity, (m/s)

Subscript

out, 0 mA = outlet of reactor at zero discharge current
out, any mA = outlet of reactor at non-zero current

References

1. Tamon H., Mizota H., Sano N., Schulze S. and Okazaki M. “New concept of gas purification by electron attachment,” *AIChE J.*, **41**, 1701-1711 (1995).
2. Sano N., Nagamoto T., Tamon H., and Okazaki M. “Removal Iodine and Methyl Iodide in Gas by Wetted-Wall Reactor based on Selective Electron Attachment,” *J. Chem. Eng. Japan*., **29**, 59-64 (1996)
3. Sano N., Development of Gas Purification Technology by Selective Electron Attachment, *Ph.D, Diss.,* Kyoto Univ., Japan (1997a).
4. Sano N., Nagamoto T., Tamon H., Suzuki T., and Okazaki M., Removal of Acetaldehyde and Skatole in Gas by Corona-Discharge, *Ind. Eng. Chem. Res.*, **36**, 3783-3791(1997b).
5. Sano N., Tamon H., and Okazaki M., Removal of the Chlorofluorocarbon 1,1,2-Trichloro-1,2,2-trifluoroethane in Gas by a Corona-Discharge Reactor, *Ind. Eng. Chem. Res.*, **37**, 1428(1998).
6. Tamon H., Sano N. and Okazaki M., Influence of Oxygen and Water Vapor on Removal of Sulfur Compounds by Selective Electron Attachment, *AICHE J.*, **42**, 1481-1486(1996).
7. Tamon H., Imanaka H., Sano N., Okazaki M., Tanthapanichakoon W., Removal of Aromatic Compounds in Gas by Electron Attachment, *Ind. Eng. Chem. Res.*, **37**, 2770-2774(1998).
8. Tanthapanichakoon W., Larpsuriyakul K., Charinpanitkul T., Sano N., Tamon H., and Okazaki M., Effect of structure of corona-discharge reactor on removal of dilute gaseous pollutants using selective electron attachment, *J. Chem. Eng. Japan*., **31**, 7-13 (1998).
9. Nishida, K. and Matsuda Y. Malodor of exhaust gas from crematory. *J. Odor Control*, 1981, 1-11 (in Japanese).
10. Nishida, K., Malodor at Cremation Facility (Part I), PPM, 1988, 3, 49-58 (in Japanese).
11. Nishida, K. Malodor at Cremation Facility (Part II), PPM, 1988, 4, 51-59 (in Japanese).

Effect of Oxygen and Water Vapor on the Removal of Styrene and Ammonia from Nitrogen by Non-pulse Corona Discharge at Elevated Temperatures

Wiwut Tanthapanichakoon*, Tawatchai Charinpanitkul, Sahat Chaiyo,
Nantamas Dhattavorn, Jintawat Chaichanawong

Department of Chemical Engineering, Chulalongkorn University
Payathai Road, Pathumwan, Bangkok 10330 Thailand
E-mail: fchwtt@eng.chula.ac.th

Noriaki Sano

Department of Chemical Engineering, Himeji Institute of Technology
2167 Shosha, Himeji, Hyogo 671-2201 Japan

Hajime Tamon

Department of Chemical Engineering, Kyoto University
Yoshida-Honmachi, Sakyo-ku, Kyoto 606-8501 Japan.

Abstract

The present work experimentally investigates the individual and combined effect of O_2 and H_2O vapor on the separate and simultaneous removal of styrene and NH_3 from N_2 at elevated temperatures via corona discharge reactions. Styrene and NH_3 are chosen to represent the trace components in crematory emission because they are chemically dissimilar. Since the crematory emission always contains some O_2 and H_2O at elevated temperatures, their effects and the effect of elevated temperature are of practical interest. It is found that the presence of O_2 in N_2 always enhances the removal of styrene and/or NH_3 from N_2. The presence of H_2O in N_2 generally enhances the removal of styrene and/or NH_3 but its presence retards that of NH_3 when H_2O concentration is too high or the temperature is 300^0C. The combined effect of O_2 and H_2O is found to substantially retard the removal of styrene and/or NH_3 compared to the sole effect of coexisting O_2. The general effect of elevated temperature is to decrease the removal efficiency of styrene and/or NH_3 compared to the case of room temperature.

***Corresponding author.**

Correspond to Wiwut Tanthapanichakoon

Department of Chemical Engineering, Chulalongkorn University,

Payathai Road, Pathumwan, Bangkok 10330 Thailand

Tel.: +66-2-218-6894 Fax : +66-2-218-6877

E-mail: fchwtt@eng.chula.ac.th

1. Introduction

Recently, a considerable number of reports on the application of discharge technology to gas purification have appeared because the technique is deemed as a powerful method to remove dilute gaseous contaminants. There are several types of electrical discharge for gas purification such as d.c. corona discharge [1,2], pulsed corona discharge [3], surface discharge [4], and electron beam [5]. Among these methods, d.c. corona discharge is considered to be superior in terms of low byproduct formation thanks to the low electron energy in the discharge region.

Nowadays air pollution in Thailand poses a serious environmental issue. There are numerous sources of air pollutants in big cities such as heavy concentration of vehicles and traffic congestion. One severe public nuisance is emission gas from the crematorium during cremation rites. There are nearly 23,000 temples nationwide, including approximately 300 temples with crematory furnaces in Bangkok Metropolitan Area alone. During cremation, various malodorous gases and particulate are often emitted without adequate treatment, causing frequent complaints from vicinal communities. A few rich temples have installed furnaces with effective after-burning systems but an overwhelming majority of the temples have inadequate systems. For this reason it is worthwhile to develop an alternative gas treatment method that achieves high efficiency at relatively low energy consumption. This similar issue may affect some other developing and even developed countries, where cremation is widely practiced.

In potential applications of corona discharge reactors, it is important to know the influence of temperature, especially the high temperature range, For example, the exhaust gas temperature from a cremating furnace may be as high as 300 °C. In spite of this practical condition, a limited number of reports on temperature effects on discharge-assisted gas purification have appeared since the reported removal of methanol and trichloroethylene from air by dielectric barrier and pulsed corona discharges under 300 ^{o}C [6]. The present work applies non-pulse corona discharge to the removal of styrene and NH_3, two dissimilar components chosen to represent crematory emission [7, 8]. Since, in addition to N_2, the crematory emission contains H_2O vapor and residual O_2 at elevated temperatures, their effects on the separate and simultaneous removal of styrene and NH_3 are investigated experimentally.

2. Experimental

Fig. 1 shows a schematic diagram of the experimental setup which consists of a non-pulse corona-discharge reactor, a test gas mixing system, a high-voltage DC generator and a temperature controller. The reactor consists of a SUS tube, 3.7 cm. inner diameter and 80 cm. length, as the anode. The cathode is a 0.5-mm stainless-steel wire suspended from a silicone plug at the top of the reactor and straightened along the central axis of the vertical anode by a small weight. A high-voltage DC generator (Matsusada, HAR-30N5) whose maximum allowable voltage is 50 kV is utilized to supply a steady stream of low-energy electrons to the corona-discharge reactor. A slim pyrex glass tube is used to sheath either end of the cathode in order to limit the corona discharge zone to an effective length of 10 cm in the middle section of the reactor and to expose the zone to an essentially flat axial temperature distribution. A type-K thermocouple is inserted into the reactor to measure the gas temperature in the discharge zone. To control the reactor temperature, 6 infrared heating lamps (700W each) are installed lengthwise around the outside perimeter of the reactor. The temperature control unit consists of a temperature controller and a thyrister power regulator.

The desired concentrations of styrene, NH_3, and/or coexisting O_2 are adjusted by diluting standard gases with pure N_2 carrier gas. Water vapor is mixed into the carrier gas by bubbling it through liquid water whose temperature is suitably controlled at 34-50 ^oC. The inlet concentrations of styrene and NH_3 are either 500 or 40 ppm, and either 400, 250, or 200 ppm, respectively. Similarly, the concentrations of coexisting O_2 and H_2O are varied from 0-25% and 0-23000 ppm, respectively. Concentrations of styrene are analyzed using a gas chromatograph (Shimadzu Corp., GC 9A) equipped with a flame ionization detector (FID). Concentrations of NH_3 are analyzed using another gas chromatograph (Shimadzu Corp., GC 14A) equipped with a thermal conductivity detector (TCD). The concentrations of byproduct O_3 and/or NO_x can separately be detected with appropriate gas detector tubes (GASTEC Co., Ltd. and Kitagawa Co., Ltd.). NH_3 can also be detected or double-checked by detector tubes. Compared to the GC method, the detecor-tube measurements were found to differ by less 12 %.

The inlet concentrations of styrene and NH_3 are deliberately set higher than their reported values in crematory emission for two reasons. First, our present and previous investigations have conclusively shown that, as the inlet concentration of a gaseous impurity rises, its removal efficiency always drops because the ratio of the number of gas molecules to the number of discharged electrons decreases. Thus the experimental results yield conservative values. Second, if the gas concentration is too low (a few ppm order or less), there may be significant uncertainty in the measurement values obtained by the gas chromatographs.

In our case, the voltages required to generate 0.05 mA in the removal of either 500 ppm styrene or 400 ppm NH_3 from N_2-O_2 (20%) mixture are, respectively, 10.1 and 10.5 kV at room temperature, and these voltages decrease to 6.4 and 5.9 kV, respectively, as temperature rises to 300^oC. The voltages in the removal from pure N_2 are significantly lower but become unstable at the same 0.05 mA. Therefore a higher current is used. Even when the current is increased 10 folds to 0.5 mA, the required voltage increases less than 10% for styrene and even decreases about 45% for NH_3. As the discharge current increases, ion wind [9] becomes stronger, causing the suspended wire cathode to sway. This effect imposes a maximum stable current, which is found to be around 0.5 mA, in our condition.

3. Results and Discussion

3.1 Definition of removal efficiency

Generally the removal efficiency is obtained by comparing the inlet and outlet gas concentrations. At high temperatures, significant thermal decomposition of styrene and ammonia in N_2 might occur, which also depends on the type and concentration of the coexisting gas. For example, 23 – 33 % of the influent styrene but less than 1.5 % of the NH_3 were found to decompose at 200 – 300 ^{o}C in pure N_2. When H_2O coexists at 20,000 – 23,000 ppm, the decomposition of styrene and NH_3 become ca. 31% and 16 - 20 %, respectively. This means that only ammonia decomposition is accelerated by the presence of H_2O. On the contrary, the decomposition of styrene in the presence of 20% O_2 and NH_3 in the presence of 5% O_2 become ca. 38 – 40 % and ca. 1.5 %, respectively This means that only styrene decomposition is accelerated by O_2. To show the sole effect of corona discharge and excludes the effect of high-temperature thermal decomposition inside the reactor, the removal efficiency ψ in this work is defined by Eq.1

$$\psi = \frac{(C_{out,0\,mA} - C_{out,any\,mA})}{C_{out,0\,mA}} \quad [-] \qquad (1)$$

Here, $C_{out,0\ mA}$ (ppm) and $C_{out,any\ mA}$ (ppm) are the outlet concentrations of the impurity gas without and with discharge current, respectively. At steady state, the equation of continuity requires that $\rho_1 \langle \upsilon_1 \rangle A_1 = \rho_2 \langle \upsilon_2 \rangle A_2$. Since $A_1 = A_2$ and ρ is a function of the gas temperature, the gas velocity at an elevated temperature T_2 will be faster than its velocity at room temperature T_1. Thus the mean residence time $\theta_2 = \frac{V}{\langle \upsilon_2 \rangle A}$ of this gas at T_2 is shorter than $\theta_1 = \frac{V}{\langle \upsilon_1 \rangle A}$ at room temperature. Here V is the effective volume of the corona discharge reactor. The removal efficiency per unit residence time, ψ', in Eq. (2) takes into consideration the shorter residence time of the hot gas in the reactor even when the inlet gas flow rate (mole basis) remains unchanged before and after the reactor temperature is elevated. Strictly speaking, this definition is scientifically correct only in the initial reaction stage where the yield is proportional to the residence time. Nevertheless, it is adopted here as a handy indicator that reasonably offsets the effect of reduced residence time.

$$\psi' = \frac{\psi \times residence\ \ time\ \ at\ 25\ \ ^{0}C}{residence\ \ time\ \ at\ T\ \ ^{0}C} \qquad (2)$$

It is a common practice to obtain reaction rate constants based on some proposed reaction system in order to elucidate detailed reaction kinetics. In the purification of N_2 contaminated with several individual sulfur compounds and CH_3CHO in a corona discharge reactor, a mathematical model based on the first-order reaction of electron attachment and the fitted ion-diffusivity is shown to correlate well with experimental results [1, 10]. However, this model is not applicable to this study in which its “electron efficiency”, the number of gas molecules removed per electron, is greater than unity. The experimental electron efficiencies obtained here range from 0.9 at 300 ^{o}C in the case of pure N_2 to 36.6 at room temperature in the case of 20% O_2. The large values indicate that not only electron attachment but other reaction paths such as radical reaction and dissociation by electron impact also play an important role. The mathematical modeling of such a highly complex reaction system is beyond the scope of the present study. To qualitatively compare the apparent “intrinsic” reaction rate of removal, the values of ψ' are handy and practical. It is reasonable to think that the overall reaction rate is higher when ψ' is higher.

3.2 Influence of temperature on removal mechanism

As mentioned in the experimental section, the voltage required for a corona discharge current of 0.5 mA decreased with the elevated temperature. This voltage drop causes the decreaed acceleration of electrons in the discaharge zone. In spite of this factor, the temperature elevation causes the gas to expand and its density to decrease, resulting in lower collision frequency of drifting electrons with gas molecules. It is also important to note that the electron energy depends on the electric field strength divided by the gas density, *E*/*N*. To approximate *E*/*N*, the electric field strength described as Eq. (3) is used.

$$E = V / \{ r \ln (D_1/D_o) \} \tag{3}$$

V, r, D_1, D_o are the applied voltage, radial distance from the cylindrical axis, inner diameter of the cylindrical anode, and diameter of the wire cathode, respectively. Thus, the mean E/N is approximated by Eq. (4).

$$\langle E/N \rangle = \frac{\int_{D_0/2}^{D_1/2} (2\pi r)(E/N)\, \mathrm{d}r}{\pi \left((D_1/2)^2 - (D_0/2)^2 \right)} = \frac{4V}{N(D_1+D_0)\ln(D_1/D_0)} \tag{4}$$

N is calculated as $p/\{\mathrm{R}(273+T)\}$, where p, R, T are total pressure, gas constant, and gas temperature, respectively. From this correlation, the average $\langle E/N \rangle$ in our case is 6.2 kV m^2 mol^{-1} and 7.2 kV m^2 mol^{-1} at room temperature and 300 ^oC, respectively,. Since the electric field strength increases only slightly when the temperature is elevated, the electron energy at 300 ^oC turns out to be approximately 13% higher than at room temperature. Generally, the electron energy level should affect the reaction mechanism. For example, electron attachment tends to occur when electron energy is relatively low [18, 19, 28], while formation of radicals may take place when electron erergy is very high.

Rigorously speaking, the relevant reactions contributing to the removal of styrene and NH_3 are affected not only by the change in electron energy level but also by other effects of the elevated temperature. To consider the reaction mechanism, one must take byproduct formation into account. As for the gaseous byproducts, O_3 and NO_x were respectively detected mainly in the low and high temperature ranges. In fact, our measurements of O_3 concentration during the removal of toluene from N_2-O_2 mixture reveal that O_3 is produced up to 1370 ppm at room temperature but it rapidly drops down to 430 ppm at 100 ^oC. When T is further increased above 300 ^oC, O_3 concentration becomes negligible [11]. This is because O_3 is unstable at high temperature [12, 13]. Therefore, oxidation by O_3 should play a negligible role in the high temperature range.

Contrary to O_3 formation, it is known that production of NO_x by the discharge process is favored at high temperature. This is also confirmed in our experiments. While the outlet concentration of NO_x was negligible at room temperature, its concentration gradually increased with temperature and reached 300 ppm at 400 ^oC. Since NO_x formation can be attributed to the reaction of discharge-induced N radicals with O_2 [14, 15], N radicals should also contribute to the removal of styrene and/or NH_3 from both N_2 and air at high temperatures. In addition, in the removal from air, there should be the extra effect of O radicals produced by electron impact to O_2 and by O_3 decomposition [12, 16, 17]. Therefore, the removal efficiency from air at high temperatures should be enhanced by O radicals, though O_3 oxidation is not effective. In fact Peyrous et al. [12] simulated the concentrations of O_3 and O radicals in pulsed corona discharge in the presence of O_2, and showed that temperature elevation brings about higher O radical concentration and lower O_3.

When H_2O is present in the gas stream, H^-, OH^- and a few O^- anions are expected to be produced by dissociative electron attachment to H_2O molecules at low temperature [18, 19]. The selectivity for these ionic products should depend on the gas temperature and electron energy. At high temperature, electron detachment would become significant so that radicals of O, H, and OH may play a more important role than their anionic counterparts. These radicals are also expected to contribute to the removal of the target gases. More specifically, OH is believed to dissociate NH_3 to produce an aminogen radical (NH_2) and H_2O [20].

In non-thermal corona discharge in the air at room temperature, electrons are sometimes captured by O_2 to form negative ions, O^-, O_2^-, O_3^-, and clusters via electron attachment. The reversed electron detachment process, however, becomes significant at high temperature, causing ion clusters to become unstable [21]. Our previous articles indicate that the corona discharge reactor plays host to electron attachment reactions and relevant ion cluster formation at room temperature [10, 22]. However, because of high temperature effects such as electron detachment and radical formation, electron attachment and ion clustering would be less and less important as the temperature rises.

The removed styrene was converted to non-volatile deposit, which was observed inside the reactor and in the gas line after the reactor. The observed conversion to non-volatile deposit is consistent with our previous report on the removal of certain aromatic compounds, benzene and p-dichlorobenzene, from N_2 and N_2-O_2 mixture at room temperature [23]. There it was discussed that negative ions induced by dissociative electron attachment initiated chain polycondensation reactions to form the deposit. The present reaction mechanism for the removal of styrene at room temperature may be considered to be analogous to the chain polycondensation found in the removal of benzene and p-dichlorobenzene because of the similar aromatic structure of these molecules. Since the terminating reaction for styrene chain polycondensation at room temperature is considered to be effected by the reactions of electron-attachment-induced ions with styrene molecules, we may likewise consider that, in the high temperature range, radical reactions involving N and O radicals and electron impact to styrene molecules, instead of ionic reactions, could initiate the chain polycondensation reaction required to form non-volatile deposit. It should be emphasized that the proposed mechanism is clearly different from the removal of methanol and trichloroethylene reported by Hsiao et al. [6], in which they are converted to CO_x by decomposition. The temperature dependency of this chain polycondensation reaction might have a role in determining the removal efficiency at various temperatures.

In the case of NH_3 removal, the removed NH_3 was converted to needle-like bright crystal, which was observed inside the reactor and the gas line after it. It is reported [24] that NH_3 does not react with O_3 to directly form NH_4NO_3. Instead the following consecutive reactions are mentioned: $2\ NH_3 + 4\ O_3 = NH_4NO_2 + H_2O_2 + 4\ O_2$; $NH_4NO_2 + H_2O_2 = NH_4NO_3 + H_2O$. Our result is also consistent with published reports that NH_4NO_3 solid is produced by corona treatment of humid air containing NH_3 [20, 25, 26]. The mechanism for NH_4NO_3 formation in the high temperature range is not clear but it may be considered that NH_3, H_2O and NO_x as well as N and H radicals could react to form NH_4NO_3.

Since our blank tests show negligible change in the concentrations of styrene and NH_3 when they are fed together to the reactor at various temperatures and no extraneous peaks are detected in the gas chromatograms, it may be considered that styrene does not react with NH_3 in the presence of air.

3.3 Effect of coexisting O_2 on removal of styrene from N_2

Fig. 2 shows the removal efficiency ψ' of styrene from N_2 versus temperature when the styrene inlet concentration is 500 ppm. Partly because of the above-mentioned swaying effect of the ion wind [9], there is a maximum fluctuation of around + 6% at some of the experimental points. It is obvious that the presence of O_2 in N_2 greatly enhances the styrene removal efficiency despite the fact that the discharge current in the N_2-O_2 case has been reduced ten folds to 0.05 mA compared to the case of pure N_2. As explained in section 3.2, this may be attributed to the fact that O_3 is produced from O_2 by the corona discharge reaction and is quite stable at room temperature. At room to moderate temperatures, electron attachment reactions contribute to, and relevant ion cluster formation enhances, the removal of numerous electro-negative compounds [10, 22]. Considered to be applicable to the removal of styrene, this mechanism is consistent with the observation that the biggest effect of coexisting O_2 is found at the highest concentration of 25% O_2.

As mentioned in section 3.2, the removed styrene was converted to non-volatile deposit, which is consistent with our previous report [23]. In addition, the reaction mechanism in the removal of styrene at room temperature may be considered to be chain polycondensation of styrene, whereas the terminating reaction is considered to be effected by the reactions of electron-attachment-induced ions with styrene molecules. In the high temperature range, radical reactions involving N and O radicals and electron impact to styrene molecules, instead of ionic reactions, could initiate the chain polycondensation reaction required to form the observed non-volatile deposit.

As the gas temperature increases, there was a gradual reduction in the removal efficiency ψ omitted here. Above 200 ^{o}C, O_3 is unstable and not detected. Instead O radicals are produced [12, 17, 18] and so are N radicals, which might be more reactive than O radicals because $N\equiv N$ bonding energy at 225 kcal/mol is much higher than that of O=O at 118 kcal/mol. Since the increased production of NO_x at higher temperatures consumes N radicals, the styrene removal efficiency tends to decrease. Coupled with the negative effect of reduced residence time, this explains why the value of the omitted ψ decreases monotonically in the high temperature range. When the effect of residence time is considered, the value of ψ' in Fig. 2 increases up to 200 ^{o}C before subsequently decreasing. In the low to moderate temperature range, the combined effect of both O_3 and N radicals results in an efficiency increase despite the reduced residence time. In the high temperature, the positive effect of diminishing N radicals turns out to be negated by the much reduced residence time.

Generally, two other types of removal efficiency are reported for a corona-discharge system. The electron-based efficiency ψ_{elec} (-) is defined as the number of gas molecules removed by one discharged electron, and the energy-based efficiency ψ_{ener} (mol gas .J^{-1}) is defined as the mole of gas removed per energy consumption (J). At 306, 373, 473 and 573 K, the experimental values of ψ_{elec} and ψ_{ener} are as follows:

Pure N_2 (I = 0.5 mA) :

ψ_{elec} = 1.6, 1.7, 1.2, 0.9; $\psi_{ener} \times 10^{-9}$ = 1.66, 1.94, 1.45, 1.21

N2 – 20% O_2 (I = 0.05 mA):

ψ_{elec} = 36.6, 28.4, 21.8, 10.6; $\psi_{ener} \times 10^{-9}$ = 186, 160, 149, 86.2

In the absence of O_2, ψ_{elec} ranges from 1.7 at 373 K to 0.9 at 573 K while ψ_{ener} ranges from 1.7×10^{-9} to 0.9×10^{-9} . In the presence of 20% O_2, ψ_{elec} and ψ_{ener} increases 22.9 - 11.8 folds and 112 – 71.2 folds, respectively, despite a 10-fold reduction in the discharge current compared to the case of pure N_2 . The remarkable enhancement effect of O_2 can be attributed to the effect of O_3 and O^- anion at low temperatures and N and O radicals at high temperatures.

Generally ψ_{elec} and ψ_{ener} tends to decrease as the gas temperature increases. This trend may be ascribed to the combined effect of reduced residence time and the shift in removal mechanism. Interestingly, in the case of pure N_2, ψ_{elec} and ψ_{ener} at 373 K become higher than at room temperature, thus indicating the possible existence of an optimal temperature.

3.4 Effect of water vapor on removal of styrene from N_2

Fig. 3 shows the styrene removal efficiency from N_2 ψ' versus temperature at various concentrations of water vapor. Regarding the general influence of H_2O, its presence significantly raises the removal efficiency despite a 5-fold reduction in the discharge current, compared to the case of pure N_2. As mentioned in section 3.2, H^-, OH^- and a few O^- anions are expected to be produced by dissociative electron attachment to H_2O molecules at low temperature [18, 19]. To gain some insight into the electron affinity of styrene and H_2O molecules, electron affinities of H_2O molecule and styrene molecule were obtained by subtracting the total energies of neutral molecules from their anionic counterparts. These calculations were carried out by Density Functional Theory at B3LYP/6-31G(d) level using Gaussian98W program [27], resulting in 88 and 403 kJ/mol for styrene and H_2O, respectively. This means that the H_2O anion is much more difficult to form than the styrene anion. The difficulty of forming H_2O anions is also confirmed by drift tube experiment [28]. As a result it may be considered that electron attachment to H_2O is dissociative. Similarly, it is reasonable to assume that electron attachment reactions to other gaseous species such as styrene and NH_3, are also dissociative. Therefore it should be more meaningful to consider electron affinity of constituent atoms in these gas species. The values of Mulliken-scale electron negativity of O, N, and H atoms, which constitutes O_2, O_3, H_2O, NH_3 and styrene, are, respectively, 3.5, 3.0 and 2.1 eV. These values mean that O^- anion is easier to produce from O_2, O_3, and H_2O than N^- and H^- from NH_3 and H^- from styrene. This explains why styrene removal efficiency is significantly enhanced by the presence of H_2O.

At high temperature, electron detachment becomes significant and as a result, radicals of O, H, and OH as well as N radicals are produced. As the gas temperature increases, the omitted styrene removal efficiency ψ decreases monotonically from room temperature to 300°C mainly because of the reduction in residence time. Fig. 3 reveals that, even when the effect of reduced residence time is taken into consideration, the value of ψ' in the presence of H_2O still decreases slightly with temperature. This trend is completely different from the removal efficiency in the absence of H_2O. As mentioned in section 3.2, NO_x formation can be attributed to the reaction of discharge-induced N radicals with O_2 [14, 15], and N radicals are considered to contribute to the removal of styrene from both N_2 and air at high temperatures. Since N radicals are consumed by their reaction with H_2O at high temperatures, the styrene removal efficiency at high temperatures decreases in the presence of H_2O. In contrast, in the absence of O_2 and H_2O, N radicals are not consumed and this results in a slight increase in ψ' in Fig. 3.

3.5 *Effect of coexisting O_2 and water vapor on removal of styrene from N_2*

A number of experiments were carried out to observe the combined effect of O_2 and H_2O on the removal of styrene from N_2. The O_2 concentrations investigated were 5, 10 and 20%. Because of space limitation, only the case of 5% O_2 is introduced here. **Fig. 4** shows the observed removal efficiency ψ' of styrene from N_2 at elevated temperatures. Again note that the discharge current in the case of pure N_2 is 10 times the case of N_2-O_2 mixture. As the gas temperature increases, the omitted ψ substantially decreases mainly because of the effect of reduced residence time. In Fig. 4, the presence of H_2O (4050 ppm, 12900 ppm and 23000 ppm) have no discernable effect on the removal efficiency ψ' at room temperature because complete removal of styrene is obtained at all H_2O concentrations. In the intermediate temperature range, the calculated value of ψ' becomes significantly higher than unity in the absence of H_2O because electron attachment reactions and O_3 cluster formation enhance the removal efficiency [10, 22] but O_3 formation is not retarded in the absence of H_2O. **Fig 5** confirms the retarding effect of water vapor on ozone generation at room temperature. At 300°C, O, OH and H radicals should be produced from O_2 and/or H_2O, thus enhancing the removal efficiency, though O_3 is hardly observed at 300^0C.

3.6 *Effect of coexisting O_2 on removal of NH_3 from N_2*

Fig. 6 shows the removal efficiency ψ' of NH_3 from N_2 at various concentrations of co-existing O_2 when the NH_3 inlet concentration is 400 ppm. As in the case of styrene, the presence of O_2 in N_2 greatly enhances the NH_3 removal efficiency despite the fact that the discharge current has been reduced 6 folds to 0.05 mA, compared to the case of pure N_2 in the same figure. As mentioned in section 3.2, this may be attributed to the facts that O_3 is produced from O_2 by the corona discharge reaction in the low to moderate temperature range, where electron attachment reactions and relevant ion cluster formation contribute to the removal of NH_3, and that the removed NH_3 is converted to non-volatile deposit, which was observed inside the reactor and the gas line after it. At room temperature NH_3 may react O_3 with to form NH_4NO_3 [24] via the following consecutive reactions: $2\ NH_3 + 4\ O_3 = NH_4NO_2 + H_2O_2 + 4\ O_2$; $NH_4NO_2 + H_2O_2 = NH_4NO_3 + H_2O$. This is consistent with the observation that the biggest effect of coexisting O_2 on ψ is found at the highest concentration of 25% O_2.

As the temperature increases, the omitted ammonia removal efficiency ψ in the presence of O_2 drops monotonically starting from room temperature to 300°C because O_3 is unstable and not detected above 200 °C. Instead O and N radicals are produced and contribute to NH_3 removal [12, 14, 17]. Since more N radicals are consumed to form NO_x as the temperature increases, the NH_3 removal efficiency significantly decreases. Coupled with the negative effect of reduced residence time, the value of ψ decreases drastically in the high temperature range. Even when the effect of residence time is considered , the value of ψ' in Fig. 6 still decreases monotonically with temperature, albeit less drastically.

3.7 Influence of H_2O on removal of NH_3 from N_2

Fig. 7 shows the removal efficiency ψ' of NH_3 from N_2 at various concentrations of coexisting water vapor. Note that the discharge current is all 0.3 mA here compared to 0.05 mA in the case of dry N_2-O_2 mixture. The effect of elevated temperature on ψ' and the omitted ψ is not straightforward but appears to depend on the H_2O concentration. When the H_2O concentration is highest at 23000 ppm, both ψ and ψ' are retarded compared to the absence of H_2O, while the effect of elevated temperature is slight. In contrast, the retarding effect at two lower H_2O concentrations (5250 and 10500 ppm) is relatively small up to 100°C. Both ψ and ψ' become enhanced at 200°C but become retarded again at 300 °C compared to the absence of H_2O. As mentioned in section 3.2, H^-, OH^- and a few O^- anions are produced by dissociative electron attachment to H_2O molecules at low temperature [18, 19]. At room temperature the required voltages for corona discharge are 8.1, 8.7, 8.3, and 8.7 (kV), respectively, for $H_2O = 0$, 5250, 10500 and 23000 (ppm). At 100, 200 and 300 °C, the corresponding sets of voltage values are (6.9, 7.2, 6.8, 6.6 (kV)), (5.1, 5.1, 5.1, 5.2 (kV)), and (3.5, 3.6, 3.7, 4.1 (kV)), respectively. The decrease in required kV against increasing H_2O concentration at room temperature means that the rate of ozone and radicals formation become lower. This explains the observed retardation effect of H_2O at low temperatures.

At 200 °C or more, electron detachment produces radicals of O, H, and OH from their anions. More specifically, OH radical is believed to dissociate NH_3 to produce an aminogen radical (NH_2) and H_2O [20]. This reversible reaction is, however, retarded by a big excess of the reaction product H_2O. Similarly, N and H radicals are produced from NH_3, especially at 300 °C. Since N and H radicals are considered to contribute more to the formation of NH_4NO_3, the high consumption of N radicals at 300 °C to form NO_x leads to the observed reatardation effect. At 200 °C fewer N radicals are consumed to form NO_x and, without excessive H_2O, the combined effect of N, H and OH radiclas lead to the observed efficiency enhancement.

3.8 Influence of coexisting O_2 and H_2O on removal of NH_3 from N_2

Experiments were carried out to observe the combined influence of H_2O and O_2 on the removal of NH_3 from N_2. **Fig. 8** shows the experimental results when O_2 concentration is 5%. In the absence of H_2O and O_2, the removal efficiency ψ' and the omitted ψ are not high even at I=0.3 mA because the electro-negativity of NH_3 is not so high. As explained in section 3.4, the presence of 5% O_2 without water vapor greatly enhances ψ and ψ' because of the generation of O_3 and O^- anions at low temperatures, and O radicals at high temperatures. The combined effect of O_2 and 5250 ppm H_2O slightly retard ψ and ψ' compared to the case of pure N_2. However, at 10500 ppm H_2O the combined effect of O_2 and H_2O becomes positive at low temperatures compared to pure N_2. As mentioned in section 3.2, H^-, OH^- and a few O^- anions are produced by dissociative electron attachment to H_2O molecules at low temperature [18, 19]. At room temperature the required voltages for corona discharge are 13.1, 8.2, and 12.9 (kV), respectively, for H_2O = 0, 5250, and 10500 (ppm). At 100, 200 and 300 °C, the corresponding sets of voltage values are (11.8, 6.7, 9.0 (kV)), and (8.3, 5.0, 6.8 (kV)), and (5.4, 3.7, 5.3 (kV)), respectively. At room temperature the U shape in the required kV against increasing H_2O concentration means that the average electron energy decreases and then increases, thus little O_3 and few O radicals are produced from O_2 at 5250 ppm. Combined with the reduced formation of N radicals, this explains the retardation effect at H_2O = 5250 ppm compared to the case of pure N_2. At H_2O = 10500 ppm, the much higher energy level leads to significant formation of O and N radicals, thus enhancing the removal of NH_3. The U shape in the required kV vs. H_2O concentration is observed at elevated temperatures, and a similar explanation is applicable up to 200 °C. When H_2O = 10500 ppm, the electron energy level at 300 °C becomes so low that the reactions of O and N radicals may be reduced.

3.9 Effect of coexisting O_2 on the simultaneous removal of styrene and NH_3 from N_2

No significant reduction in the outlet concentrations of styrene and NH_3 was observed that might indicate their spontaneous reaction at high temperature without corona discharge in the presence of nitrogen. In addition no extraneous peaks were observed in the gas chromatograms of the effluent stream. Therefore it may be considered that styrene and ammonia did not react to generate new pollutants. In fact they were observed together in the exhaust gas from the crematory furnace.

Figs. 9 and 10 show the effect of O_2 on the simultaneous removal efficiency of styrene and NH_3 from N_2, respectively. The inlet concentrations of styrene and NH_3 are 40 and 200 ppm, respectively, while the current is rather high at 0.3 mA. Obviously, the presence of O_2 has a significant enhancement effect on the simultaneous styrene removal efficiency ψ in **Fig.9**. As the temperature increases, the styrene removal efficiency remains essentially at 100% from room temperature to 300 ^{o}C, except at 5% O_2 and 300^{0}C. As expected, the presence of O_2 also has a significant effect on the simultaneous NH_3 removal efficiency in **Fig. 10**. As the temperature increases, the NH_3 removal efficiency ψ above 200^{0}C tends to significantly decrease. In either Figure, the removal efficiency enhancement is found to depend on the concentration of coexisting O_2. As mentioned previously, the improved removal efficiency for both styrene and NH_3 can be attributed to effect of O_3 and O^- anion at low temperatures and various radicals at high temperatures.

3.10Effect of coexisting O_2 and H_2O on the simultaneous removal of styrene and NH_3 from N_2

Figs. 11 and 12 show the combined effect of O_2 and H_2O on the simultaneous removal efficiency ψ of styrene and NH_3 from N_2. Compared to the case of only coexisting O_2, the simultaneous removal efficiency of both styrene and NH_3 is retarded by the presence of H_2O. In Fig. 11, the presence of H_2O significantly decreases the simultaneous removal efficiency of styrene only above 200^{0}C. In Fig. 12, however, the presence of H_2O significantly decreases the simultaneous removal efficiency of NH_3 from 100 ^{0}C upward. As explained above, an increase in the gas temperature leads to a significant drop in the importance of electron attachment reaction, while various radicals become important. N radicals produced at elevated temperature are consumed to form NO_x, thus causing a drop in the NH_3 removal efficiency.

4. Conclusion

Generally the apparent removal efficiency of styrene and/or NH_3 from N_2 tends to drop with the elevated temperature because of the reduced gas residence time, while the removal efficiency per unit residence time can increase with temperature. The presence of O_2 substantially enhances the removal efficiency of styrene and/or NH_3 because of the effect of O_3 and O^- anion at low temperatures and N and other radicals at high temperatures. The presence of H_2O in nitrogen generally enhances the removal efficiency of styrene and/or NH_3 but the presence of H_2O retards that of NH_3 when H_2O concentration is too high or the temperature is 300°C. The combined effect of O_2 and H_2O is found to significantly retard the removal efficiency of styrene and/or NH_3 compared to the sole effect of coexisting O_2.

There are still a number of points on the complex removal mechanism left for further investigation. Though negligible gaseous byproducts besides O_3 and NO_x were detected in the gas chromatograms, more detailed investigation should be also carried out.

Acknowledgement

W.T., T.C., N.D., S.C. and J.C. receive research grant from Thailand Research Fund (TRF) (High-Temperature Removal of Low-Concentration Multi-Component Air Pollutant Gases Using Electron Attachment Reaction Project). W.T. and T.C. also receive partial financial support from TRF – RTA (Research Team Award) project and from COE Project of Ratchadapisek Sompoch Fund, Chulalongkorn University. H.T. and N.S. received support from TJTTP-JBIC Project of Chulalongkorn University to carry out research collaboration at C.U.

Notation

A = cross-sectional area, (m^2)

C = concentration, (ppm)

E = electric field strength, (V/m)

N = gas density (mol/m^3)

SV = space velocity, (hr^{-1})

t_r = ratio of residence times in the corona discharge zone, (-)

V = effective volume of the corona discharge reactor, (m^3)

θ = mean residence time, (s)

$\langle \upsilon \rangle$ = superficial velocity, (m/s)

ψ = removal efficiency, (-)

ψ' = removal efficiency per unit residence time, (-)

ψ_{elec} = electron-based efficiency, (-)

ψ_{ener} = energy-based efficiency, (mol gas .J^{-1})

Subscript

in = inlet of reactor

out, 0 mA = outlet of reactor at zero discharge current

out, any mA = outlet of reactor at non-zero current

Literature Cited

[1] H. Tamon, H. Mizota, N. Sano, S. Schulze, M. Okazaki, New concept of gas purification by electron attachment, AIChE J. 41 (1995) 1701-1711.

[2] N. Sano, T. Nagamoto, H. Tamon, M. Okazaki, Removal of iodine and methyl iodide in gas by wetted-wall reactor based on selective electron attachment, J. Chem. Eng. Japan 29 (1996) 59-64.

[3] S. Masuda, Pulse Corona Induced Plasma Chemical Process -- A Horizon of New Plasma Chemical Technologies, Proc. 8th Int. Symp. on Plasma Chemistry, Tokyo, Japan (1987) 2187-2192.

[4] S. Masuda, Y. Wu, T. Urabe, Y. Ono, Pulse corona induced plasma chemical process for $DeNO_x$, $DeSO_x$, and mercury vapor control of combustion gas, Proc. Int. Conf. on Electrostatic Precipitation, Padova, Italy (1987) 667-676.

[5] K. Kawamura, Simultaneous removal of NO_x and SO_x by electron beam, Kagaku Kokaku 53, (1989) 820-821.

[6] M.C. Hsiao, B.T. Merritt, B.M. Penetrante, G.E. Vogtlin and P. H. Wallman, Plasma assisted decomposition of methanol and trichloroethylene in atmospheric pressure air streams by electrical discharge processing, J. Appl. Phys. **78** (1995) 3451-3456.

[7] K. Nishida, Malodor at cremation facility (Part I), PPM 3 (1988) 49-58 (in Japanese).

[8] K. Nishida, Malodor at cremation facility (Part II), PPM 4 (1988) 51-59 (in Japanese).

[9] A. Yabe, Y. Mori, K. Hijikata; EHD Study of the corona wind between wire and plate electrodes, AIAA J. 16 (1978) 340-345.

[10] N. Sano, T. Nagamoto, H. Tamon, T. Suzuki, M. Okazaki, Removal of acetaldehyde and skatole in gas by corona-discharge, Ind. Eng. Chem. Res. 36 (1997) 3783-3791.

[11] N. Dhattavorn, Effect of temperature on removal of toluene vapor using the electron attachment reaction, Master's degree thesis, Chulalongkorn University, 2000.

[12] R. Peyrous, P. Pignolet, B. Held, Kinetic simulation of gaseous species created by an electrical discharge in dry or humid oxygen, J. Phys. D: Appl. Phys. 22 (1989) 1658-1667

[13] J.C. Devins, Mechanism of ozone formation in the silent electric discharge, J. Electroche. Soc. 103 (1956) 460-466.

[14] J.J. Lowke, R. Morrow, Theoretical analysis of removal of oxides of sulfur and nitrogen in pulsed operation of electrostatic precipitators, IEEE Trans. Plasma. Sci. 23 (1995) 661-671.

[15] S. Mukkavilli, C.K. Lee, K. Varghese, L.L. Tavlarides, Modeling of the electrostatic corona discharge reactor, IEEE Trans. Plasma Sci. 16 (1988) 652-660.

[16] J.F. Loiseau, C. Lacassie, C. Monge, R. Peyrous, B. Held, C. Coste, Numerical simmulation of ozone axial and radial distribution in a cylindrical oxygen-fed ozonizer, J. Phys. D: Appl. Phys. 27 (1994) 63-73.

[17] S. Hadj-Ziane, B. Held, P. Pignolet, R. Peyrous, J.M. Benas, C. Coste, Ozone production in an oxygen-fed wire to cylinder ozonizer, J. Phys. D: Appl. Phys. 23 (1990) 1390-1395.

[18] S.H. Massey, Negative Ions, Cambridge Univ. Press, Cambridge, England, 1976.

[19] J.L. Moruzzi, A.V. Phelps, Survey of negative-ion-molecule reactions in O_2, H_2O, CO, and mixtures of these gases at high pressures, J. Chem. Physics. 45 (1966) 4617-4627.

[20] V.A.Bityurin, B.V. Potapkin, M.A. Deminsky, Chemical activity of discharges, electrical discharges for environmental purposes, Edited by E.M. Van Veldhuizen, Nova Science Publishers Inc., New York, 2000, pp. 49-117.

[21] A.K. Mnatsakanyan, G.V. Naydis, Y.M. Solozobov; Theory of a corona discharge in heated air, High Temperature (1987) 771-776

[22] H. Tamon, N. Sano, M. Okazaki, Influence of oxygen and water vapor on removal of sulfur compounds by electron attachment, AIChE J. 42 (1996) 1481-1486.

[23] H. Tamon, H. Imanaka, N. Sano, M. Okazaki, W. Tanthapanichakoon, Removal of aromatic compounds in gas by electron attachment, Ind. Eng. Chem. Res. 37 (1998) 2770-2774.

[24] H. Sugimitsu, Ozone no kiso to ouyo (Fundamentals and application of ozone), Korin, Tokyo, 1998 (in Japanese).

[25] S. Kanazawa, J.S. Chang, G.F. Round, G. Sheng, T. Ohkubo, Y. Nomoto, T. Adachi, Reduction of NO_x from flue gas by corona discharge activated ammonia radical showers, Combust. Sci. Technol. 133 (1998) 93-105.

[26] K. Urashima, S.J. Kim, J.S. Chang, Characteristics of aerosol particles from corona discharge ammonia radical injection desulfurization and denitrification processes for flue gases cleanings, J. Aerosol Sci. 30 (1999) S849-S850.

[27] M.J. Frisch, G.W. Trucks, H.B. Schlegel, G.E. Scuseria, M.A. Robb, J.R. Cheeseman, V.G. Zakrzewski, J.A. Montgomery Jr., R.E. Stratmann, J.C. Burant, S. Dapprich, J.M. Millam, A.D. Daniels, K.N. Kudin, M.C. Strain, O. Farkas, J. Tomasi, V. Barone, M. Cossi, R.

Cammi, B. Mennucci, C. Pomelli, C. Adamo, S. Clifford, J. Ochterski, G.A. Petersson, P.Y. Ayala, Q. Cui, K. Morokuma, D.K. Malick, A.D. Rabuck, K. Raghavachari, J.B. Foresman, J. Cioslowski, J.V. Ortiz, A.G. Baboul, B.B. Stefanov, G. Liu, A. Liashenko, P. Piskorz, I. Komaromi, R. Gomperts, R.L. Martin, D.J. Fox, T. Keith, M.A. Al-Laham, C.Y. Peng, A. Nanayakkara, M. Challacombe, P.M.W. Gill, B. Johnson, W. Chen, M.W. Wong, J.L. Andres, C. Gonzalez, M. Head-Gordon, E.S. Replogle, J.A. Pople, Gaussian 98, Revision A.9, Gaussian Inc., Pittsburgh PA, 1998.

[28] G.E. Caledonia, A survery of the gas-phase negative ion kinetics of inorganic molecules-Electron Attachment Reactions, Chem. Rev. 75 (1975) 333-351.

List of Figures

Fig. 11. Combined effect of O_2 and H_2O on simultaneous removal of styrene and ammonia from N_2 at 5% O_2 ; removal efficiency of styrene; [ammonia]= 200 ppm, [styrene]= 40 ppm, I=0.10 mA, SV= 55.8 hr^{-1} at room temperature

Fig. 12. Combined effect of O_2 and H_2O on simultaneous removal of styrene and ammonia from N_2 at 5% O_2; removal efficiency of ammonia; [ammonia]= 200 ppm, [styrene]= 40 ppm, I=0.10 mA, SV= 55.8 hr^{-1} at room temperature

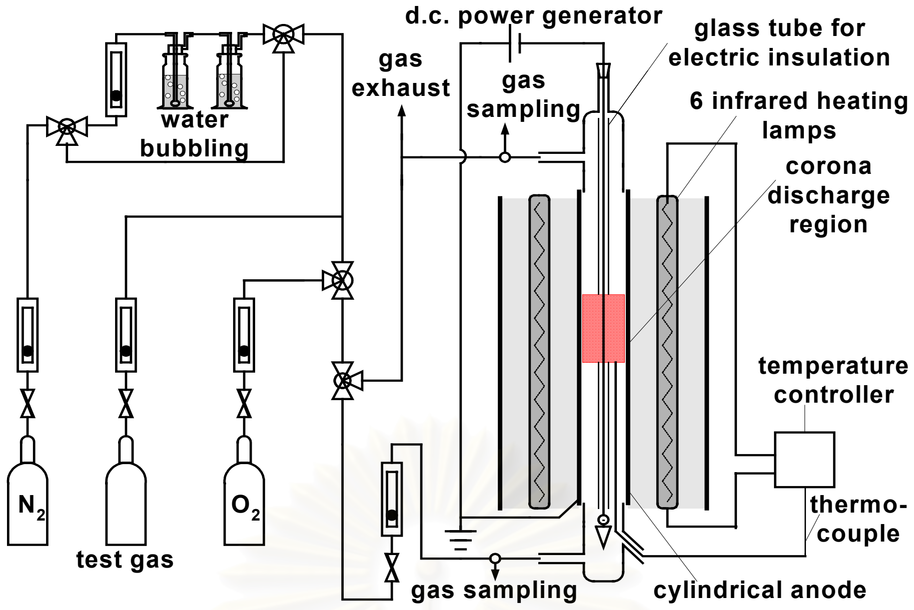

Fig.1. Experimental apparatus

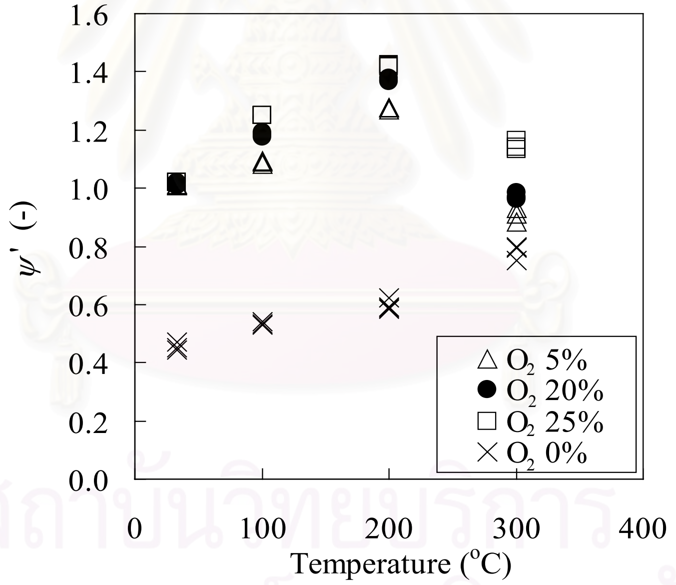

Fig. 2. Effect of coexisting O_2 on the removal efficiency ψ' of styrene from N_2; [styrene]= 500 ppm, SV= 55.8 hr^{-1} at room temperature, I = 0.05 mA (except I = 0.5 mA in the absence of O_2)

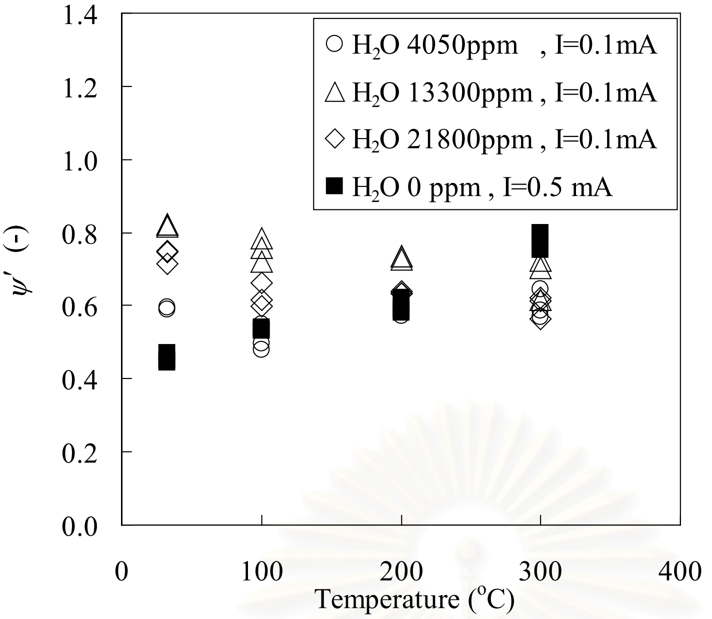

Fig. 3. Influence of water vapor on the removal efficiency ψ' of styrene from N_2; [styrene]= 500 ppm, SV= 55.8 hr^{-1} at room temperature.

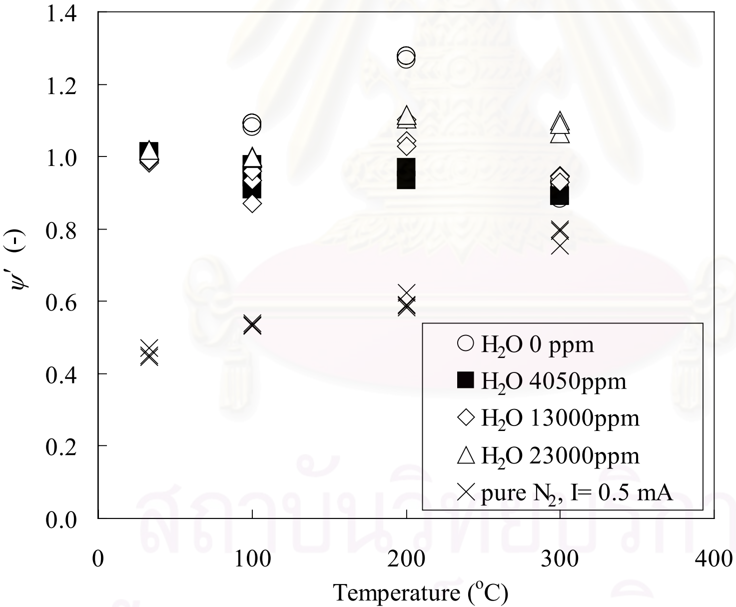

Fig. 4. Combined effect of oxygen and water vapor on the removal ψ' efficiency of styrene from N_2 at 5% O_2; [styrene]= 500 ppm, I=0.05 mA, SV= 55.8 hr^{-1} at room temperature.

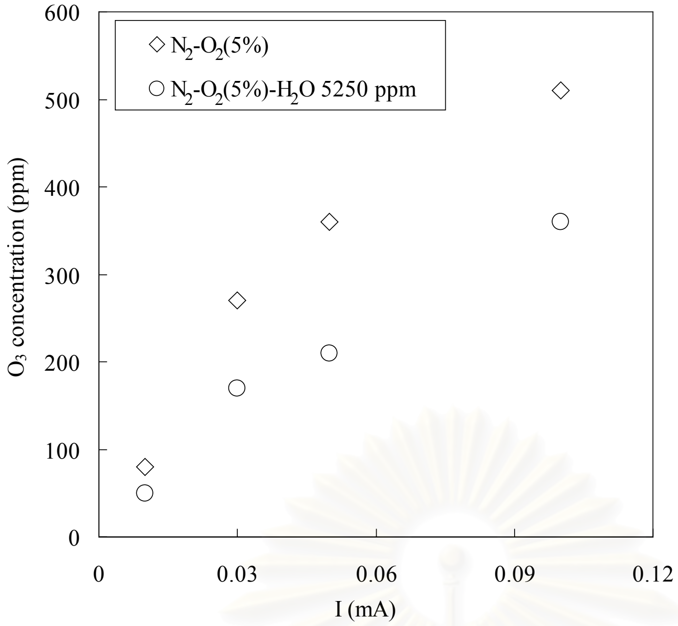

Fig. 5. Effect of water vapor on O_3 generation from 5% O_2 in N_2; SV= 55.8 hr^{-1} at room temperature.

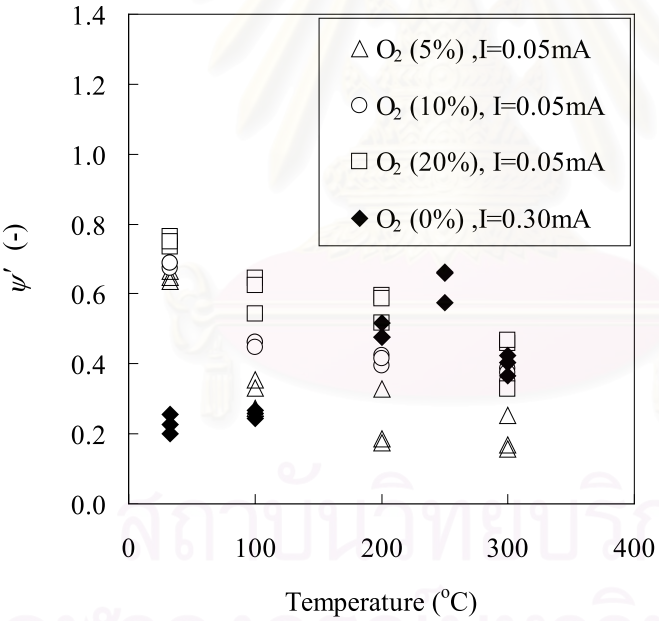

Fig. 6. Effect of coexisting O_2 on the removal efficiency ψ' of ammonia from N_2; [ammonia]= 400 ppm, SV= 55.8 hr^{-1} at room temperature.

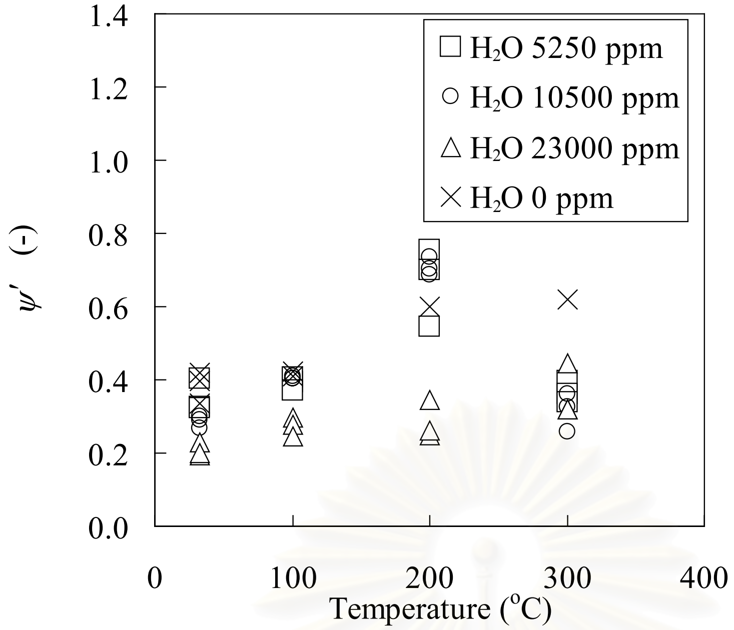

Fig. 7. Influence of water vapor on the removal efficiency ψ′ of ammonia from N_2; [ammonia]= 250 ppm, I=0.3 mA, SV= 55.8 hr^{-1} at room temperature.

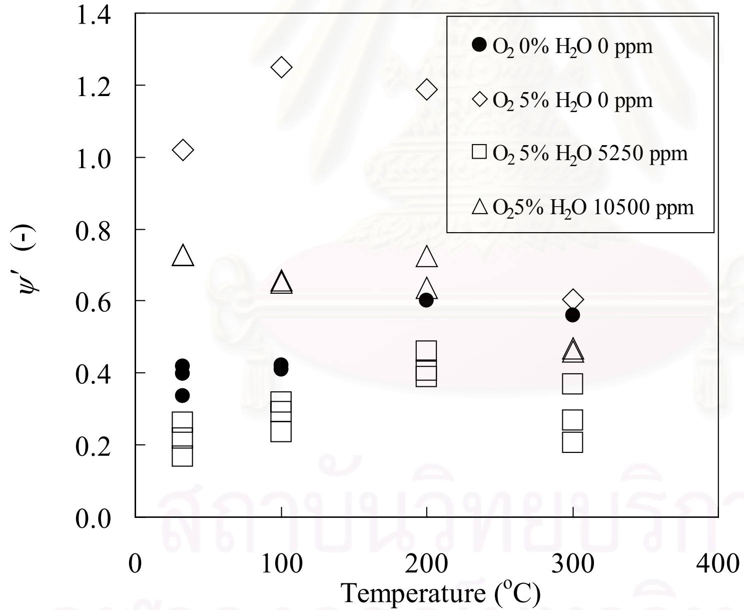

Fig. 8. Combined effect of O_2 and H_2O on the removal efficiency ψ′ of ammonia from N_2 (O_2 = 5%); [ammonia]= 250 ppm, I=0.3 mA, SV= 55.8 hr^{-1} at room temperature.

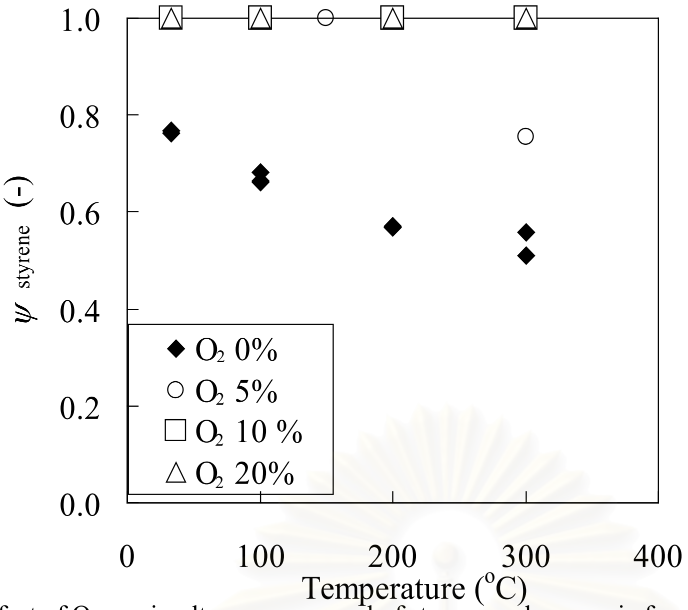

Fig. 9. Effect of O_2 on simultaneous removal of styrene and ammonia from N_2 (removal efficiency of styrene); [ammonia]= 200 ppm, [styrene]= 40 ppm, I=0.3 mA, SV= 55.8 hr^{-1} at room temperature.

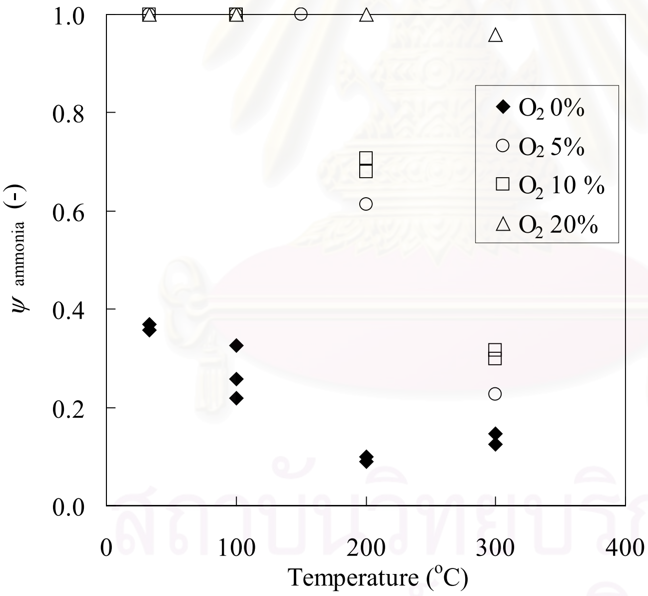

Fig. 10. Effect of O_2 on simultaneous removal of styrene and ammonia from N_2 (removal efficiency of ammonia); [ammonia]= 200 ppm, [styrene]= 40 ppm, I=0.3 mA, SV= 55.8 hr^{-1} at room temperature.

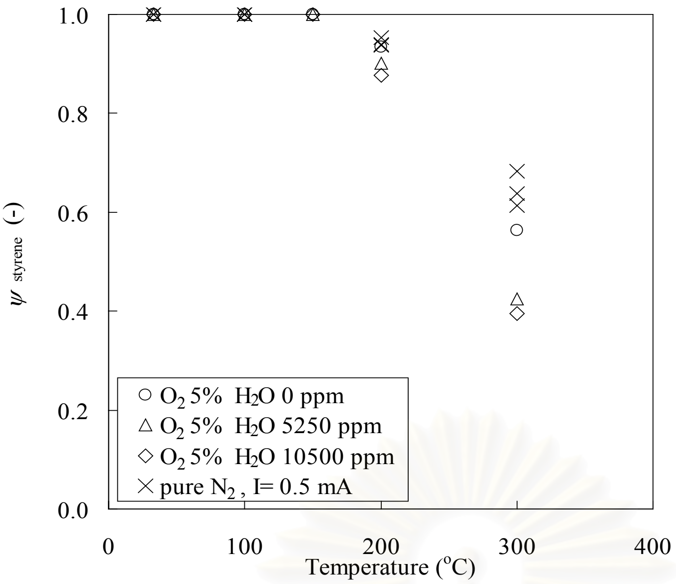

Fig. 11. Combined effect of O_2 and H_2O on simultaneous removal of styrene and ammonia from N_2 at 5% O_2 ; removal efficiency of styrene; [ammonia]= 200 ppm, [styrene]= 40 ppm, I=0.10 mA, SV= 55.8 hr^{-1} at room temperature.

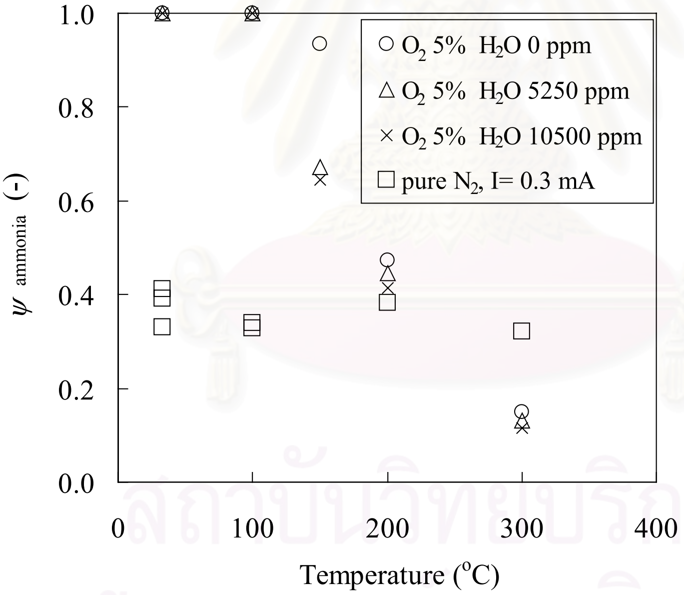

Fig. 12. Combined effect of O_2 and H_2O on simultaneous removal of styrene and ammonia from N_2 at 5% O_2; removal efficiency of ammonia; [ammonia]= 200 ppm, [styrene]= 40 ppm, I=0.10 mA, SV= 55.8 hr^{-1} at room temperature.

VITA

Mr. Jintawat Chaichanawong was born in Buriram, Thailand, on April 7, 1978, the third son of Ubon and Bang-on Chaichanawong. After completing his high-school study at Khonkaen Wittayayon school in Khonkaen, in March 1996. He entered King Mongkut's Institute of Technology Ladkrabang, Bangkok, in June, 1996. After earning the degree of Bachelor of Engineering in Chemical Engineering in March, 2000, he gained admission to the Graduate School of Chulalongkorn University in June 2000. He received financial support from Thailand Research Fund, which covered research materials and monthly expenses. In April 2003, he was awarded the degree of Master of Engineering in Chemical Engineering.